THESIS TITLE

Channel Estimation for SISO and MIMO OFDM Communication Systems

Submitted by

Olutayo Oyeyemi Oyerinde

IN FULFILLMENT OF THE DEGREE OF

Doctor of Philosophy in Electrical, Electronic and Computer Engineering, University of KwaZulu-Natal, Durban, South Africa

Date of Submission

April 2010

Supervised by

Professor S. H. Mneney

As the candidate's supervisor, I agree to the submission of this thesis.

Signed: _____

Name: _____ Date: _____

PREFACE

The research work done in this thesis was performed by Olutayo Oyeyemi Oyerinde, under the supervision of Professor Stanley H. Mneney, at the School of Electrical, Electronic and Computer Engineering at the University of KwaZulu-Natal's, Durban, South Africa. The work was supported by Deutscher Akademischer Austauschdienst/German Academic Exchange Service (DAAD) in form of DAAD/ANSTI postgraduate scholarship, and Telkom South Africa as part of the Center of Excellence Programme.

A part of this thesis has been published in the Wireless Personal Communications Journal, December 2008. The author has presented some part of this thesis during the South Africa Telecommunications Networks and Applications Conference (SATNAC) in 2008 at Wild Coast Sun, South Africa, the IEEE International Conference on Communications (ICC) in 2009 at Dresden Germany, the IEEE 1st International Conference on Wireless Communication Society, The Vehicular Technology, Information Theory and Aerospace & Electronics Systems Technology (Wireless VITAE'09) in 2009 at Aalborg Denmark, the IEEE AFRICON Conference in 2009 at Nairobi Kenya. Some other portions have been presented in IEEE International Symposium on Broadband Multimedia System and Broadcasting March 2010 in Shanghai China, and IEEE International Conference on Communications (ICC) May 2010, in Cape Town, South Africa.

The whole thesis, unless specifically indicated to the contrary in the text, is the author's work, and has not been submitted in part, or in whole to any other University.

ACKNOWLEDGEMENTS

My utmost gratitude goes to the ancient of days, the Almighty God, the author of life who has enabled me and provided opportunity to embark on this journey of acquisition of knowledge. May His name be forever praised.

My heartfelt appreciations and deepest thanks goes to my amiable supervisor, the Head of School of Electrical, Electronic and Computer Engineering, UKZN, Prof. Stanley H. Mneney for his expert guidance. His belief in me and the various privileges he gave me have helped to bring me to this end. Despite his tight schedule as the Head of School, he found time to proffer invaluable suggestions and advice towards the realization of this research work. It will be an understatement to say I have gained immensely from his pool of knowledge and persistent encouragement during the course of my PhD work.

I would like to express my heartfelt gratitude to the only love of my life, my little angel, sweet 'Fola (Rebecca Oyerinde) for her understanding and support at every stage of this PhD work. You are more than a wife to me. Thank you very much.

To my parents, brothers, sisters, uncles, aunties and cousins in Oyerinde's and Popoola's families, your supports and believe in me for this PhD work are quite appreciated.

Special appreciation to Prof. Fambirai Takawira, the Head of Center for Radio Access and Rural Technology (CRART), who also doubled as the Dean of Engineering, for various privileges I benefited from him and the Centre. Special thanks go to Prof. T.J.O. Afulo, for his fatherly love and encouragement, and to other members of staff in the CRART research group for their help.

I would like to thank Deutscher Akademischer Austauschdienst/German Academic Exchange Service (DAAD) and Telkom South Africa for their valued financial support in form of DAAD/ANSTI postgraduate scholarship, and Research Assistantship through the Centre of Excellence in the School of Electrical, Electronic and Computer Engineering, UKZN, South Africa respectively.

Lastly, my appreciation goes to my postgraduate colleagues for their help, friendship and encouragement during the course of my PhD work.

ABSTRACT

Telecommunications in the current information age is increasingly relying on the wireless link. This is because wireless communication has made possible a variety of services ranging from voice to data and now to multimedia. Consequently, demand for new wireless capacity is growing rapidly at a very alarming rate. In a bid to cope with challenges of increasing demand for higher data rate, better quality of service, and higher network capacity, there is a migration from Single Input Single Output (SISO) antenna technology to a more promising Multiple Input Multiple Output (MIMO) antenna technology. On the other hand, Orthogonal Frequency Division Multiplexing (OFDM) technique has emerged as a very popular multi-carrier modulation technique to combat the problems associated with physical properties of the wireless channels such as multipath fading, dispersion, and interference. The combination of MIMO technology with OFDM techniques, known as MIMO-OFDM Systems, is considered as a promising solution to enhance the data rate of future broadband wireless communication Systems.

This thesis addresses a major area of challenge to both SISO-OFDM and MIMO-OFDM Systems; estimation of accurate channel state information (CSI) in order to make possible coherent detection of the transmitted signal at the receiver end of the system. Hence, the first novel contribution of this thesis is the development of a low complexity adaptive algorithm that is robust against both slow and fast fading channel scenarios, in comparison with other algorithms employed in literature, to implement soft iterative channel estimator for turbo equalizer-based receiver for single antenna communication Systems.

Subsequently, a Fast Data Projection Method (FDPM) subspace tracking algorithm is adapted to derive Channel Impulse Response Estimator for implementation of Decision Directed Channel Estimation (DDCE) for Single Input Single Output - Orthogonal Frequency Division Multiplexing (SISO-OFDM) Systems. This is implemented in the context of a more realistic Fractionally Spaced-Channel Impulse Response (FS-CIR) channel model, as against the channel characterized by a Sample Spaced-Channel Impulse Response (SS)-CIR widely assumed by other authors**.** In addition, a fast convergence Variable Step Size Normalized Least Mean Square (VSSNLMS)-based predictor, with low computational complexity in comparison with others in literatures, is derived for the implementation of the CIR predictor module of the DDCE scheme. A novel iterative receiver structure for the FDPM-based Decision Directed Channel Estimation

scheme is also designed for SISO-OFDM Systems. The iterative idea is based on Turbo iterative principle. It is shown that improvement in the performance can be achieved with the iterative DDCE scheme for OFDM system in comparison with the non iterative scheme.

Lastly, an iterative receiver structure for FDPM-based DDCE scheme earlier designed for SISO OFDM is extended to MIMO-OFDM Systems. In addition, Variable Step Size Normalized Least Mean Square (VSSNLMS)-based channel transfer function estimator is derived in the context of MIMO Channel for the implementation of the CTF estimator module of the iterative Decision Directed Channel Estimation scheme for MIMO-OFDM Systems in place of linear minimum mean square error (MMSE) criterion. The VSSNLMS-based channel transfer function estimator is found to show improved MSE performance of about -4 MSE (dB) at SNR of 5dB in comparison with linear MMSE-based channel transfer function estimator.

TABLE OF CONTENTS

LIST OF ACRONYMS

1D	-	One-Dimensional
2D	-	Two-Dimensional
4G	-	Fourth Generation System
5G	-	Fifth Generation System
ANMSE	-	Asymptotic Normalized Mean Square Error
AOFDM	-	Adaptive Orthogonal Frequency Division Multiplexing
APP	-	A- Posteriori probability
APRmodRLS	-	Approximated modified Recursive Least Square
AWGN	-	Additive White Gaussian Noise
BER	-	Bit Error Rate
BICM	-	Bit Interleaved Coded Modulation
BLAST	-	Bell Laboratories Layered Space Time
BPSK	-	Binary Phase Shift Keying
BS	-	Base Station
BU	-	Bad Urban
CCs	-	Convolutional Codes
CIR	-	Channel Impulse Response
COFDM	-	Coded Orthogonal Frequency Division Multiplexing
COST	-	European Cooperation in the field Of Scientific and Technical research
CP	-	Cyclic Prefix
CSI	-	Channel State Information
CTF	-	Channel Transfer Function
DAB	-	Digital Audio Broadcasting
D-BLAST	-	Diagonal Bell Laboratories Layered Space Time
DDCE	-	Decision Directed Channel Estimation
DFT	-	Discrete Fourier Transform
DPM	-	Data Projection Method
DS-UWB	-	Direct Sequence-Ultra WideBand
DVB	-	Digital Video Broadcasting

EM	-	Expectation Maximization
EVD	-	EigenValue Decomposition
fD	-	normalized Doppler Frequency
FD-CTF	-	Frequency Domain Channel Transfer Function
FDP	-	Frequency Division Multiplexing
FDPM	-	Fast Data Projection Method
FEC	-	Forward Error Correction
FFT	-	Fast Fourier Transform
FIR	-	Finite Impulse Response
FPTA	-	Frequency Pilot Time Average
FS-CIR	-	Fractionally Spaced- Channel Impulse Response
GSM	-	Global System for Mobile
HT	-	Hilly Terrain
HIPERLAN/2	-	High Performance Radio Local Area Network type two
ICI	-	Inter-Channel (Carrier) Interference
IFFT	-	Inverse Fast Fourier Transform
IEEE	-	Institute of Electrical Electronic Engineering
ISI	-	Inter-Symbol Interference
JPL	-	Jet Propulsion Laboratory
KF	-	Kalman Filter
LAN	-	Local Area Network
LDPC	-	Low Density Parity Check
LLR	-	Log-Likelihood Ratio
LMS	-	Least Mean Square
LMMSE	-	Linear Minimum Mean Square Error
LS	-	Least Square
LORAF	-	Low Rank Adaptive Filter
MAN	-	Metropolitan Area Network
MAP	-	Maximum A-Posteriori
MB-ML	-	Multiple Burst-Maximum Likelihood
MC-CDMA	-	Multi-Carrier Code division Multiple Access
ML	-	Maximum Likelihood
MMAC	-	Multimedia Mobile Access Communication
MMSE	-	Minimum Mean Square Error

MMSEE	-	Minimum Mean Square Error Estimator
M-PSK	-	Multilevel-Phase Shift Keying
M-QAM	-	Multilevel-Quadrature Amplitude Modulation
MRT	-	Maximum Ratio Transmission
MSE	-	Mean Square Error
MVSSNLMS	-	Multiple Variable Step Size Normalized Least Mean Square
MIMO	-	Multiple Input Multiple Output
MISO	-	Multiple Input Single Output
NLMS	-	Normalized Least Mean Square
OFDM	-	Orthogonal Frequency Division Multiplexing
OPML	-	Orthogonal Pilot-based Maximum Likelihood
OSTBC	-	Orthogonal Space Time Block Code
PAPR	-	Peak to Average Power Ratio
PAST	-	Projection Approximation Subspace Tracking
PASTd	-	Projection Approximation Subspace Tracking with deflation
pdf	-	probability density function
PDP	-	Power Delay Profile
PIC	-	Parallel Interference Cancellation
PN	-	Pseudo random Noise
PSAM	-	Pilot Symbol Assisted Modulation
QAM	-	Quadrature Amplitude Modulation
QPSK	-	Quadrature Phase Shift Keying
RLS	-	Recursive Least Square
RF	-	Radio Frequency
RSC	-	Recursive Systematic Convolution
RSE	-	Recursive Systematic Encoder
SDMA	-	Space Division Multiple Access
SIC	-	Serial Interference Cancellation
SIMO	-	Single Input Multiple Output
SISO	-	Single Input Single Output
SNR	-	Signal to Noise Ratio
SOSTTC	-	Super Orthogonal Space Time Trellis Code
SOVA	-	Soft Output Viterbi Algorithm
SS-CIR	-	Sample Spaced-Channel Impulse Response

STBC	-	Space Time Block Code
ST-BICM	-	Space Time Bit Interleaved Coded Modulation
STTC	-	Space Time Trellis Code
TDMA	-	Time Division Multiple Access
TSR	-	Time Series Representation
TU	-	Typical Urban
US	-	Uncorrelated Scattering
V-BLAST	-	Vertical Bell Laboratories Layered Space Time
VLSI	-	Very Large Scale Integration
VSSNLMS	-	Variable Step Size Normalized Least Mean Square
WSS	-	Wide Sense Stationary

LIST OF NOTATIONS

det	Determinant
orthnorm	Orthonormalization process
$diag(.)$	diagonal matrix
$.^{T}$	Transpose
$.^{*}$	Complex conjugate
$.^{H}$	Hermitian (conjugate transpose)
$Cov\{.,.\}$	Covariance of two variables
$E\ .$	Expectation of random variable
$\Pr[.=.]$	Symbol probability
$\mathrm{Re}\ .$	Real part
$\|.\|$	Euclidean norm
$\|.\|^2$	Square of Euclidean norm
B_{ch}	Coherence bandwidth of the channel
B_s	Transmitted signal's bandwidth
c	Speed of light
C	Shannon capacity
$\boldsymbol{C}_H$	Symmetric, nonnegative, definite, covariance matrix
δ	Dirac's delta function
E_s	Energy per transmitted symbol
fD	Doppler spread/ Doppler Frequency
f_c	Carrier frequency
λ	Forgetting factor
$\breve{\gamma}$	*a priori* estimate of γ
$\hat{\gamma}$	*a posteriori* estimate of γ

$\boldsymbol{H}$	Channel matrix
I	Identity matrix
K	Number of subcarriers
L_{prd}	Length of predictor filter
M	Number of paths
M_T	Numbers of transmit antennas
M_R	Numbers of receive antennas
μ	Step size
μ_n	Variable step size
N_0	Gaussian noise power spectral density
σ_e^2	Ensemble error variance
σ_w^2	Gaussian noise variance
σ_H^2	Total average power of the CIR
R	Sampling rate
R_c	Code rate
τ_m	*m*th path time-variant delay
τ_d	Delay spread
T_D	Coherent time
T_s	Transmitted signal's duration
$\bar{\boldsymbol{x}}$	Soft symbol vector
v	Speed of vehicle

LIST OF FIGURES

LIST OF TABLES

CHAPTER 1

GENERAL INTRODUCTION

In the modern day world we are living today, communication has become an integral part of our lives in different forms. We communicate with one another via the avenues of telephones (fixed and mobile), radio and television, the internet on both mini and macro computer terminals, just to mention a few. Notwithstanding the type of communication Systems being used, the three major components of the communication Systems remain the same for all. These include *source*, *channel* and *sink* (*transmitter*, *channel* and *receiver* respectively). Both the *transmitter* and the *receiver* could either be fixed or mobile, and they are separated by the *channel*. The *channel* can be *wireline* or *wireless*. Irrespective of the type of channel, its effects on the transmitted signal from the *transmitter* through the *channel* to the *receiver* are similar. These effects include distortion of the transmitted signal in the form of attenuation, interference with other transmitted signals available in the channel or its own delayed version caused by the *channel*'s physical characteristics, and contamination with the channel's noise. The communication receiver is therefore vested with an important task of reconstruction of the accurate estimate of the original information-bearing signal. In a bid to do this effectively many signal processing techniques are employed at the receiver end of the communication Systems. These include, among others, compensation techniques based on the estimation of the time-varying nature of the channel, error-correction techniques to improve information received through the wireless channels, and synchronization techniques both in time and frequency domains.

1.1 Wireless Communication

Wireless communications is one of the most active areas of technology development and a rapidly growing branch of the wider field of communications Systems. It is called wireless because it involves the use of wireless channels rather than wireline channels. This rapid growth

has been coupled closely with the technological advances of our time. It is worth noting that telecommunications in the 21st century is increasingly relying on the wireless link. This is because wireless communication has made possible a variety of services ranging from voice to data and now to multimedia. As a result, similarly to what happened to wireline capacity in the late1990s, the demand for new wireless capacity is now growing at a very rapid rate. Nevertheless, the wireless communication system is consistently faced with diverse challenges. These include the sparsely available radio frequency spectrum and a complex space-time varying wireless environment. Besides these, the system is also confronted with challenges of an increasing demand for higher data rates, better quality of service, and higher network capacity [1]. Consequently, there is a migration from Single-Input Single-Output (SISO) antenna technology to a more promising Multiple-Input Multiple-Output (MIMO) antenna technology for deployment in the wireless communications Systems.

The idea of using multiple antennas at both transmit and receive ends has emerged as one of the major technical breakthroughs in modern wireless communications system. Theoretical studies and initial prototyping of MIMO Systems have shown a high order of magnitude in spectral efficiency improvements for point -to-point communication [2 - 5]. As a result, MIMO is considered a key technology for improving the throughput of future wireless broadband data Systems, which as at present are mired at data rates far below their wired counterparts.

On the subject of the transmission techniques for mitigating the physical limitation of wireless channels caused by multipath fading, dispersion, and interference, a very popular multi-carrier modulation technique which has emerged recently [6, 7] in the communication field is Orthogonal Frequency Division Multiplexing (OFDM) technique. The OFDM technique simply converts a wireless frequency selective fading channel into a parallel collection of frequency flat fading channels. The subcarriers (subchannels) have the minimum frequency separation required to make their time domain waveforms orthogonal while the signal frequency spectrum corresponding to the different subcarriers overlap. As a result, the available bandwidth is utilized more efficiently. In general OFDM technique for wireless communication Systems has a high spectral efficiency compared with Frequency Division Multiplexing (FDM) scheme. In addition, it is very robust to selective fading and has a low computational complexity due to the type of computational method with which it is implemented.

1.2 Wireless Communication Channels

The undesirable effects of a wireless communication channel on the signals transmitted through the channel are as a result of the physical properties of the channel. The transmitted signals interact with the environment in a very complex way. In the channel between the transmitter and the receiver, there are always reflections due to large objects, diffraction of the electromagnetic waves around obstructing objects as well as signal scattering. The overall effects of these interactions result in many signal copies (or *multipath* signals) with different attenuation, distortion, delays and phase shift arriving at the receiver. These *multipath* signals can interfere with each other constructively or destructively. In the case when destructive interference occurs, the signal power can be significantly diminished. This phenomenon is termed as *fading*. In the case of strong destructive inference, the channel will experience what is always referred to as a *deep fade* and may eventually lead to a temporary failure of communication as a result of severe drop in the channel signal to noise ratio (SNR). Basically, there are two types of fading effects that are associated with wireless communication channels. These include large-scale fading and small scale fading [8]. Large-scale fading corresponds to the average signal power attenuation or path loss attributable to motion over large areas. Small-scale fading is due to dramatic alterations in amplitude and phase of transmitted signal that can mostly be experienced due to slight changes in the spatial separation between a receiver and transmitter. Small-scale fading is referred to as *Rayleigh fading* provided the multiple reflective paths are large in number and there is no line of sight signal component, hence the envelope of the received signal can be statistically described by a Rayleigh probability density function (pdf). However, if there is a dominant non-fading signal component present, such as a line-of-sight propagation path, such small scale fading envelope can be illustrated by a Rician pdf [8]. *Doppler shift* is another property of wireless communication channel. *Doppler shift* is caused as a result of relative motion between the transmitter and the receiver as well as motion of any other objects in the wireless channel. This also results in the time-varying nature of the wireless channel. Figure 1.1 shows a typical wireless communication channel with *multipath* effect. As a result of different environmental paths, each multipath signal arriving at the base station from the mobile transmitters, local scatterers and the remote dominant reflector, will have different amplitude, carrier phase shift, time delay, and Doppler shift. If the transmitters are in motion, these multipath signals parameters will also be time-varying.

1.2.1 Parameters of Fading Channels

The following parameters, among others, are always used to characterize wireless communication

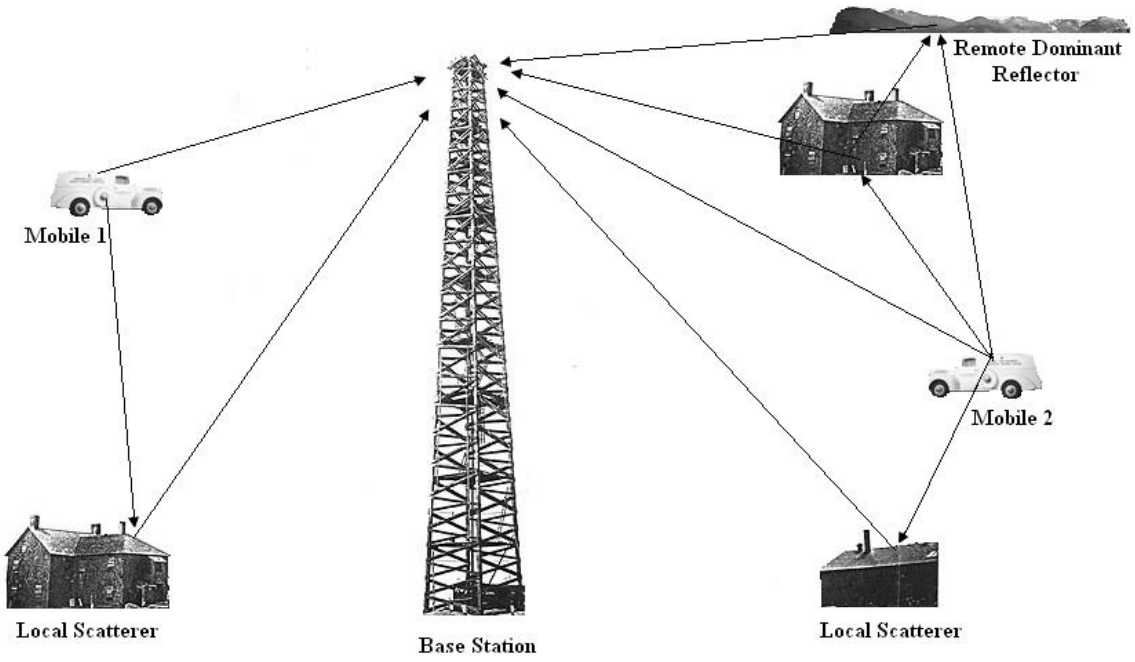

Figure1.1 Multipath propagation in wireless communication channel

channels [9].

- *Delay spread* (τ_d): This is defined as the largest of the delays among the various paths, which is due to reflected and scattered propagation paths in a radio channel.

- *Coherence bandwidth of the channel* (B_{ch}): This is inversely proportional to the delay spread ($B_{ch} \alpha \, 1/\tau_d$). It represents a frequency range over which frequency components exhibit a strong potential for amplitude correlation. Thus a signal's spectral components in such frequency range will undergo similar channel fading effects.

- *Doppler Spread* (fD): This is defined as the largest of the frequency shifts of the various paths of the multipaths in the wireless communication channel. If the receiver and transmitter are in relative motion with constant speed, the received signal will be subjected to a constant frequency shift called Doppler spread. The Doppler spread is given as

$$fD \approx f_c \frac{v}{c}, \qquad 1.1$$

where f_c is the carrier frequency, v is the speed of the vehicle, and c is the speed of light.

- *Coherent Time* (T_D): This is defined as the inverse of the Doppler spread. It is a measure of the expected time duration during which the channel's response is approximately invariant.

1.2.2 Fading Channel Classification

Classification of fading channels is a direct function of both the transmitted signals characteristics and the channel's parameters. If B_s denotes the bandwidth of the transmitted signal and its reciprocal ($1/B_s$) is the duration of the signal (T_s), the fading channel, based on time and frequency dispersion mechanism, can be classified as follow.

- **Frequency Selective Fading channel:** This is the type of fading that occurs if the bandwidth of the transmitted signal (B_s) is large compared with coherent bandwidth of the channel (B_{ch}), that is $B_s > B_{ch}$ [9]. In this case the symbol duration, T_s is less than the delay spread of the channel, i.e. $T_s < \tau_d$. Under these circumstances, the channel's output signal that arrives at the receiver will include multiple versions of the transmitted signal, which are faded and delayed in time, resulting in intersymbol interference (ISI) problem. As such, different frequency components of the transmitted signal would then undergo different degrees of fading.

- **Non-Frequency Selective (Flat) Fading:** This type of fading occurs if the bandwidth of the transmitted signal (B_s) is small compared with coherent bandwidth of the channel (B_{ch}), that is $B_s << B_{ch}$ [9]. In this case, the symbol duration, T_s is large compared with the delay spread of the channel, i.e. $T_s > \tau_d$. Under these conditions, delays between different paths are relatively small with respect to the symbol duration. Hence, the channel transfer function can be taken as constant and different frequency components of the transmitted signal experience the same type of fading referred to as flat (i.e., non-selective) fading in frequency.

- **Slow fading channel:** The term "slow fading" is used to describe a channel that has its impulse response varying at a rate much slower that the rate of change of the transmitted signal. In this case, the time duration of a transmitted symbol is small compared with the channel coherent time (i.e. $T_s < T_D$) [9]. Such a channel can be assumed to be time-

invariant over a number of symbol intervals. This type of fading can be due to phenomenon such as shadowing, where a large obstacle such as hill or large building obscures the main signal path between the transmitter and the receiver.

- **Fast fading channel:** A channel is said to be introducing fast fading if its impulse response changes rapidly within the symbol duration of the transmitted signal. The time duration over which the channel behaves in a correlated way is short in comparison with the time duration of a symbol. This implies that the coherence time of the channel is smaller than the time duration of a transmitted symbol (i.e. $T_D < T_s$).

All these classification, in turn, give rise to four different types of channels as listed below and their relationship in both frequency and time domains illustrated in Figure 1.2.

- Frequency selective fast fading channel
- Frequency non-selective (flat) fast fading channel
- Frequency selective slow fading channel
- Frequency non-selective (flat) slow fading channel

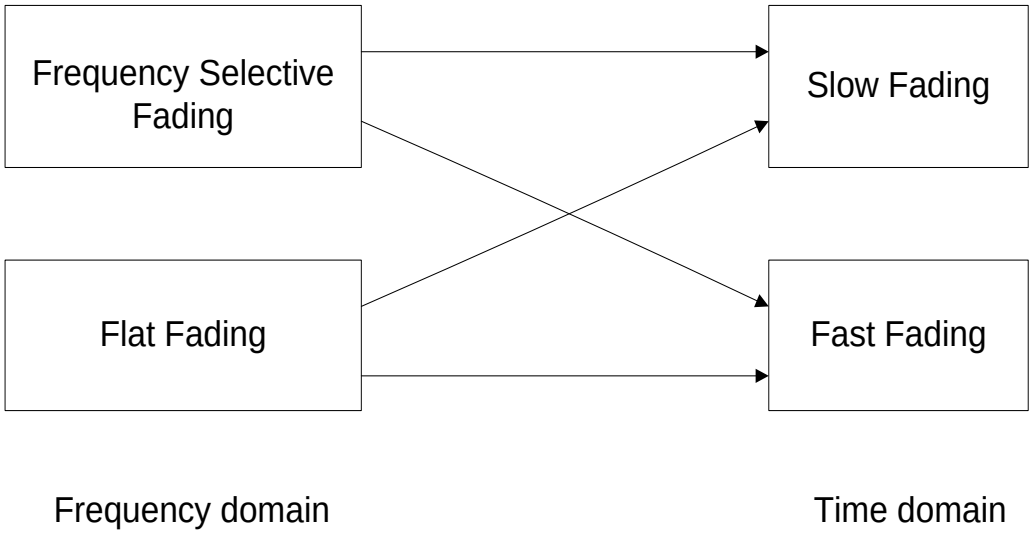

Figure1.2 Relationship between fading channel classification

The effect of fading is undesirable in wireless communication system. It results in performance deterioration in the communication Systems because the quality of the communications link depends on the channel and due to fading there is a significant probability that the channel will undergo a *deep fade effect* (strong destructive interference of signal of interest by some unwanted or delayed version of the signals due to multipaths in the channel). Different techniques have been proposed in a bid to overcome the effects of fading in the communication channel. Others even possess the capability of turning to gain some of these negative effects. Examples of these are the use of multiple antennas at the transmitter and/or the receiver end of the communication system, OFDM transmission scheme, and MIMO-OFDM scheme as earlier mentioned. These are briefly described in the next section.

1.3 MIMO-OFDM for Wireless Communication Systems

The combination of MIMO methods with OFDM known as MIMO-OFDM is considered as a promising solution to improve the signal rate of future broadband wireless communication Systems. The idea of this scheme is developed in [4] with the intention to compute the information-theoretic capacity in a frequency-selective MIMO channels. The great finding was that the well-known flat-fading MIMO algorithms can be re-used on a carrier-by-carrier basis since the channel becomes orthogonal in the frequency domain with the use of OFDM scheme. This reduces the computational effort and makes MIMO-OFDM technique attractive for mobile applications. In this section, brief overviews of MIMO, OFDM and MIMO-OFDM for wireless communication Systems are presented.

1.3.1 MIMO Systems

The use of spatial diversity technique is the main idea of multiple antennas Systems originated from the single antenna Systems, the SISO Systems. An early type of antenna diversity is the receive diversity. In this technique, multiple antennas are used at the receiver end of the communication link alone. This results in what is known as Multiple-Input Single-Output (MISO) Systems. Some years later it was observed that many of the benefits of receive diversity can be obtained by using transmit diversity. In transmit diversity technique multiple antennas are used at the transmitter end alone to form Single -Input -Multiple Output (SIMO) Systems. An incentive for the usage of transmit antenna diversity is that in a cellular communication Systems, the extra antennas will be at the base station so that the mobile station needs not to have multiple antennas.

Consequently, the cost of extra antennas at base station can then be paid by service provider. The Multiple-Input Multiple-Output (MIMO) combined the performance gains that are achievable in both the transmit antenna diversity and the receive antenna diversity Systems with the use of multiple antennas at both end of the communication link. The main idea behind MIMO is that signals sampled in the spatial domain at both ends are combined in such a way that they either create effective multiple parallel spatial data channels (therefore increasing the data rate), and/or add diversity to enhance the bit-error rate (BER) performance of the Systems. The idea of spatial diversity is that in the presence of random fading occasioned by multipath propagation, the signal-to-noise ratio (SNR) is significantly improved by combining the output of decorrelated antenna elements. The early 1990s witnessed new proposals for using antenna arrays to increase the capacity of wireless links thereby creating several opportunities beyond just diversity [1].

1.3.1.1 Performance gain in MIMO Systems

The performance benefits available as a result of using the MIMO Systems are largely due to spatial multiplexing gain, diversity gain, array gain, and interference reduction.
Each of these is briefly described below with assumption of having M_T and M_R numbers of transmit and receive antennas respectively.

- **Spatial multiplexing gain**: Spatial multiplexing technique is the simultaneous transmission of multiple data signals from transmitter to the receiver, with both equipped with more than one antenna. Consequently, MIMO system is able to offer a linear capacity proportional to the minimum number of either the transmit antennas or the receive antennas (i.e. $\min M_R, M_T$), in comparison with Systems employing single antenna at one or both end of the links, for no extra power or bandwidth expenditure [2-5], [12]. This gain which is commonly referred to as multiplexing gain, is possible if the propagation channel exhibits rich scattering. The receiver takes advantage of differences in the spatial signatures induced into the multiplexed signals by the MIMO channels to separate the different streams of data transmitted, thereby realizing a capacity gain.
- **Diversity gain**: As earlier described in the previous section, diversity is a powerful technique to reduce the effect of fading in wireless links where signal power fluctuates randomly. Diversity gain is achieved by transmitting the signal over multiple, independently fading paths in time, frequency or space. Spatial (antenna) diversity is however preferred over time/frequency diversity because it does not involve expenditure of either transmission time or bandwidth [12]. Provided that the $M_T M_R$ links comprising

the MIMO channels fade independently and the transmitted signal is suitably constructed, the MIMO Systems' receiver can combine the arriving signals such that the resultant signal exhibits considerably reduced amplitude variability in comparison to a SISO link. Consequently, $M_T M_R$ –*th* order of diversity will be obtained.

- A**rray gain:** MIMO Systems increases antenna gain by beamforming. The gain can be achieved both at the transmitter and the receiver, but depends on the number of transmit and receive antennas. Besides, transmit/receive array gain requires channel knowledge in the transmitter and receiver respectively [12].
- **Interference reduction**: The differentiation between the spatial signatures of the desired signal and co-channel signals, when multiple antennas are used, can be employed to reduce co-channel interference which occurs due to frequency reuse in wireless channels [12]. Just like the case with array method for MIMO Systems, interference reduction also requires knowledge of the desired signal's channel. Interference reduction allows aggressive frequency reuse and thereby increases the system capacity.

1.3.1.2 MIMO Systems Capacity

The capacity metrics to represent the quality of the MIMO channels presented in different literatures, by various authors, have some slight differences which are due to differing assumptions made about the channel. In general, the singular values of the MIMO channels matrix, $\boldsymbol{H}$, of dimension $M_R \times M_T$, remains the determinant factor of the MIMO Systems capacity. In particular, what the transmitter knows about the channel has a great bearing on the transmission scheme, and ultimately the achievable capacity.

In [13] it is shown that the usual equation of Shannon capacity (in bit/sec/Hz) given as

$$C = \log_2 \left(1+\rho\right), \tag{1.2}$$

for SISO Systems can be extended to derive the capacity expression for MIMO Systems which is given as

$$C = \log_2 \left[\det\left(I_{M_R} + \frac{\rho}{M_T} \boldsymbol{H}\boldsymbol{H}^H \right) \right], \tag{1.3}$$

where I_{M_R} denotes the identity matrix of size M_R, ρ is the average signal-to-noise ratio (SNR) at any receiving antenna, *det* is the determinant, superscript '*H*' stands for Hermitian (conjugate transpose), and $\boldsymbol{H}$ is the $M_R \times M_T$ channel matrix with elements which are complex Gaussian

with zero mean and unit variance. It has been however established in [4, 10] that at high SNR the MIMO Systems capacity can be approximated to

$$C = \min\ M_R, M_T\ \log_2\ 1+\rho\ . \qquad 1.4$$

The capacity expression in (1.4) shows clearly that there is a linear increase in capacity of MIMO Systems proportional to the minimum of the number of transmit and receive antennas. This confirms the main reason for its deployment in the wireless communication Systems.

1.3.2 OFDM Systems

The OFDM technology has become a popular transmission technique for signals over wireless channels. The origin of OFDM can be traced back to the Chang's paper [6] on *the synthesis of bandlimited orthogonal signals for multichannel data transmission* published in 1966. In the paper, a new concept of simultaneous transmission of signals over a bandlimited channel without the inter-channel interference (ICI) and the inter-symbol interference (ISI) was presented. A year later, performance analysis of effective signal transmission in parallel form was presented by Saltzburg [7]. Saltzburg concluded in his paper that in designing an effective parallel system, effort should be concentrated on reduction of crosstalk between adjacent channels rather than endeavoring to perfect the individual channels. Today, OFDM has become a widely accepted multi-carrier modulation method for signals transmission over wireless channels. Several wireless technologies and standards such as digital audio broadcasting (DAB), digital video broadcasting (DVB), high-rate wireless LAN standard [14] such as the IEEE 802.11a [15], high-performance radio LAN type two (HIPERLAN/2) [16], multimedia mobile access communication (MMAC) [17, 18], and the IEEE 802.16a [19] metropolitan area network (MAN) standard, are all based on OFDM technique [20]. OFDM is also seen as a potential candidate for the future generation of the mobile wireless Systems, especially the fourth generation (4G) Systems [20, 32].

The OFDM concept is based on the splitting of data stream with a high-rate into a number of lower rate streams that are transmitted simultaneously over a number of subcarriers. Thus, there is an increase in symbol duration for the lower rate parallel subcarriers which in turn reduces the relative amount of dispersion, that is caused by multipath delay spread, in time. However, in a bid to completely eliminate the intersymbol interference (ISI), a guard time is introduced in every OFDM symbol. As such, OFDM technology is seen as a scheme that transforms a frequency selective fading channel to a set of parallel flat fading sub-channels. Consequently, the receiver structure is drastically simplified, and the time domain waveforms of the sub-carriers become orthogonal to each other. In contrast to the normal Frequency Division Multiplexing (FDM)

scheme where the subcarriers are non-overlapping, the signal frequency spectrum associated with different subcarriers overlap in frequency domain as shown in Figure 1.3. The introduction of guard band between the different carriers in the conventional FDM, in a bid to get rid of the interchannel interference, results in an inefficient use of the scarce and costly frequency spectrum resource. The overlapping of these subcarriers in the OFDM Systems makes possible efficient utilization of available bandwidth without causing the inter-carrier interference (ICI).

Direct implementation of OFDM Systems is computationally complex because of the large number of subcarriers involved which would require an equal number of sinusoidal oscillators for coherent demodulation. However, a breakthrough to the OFDM implementation came in 1971 when Weinstein and Ebert [21] proposed an effective way of implementing the scheme through the application of Discrete Fourier Transform (DFT), which drastically reduces the implementation complexity of the OFDM modems. This substantial reduction in implementation complexity was attributable to the simple realization that the DFT makes use of a set of harmonically related sinusoidal and cosinusoidal basis functions, whose frequency is an integer multiple of the lowest nonzero frequency of the set, which is referred to as the basis frequency.

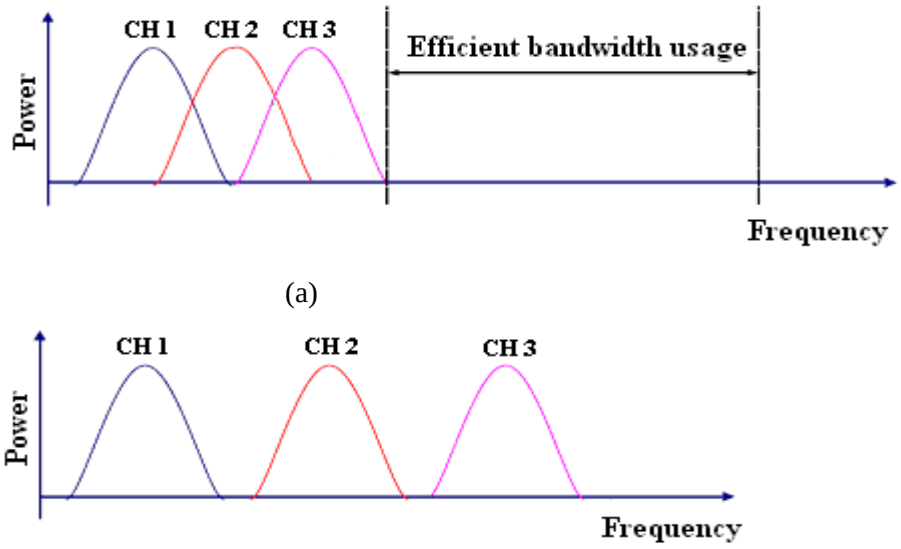

Figure1.3 Comparison between (a) OFDM and (b) Conventional FDM

These harmonically related frequencies can therefore be used as the set of carriers required by the OFDM system. By employing a Fast Fourier Transform (FFT), an efficient implementation of the DFT, the computational complexity of OFDM could further be reduced. Recent advances in very-large-scale-integration (VLSI) technology have, however, enabled the availability of economical, high-speed and large-size integrated circuits for the implementation of FFT and (Inverse Fast Fourier Transform) IFFT. The use of these IFFT and FFT methods for the implementation of both the OFDM transmitter and receiver respectively reduces the number of operation to $Klog_2K$ from K^2, if DFT techniques are used instead, where K is the number of subcarriers [22].

1.3.2.1 Advantages and Disadvantages of OFDM Systems

The various advantages and disadvantages of OFDM Systems can be highlighted as follows [23, 24]:

- **Advantages of OFDM Systems**:

i. OFDM has immunity to delay spread. Hence the scheme is an efficient way to deal with the problem of multipath.
ii. It has resistance to frequency selective fading because each of the subchannels in OFDM is almost flat fading.
iii. It exhibits efficient bandwidth usage, since the subchannels are kept orthogonal in the time domain but overlap in the frequency domain.
iv. The implementation of OFDM Systems is simple by using FFT (Fast Fourier Transform).
v. The system's receiver complexity is low because of absence of multi-taps equalizer/detector.
vi. OFDM possesses high flexibility in terms of link adaptation.
vii. OFDM is robust against narrowband interference, because such interference affects only a few numbers of the subcarriers.

- **Disadvantages of OFDM Systems**:

i. The scheme is sensitive to frequency offsets (caused by frequency differences between the local oscillators in the transmitter and the receiver), timing errors and phase noise.

ii. It exhibits quite a high peak-to-average power ratio (PAPR) in comparison with single carrier system that seeks to lower the power efficiency of the Radio Frequency (RF) amplifier.

1.3.3 MIMO-OFDM Systems

The multiple transmitting and receiving antennas can be employed with OFDM to enhance the communication capacity and quality of mobile wireless Systems [25-28]. MIMO as described above is known to boost capacity. In the case of high data-rate transmission, the multipath nature of the communication environment causes the MIMO channels to become frequency-selective. However, as elucidated earlier, OFDM transmission scheme can convert such frequency-selective MIMO channels into an array of parallel frequency-flat MIMO channels by which the receiver complexity is drastically reduced. The combination of these two powerful techniques, MIMO and OFDM to form Multiple Input Multiple Output-Orthogonal Frequency Division Multiplexing (MIMO-OFDM) Systems, is very attractive, and is considered one of the most promising solutions to improve the signal rate of broadband wireless communication Systems.

A schematic diagram of a MIMO-OFDM system is shown in Figure1.4. Assuming a MIMO-OFDM system employing M_T transmit and M_R receive antennas with N OFDM subcarriers, channel encoded bits are first interleaved with a channel interleaver π and then mapped onto a number of data symbols via some modulation type such as Quadrature Amplitude Modulation (QAM) or Multilevel Phase Shift Keying (M-PSK). These symbols are then passed through the transmit diversity processor (e.g. a space-time encoder) that transforms them into M_T different signals. Each of these signals forms an OFDM block, and they are passed through classical OFDM modulators (IFFT followed by cyclic prefix insertion) of K carriers. The resulting OFDM symbols are transmitted simultaneously from the individual transmit antennas. At the receiver, the individual signals are passed through OFDM demodulators which first discard the cyclic prefix and then perform the K-point FFT on the received signals. The outputs of the OFDM demodulator are passed through the diversity gain processor in a bid to achieve transmit diversity gain. The diversity gain processor's outputs are de-interleaved with a channel de-interleaver π^{-1} and then demapped from the QAM or M-PSK constellations. Thereafter channel decoder is used to decode the transmitted bits. Detailed of the basic concepts of the MIMO-OFDM system are well documented in [29, 30].

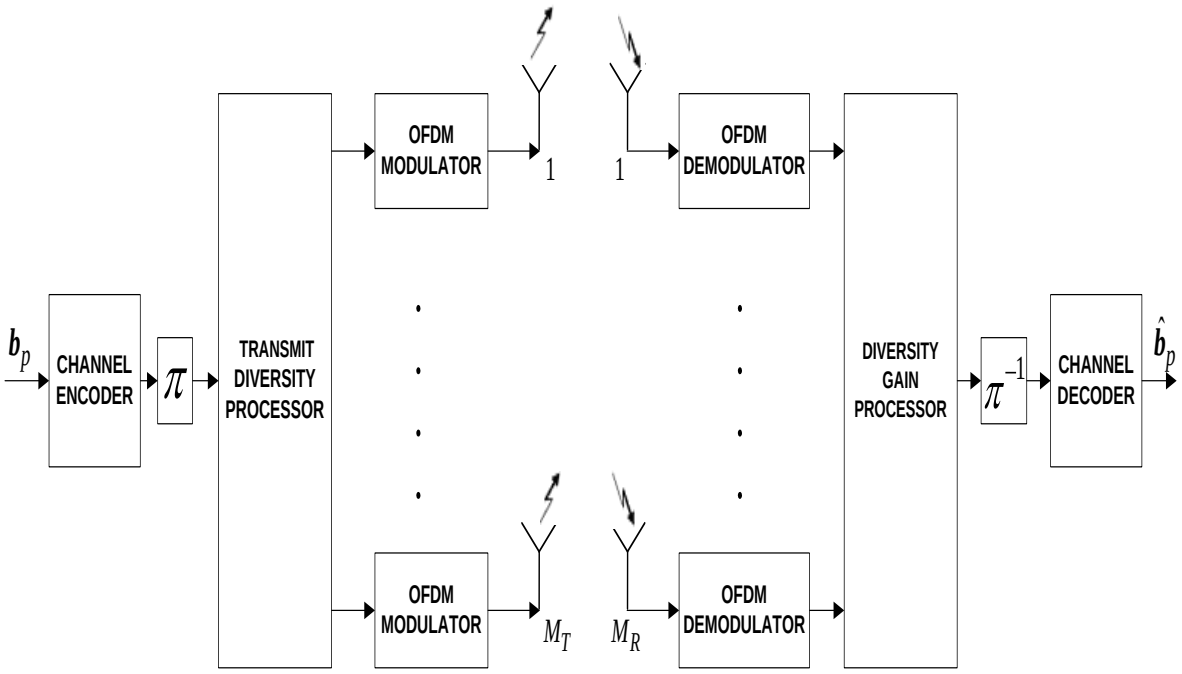

Figure1.4 Schematic diagram of MIMO-OFDM system

Irrespective of the techniques being employed in wireless communication System (such as OFDM, MIMO, or MIMO-OFDM techniques) to combat the effects of the channel on the transmitted signals, the availability of the channel state information (CSI) at the receiver end of the communication system remains a crucial factor for effective functioning of these techniques as well as for the successful recovery of the transmitted signal.

1.4 Research Motivation

The ever increasing growth of wireless communication Systems has continued to drive the research efforts towards obtaining novel techniques by which system capacity can be increased, and at the same time maintaining high-quality of services. This, as earlier mentioned, has brought about the migration from single antenna, single input single output (SISO) Systems to deployments of multiple antennas at both ends of the wireless communication Systems. Emerging from this migration is the multiple-input multiple-output (MIMO) Systems. From the spectral efficiency angle of wireless communication is the emergence of orthogonal frequency division

multiplexing (OFDM) which finds deployment in both single antenna and multiple antenna wireless communication Systems. The concepts of MIMO and OFDM were combined with the emerging intent of exploiting the advantages of both techniques. This combination has given the development to MIMO-OFDM wireless communication Systems with the expectation of having spectrally efficient, high data rate system that is robust to frequency selective fading channels.

With the area of applications of the MIMO-OFDM system expanding very fast, the requirement for an improved functioning of the Systems is becoming very high. As a result, more research efforts are being directed towards achieving better MIMO-OFDM Systems performance. However, one of the major challenges to either single antenna, SISO OFDM, or MIMO-OFDM communication Systems is means of providing accurate channel state information (CSI) at the receiver end of the Systems for coherent detection of the transmitted signal. If the CSI is not available at the receiver, the transmitted signal could only be demodulated and detected through a non-coherent method such as the differential demodulation technique. However, the employment of non-coherent detection method is at the expense of about 3-4 dB loss in signal-to-noise ratio (SNR) compared with using the coherent detection method [31]. In order to eliminate such a huge loss, it is imperative to develop an efficient and cost effective technique of providing channel state information at the receiver for coherent detection of the transmitted information in MIMO-OFDM wireless communication Systems.

There are different techniques by which channel state information can be obtained and these are classified as *pilot-assisted (training-based), blind* and *decision-directed* channel estimation methods. In the context of *pilot-assisted* channel estimation scheme, training-data that is known *a priori* at the receiver is transmitted along with the message data from the transmitter. These training data is then used to obtain the samples of CSI at the training data's locations. The CSI at the message data's locations are obtained from CSI at the training data's locations by means of interpolation techniques. The insertion of the training data within the message signal will definitely induce additional overhead and thus reducing the data throughput. In *blind* channel estimation method, no training data sequence is needed; instead the statistical properties of the channel and certain information about the transmitted signal are employed to obtain the CSI. Consequently, there is saving in the bandwidth usage while employing blind channel estimation method in comparison with the *training-based* method. Though the *blind* channel estimation method has its advantage in that it has no overhead loss, unfortunately it can only be applied to slowly time-varying fading channels. This is because it will have to memorize the data record for

a long time. Thus, it can not be applied in fast-varying channel scenarios that are peculiar to mobile wireless communication Systems. Besides, *blind* channel estimation methods also tend to become heavier in terms of computational complexity [74].

Consequently, in this thesis we investigate the *training-based* channel estimation schemes for single antenna system rather than the *blind channel* estimation method. Our investigation leads us to develop a low complexity adaptive algorithm that is robust against both slow and fast fading channel scenarios, in comparison with other algorithms employed in literatures, to implement soft iterative channel estimator for turbo equalizer based receiver for single antenna communications Systems.

In the *decision directed* channel estimation method, all the detected data at the receiver are used for channel estimation. Hence, few numbers of pilots, in comparison with the *pilot- assisted* method, are required to commence the estimation process in the *decision directed* channel estimation method. The gain obtainable with this method in comparison with purely *pilot-assisted* scheme has motivated this research to focus on the decision directed channel estimation method for single antenna OFDM Systems and MIMO-OFDM Systems. In this thesis a faster and low complexity subspace algorithm, in comparison with other algorithms employed by some other authors in literature, is proposed for parametric estimation of the channel impulse response of SISO-OFDM and MIMO-OFDM Systems. Besides, a low complexity adaptive predictor, in comparison with other available ones in literature, is derived for implementation of the adaptive predictor module of the proposed *decision directed* channel estimation method for the SISO OFDM and MIMO-OFDM Systems. In addition, the low complexity adaptive algorithm we proposed for channel estimator in single antenna communication Systems is also proposed for use to implement the temporary channel transfer function estimator module of the proposed *decision directed* channel estimation method for the SISO-OFDM and MIMO-OFDM Systems.

In addition, iterative technique that is based on turbo principle is employed for the channel estimation schemes proposed in this thesis for the single antenna Systems and MIMO-OFDM wireless communication Systems.

1.5 Scope of the Thesis and Assumptions

The main objectives of this thesis include:

i. Identification of the limitations associated with some existing channel estimation techniques for both single and multiple antenna Communication Systems.

ii. Deployment of OFDM transmission scheme to address the problem of ISI in both SISO and MIMO wireless Communication System.

iii. Designing effective channel estimation models for SISO-OFDM and MIMO-OFDM wireless Communication Systems.

iv. Deriving and proposing effective and less complex adaptive algorithms for implementation of the channel estimation for Turbo equalizer based SISO receiver.

v. Employment of fast subspace algorithm for implementation of CIR estimator for both SISO-OFDM and MIMO-OFDM wireless Communication Systems.

vi. Deriving an effective and less complex adaptive predictor for prediction of time varying channel for SISO-OFDM and MIMO-OFDM wireless Communication Systems.

Equalizer techniques for both SISO and MIMO Systems, channel coding techniques and channel decoding schemes are not addressed in this thesis. Existing techniques and schemes found in literature are employed throughout the Thesis. Furthermore, the problems of frequency and time synchronization are not addressed in the thesis, rather it is assumed, through out the Thesis, that both the transmitter and receiver of the Communication Systems are perfectly synchronized both in time and frequency. Lastly, in all the simulation presented in this Thesis, single user rather than multiple users is assumed.

1.6 Organization of the Thesis

This thesis is divided into seven chapters including this general introduction. The rest of the thesis is organized as follows:

In Chapter 2, channel impulse response models employed in this thesis are presented. In addition, some channel estimation techniques presented in literature are reviewed for both single antenna Systems as well as for MIMO-OFDM Systems.

Soft iterative channel estimation for Turbo equalizer proposed for estimation of time-varying frequency selective channels of single antennal Systems is presented in Chapter 3.

In Chapter 4, Decision Directed channel estimation employing a robust subspace tracking algorithm and efficient and less complex adaptive predictor is proposed for SISO-OFDM Systems.

In Chapter 5, iterative technique based on turbo principle is proposed for the Decision Directed Channel Estimation employed for SISO-OFDM Systems of Chapter 4.

Iterative channel estimation technique for SISO-OFDM Systems of Chapter 5 is extended to MIMO-OFDM Systems in Chapter 6. Channel transfer function estimator presented in Chapter 3 for single antenna Systems is also adapted and re-derived in the context of MIMO channel for the implementation of the channel transfer function (CTF) estimator of the proposed channel estimation schemes for MIMO-OFDM system.

Finally, Chapter 7 concludes the thesis and summarizes the various results of this research work. This chapter is concluded by suggesting some open research problems for future work in the area of MIMO-OFDM wireless communication Systems.

1.7 Original Contributions

The main contributions of this thesis are the development of channel estimation algorithms for single antenna Systems, single input single output OFDM (SISO-OFDM) Systems, and multiple input multiple output OFDM (MIMO-OFDM) Systems:

i. We developed low complexity adaptive algorithms (VSSNLMS and M-VSSNLMS algorithms) that are robust against both slow and fast fading channel scenarios, in comparison with other algorithms employed in literatures, to implement the proposed soft iterative channel estimator for turbo equalizer base receiver for single antenna communications Systems.

ii. A faster and low complexity subspace algorithm in comparison with other employed in literatures is proposed for parametric estimation of the channel impulse response

of the proposed *decision directed* channel estimation method for the SISO-OFDM and MIMO-OFDM Systems.

iii. We also developed a low complexity adaptive predictor, in comparison with other available ones in literature, for implementation of the adaptive predictor module of the proposed *decision directed* channel estimation method proposed for the SISO-OFDM and MIMO-OFDM Systems.

iv. Lastly, the low complexity adaptive algorithm we proposed for channel estimation in single antenna communication Systems is also proposed for use and re-derived in the context of MIMO channel for implementation of the temporary channel transfer function estimator of the *decision directed* channel estimation method put forward for the MIMO-OFDM Systems.

All these algorithms that we proposed for the implementation of channel estimator for single antenna Systems, SISO-OFDM Systems and MIMO-OFDM Systems are confirmed to provide near optimal performance with low complexity in comparison with some other ones in literature through computer simulations. These contributions are detailed in four chapters of this thesis as summarized below.

In Chapter 3, computationally efficient iterative channel estimation for Turbo equalizer-based communication receiver employing Variable Step Size Normalized Least Mean Square (VSSNLMS) algorithm [17] and Multiple-Variable Step Size Normalized Least Mean Square (M-VSSNLMS) algorithm are proposed for single antenna wireless communication Systems. The VSSNLMS and M-VSSNLMS algorithms employed for the implementation of the iterative channel estimation is proposed in order to address the problem of slow convergence rate associated with the Least Mean Square (LMS)-based channel estimation algorithm proposed in literature for single antenna communication system. It is also our intention to put forward a less complex algorithm compared with the well known Recursive Least Square (RLS) algorithm.

In Chapter 4, Fast Data projection Method (FDPM) subspace tracking algorithm-based Channel Impulse Response Estimator is proposed for implementation of the Decision Directed Channel Estimation (DDCE) scheme for SISO-OFDM Systems. This is carried out in the context of a more realistic Fractionally Spaced-Channel Impulse Response (FS-CIR) channel model, as against the channel characterized by a Sample Spaced- Channel Impulse Response (SS)-CIR**.** In this chapter, we also derive a fast convergence Variable Step Size Normalized Least Square-

based predictor, with low computational complexity in comparison with other in literature, for the implementation of the CIR predictor module of the DDCE scheme.

In Chapter 5, we designed a novel iterative receiver structure for the FDPM-based Decision Directed Channel Estimation scheme for SISO-OFDM system. The iterative design is based on Turbo iterative principle. It is shown that a significant improvement in the performance can be achieved with the iterative DDCE scheme for OFDM Systems in comparison with the non-iterative scheme presented in Chapter 4.

In Chapter 6, Iterative receiver structure for FDPM-based DDCE scheme of Chapter 5 is extended to MIMO-OFDM Systems. In addition, Variable step size Normalized Least Mean Square (VSSNLMS)-based channel transfer function estimator is derived in the context of MIMO Channel, following the idea presented in Chapter 3, for the implementation of the CTF estimator module of the iterative Decision Directed Channel Estimation scheme for MIMO-OFDM Systems.

1.8 Publications

During this research work, the following conference and journal papers have been published.

1.8.1 Journal Papers

1. Olutayo O. Oyerinde and Stanley H. Mneney, "Improved Soft Iterative Channel Estimation for Turbo Equalization of Time Varying Frequency Selective Channels," *Wireless Personal Communication Journal*, vol. 52, no.2, pp. 325-340, ISSN: 0929-6212, January 2010.

2. Olutayo O. Oyerinde and Stanley H. Mneney, "Variable Step Size Algorithms for Network Echo Cancellation," *Ubiquitous Computing and Communication (UBICC) Journal*, vol. 4, no. 3, pp. 746-757, *ISSN:* 1992-8424, August 2009.

1.8.2 Conference Papers

1. Olutayo O. Oyerinde and Stanley H. Mneney, "Iterative Decision Directed Channel Estimation for BICM-based MIMO-OFDM Systems," in *Proceedings IEEE International Conference on Communications*, South Africa, 5 pages, 23rd - 27th May 2010.

2. Olutayo O. Oyerinde and Stanley H. Mneney, "FDPM Aided Decisison Directed Channel Estimation with VSSNLMS-based Predictor for OFDM Systems," in *Proceedings IEEE International Symposium on Broadband Multimedia System and Broadcasting*, Shanghai, China, 6 pages, 24th -26th March 2010.

3. Olutayo O. Oyerinde and Stanley H. Mneney, "Iterative OFDM Receiver with Decision Directed Channel Estimation," *in Proceedings of IEEE AFRICON 2009*, Nairobi, Kenya, 6 pages, 23rd -25th September 2009.

4. Olutayo O. Oyerinde and Stanley H. Mneney, "Adaptive CIR Prediction of Time-Varying Channels for OFDM System," *in Proceedings of IEEE AFRICON 2009*, Nairobi, Kenya, 5 pages, 23rd -25th September 2009.

5. Olutayo O. Oyerinde and Stanley H. Mneney, "Decision Directed Channel Estimation for OFDM Systems employing Fast Data Projection Method Algorithm," *in Proceedings of IEEE International Conference on Communication (ICC)*, Dresden, Germany, 5 pages. 14th -18th June 2009.

6. Olutayo O. Oyerinde and Stanley H. Mneney, "Soft Iterative Decision Directed Channel Estimation for OFDM Systems employing Adaptive Predictor," *in Proceedings of IEEE 1st International Conference on Wireless Communication Society, Vehicular Technology, Information Theory and Aerospace & Electronics Systems Technology (Wireless VITAE'09),* Aalborg, Denmark, pp.857-861, 17th - 20th May 2009.

7. Olutayo O. Oyerinde and Stanley H. Mneney, "Soft Input Iterative Channel Estimation for Turbo Equalization over Time Varying Frequency Selective fading Channel," *in Proceedings of South Africa Telecommunication Networks and Applications Conference (SATNAC)* 2008, Wild Coast Sun, Eastern Cape Coast, South Africa, pp. 77-82, 7th-10th September, 2008.

8. Olutayo O. Oyerinde and S. H. Mneney, "Single and Multiple - Variable Step Size Normalized Least Mean Square Algorithms for Network Echo Cancellation," *in Proceedings of the 5th International Conference on Cybernetics and Information Technologies, Systems and Applications: CISTA 2008, in the context of International Multi-Conference on Engineering and Technological Innovation: IMETI 2008*, pp 1-5, Orlando, Florida, USA, 29th June - 2nd July, 2008.

CHAPTER 2

CHANNEL MODELS AND OVERVIEW OF CHANNEL ESTIMATION TECHNIQUES

2.1 Introduction

In this chapter, channel impulse response (CIR) models for both Single Input Single Output (SISO) and Multiple Input Multiple Output (MIMO) Systems, which are employed in the subsequent chapters, are presented. These include the Symbol (Sample)-Spaced Channel Impulse Response (SS-CIR) and the Fractionally-Spaced Channel Impulse Response (FS-CIR) models. It is shown in this chapter how FS-CIR model is more fit into realistic channel conditions than its SS-CIR model's counterpart. The review of channel estimation techniques for single antenna, SISO-OFDM and MIMO-OFDM Systems is also presented in this chapter. These techniques include *pilot-assisted (training-based) channel estimation* methods, *blind and semi-blind channel estimation* schemes, and decision *directed channel estimation* techniques. The chapter emphasizes the advantages of the decision directed channel estimation techniques over the other two channel estimation schemes.

The rest of the chapter is organized as follows. Classification of multipath channel impulse response models are briefly described in Section 2.2. SISO Channel model is presented in Section 2.3, while Section 2.4 described MIMO channel model. In Section 2.5 channel estimation techniques are reviewed, and Section 2.6 gives the summary of the chapter.

2.2 Multipath Channel Impulse Response Models

Channel model, according to [32], *is the bread and butter for telecommunication engineers*. This is because the foundation on which mobile communication Systems is developed is the channel

model. A number of different models have been proposed for the simulation of Rayleigh fading channels (both flat and frequency selective fading channels) in the past years. The classification of these models can be divided into two categories: the statistical and deterministic models. In the statistical models, the power spectral densities of white Gaussian random processes are shaped by either time-domain or frequency-domain filtering [33-36], whereas the Gaussian processes are approximated by the superposition of finite properly selected sinusoids in the deterministic models [37-41]. Details of the rigorous derivation of these models could be found in the cited references.

In the subsequent sections, channel impulse response models employed in this thesis for both single antenna and multiple antenna Systems are presented. The impulse response of a channel is essential for the characterization of the channel. It contains all the information necessary to simulate and analyze any type of transmitted signal in the channel. By way of definition, the channel impulse response (CIR) can be defined as the instantaneous state of the dispersive channel encountered. It corresponds to the vector of the instantaneous amplitudes that is associated with different multipath components.

2.3 Single Input Single Output (SISO) Channel Model

Let the transmitted signal $s(t)$ in a Single Input Single Output (SISO) wireless communication link characterized by multipath fading as shown in Figure 2.1 be given as

$$s(t) = \mathrm{Re}\ \ x(t)e^{j\omega_c t}\ , \tag{2.1}$$

where the complex signal $x(t)$ is the equivalent baseband form of $s(t)$, $w_c = 2\pi f_c$ is a carrier/center frequency, and Re{} denotes the real part. The received signal $r(t)$ can be written as

$$\begin{aligned} r(t) &= \sum_{m=0}^{M-1} \gamma_m(t) s(t-\tau_m(t)) \\ &= \mathrm{Re}\left\{ \sum_{m=0}^{M-1} \gamma_m(t) e^{-jw_c\tau_m(t)} x(t-\tau_m(t)) e^{jw_c t} \right\}, \end{aligned} \tag{2.2}$$

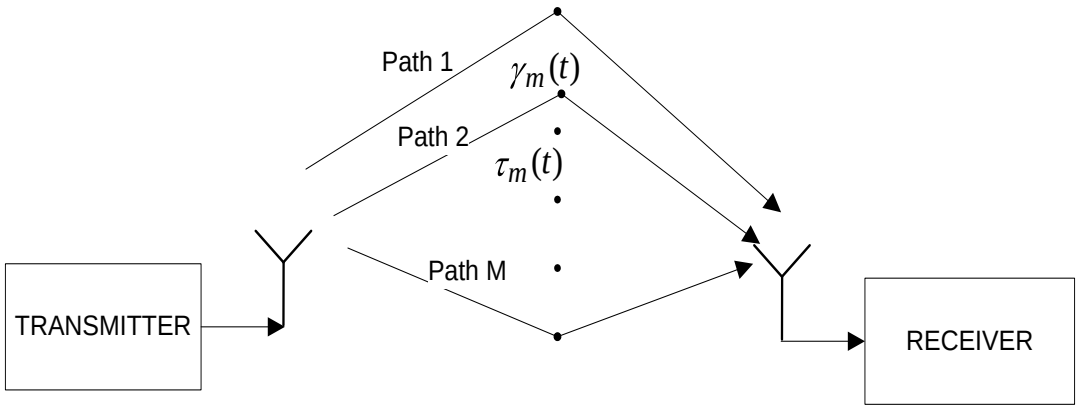

Figure 2.1 Single Input Single Output (SISO) multipath fading channel

where $\gamma_m(t)$, $\tau_m(t)$ and M are the time-variant complex amplitude, the time-variant delay associated with the *m*th path, and the number of paths, respectively. Assuming that the received signal is corrupted by additive bandlimited Gaussian noise that has effective bandwidth of $B(Hz)$ and a power spectral density of N_0 (W/Hz), the equivalent baseband noise signal $w(t)$ will be circularly symmetric complex Gaussian noise (i.e. the real and imaginary parts of the noise are independent Gaussian variables with zero means and equal variance) and has a variance given as

$$\sigma_w^2 = N_0 B = E\ w(t)w^*(t)\ . \tag{2.3}$$

The equivalent baseband form of the received signal $r(t)$, corrupted with complex additive white Gaussian noise $w(t)$, is then given as

$$z(t) = \sum_{m=0}^{M-1} \gamma_m(t) e^{-jw_c\tau_m(t)} x(t-\tau_m(t)) + w(t)$$

$$= \int_{-\infty}^{\infty} h(t,\tau)x(t-\tau)d\tau + w(t)\ \text{[47]}, \tag{2.4}$$

for all possible delays $\tau \in -\infty, +\infty$, where $h(t,\tau)$ is the equivalent baseband impulse response of the multipath fading channel at time instant *t*. The channel impulse response $h(t,\tau)$ corresponds to the model usually used for mobile wireless channels and is given by

$$h(t,\tau) = \sum_{m=0}^{M-1} \gamma_m(t) e^{-jw_c\tau_m(t)} \delta(\tau - \tau_m(t)), \tag{2.5}$$

where δ is the Dirac's Delta function.

The corresponding continuous Channel Transfer Function (CTF) is obtained by taking the Fourier transform of $h(t,\tau)$ with respect to τ as [47]:

$$H\ t,f\ = \int_{-\infty}^{\infty} h(t,\tau)e^{-j2\pi f\tau}d\tau$$

$$= \sum_{m=0}^{M-1} \gamma_m(t)e^{-j2\pi\ f+f_c\ \tau_m(t)}\ . \qquad (2.6)$$

In a bid to make the mobile channel model mathematically tractable, wide sense stationarity assumption is usually made for the channel. A channel is said to be wide sense stationary if the second order statistics of $h(t,\tau)$ not vary with *t*. If this assumption is made, we have the usual linear time-invariant channel and the Channel impulse response in (2.5) can then be reduced to [48]:

$$h(\tau) = \sum_{m=0}^{M-1} \gamma_m e^{-jw_c\tau_m}\delta(\tau-\tau_m) \qquad (2.7)$$

2.3.1 Channel Impulse Response Statistics

In some of the proposed models for wireless mobile channels, each of the CIR component γ_m associated with an individual channel path is always modeled by a Wide Sense Stationary (WSS) narrow-band complex Gaussian process [42]. For this type of WSS modeled channel, the time-domain correlation function that characterizes the CIR component γ_m associated with an individual channel path delay τ_1 and the one associated with path delay τ_2 is characterized by [42]:

$$r_\gamma\ \Delta t,\tau_1,\tau_2\ = E\ \gamma_{\tau_1}\ t\ \gamma_{\tau_2}^{*}\ t-\Delta t\ \ . \qquad (2.8)$$

Furthermore, if the assumption of Uncorrelated Scattering (US) is applied to (2.8) which implies that the amplitude and phase shifts associated with different CIR delay of $\tau_1 \neq \tau_2$, then the time-domain correlation function reduces to

$$r_\gamma\ \Delta t,\tau_1,\tau_2\ = r_\gamma\ \Delta t,\tau_1\ \ \delta\ \tau_1-\tau_2\ \ . \qquad (2.9)$$

By setting $\Delta t = 0$, the function $r_\gamma\ \Delta t,\tau_1$ reduces to $r_\gamma\ 0,\tau_1 \equiv r_\gamma\ \tau$, where $\tau=\tau_1$. This reduced form is known as the multipath intensity profile or delay power spectrum (Power Delay Profile) of the Channel, and it describes the channel's average power output as a function of the time delay τ . The channel's Power Delay Profile (PDP) is useful in determining the channel impulse response's (CIR) statistical distribution. For a time-varying multipath fading channel, the power delay profile is obtained from the magnitude square of (2.5) and it is given as [8, 9]

$$p(t,\tau)=\left|h(t,\tau)\right|^2 . \tag{2.10}$$

Examples of different commonly used power delay profile for COST 207 (*European Cooperation in the Fields of Scientific and Technical Research*) channel models are listed in Table 2.1 [43, 44]. Its corresponding tapped delay line implementation is described in Table 2.2 [43, 47].

2.3.2 Discrete-Time Channel Model

Let the pulse train transmitted symbol $x(t)$, with symbol rate T_s, that passed through a transmitter filter $g_{Tr}(\tau)$ (typically a root raised cosine Nyquist filter) and a time varying channel impulse response $h(t,\tau)$, and corrupted with Gaussian white noise $w(t)$ be represented by

$$x(t)=\sum_{n=-\infty}^{\infty} x_n \delta\ t-nT_s\ . \tag{2.11}$$

At the receiver, the continuous-time received signal $z(t)$ after passing through the receiver filter $g_{Rc}(\tau)$, before sampling is

$$\begin{aligned} z(t) &= h_e(t,\tau) * x(t) + w(t) \\ &= \int_{-\infty}^{\infty} h_e(t,\tau) x(t-\tau) d\tau + w(t), \end{aligned} \tag{2.12}$$

Table 2.1 Power delay profile of COST 207 [44]

Profile	Power delay Profile (PDP), (delay τ is in μs)
Rural Area (RA)	$\begin{cases} 9.21\exp(-9.2\tau) & 0 \le \tau < 0.7 \\ 0 & else \end{cases}$
Typical Urban (TU)	$\begin{cases} \exp(-\tau) & 0 \le \tau < 7 \\ 0 & else \end{cases}$
Bad Urban (BU)	$\begin{cases} 0.67\exp(-\tau) & 0 \le \tau < 5 \\ 0.335\exp(5-\tau) & 5 \le \tau < 10 \\ 0 & else \end{cases}$
Hilly Terrain (HT)	$\begin{cases} 3.08\exp(-3.5\tau) & 0 \le \tau < 2 \\ 0.1232\exp(15-\tau) & 15 \le \tau < 20 \\ 0 & else \end{cases}$

Table 2.2 Tapped Delay Line Implementation of COST 207 Channel Models [47]

Tap No.	Delay (μs)	Power (dB)	Doppler Spectrum
Rural Area			
1	0	0	Ricean
2	0.2	-2	Classical(Jakes)
3	0.4	-10	Classical(Jakes)
4	0.6	-20	Classical(Jakes)
Typical Urban (TU)			
1	0	-3	Classical(Jakes)
2	0.2	0	Classical(Jakes)
3	0.6	-2	Gaussian
4	1.6	-6	Gaussian
5	2.4	-8	Gaussian
6	5.0	-10	Gaussian
Bad Urban (BU)			
1	0	-3	Classical(Jakes)
2	0.4	0	Classical(Jakes)
3	1.0	-3	Gaussian
4	1.6	-5	Gaussian
5	5.0	-2	Gaussian
6	6.6	-4	Gaussian
Hilly Terrain (HT)			
1	0	0	Classical(Jakes)
2	0.2	-2	Classical(Jakes)
3	0.4	-4	Classical(Jakes)
4	0.6	-7	Classical(Jakes)
5	15.0	-6	Gaussian
6	17.2	-12	Gaussian

where $*$ denotes the convolution product, and $h_e(t,\tau)$ is the time-varying equivalent channel impulse response obtained as

$$h_e(t,\tau) = h(t,\tau) * g_T(\tau)$$

$$= \int_{-\infty}^{\infty} h(t,\tau) g_T(\tau - \alpha) d\alpha \ . \tag{2.13}$$

In (2.13), $g_T(\tau)$ is the convolution product between $g_{Rc}(\tau)$ and $g_{Tr}(\tau)$ given as

$$g_T(\tau) = g_{Rc}(\tau) * g_{Tr}(\tau) . \tag{2.14}$$

Because of the presence of the radio filters $g_{Rc}(\tau)$ and $g_{Tr}(\tau)$, the condition of the Uncorrelated Scattering (US) is violated. Consequently the time-varying equivalent channel impulse response $h_e(t,\tau)$ is no longer Wide Sense Stationary (WSS). Besides, the noise $w(t)$ in (2.12) is not white again by reason of $g_{Rc}(\tau)$ at the receiver. By making substitution for $x(t)$ and $h_e(t,\tau)$ in (2.12) from (2.11) and (2.13) respectively, the received baseband signal is given by

$$z(t) = \sum_{i=-\infty}^{\infty} x_i \int_{-\infty}^{\infty} h(t,\tau) g_T(t - iT_s - \tau) d\tau + w(t) . \tag{2.15}$$

2.3.2.1 Symbol-Spaced Channel Impulse Response Model

If the continuous-time received signal $z(t)$ of (2.15) is sampled at a rate of $1/T_r = 1/T_s$, the equivalent discrete-time representation given as

$$z\ n = z(nT_r) , \tag{2.16}$$

can be obtained by substituting (2.16) into (2.15) to give [45]

$$z\ n = z(t)|_{t=nTr} = \sum_{i=-\infty}^{\infty} x[i] \int_{-\infty}^{\infty} h\ nT_r, \tau\ \ g_T(nT_r - iT_s - \tau) d\tau + w(nT_r) . \tag{2.17}$$

By substituting $m = n - i$, (2.17) becomes (using square bracket instead of subscript)

$$z\ n = \sum_{m=-\infty}^{\infty} x\ n-m \int_{-\infty}^{\infty} h\left[nT_s, \tau\right] g_T(mT_s - \tau) d\tau + w\ n \ , \tag{2.18}$$

where T_s is the sampling period.

The symbol-spaced discrete-time channel impulse response (SS-CIR) model is then given by

$$h\ n,m = \int_{-\infty}^{\infty} h\left[nT_s, \tau\right] g_T(mT_s - \tau) d\tau , \tag{2.19}$$

hence,

$$z\ n = \sum_{m=-\infty}^{\infty} h\ n,m\ x\ n-m\ + w[n], \tag{2.20}$$

where

$$w\ n = \int_{-\infty}^{\infty} g_{Rc}\ \tau\ w(nT_s - \tau)d\tau\ . \tag{2.21}$$

If $h\ n,m = 0$ for all $m < 0$ and $m \geq M$, where M is the length of the equivalent CIR measured in symbol intervals, and the discrete-time channel impulse response is written in a vector form as

$$\boldsymbol{h}\ n = \left[h\ n,0\ , h\ n,1\ , ..., h\ n,M-1\ \right]^T, \tag{2.22}$$

the discrete-time received signal $z\ n$ of (2.18) can then take the form

$$\begin{aligned} z\ n &= \sum_{m=0}^{M-1} h\ n,m\ x\ n-m\ + w[n] \\ &= \boldsymbol{h}^T\ n\ \boldsymbol{x}\ n\ + w[n]. \end{aligned} \tag{2.23}$$

In the case where the transmitter and receiver's filters are ignored, the symbol-spaced CIR of (2.19) will be given as

$$h\ n,m = h\ nT_s, mT_s\ , \tag{2.24}$$

where $0 \leq m \leq M-1$.

2.3.2.2 Fractionally-Spaced Channel Impulse Response Model

The symbol-spaced CIR model presented in Section 2.3.2.1 is not feasible in the real-time implementation. This is because, for the model to hold, the receiver's filter $g_{Rc}\ \tau$ must be implemented as a "channel matched filter" in order to match the convolution of the transmitter's filter $g_{Tr}\ \tau$ and the time varying channel impulse response $h(t,\tau)$. This in turn will make the received samples $z\ n$ sufficient statistics for adequate recovery of the transmitted samples. However, in reality, the receiver's filter $g_{Rc}\ \tau$ cannot be implemented as a channel matched filter due to the fact that the CIR will be time-varying and might not be known *a priori*, which makes symbol-spaced CIR model not fit into the real-time channel condition. A way out of this is to adopt the realistic fractionally-spaced channel impulse response (FS-CIR) model presented in this section. In such a realistic channel scenario, the continuous-time received signal $z(t)$ of (2.15) is sampled several time (e.g $R > 1$) per symbol period such that $T < T_s$. Hence, there will be R values of z_i at each symbol period n.

Suppose the received signal $z(t)$ of (2.15) is sampled at the rate of R times the sampling rate such that $T_r = T_s / R$, using a time series representation (TSR) of [46] the received sampled $z_i\ n$ can be given by

$$z_i\ n = \sum_{m=-\infty}^{\infty} x\ n-m \int_{-\infty}^{\infty} h\ nT_r R+iT, \tau\ \ g_T(mT_r R+iT_r-\tau)d\tau + w_i\ n\ , \tag{2.25}$$

where the fractionally-spaced channel impulse response (FS-CIR), represented as R symbol-spaced time varying impulse response, is given by

$$h_i\ n,m = \int_{-\infty}^{\infty} h\left[nT_s+iT_r,\tau\right] g_T(mT_s+iT_r-\tau)d\tau \qquad i \in 0,1,2,...,R-1\ , \tag{2.26}$$

then

$$z_i\ n = \sum_{m=-\infty}^{\infty} h_i\ n,m\ x\ n-m\ + w_i[n] \qquad\qquad i \in 0,1,2,...,R-1\ , \tag{2.27}$$

and

$$w_i\ n = \int_{-\infty}^{\infty} g_{Rc}\ \ \tau\ \ w(nT_s+iT_r-\tau)d\tau\ . \tag{2.28}$$

Similarly to the SS-CIR case, by assuming that $h_i\ n,m = 0$ for all $m<0$ and $m \geq M$ the FS-CIR can be written in a vector form as

$$\boldsymbol{h}_i\ n = \left[h_i\ n,0\ , h_i\ n,1\ ,...,h_i\ n,M-1\ \right]^T\ . \tag{2.29}$$

Consequently, the received sampled $z_i\ n$ of (2.23) then simplifies to

$$\begin{aligned} z_i\ n &= \sum_{m=0}^{M-1} h_i\ n,m\ x\ n-m\ + w_i[n] \\ &= \boldsymbol{h}_i^T\ n\ \boldsymbol{x}_i\ n\ + w_i[n]\ . \end{aligned} \tag{2.30}$$

From the foregoing, it implies that for each transmitted symbol $x\ n$, R values of z_i observation are obtained from the received signal. These are made possible by passing $x\ n$ through R different time varying filters $\boldsymbol{h}_i\ n$. The result of using $R>1$ different time varying filters in fractionally spaced channel model is that the received samples $z_i\ n$ will be sufficient statistics enough for the recovery of the transmitted samples, even when the receiver's filter $g_{Rc}\ \tau$ is not channel marched filter. This is the reason why fractionally spaced channel model is more fit into realistic channel conditions than its symbol-spaced CIR model counterpart presented in Section 2.3.2.1.

2.4 Multiple Input Multiple Output (MIMO) Channel Model

In the previous section, channel impulse response for Single Input Single Output (SISO) Systems is described. In this section the SISO scenario is extended to the MIMO Systems. Figure 2.2 depicts a MIMO wireless communication system using M_T transmit and M_R receive antennas. The MIMO channel consists of $M_R \times M_T$ propagation links between the transmitter and the receiver ends. Each of these links, in an ideal situation, is made up of a number of statistically independent paths. Thus, it could be said that the MIMO channel consist of M_R by M_T $M_R \times M_T$ Single Input Single Output (SISO) links. Consequently, the channel impulse expression for SISO system in (2.23) can be extended to the case of MIMO system. As a result, M_T signals $x_i\ n$, $1 \le i \le M_T$, constitute the input of the MIMO system at each time instant n. At the receiver end of the system, we have M_R received signals $z_j\ n$, $1 \le j \le M_R$. Each pair i, j of inputs and received signals is connected by a channel impulse response $h_{j,i}\ n,m$ as shown in Figure 2.2. The jth received signal at time instant *n* can now be expressed as [44]

$$z_j\ n = \sum_{i=1}^{M_T} \sum_{m=0}^{M-1} h_{j,i}\ n,m\ x_i\ n-m\ + w_j[n] \ , \tag{2.31}$$

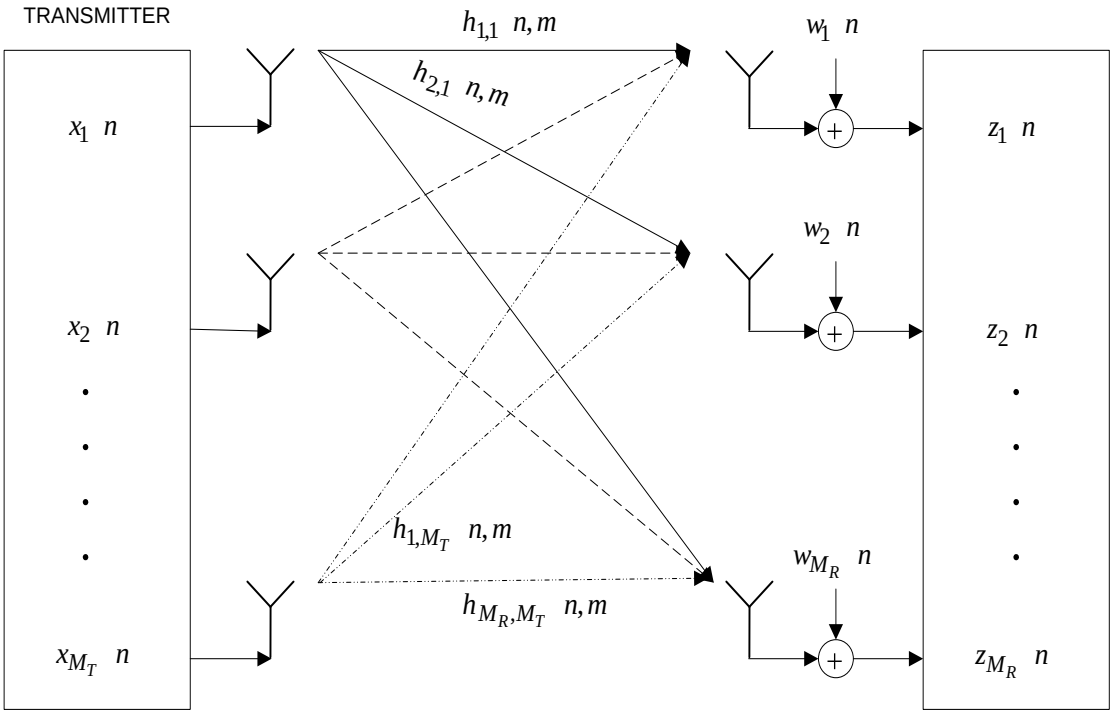

Figure 2.2 MIMO Channel with MT transmit and MR receive antennas

where M, in this case, is the largest number of taps among all the contributing channels.
The above equation, (2.31) can be written in a vector notation as

$$\boldsymbol{z}\ n = \sum_{m=0}^{M-1} \boldsymbol{H}\ n,m\ \boldsymbol{x}\ n-m\ + \boldsymbol{w}[n], \tag{2.32}$$

where $\boldsymbol{H}\ n,m$ is the MIMO channel matrix, and can be expressed as

$$\boldsymbol{H}\ n,m = \begin{bmatrix} h_{11}\ n,m & . & . & . & h_{1M_T}\ n,m \\ . & . & & & . \\ . & & . & & . \\ . & & & . & . \\ h_{M_R1}\ n,m & . & . & . & h_{M_RM_T}\ n,m \end{bmatrix}. \tag{2.33}$$

2.5 Channel Estimation Techniques

In wireless communication Systems, the time-varying nature of the channel as well as its frequency selectivity in a multipath scenario is considered as one of the major challenges. For accurate transmitted signal demodulation, equalization, decoding, and a host of other baseband processing applications, the provision of perfect and up to date channel knowledge is very vital. Consequently, channel estimation remains an important block in the signal processing stages at the receiver of both the existing and the evolving wireless communication Systems.

In the recent years, research efforts have been directed towards producing efficient channel estimation techniques for employment in single antenna based communication Systems, single input single output-assisted OFDM (SISO OFDM) Systems and multiple input multiple output-based OFDM (MIMO-OFDM) Systems. In general, the various techniques for channel estimation that have been put forward, some of which can be used in different technologies of wireless communication Systems (such as WiMAX, LTE, WiFi, etc), can be categorized into three classes. These include [48] the *pilot-assisted (training-based) channel estimation* methods, *blind and semi-blind channel estimation* schemes, and decision *directed channel estimation* techniques. Figure 2.3 shows the three main classification of channel estimation techniques briefly reviewed in this chapter, and how they interlinked with each other.

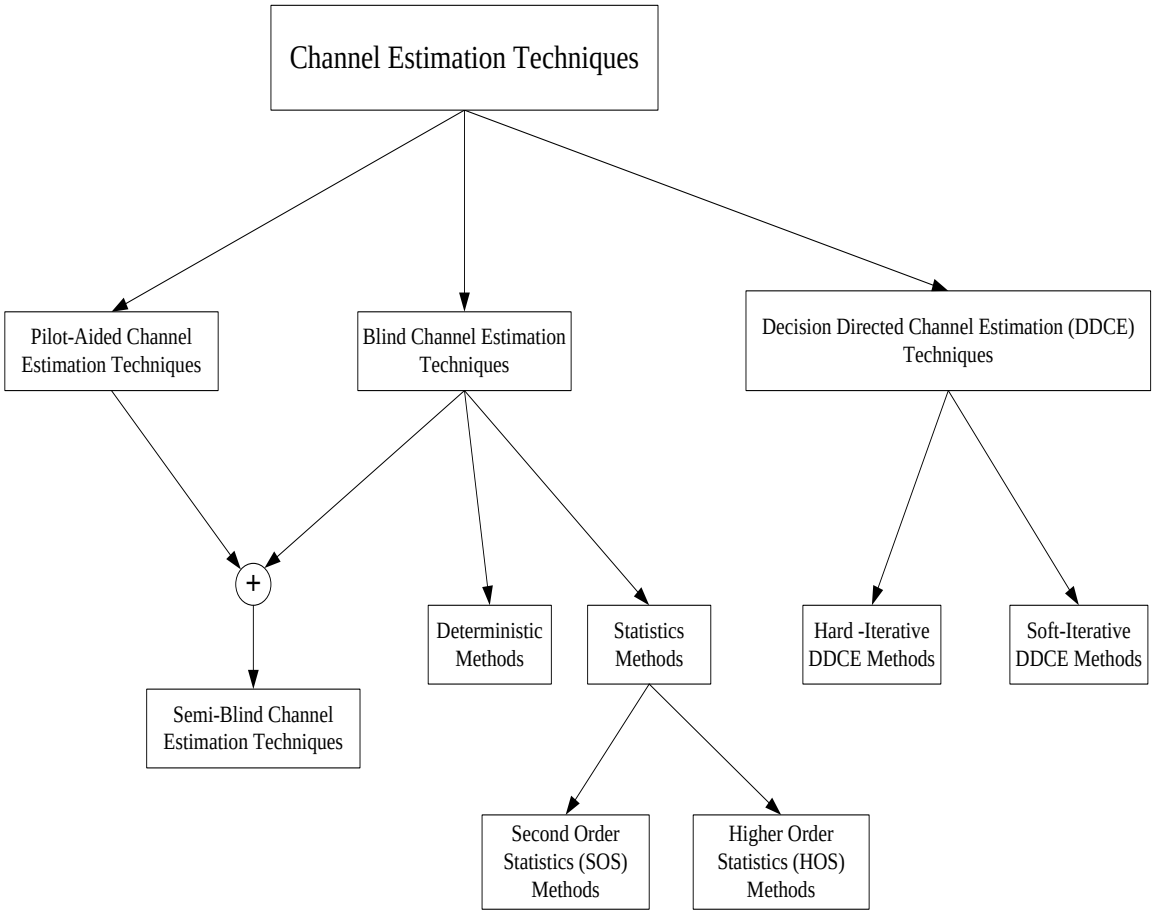

Figure 2.3 Channel Estimation Techniques Classification

2.5.1 Pilot-Assisted Channel Estimation Techniques

Pilot-assisted channel estimation technique, which is also known as training-based channel estimation scheme, is a conventional way of obtaining channel estimate for communication Systems. In this technique, training sequences of data known to the receiver are multiplexed with the transmitted information symbols at a pre-determined position before transmission. These training data are used at the receiver for estimating the channel state information corresponding to their positions. The channel state information corresponding to the information data positions is then obtained by means of interpolating between different channel estimates earlier obtained from the training data sequence.

Quite a number of works have been reported in literature with regards to the pilot-assisted channel estimation techniques. In [49, 51], pilot symbol assisted modulation (PSAM) was proposed as an alternative to the use of a pilot tone earlier in use to mitigate the effects of fading in wireless communication Systems. The various studies of PSAM in [49, 51] were based on simulation and experimental implementation, demonstrating the feasibility of the approach. The performance analysis of the approach is provided in [52]. In [53] superimposed pilot assisted modulation techniques was compared with that of PSAM, and the conclusion arrived at was that the superimposed pilot assisted modulation scheme is 4 dB worse in bit error rate (BER) performance than the PSAM scheme. The two pilot-assisted schemes were considered in the context of slow (quasi-static) fading environment [54], where it was observed that both approaches show the same error performance. It was further shown that a superimposed pilot method achieve better BER performance in fast fading channel in comparison with PSAM but with higher computational complexity than PSAM that employs interpolation method. The exact BER of multilevel quadrature amplitude modulation (M-QAM) in flat fading with imperfect channel estimates is investigated in [55]. In the investigation carried out in [55], the distribution of the amplitude and the estimates of the phase by employing a PSAM technique is used to obtain the exact BER of the M-QAM. An optimal pilot symbols insertion pattern called time division multiplexed training with regular periodic placement is proposed in [56]. The results obtained with the new pattern are compared with that of superimposed training scheme for a time-varying flat fading channel scenario. It is concluded that the proposed scheme performs better at high SNR and for slowly varying channel; however it is found out that the superimposed training scheme exhibits better performance than the proposed scheme in the other regimes. In [57] adaptive PSAM approaches that address both channel estimation and prediction errors in adaptive modulation in order to meet a target BER are proposed. In the proposed scheme, the authors optimized the spacing between pilot and data symbols and the power allocation between pilot and data symbols in order to maximize spectral efficiency. In their results the authors claimed that the adaptive PSAM scheme work well even when the feedback delay is relatively large.

With respect to the single antenna-assisted multi-carrier modulation (OFDM) Systems, different contributions to training-based channel estimation technique have been published in literature. The early publications on training symbols-based channel estimation for OFDM system only considered periodic one-dimensional (1D) pilot patterns that span the frequency direction only. However, in some recent publications the theory of two-dimensional (2D) pilot pattern that is made to span both the time and frequency directions is exploited [48]. Some of these publications

include the 2D-finite impulse response (FIR) and cascaded 1D-FIR Wiener filtering based channel estimation schemes of [58, 59, 60]. Channel estimator based on piecewise-constant and piecewise-linear interpolations between pilots is proposed for OFDM Systems in [61], with the drawback that it needs a large number of pilots to get satisfactory performance which of course is costly in terms of bandwidth requirement. Maximum likelihood estimator for OFDM system is studied in [62], while Channel interpolation was performed by the two-dimensional interpolation between pilots in [63], though the approach is robust to Doppler frequency shifts, it however exhibits performance degradation with lower Doppler frequencies. A time domain channel estimation approach, the frequency Pilot Time Average (FPTA), wherein intra-symbol time-domain averaging of identical parts of the pilot signal applied for estimation purpose is investigated in [64]. Two types of pilot-aided channel estimation schemes, namely the Maximum likelihood estimator and the Bayesian minimum mean squared error estimator (MMSEE), are compared in [65]. It is established that the former is simpler to implement since it requires no information about the channel statistics, while at low SNR MMSEE is confirmed to exhibit better performance because it exploit *prior* information about the channel. However at intermediate and high SNRs the two schemes are found to have similar performance. In [66] windowed Discrete Fourier Transform (DFT)-based MMSE channel estimator is proposed for OFDM system, and in [67] pilot-assisted channel estimation method based on nonlinear regression channel models is proposed for OFDM signals in Rayleigh fading channel environment. In the context of MIMO Systems, different contributions have been published with regards to the pilot-assisted channel estimation techniques of which some of them could be found in [68, 69].

In addition, different pilot patterns have been proposed for the implementation of the pilot-assisted channel estimation techniques for both single antenna and multiple antenna Systems. Optimal training for single antenna-aided OFDM with respect to the Mean Square Error (MSE) of the Least Square (LS) channel estimate as well as the MSE at the output of a zero-forcing receiver employing LS channel estimate is studied in [70]. However, in [71] optimal training for single input single output OFDM (SISO-OFDM) Systems with respect to the capacity based on Linear Minimum Mean Square Error (LMMSE) channel estimate is proposed. Channel estimation techniques based on pilot arrangement in OFDM system are studied in [72], while optimal training and pilot design for OFDM Systems operating over Rayleigh fading channel is investigated in [73]. In [74, 75, 76, 77] optimal training designs for MIMO OFDM Systems are presented.

In general, irrespective of the various improvement that have been brought upon the use of the pilot-assisted channel estimation technique by different research investigations, the fact that the technique brings about wastage in the scarce communication bandwidth still remains a major setback in its deployment for channel estimation. Another drawback of the pilot scheme is that they make channel estimate to depend on the pilot symbols alone, and the interpolation techniques that is applied to estimate for data points, as expected, can never be hundred percent perfect, hence there would be unresolved error introduced into the estimation process.

2.5.2 Blind and Semi-blind Channel Estimation Techniques

Consequent upon the wastage of bandwidth that is peculiar to the usage of pilot-assisted channel estimation technique presented in the previous section, blind channel estimation techniques have been investigated. In the blind channel estimation techniques, the use of pilot (training) symbols that consume valuable channel capacity is avoided, but instead the channel is estimated by employing inherent information in the received signals as well as the transmitted signals' structural properties. In contrast, the semi-blind channel estimation techniques employ the combination of the training based estimation and blind channel estimation methods. In this technique, information about the known training symbols as well as inherent information in the unknown received signals is used for channel estimation purpose. Existing blind channel estimation techniques can be classified as statistical and deterministic. In the class of statistical method, the cyclic statistic properties of the received signals are explored in estimating the channel, whereas in the deterministic approach the statistic properties of the received signals are not used, instead both the received signals and the channel coefficients are considered to be deterministic quantities [78].

In various works published in [79, 80, 81, 82, 83, 84] the higher-order statistics of the received signals are exploited for channel estimation. Despite the robustness of the idea presented in the cited references, in some cases, large number of data samples is required which results in complexity in the computation process. These problems are reduced by exploring second-order cyclic statistics of the over-sampled channel output in [85, 86, 87, 88]. Algorithms using second-order statistics for blind channel estimation are compared based on the Asymptotic Normalized Mean Square Error (ANMSE) of channel estimates in [89], while in [90] hidden Markov model is applied to the issue of blind channel estimation. In [91] *a priori* knowledge of the transmitted data is utilized for blind channel estimation in a fixed wireless sparse multipath channel scenario; and frequency-domain blind channel estimation method is proposed in [92]. The problem of

blindly estimating the finite impulse response (FIR) of single input single output (SISO) channel is considered in [93], by employing second order statistics of transformed data in the channel estimation process. Identifiable conditions for channel estimation are derived in the paper. It is however noted in the paper that some channels are not identifiable. Examples of deterministic channel estimation in single antenna communication Systems can be found in [94, 95, 96].

Examples of statistical blind channel estimation methods for single antenna OFDM Systems include those using correlation techniques [97] and cumulant fitting methods [98, 99]. Redundancy introduced by OFDM cyclic prefix is employed in [100, 101, 102, 103] to develop different blind channel estimation methods, while different subspace blind channel estimation approaches are published in [104, 105, 106, 107, 108, 109]. In [110] finite alphabet approach is employed to implement blind channel estimation for OFDM, whereas the authors in [111] investigate blind channel estimation for IEEE 802.11a based on both finite alphabet approach and clustering of subcarriers. In [112, 113, 114], iterative Bayesian method that swings between channel estimation and symbol detection (and decoding) is proposed for coded OFDM Systems, and deterministic blind channel estimation approach based on maximum likelihood (ML)-principle is applied to OFDM Systems in [115], while in [116] the basic ML-method of [115] is modified for phase shift keying (PSK) signals of OFDM Systems.

Blind channel estimation in MIMO-OFDM Systems is considered in [117], where periodic precoding is applied at the inputs and the channel estimation is carried out based on cyclic correlation of the Systems output. Subspace approach is utilized in [118] for blind channel estimation for MIMO-OFDM Systems. A blind source separation techniques using second order statistic is employed for extracting the inputs in the blind channel estimation algorithm presented in [119], while a symbol-rate blind estimation method that relies on second order statistics is proposed in [120, 121]. Higher order statistic based blind channel estimation methods for MIMO Systems are presented in [122, 123, 124, 125, 126, 127]. A deterministic blind symbol estimation technique is developed in [128] for single input multiple output (SIMO) Systems by exploiting a special data structure of the oversampled channel output. Subspace-based channel estimation approaches are presented in [129], using the projection approximation subspace tracking combined with deflation (PASTd), and in [130] with short averaging periods, exploiting the frequency correlation among adjacent OFDM subcarriers.

Comparing between deterministic and statistical blind channel estimation methods, the deterministic method converges much faster than statistical one. However, the computation complexity of deterministic is very high and even become higher as the constellation order of the modulator employed at the transmitter increases [117]. Statistical approaches too, do suffer from finite data effect when dealing with an extremely short sample sequence [128].

Because the blind techniques require no training symbols for the channel estimation, the techniques are attractive in that they utilize the bandwidth efficiently. However, in general, blind channel estimation techniques suffer from others deficiencies. One of these is their requirement of a long data record which result in slow convergence rate of the methods, and they also tend to become heavier from a computational complexity point of view [74]. Furthermore, the techniques, especially the deterministic and the second order statistic approaches, do leave indeterminacy in the channel. Besides, the methods are very sensitive to channel order over-estimation. Lastly, the blind channel estimation methods do require the channel to be time-invariant, consequently the techniques are always limited to slowly time-varying channels and can not be applied to a fast time-varying channel which is peculiar to mobile wireless communications Systems.

In the class of semi-blind channel estimation techniques belong the algorithms in [131, 132, 133], where superimposed periodic pilot sequences are used to estimate channel coefficients based on the first or second order statistics of the channel. In [134] a semi-blind estimation framework is analyzed in which the standard least-squares estimator, based on a known pilot sequence, is enhanced by using the statistical structure of the observation. Algorithms for semi-blind channel estimation for parallel data and training signal case are developed in [135], however in [136], the identifiability conditions for blind and semi-blind finite impulse response (FIR) multichannel estimation in terms of channel characteristics, length of received data, and excitation modes of input symbol, with number of known symbols for semi-blind estimation are investigated. Semi-blind channel estimation for block precoded space-time OFDM transmissions is presented in [137]. In the case of MIMO system, semi-blind channel estimation is considered for MIMO channel in [138], while an approach that can learn channel coefficient when a small amount of training data area available is proposed in [139] for frequency selective MIMO Systems. An orthogonal pilot-based maximum-likelihood (OPML) semi-blind estimation scheme is proposed in [140, 141, 142]. In this approach, the channel matrix is factored into the product of a whitening matrix and a unitary rotation matrix, the whitening matrix is estimated from the data using a blind

algorithm, while the unitary rotation matrix is estimated exclusively from the training data using the OPLM algorithm. In [143], comparative study of training based and semi-blind MIMO flat-fading channel estimation schemes, when the transmitter employs maximum ratio transmission (MRT), is carried out.

Despite the fact that semi-blind channel estimation techniques (that exploit the statistics of the unknown data, as well as the known pilot signal) are provide better performance than the pilot-based and blind channel estimation techniques separately [135], the techniques are outperformed by the decision directed channel estimation techniques as well as their iterative versions described in the following section. In the case where the same number of pilot symbols employed by the semi-blind techniques are assigned to the iterative (decision directed) channel estimation techniques, the iterative (decision directed) channel estimation techniques will exhibit better performance than the semi-blind techniques and far better than the blind and pilot-assisted channel estimation techniques. This understanding as well as the knowledge of various shortcomings of the approaches described hitherto, informed our drive to focus on the family of decision directed channel estimation techniques in this thesis.

2.5.3 Decision Directed Channel Estimation Techniques

In the Decision Directed Channel Estimation (DDCE) techniques, both the pilot symbols as well as the re-modulated detected message symbols are employed for channel estimation [48]. By this process, the DDCE schemes provide a more reliable channel estimate than its pilot-assisted channel estimation method counterpart. The reason for this is because in the absence of transmission errors, DDCE scheme could be viewed as pilot-assisted channel estimation scheme that is employing approximately hundred percent pilot information symbols for channel estimation in comparison with the purely pilot-assisted scheme with sparse available pilot symbols for the same estimation. By using these techniques, the number of pilot symbols being used for channel estimation could be drastically reduced. The mode of operation of the DDCE techniques is that the initial *a posteriori* channel transfer function (CTF obtained based on the available present received and detected symbols) associated with the current detected symbol is estimated on the basis of the pilot symbols and the re-modulated message symbols. This *a posteriori* CTF is then employed as an *a priori* channel estimate during the demodulation of the next symbols received in the next time slot. In these techniques, very few pilot symbols are required for the purpose of initializing the estimation process.

In [144] van de Beek *etal* employ both training symbols and quantized decision variable in the decision directed channel estimators (Minimum Mean Square Error and Least Square channel estimators) proposed for OFDM Systems. In their methods *a priori* knowledge of noise variance and channel covariance is assumed, the assumption that does not hold in real world scenarios. Edfords *etal* in [145, 146] propose a low-rank approximation to the frequency-domain linear Minimum Mean Squared Error Estimator (MMSEE) making use of singular value decomposition method. The major problem with the approach is that it requires knowledge of the channel frequency correlation, which might not be available, and the operating SNR. In [31] a two-dimensional (2D)-MMSE estimator is proposed for OFDM system which makes full use of the time-and frequency-domain correlations of the frequency response of time varying dispersing fading channel, and also capitalizes on the availability of an infinite number of previous initial *a posteriori* channel estimates associated with past OFDM symbols. This assumption of utilizing an infinite number of initial *a posteriori* channel estimates associated with the past OFDM symbols is quite unrealistic. In [147] the idea in [31, 144] is extended to the case of clustered OFDM system where new transforms, that are independent of the channel delay profile, is used for the proposed channel estimator. However, in [148] the performance of an adaptive OFDM (AOFDM) transceiver that employs decision directed channel estimation and modulation mode adaptation is studied.

A decision directed channel estimation method is proposed in [149] for both OFDM and Multi-Carrier Code Division Multiple Access (MC-CDMA) Systems, where a channel characterized by a Sample Spaced Channel Impulse Response (SS-CIR) is assumed. As it is indicated earlier in section 2.3.2.2, this assumption is not feasible in a realistic channel conditions. Achievable performance of the estimation method proposed in [149] in conjunction with a more realistic Fractionally Spaced Channel Impulse Response (FS-CIR) model described in section 2.3.2.2 is analyzed in [150]. Recently, a subspace algorithm namely the deflated version of the Projection Approximation Subspace Tracking (PASTd) algorithm of [151], and the adaptive Recursive Least Square (RLS) predictor of [152], are deployed to implement the decision directed channel estimation scheme in [153, 154] for OFDM Systems in a realistic fractionally spaced mobile channel scenario. The major drawback with the proposed scheme by the authors in [153, 154] is associated with the algorithms deployed. In the case of the PAST algorithm, it is highlighted in [151] that the deflation technique applied on PAST algorithm to arrive at PASTd version causes a stronger loss of orthonormality between eigenvectors of the transformation matrix utilized in the algorithm. Therefore, if there are some post-processing methods that use the signal subspace

estimate, from which an orthonormal basis of the signal subspace is required, in order to extract the desired signal information, the transformation matrix has to be re-orthonormalized. This of course will result in increase of computational complexity. Another shortcoming mentioned in [151] is the fact that PASTd algorithm exhibits an increase in computational complexity if the number of OFDM subcarriers, K, is much greater than the number of the Fractionally Spaced (FS) channel paths M (i.e. if $K \gg M$). Although the RLS converge faster than its Normalized Least Mean Square (NLMS) counterpart, it is emphasized in [152] that the coefficient update complexity is more costly for RLS-based predictor compared with that for NLMS predictor. This obviously will limit the deployment of RLS-based predictor in a real time implementation. In this thesis, these two drawbacks are addressed in the proposed decision directed channel estimation methods presented in Chapter 4.

In [26] a decision directed channel parameter estimation and optimum training sequences for OFDM with multiple transmit antennas is proposed. The method involves the inversion of a large matrix in order to decouple the inter-antenna interference. A simplified channel estimator is then presented in [155] based on optimum training sequences for OFDM Systems with multiple transmit antenna, in order to reduce the complexity involved in the approach of [26]. However, it is noted in [155] that the substitution made to reduce the computational complexity of the simplified channel estimator proposed may cause some performance degradation. The techniques in [26, 155] is extended to MIMO OFDM Systems in [156] where the estimated channel delay profile of the various independent channels are exploited for channel parameter estimation. Other contribution to the DDCE scheme for MIMO Systems includes the presentation in [157] where the application of the RLS algorithm for adaptation of the CIR-related tap predictors' coefficient in the context of parallel interference cancellation (PIC)-assisted DDCE designed for OFDM Systems employing mulitiple transmit antennas is studied. A subspace-based decision directed channel estimation employing a modified Low Rank Adaptive Filter (*LORAF*) *1* algorithm in [158] is proposed for MIMO-OFDM system in [159]. Unfortunately it is observed from the simulation results presented in [159] that the performance of the proposed subspaced-based channel estimator is worse at low SNR, which is explained as due to the subspace tracking error caused by strong noise. The PIC-assisted DDCE designed for OFDM Systems that support multiple users and employ multiple transmit antennas at base station (BS) is investigated in [160]. Recently, the decision directed channel estimation proposed for single antenna-based OFDM Systems in [150] is extended to MIMO-OFDM Systems in [161] with the modification made to the channel transfer function (CTF) estimator module of the scheme. The CTF estimator module

of the DDCE scheme is made up of the complex RLS algorithm that exploits the probability-related soft information available at the output of the MIMO-OFDM system's detector rather than the decision-based estimates of the transmitted symbols employed in [150] which are prone to decision error and might cause error propagation which will eventually result in substantial performance degradation in the case of MIMO-OFDM Systems.

2.5.3.1 Iterative Decision Directed Channel Estimation Techniques

In the iterative schemes, the channel estimator employs the increasingly refined soft or hard symbol information computed by either the detector/equalizer or the decoder and fed back to the estimator in order to improve the quality of the channel estimates as the number of iteration increases. In the process, the detector/equalizer or the decoder also benefits from the improved channel estimates and then outputs better soft or hard symbol information which in turn is fed back into the channel estimator. Hence the detector/equalizer or the decoder operates in an iterative mode with the channel estimator. If hard symbol information is employed, the channel estimator makes use of the hard decided output of either the detector/equalizer or the decoder. Such channel estimation schemes are then referred to as *hard iterative channel estimation*. On the other hand, if the soft symbol information is utilized, the channel estimator will use the log-likelihood ratios (LLR) on the coded bits calculated by either the detector/equalizer or the decoder for channel estimation. Similarly, such schemes are referred to as *soft iterative channel estimation.*

The iterative method based on expectation-maximization (EM) algorithm is presented in [162] for joint channel parameter estimation and symbol detection. With EM algorithm, the quality of the channel estimate is not guaranteed throughout the iteration process. Hard decision from decoder is used to refine the channel estimate in the iterative method presented in [163] for coded OFDM (COFDM) Systems, while in [164] iterative channel estimation methods is presented, where soft and hard decision feedback from equalizer are used separately to improve the channel estimate. It is however verified in [164] that soft decision feedback performs about 0.15dB better than hard decision feedback, for both channel sounding and least square estimation. The soft statistics in the form of *a posteriori* probability are exploited in [165] to estimate and track the random fluctuations occasioned by time division multiple access (TDMA)-based mobile radio links that is impaired by time-varying frequency-selective multipath channel. A recursive version of EM algorithm employed in [162] is applied to channel estimator proposed in [166]. The performance of a coherent COFDM system in the presence of a time-varying frequency-selective fading

channel using a predictor-based channel estimator is investigated in [167]. The channel estimation method presented is based on a decision directed adaptive technique that uses decisions at the output of either the detector or the decoder. Iterative estimation and decoding of turbo codes over fading channels employing both hard and soft feedback from turbo decoder is presented in [168, 169]. It is further confirmed from the simulation results presented in [168, 169] that channel estimate based on soft decision feedback outperforms its counterpart based on hard decision feedback by about 0.5dB. A wireless communication systems receiver based on joint iterative channel and data estimation, exploiting both the power of pilot-symbol assisted modulation and turbo coding for fading channels, is proposed in [170]. However in [171] the iterative channel similar to the one considered in [164] is proposed for fast fading GSM (Global System for Mobile) channel with feedback from decoder rather than from the equalizer. However, as expected, the performance in this case is better than when the feedback is obtained from the equalizer. The reason for this is due to the fact that the feedback from the decoder has been further refined after leaving the equalizer stage, and it is lower in error in comparison with the feedback from the equalizer as a result of the decoding process. A receiver that performs joint channel estimation and turbo decoding, where the two processes benefit from each other, is presented in [172]. An iterative channel estimator based on EM algorithm as well as an estimator based on bootstrap process using linear pseudo-inverse are presented in [173]. Iterative soft serial interference cancellation (SIC) algorithm for joint data detection and channel parameter estimation based on soft-in soft-out single user decoders and soft interference cancellation is presented in [174], while joint channel estimation and decoding approach is presented in [175]. A new way of initial estimation of amplitudes of fading channel with delayed turbo decoding initialization is proposed in the iterative channel estimation technique presented in [176], while iterative channel estimation is invoked in [177] to design a trellis-based turbo equalizer. In the iterative scheme proposed in [178] channel estimation, signal detection, decoding, and retransmission are achieved in a disjoint iterative mode. In the papers, hard decision rather than soft decision is fedback from decoder to the estimator. Two different iterative channel estimators for mobile OFDM Systems, the first one based on iterative filtering and decoding while the second one uses an *a posteriori* probability, are investigated in [179]. The two estimators are said to perform equally at low to moderate Doppler frequency shifts, however the second estimator outperformed the first one for a channel with very large Doppler frequency shifts. An EM sub-optimal two-step iterative channel estimation and decoding algorithm using some approximations is proposed in [180], whereas in [181] the application of the iterative channel estimation and coherent detection is proposed for implementation of the Direct Sequence Ultra Wideband (DS

UWB) technology. Iterative channel estimation technique proposed in [169] is extended to the case of frequency selective fading channels in [182].

Four different algorithms-based iterative channel estimators, the least mean square (LMS), recursive least square (RLS), the modified RLS, and the Kalman-based algorithms, are compared in [183, 184]. In these papers both hard and soft decision feedback from decoder are considered. The results from the papers further confirmed that the estimation with soft decision generally performs better than the one with hard decision feedback. The authors observed that though LMS shows slow convergence during the initial training sequence, it however performs well in the remainder of the frame. Besides, while using soft feedback from decoder, LMS performs only slightly worse than modified RLS and much better than ordinary RLS using soft or hard decisions. In addition, the authors in the papers concluded that by using soft feedback for iterative estimation, the LMS-based estimator is always close to the best performing estimator among those employed. Hence, since the LMS algorithm is the simplest algorithm, it is suggested by the authors that LMS with soft feedback should be used for iterative channel estimation.

Despite the fast convergence of the RLS algorithm, according to the authors in [183, 184], its deployment in the real-time implementation is to be avoided because of its costly computational complexity. Because of the limitation of the RLS algorithms and the performance exhibits by LMS algorithm as confirmed in [183, 184], in Chapter 3 of this thesis we seek to develop an improved version of LMS-based iterative channel estimator that will take care of the slow convergence of the LMS algorithm and brings about improvement on its performance.

An iterative channel estimation technique that exploits coding gain to achieve a channel estimation that yields an overall system performance is proposed in [185] for mobile fourth generation coherent OFDM Systems. In [186] soft input weighted recursive least square error estimator and soft input Kalman channel estimator (obtained by restructuring the channel estimation problem of one of the Kalman state estimation, revealing the soft information from the decoding process, into the statistical description of the channel) are proposed. Non-data maximum likelihood channel estimation is improved in [187] by using convolutional encoder at the transmitter and a soft-input soft-output decoder that works iteratively with channel estimator at the receiver. Local linear and parabolic B-splines are applied in [188] for iterative channel estimation over fast flat fading channels, while in [189] a method to measure the channel statistics and operating signal-to-noise-ratio (SNR) from the received signal is proposed for iterative

detection in OFDM Systems. Pilot-symbol-aided iterative channel estimation method for coded OFDM-based Systems is considered in [190] by using the least-squares (LS) technique with discrete Fourier transform (DFT)-based interpolation in the frequency domain and linear interpolation in the time domain. Virtual pilots are formed from the *a posteriori* probability (APP) provided by the channel decoder. Iterative coded OFDM is investigated in [191] where the reliability of the soft symbols is improved by feeding back *a posteriori* log-likelihood ratio values (LLR-values) instead of *extrinsic* LLR-values to the channel estimator. Recently, an iterative detector comprises Turbo decoder and a channel estimator is proposed for OFDM Systems in [192]. As usual, the proposed modules operate in an iterative mode during which they exchange soft information with one another. In [193], a channel estimation method for OFDM Systems in fast fading channel scenario is proposed, while sliding window approach is used to compensate the inter-carrier interference (ICI) terms for pilot tones. An adaptive soft-based multiple burst maximum-likelihood (MB-ML) technique is presented [194] for channel estimation in turbo receiver. In the presented technique, *a priori* information on the coded bits available at the iterative receiver is exploited while employing a subspace tracking approach with the aim of reducing the computational complexity of the eigenvalue decomposition (EVD) as well as improving the tracking performance in a scenario where the multipath pattern gradually changes over the time. In [195] an iterative channel estimation, equalization, and decoding scheme for pilot symbol assisted transmission over a frequency selective Rayleigh fading channel is proposed. The scheme employed a channel estimator that is separated from equalizer soft-input soft-output module similar to the type presented in [183, 184]. Significant performance improvement is observed for the scheme with iteration as opposed to its non-iterative counterpart. Specifically, it is observed in the paper that there is performance degradation of about 2.7dB for slower fade rate and 5.7dB for the faster fade rate compared with the iterative channel estimator at a BER of 10^{-3}.

Channel matrix of a MIMO channel is estimated with the aid of soft decision from a Turbo decoder in the proposed pilot aided joint channel estimation and data detection method for MIMO communication Systems presented in [196]. An iterative method for decision directed channel estimation for OFDM is presented in [197], where its application to joint channel estimation and data decoding for space time coded system is illustrated. Similarly, in [198] iterative equalization algorithm is proposed for frequency selective MIMO channels, in which the proposed algorithm works jointly with the iterative estimator. In [199] joint channel estimation and data detection is proposed. A joint iterative channel estimation scheme is proposed in [200] for mitigating the

effect of multiple-access interference and multipath channel distortion on the space-time multiuser detector. Adaptive filtering-based iterative channel estimation techniques using hard decisions are proposed in [201] where it is concluded that the LMS estimator is a reasonable choice in terms of computational efficiency, with a minimum performance loss gain compared with RLS and the Kalman filter (KF) estimators. This conclusion still reinforce our drive to avoid the use of the more complex RLS algorithm in the various channel estimation schemes proposed in this thesis, but rather put forward with a more efficient version of the LMS algorithm with a negligible higher computational complexity compared with the LMS algorithm. In [202] an iterative channel estimation method for the space time block coded (STBC) OFDM system with cyclic prefix reconstruction is proposed, while in [203] an iterative joint channel estimation and signal detection approach is proposed for MIMO-OFDM system. An iterative channel estimation algorithm based on time domain filtering, and which can iteratively reduce the multi antenna sub-channel interference and the effect of additive white Gaussian noise (AWGN) is proposed in [204].

In [205] a turbo MIMO-OFDM receiver that is made up of a soft-feedback decision directed MIMO channel estimator, a soft-input-soft-output space-time detector and a soft-input-soft-output parallel-concatenated turbo decoder is proposed. These three components of the receiver iteratively exchange soft bit related information over a number of iterations. The soft-feedback decision directed MIMO channel estimator that is made up of the same decision directed channel estimation method is proposed by the authors in [153, 154] except that the CTF estimator is based on the RLS algorithm used by the authors in [183, 188]. As such, the soft-feedback decision directed MIMO channel estimator comprises RLS-based CTF estimator, PASTd-based CIR estimator and RLS-based CIR predictor. Recently in 2009, comparative results are also presented in [206] for soft-feedback iterative DDCE scheme using the structures in [161, 205] with Turbo codes and Low Density Parity Check (LDPC) codes as the channel error-correcting coding scheme. It is obvious, based on the drawbacks with the use of the RLS algorithm and the PASTd subspace tracking algorithm, as a result of their complexity that has earlier been mentioned, that the proposed soft-feedback decision directed MIMO channel estimator will be so complex that it can not be practically implemented. Hence in this thesis, a less complex decision directed channel estimation and iterative decision directed channel estimation techniques for SISO-OFDM Systems are presented in Chapter 4 and 5 respectively. The iterative decision directed channel estimation technique of Chapter 5 is extended to the case of MIMO-OFDM Systems in Chapter 6. The authors in [205] with another author, also proposed a Generic Algorithm (GA) assisted

iterative joint channel estimation and multi-user detection approach in [207] for multi-user MIMO Space Division Multiple Access (SDMA)-OFDM Systems in a bid to resolve the problem associated with the rank-deficient scenarios (a situation where the number of users are higher than the number of receive antennas). Lastly, an iterative receiver for MIMO-OFDM system with joint intercarrier interference (ICI) cancellation and channel estimation is presented in [208]. The authors concluded, based on their simulation results, that for mobile transmission scenarios the proposed method can effectively compensate the effect of intercarrier interference.

2.6 Chapter Summary

In this Chapter, multipath channel impulse response (CIR) models for both SISO and MIMO Systems are presented. The statistics of the channel impulse response model in terms of the correlation function and power delay profile are described and their expressions given. Examples of different commonly used power delay profile for COST 207 are also tabulated. Discrete time channel models including the Symbol (Sample)-Spaced Channel Impulse Response (SS-CIR) and the Fractionally-Spaced Channel Impulse Response (FS-CIR) models employed in the subsequent chapters of this thesis are presented. Thereafter, overviews of the three main types of channel estimation techniques, namely the pilot-aided channel estimation, blind channel estimation and decision directed channel estimation techniques are presented, while the various shortcomings associated with these methods are discussed.

Based on the various shortcomings associated with the blind and purely pilot-based channel estimation schemes, as observed in the review carried out in this chapter, the subsequent chapters, except chapter 3, focus on the family of decision directed channel estimation technique. Chapter 3 exploits pilot-based channel estimation technique in an iterative mode in order to document the comparative performances of the proposed algorithms to be used in the subsequent chapters.

CHAPTER 3

CHANNEL ESTIMATION FOR SINGLE ANTENNA COMMUNICATION SYSTEMS

3.1 Introduction

This chapter focuses on channel estimation for single antenna communication Systems. Specifically, soft input based iterative channel estimation is proposed for turbo equalization over frequency selective fading channel of single antenna communication Systems. Robust algorithms for implementation of the channel estimation scheme are proposed, and the comparative results with other algorithms in the literature are presented. The specific purpose of this chapter is to document the achievable performance of the proposed algorithms which are used in the subsequent chapters for implementation of decision directed channel estimation schemes.

The rest of this chapter is organized as follows. Soft input based iterative channel estimation is introduced in Section 3.2. Section 3.3 describes the system model employed in this chapter. The proposed soft input channel estimation algorithms are presented in Section 3.4, while comparative simulation results and discussion are given in Section 3.5. Computational complexity of the proposed algorithms in comparison with some others is presented in Section 3.6. Section 3.7 summarized the chapter.

3.2 Soft input based Iterative Channel Estimation

Emergence of Turbo code through the novel contribution of Berrou et al [209, 210] opens the gate to iterative processing techniques in communication Systems. This has been extended to equalization, synchronization, and channel estimation in conjunction with forward error

correcting code in various communication Systems. In a single antenna communication system, an equalizer is employed, basically, to reduce the effect of inter-symbol interference occasioned by multipath activities in the communication channel. However, the equalizer depends on accurate channel state information provided by channel estimate for its optimum performance. Among the different types of equalizers is the Turbo equalization scheme based on finite impulse response (FIR) filter proposed by Tuchler *et al*. [211, 212]. This equalization-based receiver jointly performs an iterative process between the equalizer and the decoder whereby both the equalizer and the decoder, exchange soft information in the form of log-likelihood ratios (LLR) on the code bits during the iterative cycle. In [183, 184] channel estimations scheme based on some adaptive algorithms are proposed for Turbo equalization. The estimator works in an iterative mode with both turbo equalizer and Turbo decoder. During the course of iteration, the quality of the channel estimation can be improved as the number of iterations increases. This requires that the channel estimator be fed with the feedback information from the decoder. This requirement will lead to either the hard decision or soft decision information on the code bits being feedback, as input reference signal, to the channel estimator. This will then result in either hard or soft iterative channel estimation scheme. Both hard and soft input based iterative channel estimators have been proposed in literatures, however it is established in [164, 183, 184] that estimation with soft input information generally performs better than estimation with hard decision input information.

Different types of adaptive algorithms have been proposed over the years for the purpose of updating the channel estimates used by Turbo equalizer for detection of the transmitted symbols at every symbol interval. Examples of these are the simple least mean square (LMS) algorithm and the more complex recursive least squares (RLS) algorithm. Simulation results are presented in [183, 184] in order to document comparative performance of LMS and RLS based soft input iterative channel estimator alongside estimators based on the modified version of RLS, modified RLS and approximated modified RLS algorithms (APRmodRLS). It is concluded that though LMS shows slowest convergence during the initial training sequence using soft feedback, its performance is close to the best performing algorithm of all the algorithms employed. Since LMS is the simplest algorithm, it is proposed, based on the results obtained, that LMS is to be used for iterative channel estimation while employing soft information feedback from decoder/equalizer. It is based on this conclusion that improved versions of LMS, variable step size Normalized LMS (VSSNLMS) and multiple-variable step size Normalized LMS (MVSSNLMS) algorithms, are

derived and proposed for implementation of soft input iterative channel estimation for Turbo equalization in single antenna communication Systems in this chapter.

3.3 System Model

Figure 3.1 shows the block diagram of the system model considered in this chapter. At the transmitter end of the system, binary source bits, $\boldsymbol{b}_p \in \{1, 0\}$ are encoded with the aid of a channel encoder. The output bits of the encoder, $\boldsymbol{c}_k \in \{1, 0\}$, are intearleaved to $\boldsymbol{c}_k^{'} \in \{1, 0\}$ by employing a channel interleaver. The interleaved code bits are thereafter mapped to *M*-ary signal constellation. Sequences of pilot symbol $\boldsymbol{t}_n$, known at the receiver, are multiplexed with the modulated message symbols. The multiplexed stream of symbols is then transmitted over an M-tap frequency selective Rayleigh fading channel.

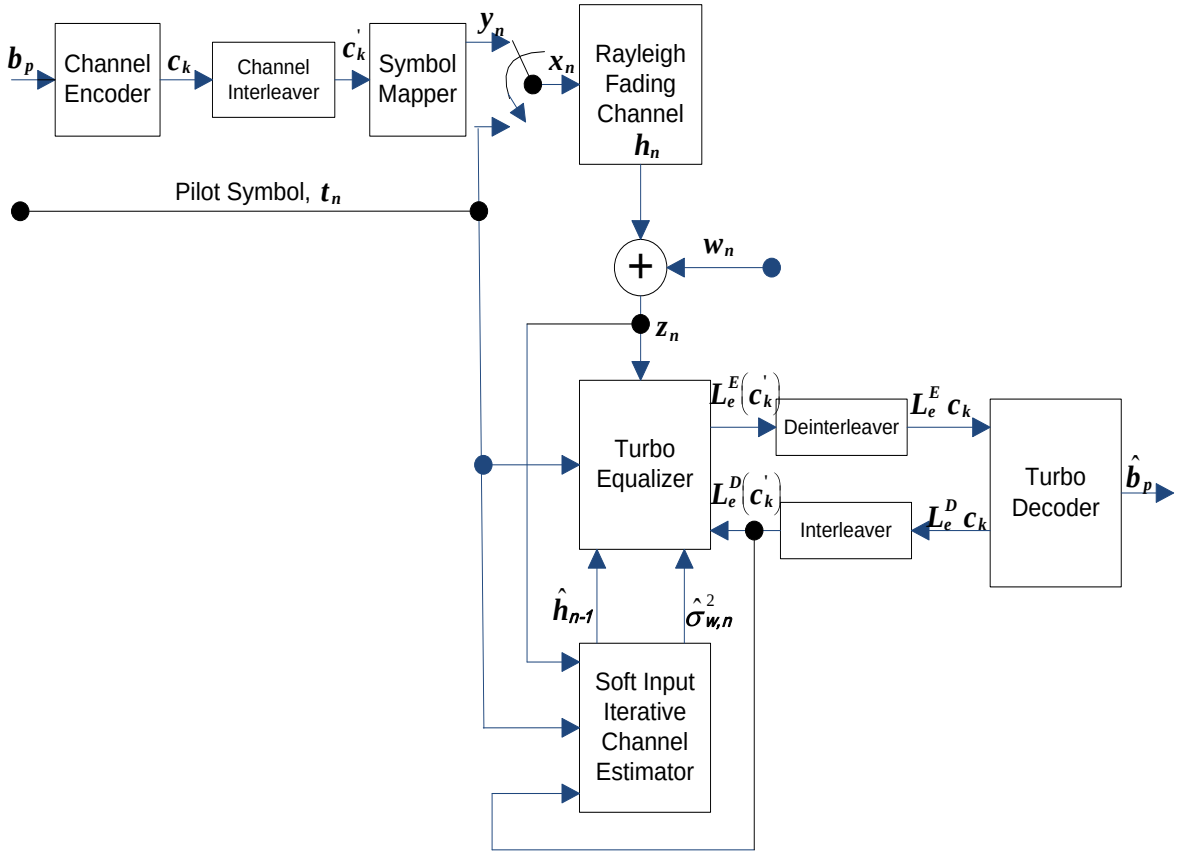

Figure 3.1 System model employing turbo equalizer-based receiver with soft input-based iterative channel estimator [184]

3.3.1 Channel Interleaver

This is a simple single input single output mechanism that takes symbols from a fixed alphabet as input and produces an identical set of symbols at the output in an altered temporary order [213]. Invariably, interleaver acts to shuffle the order of a sequence of symbols. Traditionally, interleaving is used to "randomize" the locations of errors caused by busty (correlative) channels, which in turn improves the performance of classic block and convolutional coding schemes designed and optimized for non-correlative channels, such as the Additive white Gaussian noise (AWGN) channel. With iteratively decoded concatenated coding schemes like Turbo code, interleavers are used mainly to decrease the correlation between the information encoded by different convolutional codes (CCs) encoders in the Turbo code, thereby improving the distance properties of the resultant concatenated code.

The implementable interleavers can be divided into two categories: Deterministic and Random interleavers. In the class of deterministic interleavers are the classic block interleavers, *Berrou-Glavieux* interleavers and Jet Propulsion Laboratory (JPL) interleavers. Pseudo-random (PN) generator interleavers, random number generator interleavers and semi-random(s-random) interleavers constitute the random interleavers [213]. Due to its efficiency, a type of the random interleavers (random number generator interleaver) is employed in the simulation work in this chapter and the subsequent chapters.

3.3.2 Random Block Interleaver

A Random interleaver can be described as a block interleaver with a mapping function generated from a permutation, based on the outputs of a random noise source [213]. The basic idea behind the design of random block interleavers is to eliminate regular pattern of the input signal bit sequence, resulting in extremely long interleaver periods.

In the whole of this thesis, random number generator described in the following is employed. Using any type of uniform number generator, a period N random number generator interleaver's mapping function is determined as follow [213].

1. N random numbers are generated. These numbers are stored in a length-N vector, denoted by $\overline{\boldsymbol{U}} = U_0, U_1, ..., U_{N-1}$.
2. The elements contained in $\overline{\boldsymbol{U}}$ are re-ordered to range from the smallest to the largest value. The result is stored in a length-N vector, denoted by $\overline{\boldsymbol{V}} = V_0, VU_1, ..., V_{N-1}$.

3. For every *i*, with $0 \le i < N$, the index *j* is determined such that $\boldsymbol{U}_i = \boldsymbol{V}_i$. The mapping function of the interleaver is then simply represented as $\pi(i) = j$.

3.3.3 Channel Model

Since the purpose of this chapter is to document the achievable performance of the proposed algorithms ,in comparison with the ones put forward by the authors in [184], which are used in the subsequent chapters for implementation of decision directed channel estimation schemes, the symbol space channel model used in [184] is employed in this chapter. The Channel impulse response (CIR), including transmitter and receiver filters, is modeled as a symbol-spaced time-varying linear filter $\boldsymbol{h}_n = \left[h_{n,0}, h_{n,1}, ..., h_{n,M-1} \right]^T$ as described in Chapter 2, with length *M*. Each of $h_{n,i}$ are mutually independent Rayleigh fading taps with a Gaussian Doppler spectrum [214], where the fading rate is defined as the value of the Doppler spectrum. The tap energies are equal and normalized to yield $E\ h_n^H h_n = 1$, where superscript '*H*' stands for Hermitian (conjugate transpose). The noise w_n are real value of zero mean white Gaussian noise with variance $\sigma_w^2 = N_0$.

The Rayleigh fading taps are modeled by employing Watterson Channel model of [214]. The Watterson Channel model views the radio frequency (RF) channel as a transversal filter where the taps are complex and vary with time. The time-varying taps, $h_{n,i}$, can be obtained by filtering complex additive white Gaussian noise (AWGN) with filters whose frequency-domain power spectra have a Gaussian shape. The Doppler spread d_i of interest is indirectly incorporated into the filter by ensuring that the standard deviation σ_i of each Gaussian-shaped power spectrum is set to $d_i / 2$ [214]. In equation form the amplitude of the filter taps in frequency domain is given by [214]:

$$\left\| H_{i(f)} \right\|^2 = \frac{e^{-2f^2/d_i^2}}{\sqrt{\frac{\pi d_i^2}{2}}} \quad , -\infty < f < \infty. \tag{3.1}$$

A time domain expression for the amplitude of the filter taps can be obtained by computing the Inverse Fourier Transform of (3.1) which gives:

$$h_i(t) = \sqrt{2} e^{-\pi^2 t^2 d_i^2} \tag{3.2}$$

The resulting time-domain equation has a Gaussian shape. However, in order to ensure a power gain of one the taps computed using (3.2) have to be normalized.

3.3.4 System Receiver

At the system receiver, the received distorted and noise corrupted signal $\boldsymbol{z}_n$ is given as

$$\boldsymbol{z}_n = \boldsymbol{w}_n + \boldsymbol{h}_n^T \boldsymbol{x}_n, \tag{3.3}$$

where $\boldsymbol{h}_n = \left[h_{n,0}, h_{n,1}, \ldots, h_{n,M-1} \right]^T$ is the length M time-varying discrete-time CIR, $\boldsymbol{x}_n = \left[x_n, \ldots, x_{n-M+1} \right]^T$, and $\boldsymbol{w}_n$ are as described above. Iterations are performed between three soft input based devices: the turbo equalizer, the turbo decoder, and the soft input iterative channel estimator. The sequence of pilot symbols is used to aid the channel estimation process. In the first equalization and decoding iteration, the channel estimates are derived from the pilot symbols only. However, they are mostly not accurate enough due to the small number of pilot symbols multiplexed with the message symbols at the transmitter end of the system. Hence, this will result in error propagation in the system. The pilot symbols are usually made to be few in numbers because on their own, they waste transmission bandwidth power. Immediately after the first iteration, when the soft decision from the decoder is available, the estimation can be refined, since to some degree, all the data symbols can be treated as pilot symbols. In this way, the whole receiver: the estimator, the equalizer and the decoder work in a fully iterative way and the overall performance is expected to improve as the number of iterations increase. The turbo decoder uses the deinterleaved extrinsic log-likelihood ratios (LLRs), $L_e^E(c_k')$, from the equalizer to estimate the transmitted data bits and also calculate the extrinsic LLRs $L_e^D(c_k')$ for the equalizer and the channel estimator to be used in the subsequent iterations. In addition, the decoder produces estimate $\hat{\boldsymbol{b}}_p$ of the transmitted messaged bits $\boldsymbol{b}_p$.

3.3.5 Computation of Mean and Variance of the Message Symbols

From the code bit LLRs $L_e^D(c_k)$ fedback from the decoder, the mean $\bar{y}_n = E\{y_{n'}\}$ and the variance $v_{y_{n'}}$ of each transmitted message symbol y_n is calculated respectively as:

$$\bar{y}_n = E\ y_n$$

$$= \sum_{s \in S} s.\Pr\{y_n = s\}, \tag{3.4}$$

$$v_{y_n'} = Cov\{y_n, y_n\}$$

$$= E\left[y_n' \, y_n'^{*} \right] - \bar{y}_n \bar{y}_n^{*}$$

$$= \left(\sum_{s \in S} s s^{*}.\Pr\left[y_n = s \right] \right) - \bar{y}_n \bar{y}_n^{*}, \tag{3.5}$$

where S is the vector of symbols in the M-ary signal constellation. The symbol probabilities $\Pr[y_n = s_i]$ are calculated from the code bit probabilities $\Pr[c_k = 0,1]$ which are given by the input LLRs [212] as

$$\Pr[c_k = 1] = \frac{1}{2}\left(1 + \tanh\frac{L(c_k)}{2}\right), \tag{3.6}$$

and

$$\Pr[c_k = 0] = \frac{1}{2}\left(1 - \tanh\frac{L(c_k)}{2}\right) \quad . \tag{3.7}$$

In the case where S is from M-phase shift keying (M-PSK) constellation, we have $s_i s_i^{*} = 1$ for all $s_i \in S$, such that (3.5) simplifies to $v_{y_n'} = 1 - \bar{y}_n \bar{y}_n^{*}$. By using 8-PSK constellation, we have by following [212]

$l_j = \tanh(L(C_{n,j})/2)$, for j = 1, 2, 3. (3.8)

Consequently, (3.4) becomes

$$\bar{y}_n = \left((1+\sqrt{2})i - 1\right)/4l_1 - \left(1 + \sqrt{2} + i\right)/4l_2 + l_3.\left((1-\sqrt{2}+i)/4l_1 + (1+(\sqrt{2}-1)i)/4l_2\right), \tag{3.9}$$

while (3.6), by taking pilot symbols into consideration, becomes

$$v_{y_n'} = 1 - \left|\bar{x}_n\right|^2. \tag{3.10}$$

Using the statistics $\bar{y}_n$ and $v_{y_n'}$, the transmitted symbols $\boldsymbol{x}_n$ is written as:

$$\boldsymbol{x}_n = \bar{x}_n + \chi_n, \tag{3.11}$$

where χ_n is a discrete-valued noise variable (having Gaussian distribution) with variance $E\{\chi_n, \chi_n^{*}\} = v_n$ and zero mean. During the period that the message symbols y_n have been transmitted, the mean $\bar{x}_n = \bar{y}_n$, and variance $v_n = v_{y_n'}$. However, when pilot symbols t_n have been transmitted, the mean $\bar{x}_n = t_n$. This implies that there is a perfect *a priori* information about the symbols, and $\bar{y}_n \bar{y}_n^{*} = 1$. Hence, from $v_{y_n'} = 1 - \bar{y}_n \bar{y}_n^{*}$, variance $v_n = 0$.

3.4 Proposed Soft Input Channel Estimation Algorithms

The soft input channel estimator provides time-varying channel estimates of CIR $\hat{h}_n$ as well as estimated noise variance $\hat{\sigma}^2_{w,n}=\left[\hat{\sigma}^2_{w,0},\hat{\sigma}^2_{w,1},...,\hat{\sigma}^2_{w,n}\right]$ at each time step *n* to be used by the turbo equalizer. Two improved version of the LMS algorithm employed in [183] are proposed herein for the updating of the CIR. These are derived in the following sections.

3.4.1 Variable Step Size Normalized Least Mean Square Algorithm

The LMS algorithm [215] is given more attention in real-time applications because it exhibits a good balance between computational cost and performance. This is the reason why it is suggested in [183], based on the simulation results presented, that the LMS rather than RLS algorithm should be used for updating the channel estimate at every symbol interval for communication receivers because its structure is less complex. However, a very serious problem associated with the LMS and its improved version, Normalized LMS algorithms is the choice of the step-size (μ) parameters which is responsible for the rate of convergence as well as the obtainable excess mean square error associated with the algorithms.

With the LMS algorithm, the CIR is updated as

$$\hat{\boldsymbol{h}}_{n+1}=\hat{\boldsymbol{h}}_n+\mu e_n\bar{\boldsymbol{x}}_{\boldsymbol{n}}, \tag{3.12}$$

where e_n is the error signal while using the soft symbol $\bar{\boldsymbol{x}}_{\boldsymbol{n}}$ for channel estimation. This error signal e_n is given as [183]

$$e_n=z_n-\hat{\boldsymbol{h}}_n^T\bar{\boldsymbol{x}}_{\boldsymbol{n}}. \tag{3.13}$$

By employing the LMS algorithm as given above, the correction $\mu e_n\bar{\boldsymbol{x}}_n$ applied to the CIR vector $\hat{\boldsymbol{h}}_n$ at the (*n*+1) time index is directly proportional to the input soft symbol vector $\bar{\boldsymbol{x}}_{\boldsymbol{n}}$. Consequently, when $\bar{\boldsymbol{x}}_{\boldsymbol{n}}$ is large, the LMS algorithm experiences a gradient noise amplification problem [215]. In order to overcome this difficulty, the correction that is applied to the CIR vector $\hat{\boldsymbol{h}}_n$ at next time index (*n*+1) is normalized with respect to the squared Euclidean norm of the input soft symbol vector $\bar{\boldsymbol{x}}_{\boldsymbol{n}}$ at the present time index *n* in order to obtain the NLMS algorithm for updating of CIR given as

$$\hat{\boldsymbol{h}}_{n+1}=\hat{\boldsymbol{h}}_n+\mu e_n\frac{\bar{\boldsymbol{x}}_n}{\left\|\bar{\boldsymbol{x}}_n\right\|^2}, \tag{3.14}$$

where $\|\bar{\boldsymbol{x}}_n\|^2$ denotes the square of Euclidean norm of the input vector $\bar{\boldsymbol{x}}_n$. A small value of step size μ in (3.12) and (3.14) will ensure small misadjustments in the steady state, but the algorithms will converge slowly and may not track the nonstationary behaviour of the operating environment very well. On the other hand, a large value of μ will, in general, provide faster convergence and better tracking capabilities at the cost of higher misadjustment. Any selection of the step-size must therefore be a trade-off between the steady-state misadjustment and the speed of adaptation. The idea of variable step size is to ensure that the proposed variable step size normalized least mean square (VSSNLMS) algorithm detects the rate at which the optimal coefficients of the channel are changing, during both slow and fast fading channel scenarios, and select the best value μ that can result in estimates that are close to the best possible one in terms of mean square error.

Since the NLMS algorithm exhibits a better performance than LMS algorithm due to the normalization introduced into the algorithm [215], VSSNLMS algorithm [17] is therefore obtained for NLMS algorithm and it updates the CIR as

$$\hat{\boldsymbol{h}}_{n+1} = \hat{\boldsymbol{h}}_n + \mu_n e_n \frac{\bar{\boldsymbol{x}}_n}{\|\bar{\boldsymbol{x}}_n\|^2}. \tag{3.15}$$

The variable step-size expression for the VSSNLMS algorithm proposed for updating the channel estimate of CIR in this chapter is obtained by extending the approach used in [216, 217]. This is achieved by adapting the step-size sequence using a gradient descent algorithm so as to reduce the squared-estimation error at each time index. The variable step-size μ_n is then updated as:

$$\begin{aligned}\hat{\mu}_n &= \mu_{n-1} - \frac{\rho}{2}\frac{\partial e_n^2}{\partial \mu_{n-1}} \\ &= \mu_{n-1} - \frac{\rho}{2}\frac{\partial^T e_n^2}{\partial \hat{\boldsymbol{h}}_n}.\frac{\partial \hat{\boldsymbol{h}}_n}{\partial \mu_{n-1}} \\ &= \mu_{n-1} + \frac{\rho e_n e_{n-1} \bar{\boldsymbol{x}}_{\boldsymbol{n}}^{\boldsymbol{T}} \bar{\boldsymbol{x}}_{\boldsymbol{n-1}}}{\|\bar{\boldsymbol{x}}_{\boldsymbol{n-1}}\|^2}.\end{aligned} \tag{3.16}$$

Symbol ρ in (3.16) is a small positive constant that controls the adaptive behavior of the step-size sequence μ_n. Deriving conditions on ρ, so that convergence of the adaptive system can be guaranteed appears to be very difficult. However, the initial convergence speed of the VSSNLMS algorithm will be insensitive to the choice of ρ if it is chosen to be very small in comparison with

the initial value of μ_n[17]. Hence, the convergence of the algorithm can be guaranteed by restricting μ_n to always stay within the range that would ensure convergence as stipulated for LMS and NLMS algorithms [215, 218]. Therefore, the step-size obtained from (3.16) would not be used for updating of the channel estimate at any particular time index if it falls outside the values that guarantee convergence of the NLMS algorithm. Consequently, the step-size sequence μ_n will be restricted to within the range $0 < \mu_n < 2$, the limit within which convergence of the NLMS algorithm is guaranteed as analyzed in [218]. The limit for the variable step size μ_n, in order to make for convergence of the VSSNLMS algorithms-based channel estimator, is given as follows

$$\mu_n = \begin{cases} \mu_{\max} & if \quad \hat{\mu}_n > \mu_{\max} \\ \mu_{\min} & if \quad \hat{\mu}_n < \mu_{\min} \\ \hat{\mu}_n & otherwise \end{cases} \tag{3.17}$$

where $0 < \mu_{\min} < \mu_{\max} < 2$.

3.4.2 Multiple-Variable Step Size Normalized Least Mean Square Algorithm

The multiple-VSSNLMS algorithm proposed herein is similar to the VSSNLMS algorithm of section 3.4.1 except that instead of using a single variable step-size for updating the channel estimate of CIR vector, $\hat{\boldsymbol{h}}_n$, each of $\hat{h}_{n,0}, \hat{h}_{n,1}, ..., \hat{h}_{n,M-1}$ is updated with a unique variable step-size resulting in multiple-VSSNLMS algorithm. As a result, the variable step-size μ_n in (3.15) becomes a vector given as $\boldsymbol{\mu}_n = \left[\mu_{n,0}, ..., \mu_{n,M-1} \right]^T$. Thus, multiple-VSSNLMS algorithm is M-time more complex than VSSNLMS algorithm. The multiple variable step size vector is similarly obtained as:

$$\hat{\boldsymbol{\mu}}_n = \hat{\boldsymbol{\mu}}_{n-1} + \frac{\rho e_n e_{n-1} \bar{\boldsymbol{x}}_{\boldsymbol{n}}^{\boldsymbol{T}} \bar{\boldsymbol{x}}_{\boldsymbol{n-1}}}{\left\| \bar{\boldsymbol{x}}_{\boldsymbol{n-1}} \right\|^2}. \tag{3.18}$$

In the same way as the case of single variable step size of section 3.4.1, each of the variable step-size, $\mu_{n,m}$ (for m = 0… M-1) in the multiple-variable step size vector $\boldsymbol{\mu}_n$ is restricted to within the range as given in (3.17).

3.5 Simulation Results and Discussion

In this section two set of simulations are carried out in order to validate the performance of the proposed algorithms for soft input channel estimation. In the first round of simulation, the

simulation set up is similar to the one used in [183, 184], and is based on the system model of Figure 3.1. Blocks of data bit $\boldsymbol{b}_p \in \{1, 0\}$ are generated randomly and encoded with rate ½ (2, 1, 4) Convolutional codes encoder. The encoder output bits, $\boldsymbol{c}_k \in \{+1, -1\}$, are intearleaved to $\boldsymbol{c}_k' \in \{1, 0\}$ using a random-interleaver. Interleaved code bits are then mapped to message symbols y_n using Gray-coded 8-PSK signal constellation *S*. Pilot symbols $\boldsymbol{t}_n$ are generated also from a Gray coded 8-PSK by mapping random generated bits to $\boldsymbol{t}_n$. The message symbols $\boldsymbol{y}_n$ and the pilot symbols $\boldsymbol{t}_n$ are multiplexed into frames, where a frame consists of 160 initial pilot symbols followed by three sequences of 150 message symbols and 30 pilot symbols. The energy Es per transmitted symbol $\boldsymbol{x}_n$ is one. The symbols $\boldsymbol{x}_n$ are transmitted over a time-varying ISI channel of length $M' = 6$. $\boldsymbol{h}_{i,n}$ are mutually independent Rayleigh fading taps with a Gaussian Doppler spectrum modeled according to [16], where the fading rate f_d is defined as the 2σ value of the Doppler spectrum. The tap energies are made equal and normalized to yield $E\ h_n^H h_n = 1$. The noise $\boldsymbol{w}_n$ has variance $\sigma_w^2 = N_0$. At the receiver end, the LLRs $L_e^D(c_k)$ fed back from the decoder are modeled as independent real Gaussian random variables with average value $c_k \times \sigma_L^2$ and variance σ_L^2 .This is a common model for the LLRs produced by a decoder during iterative decoding [164], and the actual distribution of LLRs is computed directly from bits transmitted over a simple AWGN channel. The value of $\sigma_L = 0$ corresponds to poor soft information, all $L_e^D(c_k)$ are 0, and an increasing σ_L corresponds to more and more reliable soft information.

At this stage of the simulation, one of the proposed algorithms for implementation of the soft iterative channel estimation scheme, the VSSNLMS algorithm and those in [183, 184] have been used to generate a time-varying channel estimate $\hat{\boldsymbol{h}}_n$ of length $M = M'+2 = 8$ (to account for the fact that M' is not known in reality) and the error signal $\boldsymbol{e}_n$ has been recorded. In total, 10,000 frames have been simulated in order to estimate the (ensemble) error variance $\sigma_{e,n}^2 = E\ e_n e_n^*$ at each symbol interval. The parameters $\boldsymbol{b}_p$, $\boldsymbol{h}_n$, $\boldsymbol{t}_n$, and $L(c_k)$ are randomly different for each frame. For all the algorithms, the variance $\hat{\sigma}_{w,n}^2$ is obtained as $\hat{\sigma}_{w,n}^2 = \sigma_{e,n}^2 = E\ e_n e_n^*$. Forgetting factor, $\lambda = 1+\mu_0$ is used for RLS and the APRmodRLS algorithms while μ_0 is used for LMS and to initialize VSSNLMS algorithms. In addition to the (ensemble) error variance and the bit error rate (BER) used as performance index for the channel estimation algorithms, the mean-squared error of the channel estimator is also obtained, at this stage of the simulation work, in order to

establish the performance of VSSNLMS algorithm in comparison with the other three algorithms. The Normalized Mean-Squared Error (NMSE) used is given as [168]

$$NMSE = \frac{\sum_n E\left\{\left|\boldsymbol{h}_n - \hat{\boldsymbol{h}}_n\right|^2\right\}}{\sum_n E\ \left|\boldsymbol{h}_n\right|^2}, \tag{3.19}$$

while

$$MSE = \sum_n E\left\{\left|\boldsymbol{h}_n - \hat{\boldsymbol{h}}_n\right|^2\right\}. \tag{3.20}$$

In order to obtain the Normalized MSE, accurate tracking of channel length is assumed and a singular frame is considered. Figures 3.2, Figure 3.3, Figure 3.4 and Figure 3.5 show convergence of the algorithms as well as the variation of the ensemble error variance, σ_e^2 throughout the frame. Significant decreases in ensemble error σ_e^2 with time are observed when the pilot symbols are used for estimation whereas it increases when soft message symbols are used. From the plots it could be seen that RLS based channel estimator show best convergence and it is followed closely by the proposed VSSNLMS based channel estimator. The LMS based channel estimator show poor performance among the algorithms compared. On the order hand, RLS exhibit the best performance in the steady state region of the plots, while the performances of both the VSSNLMS and APRmodRLS based channel estimators are close to each other. The LMS based channel estimator also show poor performance in the steady state region. However, it is observed that the results of error variances of Figure 3.2 to Figure 3.5 are slightly larger than those presented in [184]. The slight difference might be associated with the fact that there are differences in the simulation approaches presented in this Chapter in comparison with that of [184]. In [184], y_n and t_n are generated randomly, there is no encoding and interleaving processes. Conversely, in this Chapter, blocks of data bit $\boldsymbol{b}_p$ are encoded, interleaved before being multiplexed with t_n. Figures 3.6 and Figure 3.7 show the Normalized MSE and corresponding MSE for these algorithms. In the aggregate, it is obvious from the simulation results that the performance of VSSNLMS-based channel estimation algorithm is far better than those of the APRmodRLS algorithm and the LMS algorithm proposed for soft input channel estimation in [183, 184] and close to that of RLS-based channel estimator. The reason for this could be associated to that fact that the modified RLS (APRmodRLS) algorithm reduces to LMS algorithm while using soft symbols for channel estimation as stated in [184].

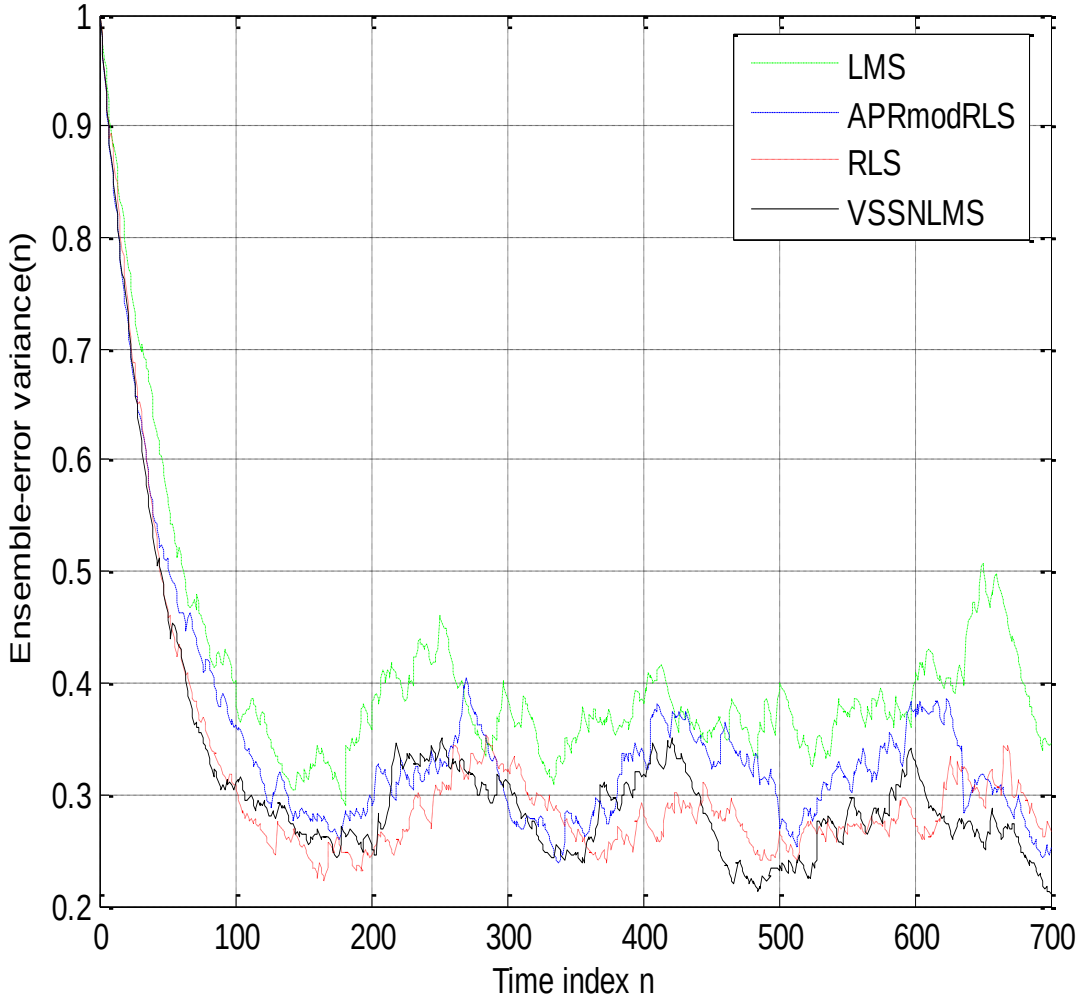

Figure 3.2 Simulated ensemble error variance for the channel estimation algorithms, at each symbol interval n in a frame of pilot and message symbols. Simulation setup: Es/N0 = 10 dB; ρ=0.02, σ_L =1, fD /fs =1/2400 (slow fading channel), and λ=0.98.

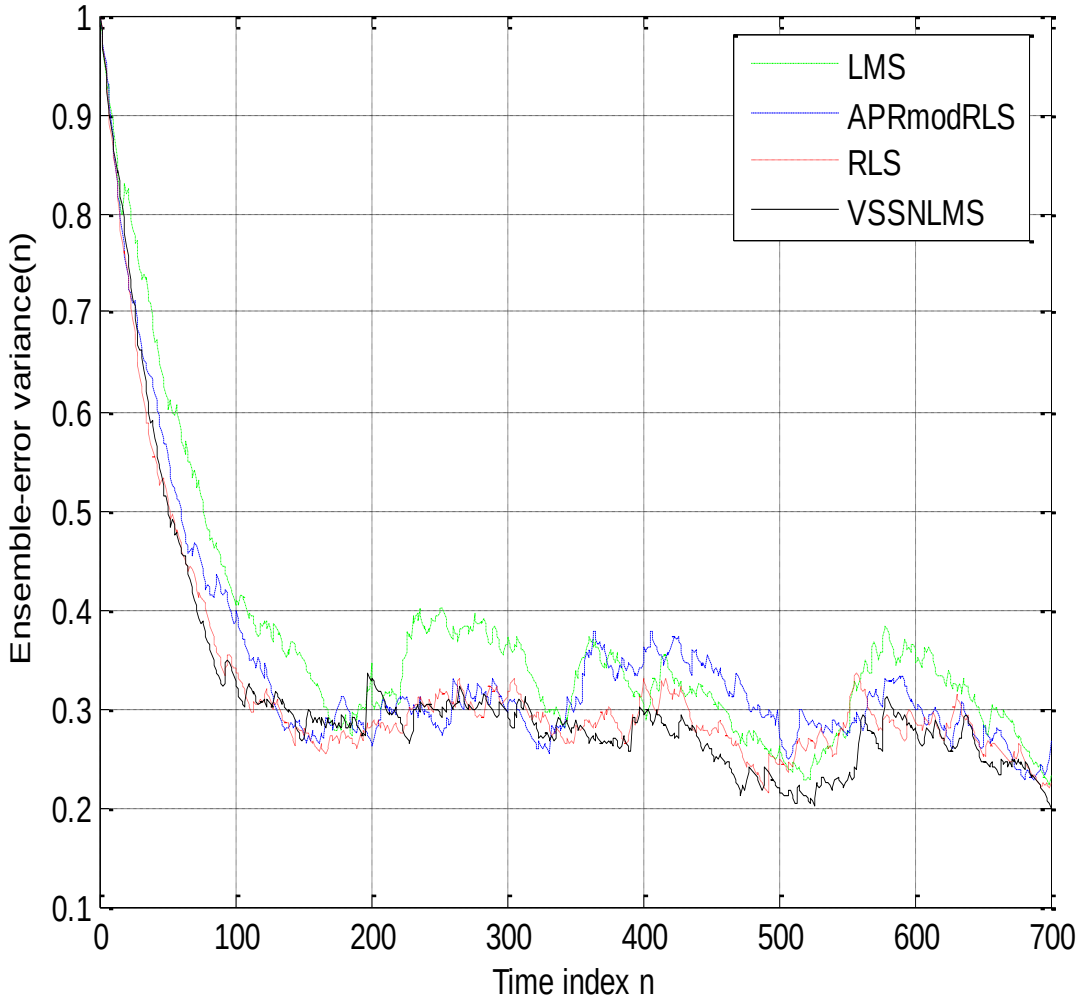

Figure 3.3 Simulated ensemble error variance for the channel estimation algorithms, at each symbol interval n in a frame of pilot and message symbols. Simulation setup: Es/N0 = 10 dB; ρ=0.02, $\sigma_{L=}$=3, fD /fs =1/2400 (slow fading channel), and λ=0.98.

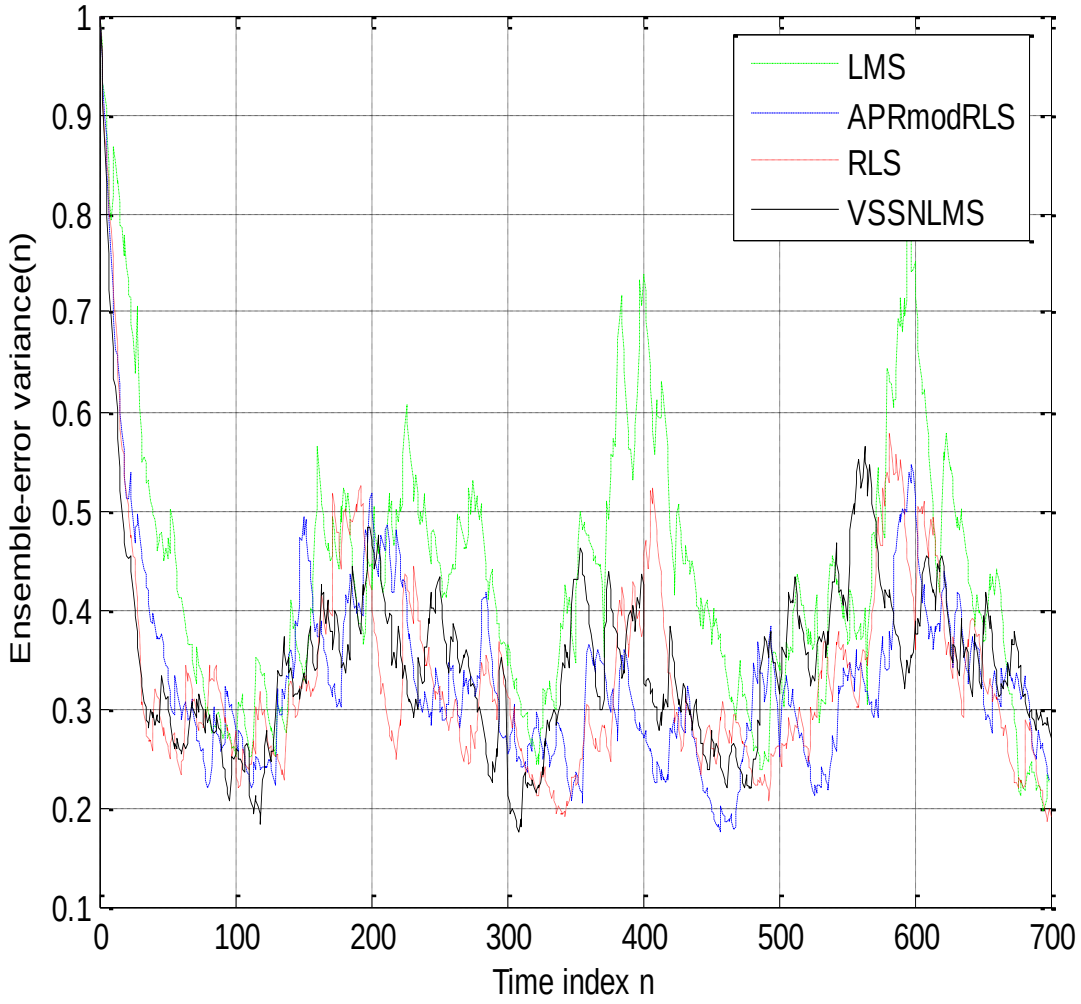

Figure 3.4 Simulated ensemble error variance for the channel estimation algorithms, at each symbol interval n in a frame of pilot and message symbols. Simulation setup: Es/N0 = 10 dB; ρ=0.02, σ_L =1, fD /fs =5/2400 (fast fading channel), and λ=0.95.

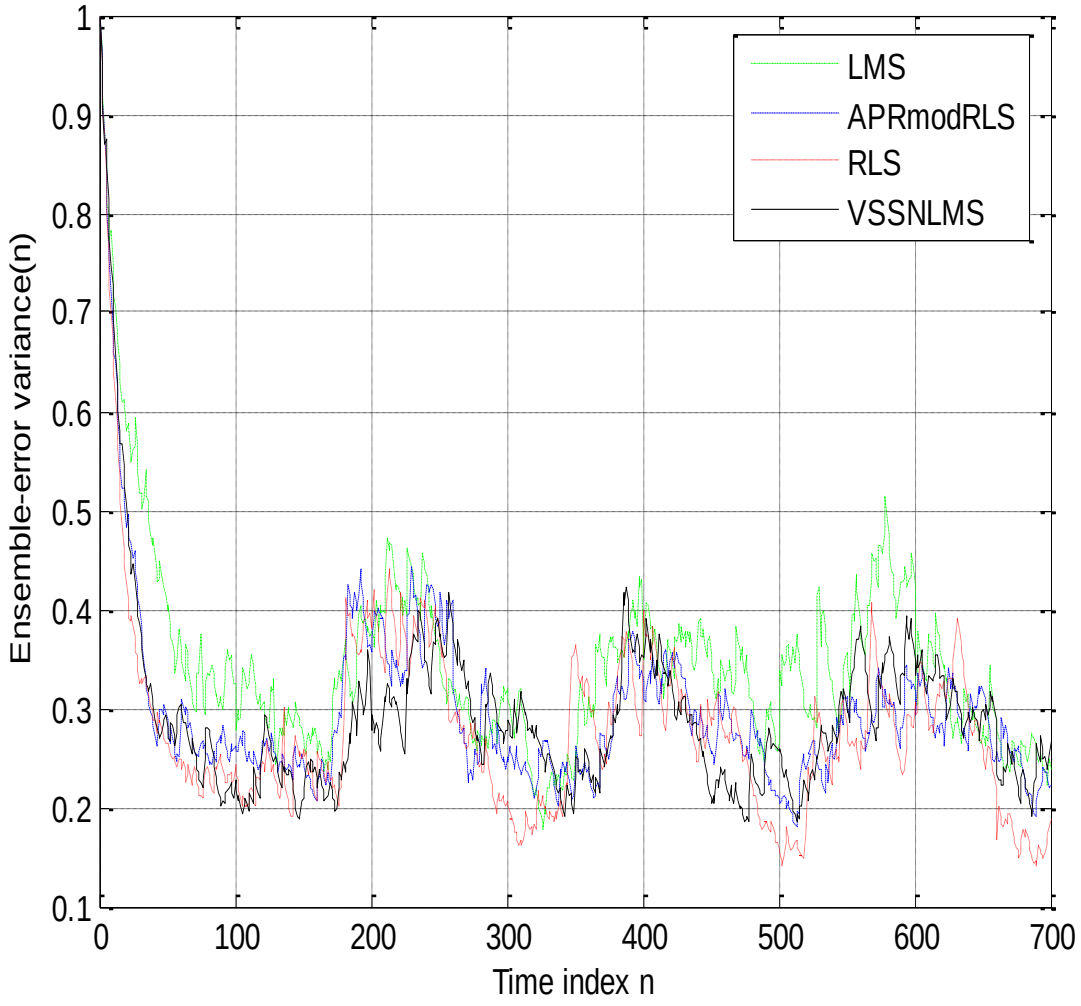

Figure 3.5 Simulated ensemble error variance for the channel estimation algorithms, at each symbol interval n in a frame of pilot and message symbols. Simulation setup: Es/N0 = 10 dB; ρ=0.02, σ_L =3, fD /fs =5/2400 (fast fading channel), and λ=0.95.

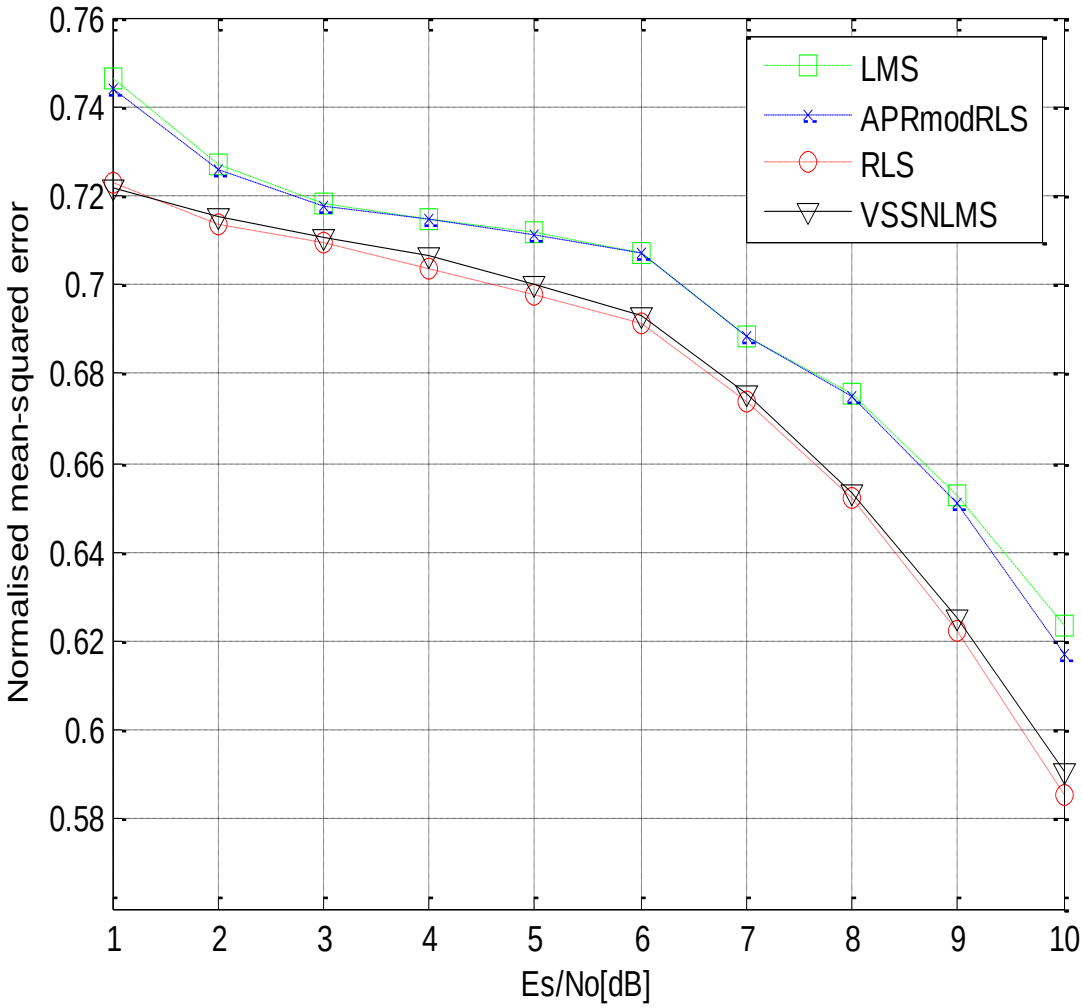

Figure 3.6 Normalized MSE for the channel estimation algorithms, at each Es/N0 in a frame of pilot and message symbols. Simulation setup: ρ=0.02, σ_L =1, fD /fs =1/2400, and λ=0.98.

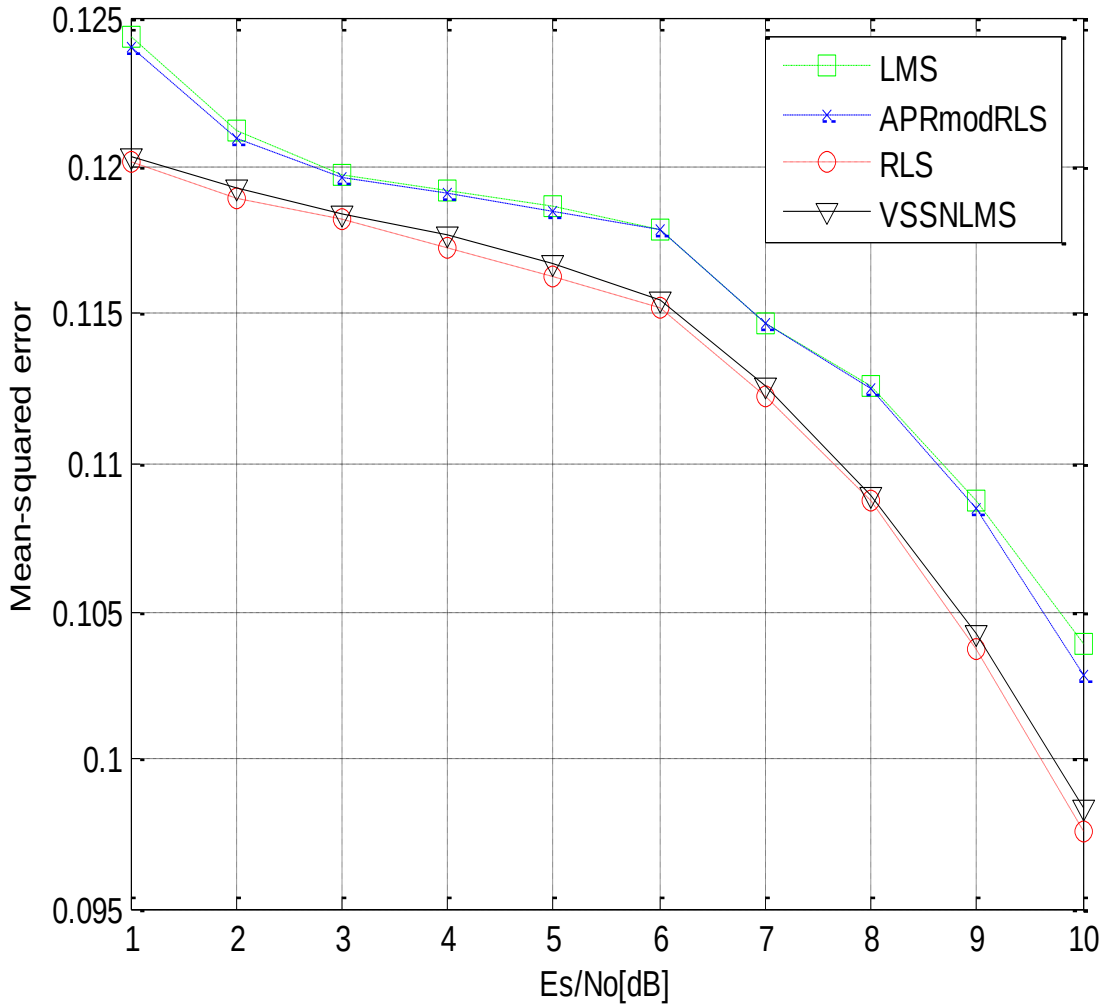

Figure 3.7 MSE for the channel estimation algorithms, at each Es/N0 in a frame of pilot and message symbols. Simulation setup: ρ=0.02, σ_L =1, fD /fs =1/2400, and λ=0.98.

In the second phase of the simulation work, a rate 1/3, 16 state, 512 data bit turbo code with generator matrix (031,027) is employed to encode blocks of data bit $\boldsymbol{b}_p \in\{+1, -1\}$. The encoder output bits , $\boldsymbol{c}_k \in\{+1, -1\}$ are interleaved to $\boldsymbol{c}_k^{'} \in\{+1, -1\}$ and then modulated with BPSK modulator to $\boldsymbol{y}_n$. Random interleavers are used in the turbo encoder and as channel interleavers. Sequences of 15 known pilot symbols, $\boldsymbol{t}_n$, obtained by mapping randomly generated bits to BPSK are regularly inserted into the frames, with 64 data symbols between each pilot sequence. The pilot symbols are used to aid the channel estimation process. They are also used by the equalizer as *a priori* information during the first-time equalization. The symbols $\boldsymbol{x}_n$ are transmitted over a time-varying ISI channel. The time-varying frequency-selective Rayleigh fading channel,

$\boldsymbol{h}_n = \left[h_{n,0}, h_{n,1}, \ldots, h_{n,M-1} \right]^T$ of length M = 4 is generated employing Rayleigh fading simulator presented in [219]. The tap energies of the CIR are made equal and normalized to yield $E\ h_n^H h_n = 1$. The w_n are real valued samples of zero-mean white Gaussian noise with variance $\sigma_w^2 = N_0$. The receiver, in this case, performs turbo equalization using the turbo equalizer structure of Figure 3.8 that is based on MMSE criterion and time recursive update algorithm derived by authors in [211, 212] for a time-invariant channel and re-derived by authors in [220] for a time-varying communication channel. The filter length of the linear SISO equalizer is $N = (N_1 + N_2 + 1) = 11$, where $N_1 = 7$ and $N_2 = 3$. This ensures that the transmitted symbols x_n starts with a preamble of at least $N+M$ pilot symbols known to the receiver in order to bootstrap the time-recursive update algorithm of the equalizer [211, 212]. During the first-time equalization, the known pilot symbols are used as input to the channel estimator and the channel estimates are kept constant between the pilot sequences. In the subsequent iterations, the pilot symbols and the soft symbols, $L_e^D(c_k)$, feedback from the decoder are used to calculate both $\bar{x}_n$

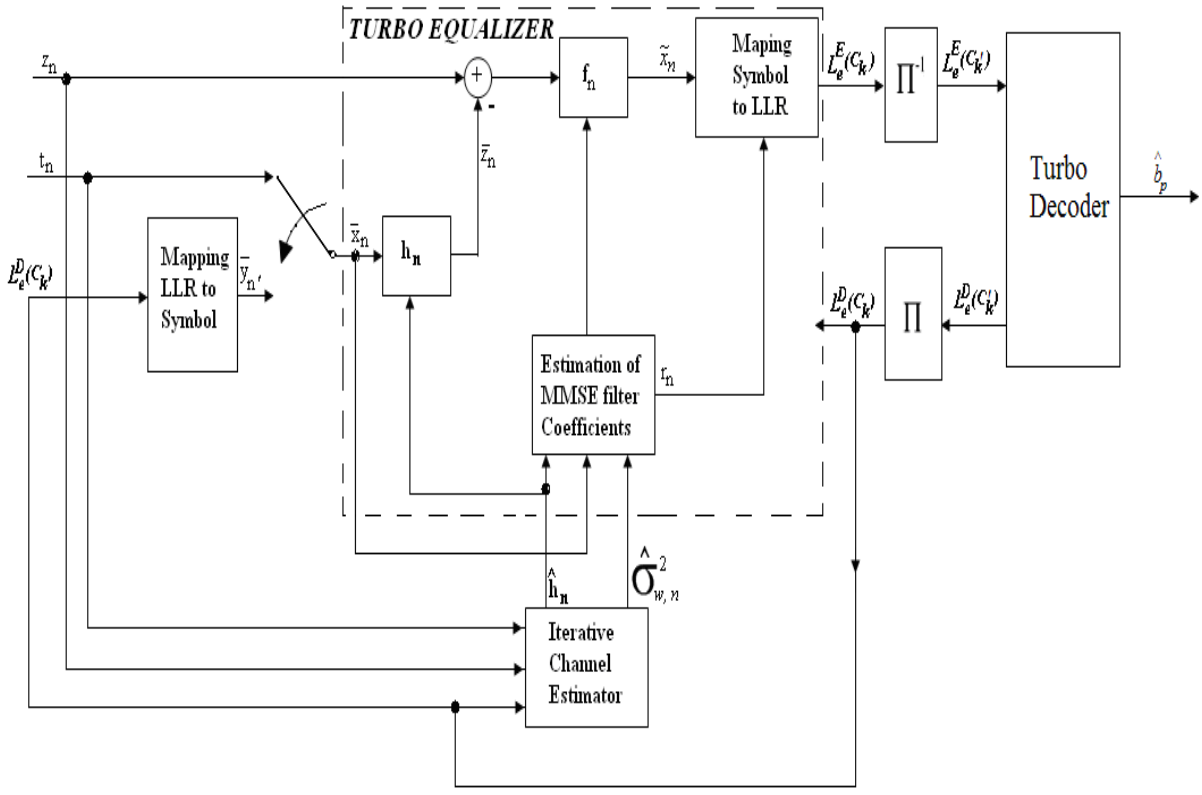

Figure 3.8 Receiver block diagram using soft-input soft output linear equalizer, iterative channel estimator and turbo decoder [220].

and v_n according to (3.4) and (3.5). The mean and the variance are used by the equalizer and the channel estimators in the subsequent iterations. The optimal *soft-input soft output* decoder for a turbo code, the Maximum A-Posteriori (MAP) decoder implemented as log-MAP in [221] is employed at this stage of simulation. In total, 10,000 frames are used for all simulations and the BER performances measured. Forgetting factor $\lambda = 1-\mu_0$ is used for RLS algorithm, while $\mu_0 = 0.02$ is used for LMS and NLMS algorithms and to initialize both VSSNLMS and multiple-VSSNLMS algorithms, ρ is set to 0.002.

Known channel state information at the receiver is assumed for the first round of simulations to ascertain the iteration stage at which the improvement in BER starts declining, that is the stage where further iterations do not bring about improved results to the system. This is found for both fast and slow fading channel to be after the seventh iteration as shown in Figure 3.9 and Figure 3.10. It is observed that there is an improvement in the BER performances from the first iteration until the seventh iteration, after which no improvement in the result is visible. This lends credence to the improved performance obtainable when iterative receiver is used in a communication system. Subsequent simulations are then run for just five iterations and the BER performances at the seventh iteration are measured. Subsequently, the VSSNLMS and multiple-VSSNLMS algorithms are used along side LMS, NLMS and RLS algorithms, to estimate channel state information (CSI) for the case where channel knowledge is not known at the receiver. The results after the seventh iteration for both slow and fast fading channel, $fDT_s = 0.005$ and $fDT_s = 0.01$ are shown in Figure 3.11 and Figure 3.12 respectively. The performance curves denote as known channel in Figure 3.11 and Figure 3.12 serves as a benchmark and performance lower bound for the system. It is observed that the performances of the proposed algorithms are far better than those of LMS and NLMS algorithms and are close to that of RLS algorithm. The reason for these better performances is because of the variability in the step-sizes which drives the proposed algorithms step-size to the optimum values, and then results in faster convergence of the algorithms with better tracking capabilities. The performances of all the algorithms for fast fading channels appear to be lower when compared with that of the slow-fading channel. This implies that all the algorithms find it easy to track the slow fading channel as opposed to the fast fading channel. It is necessary to, however, state that the length of linear SISO equalizer, number of pilot symbols and the time varying channel CIR generator employed in this Chapter are different from

those used in [183, 184]. These and some other factors might be responsible for the differences in the results presented in this Chapter and that of [183, 184]. A lower length of the linear SISO equalizer is chosen in order to reduce the complexity for the sake o smooth simulation on Computer. It is noted that the iteration result converges at 7th iteration in this Chapter, however in [183, 184] results at 3rd and 4th iteration are displayed. The iteration stage at which the convergence occurs is not stated in [183, 184]. Obviously, the complexity of the equalizer did not allow higher iteration to be reached. Regarding duration each iteration takes for the simulation to complete, this varies with the SNR and the speed of the personal computer employed. Estimated times in seconds for each of the iteration, for SNR of 1dB, 5dB and 9dB in the simulation presented in this chapter are 0.172, 0.187, and 0.204 respectively.

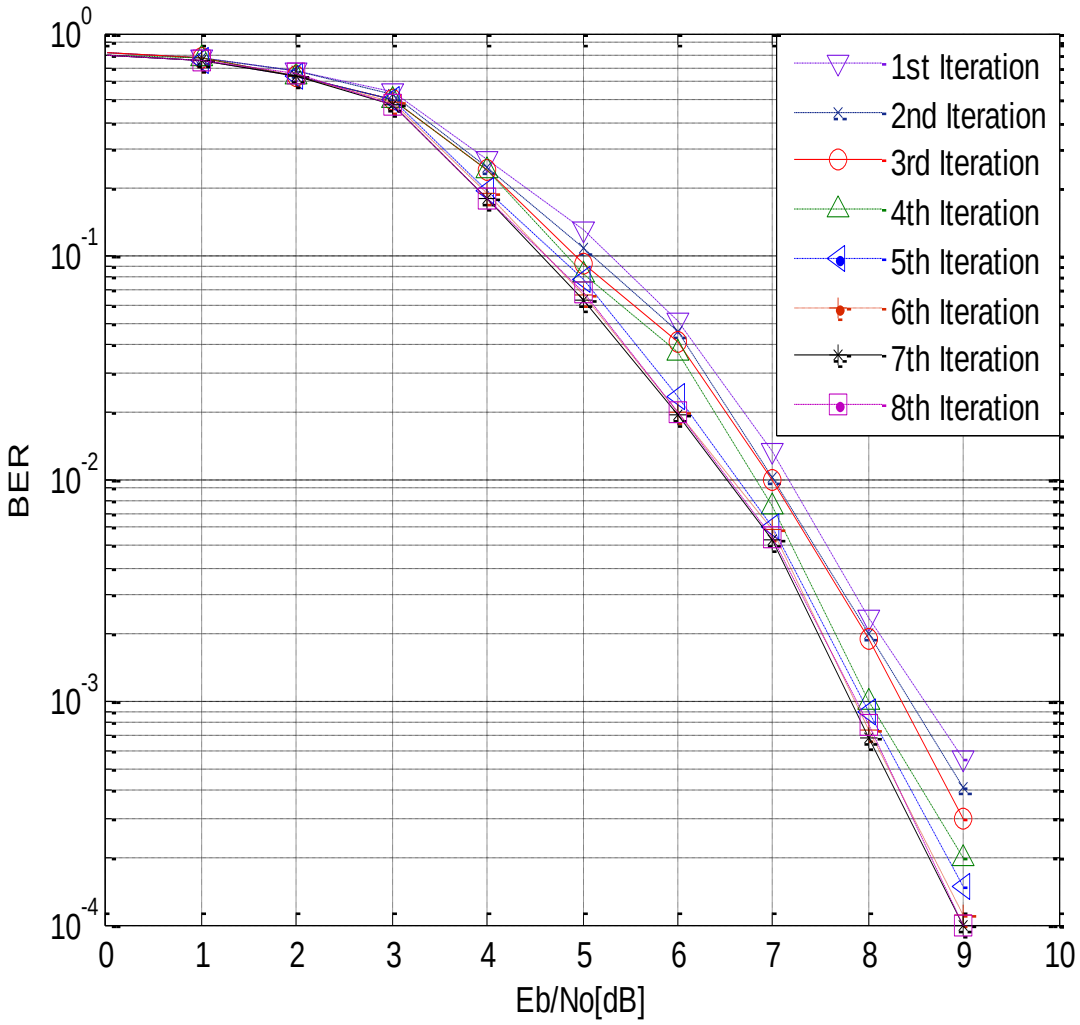

Figure 3. 9 BER for different number of iteration for known channel state information (CSI) at the receiver, $fDT_s = 0.005$

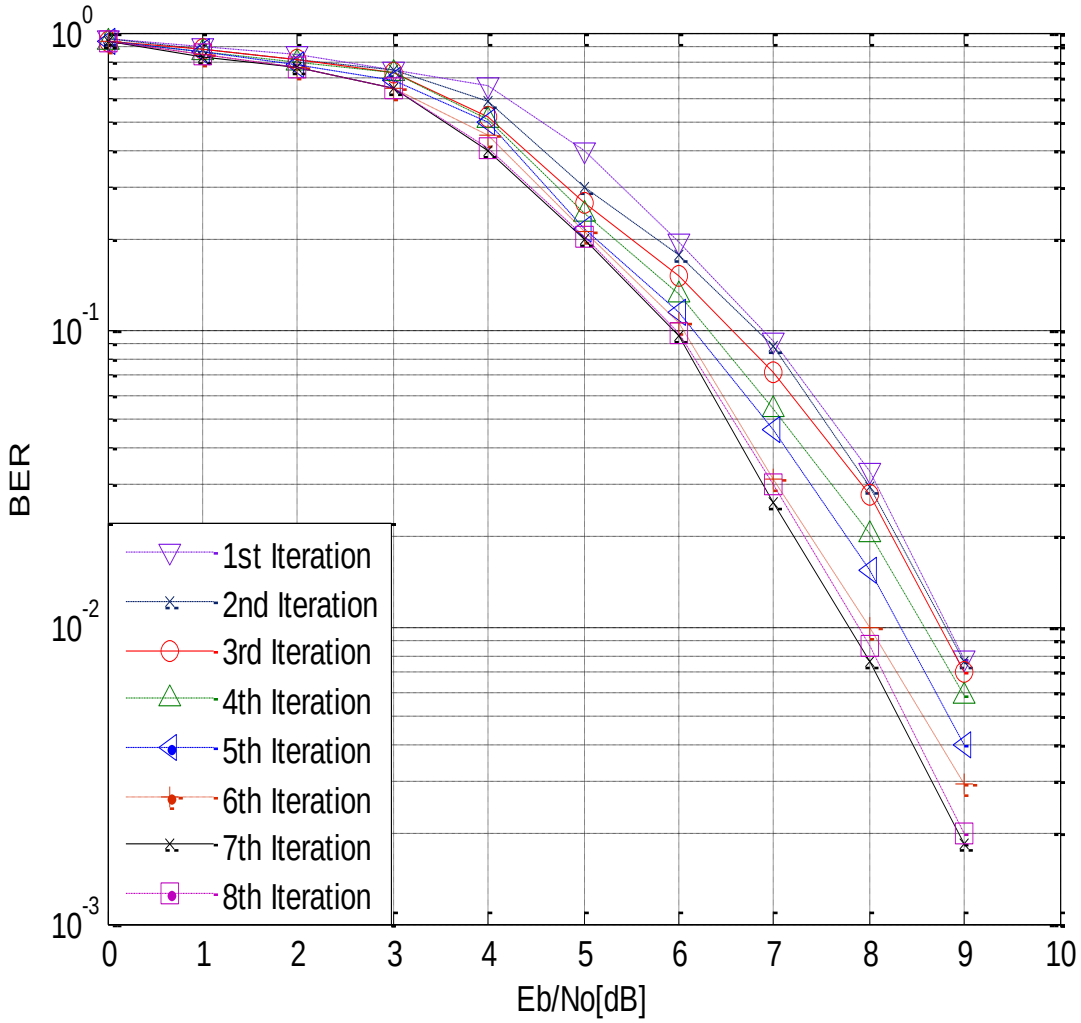

Figure 3.10 BER for different number of iteration for known channel state information (CSI) at the receiver, $fDT_s = 0.01$

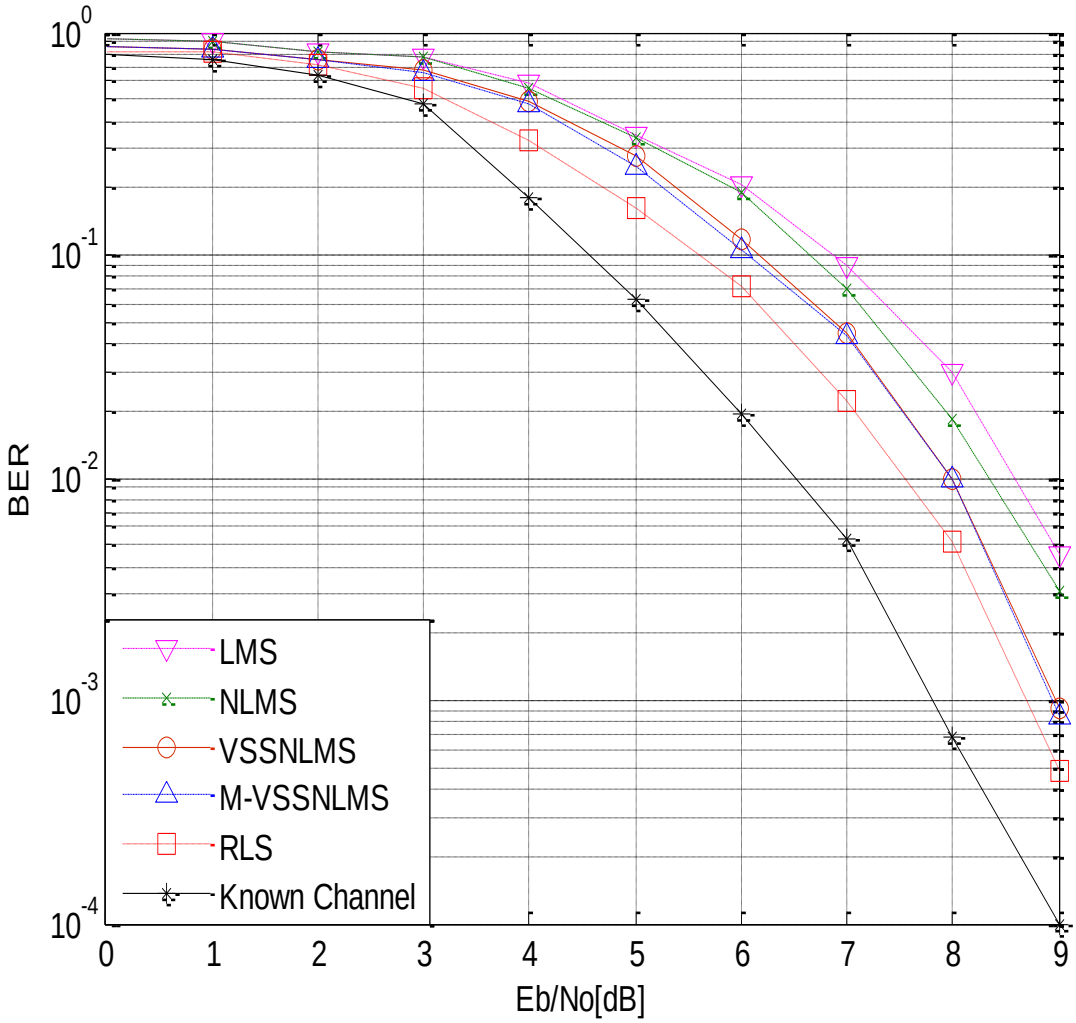

Figure 3.11 BER for different iterative channel estimator algorithms, fDT= 0.005

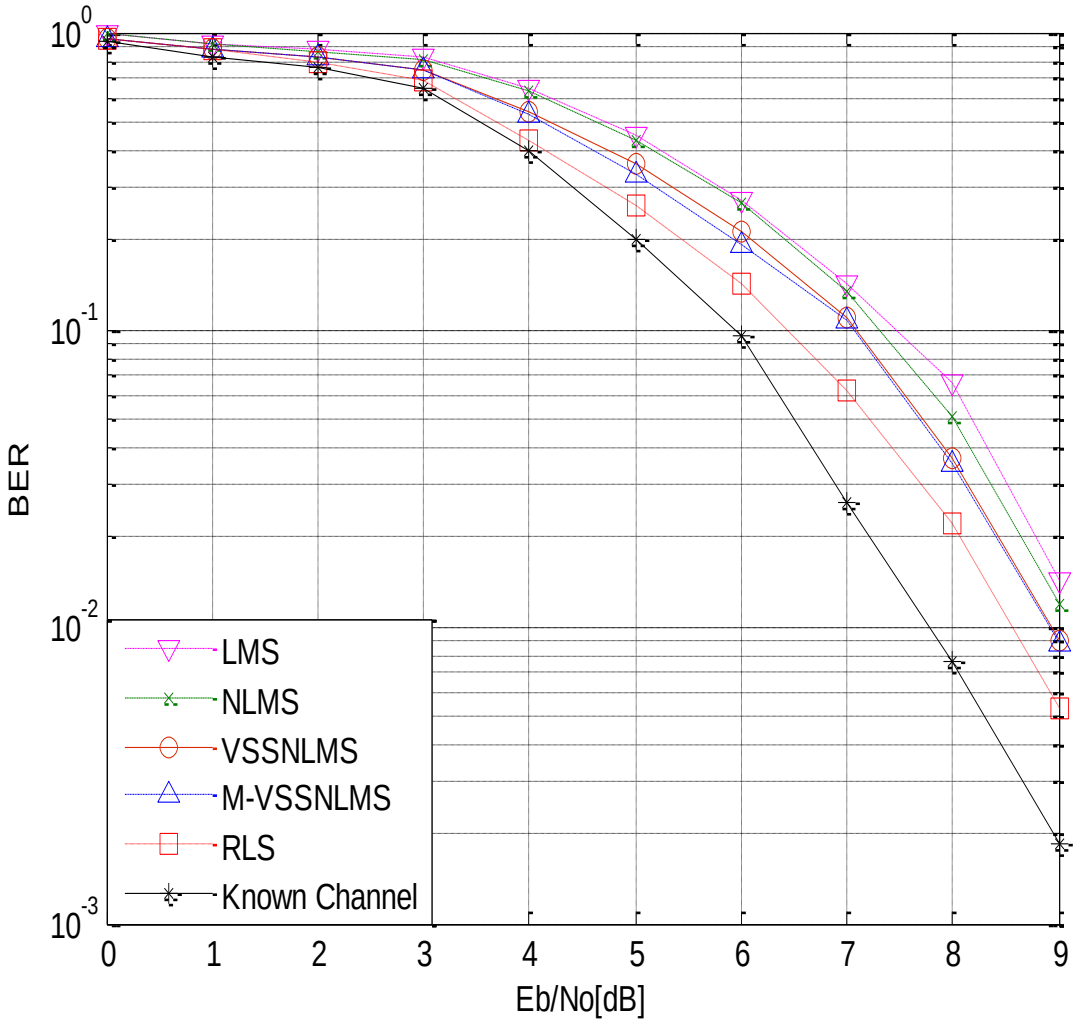

Figure 3.12 BER for different iterative channel estimator algorithms, fDT =0.01

3.6 Computational Complexity of the proposed Algorithms

Comparative computational complexity in terms of coefficient update are given in [152] for both NLMS and RLS algorithms to be of order $O(ML)$ and $O(ML^2)$ respectively, where L is the filter length and M is the channel maximum delay. However, the VSSNLMS algorithm only requires L extra additions and $(L+4)$ extra multiplications (divisions) compared with NLMS algorithm. It then turns out to be that the coefficient update of VSSNLMS-based channel estimator will be of order $O[(3L+4)M]$, which is still far lower than that of RLS-based channel estimator for a large filter length such as $L = 10$ or higher depending on the available chip's memory. In the case of multiple-VSSNLMS-based channel estimator, this requires ML extra addition and $M(L+4)$ extra multiplications (divisions) compared with NLMS algorithm. Consequently, computational complexity in terms of coefficient update for the multiple-VSSNLMS-based channel estimator is of order $O[(3L+4)\ M^2]$. Obviously, it is expected that due to the multiple step-size being employed by multiple-VSSNLMS algorithm, the algorithm would be of higher complex structure in comparison with VSSNLMS algorithm that uses single variable step-size for the estimation of all the CIR taps.

3.7 Chapter Summary

In this chapter, soft input iterative channel estimation for single antenna communication Systems has been considered. The benefits of the iterative receiver are verified through the presented simulations results. Two variable step-size algorithms are also proposed for iterative channel estimation of communication Systems in a bid to address the problem of slow convergence rate and channel tracking capabilities associated with the LMS and NLMS-based channel estimation algorithms. The chapter also put forward the use of a less complex algorithm that is realizable in a real-time application. From the results in the first phase of the simulation carried out in this chapter, it is obvious that the VSSNLMS-based iterative channel estimation algorithm shows a faster convergence rate than both APRmodRLS algorithm and the recommended LMS algorithm of [183, 184]. In the second phase of the simulation work, it is observed from the simulation results that both single and multiple-VSSNLMS-based iterative channel estimation algorithms outperform both LMS and NLMS algorithms and their performances are close to that of RLS algorithm. The performances of the various algorithms in this chapter are summarized in Table 3.1.

Table 3.1 Summary of the Performances of the Channel estimation algorithms

Algorithms	Performance indexes	
	MSE	BER
LMS	Fair	Fair
NLMS	Fair	Fair
APRmodRLS	Good	-
VSSNLMS	Very good	Good
M-VSSNLMS	-	Good
RLS	Very good	Very good

Consequent upon the negligible difference in the performance of the VSSNLMS and multiple-VSSNLMS algorithms, it could be concluded that the VSSNLMS algorithm which is less complex than both multiple-VSSNLMS and RLS algorithms is suitable for the tracking and the estimation of a fast-varying channels in single antenna communication Systems. The proposed algorithms have similarly been deployed for network echo cancellation and the results obtained which are presented in [222, 223] further confirmed the efficiency of these algorithms.

CHAPTER 4

DECISION DIRECTED CHANNEL ESTIMATION FOR OFDM SYSTEMS

4.1 Introduction

Due to the growth of mobile communications over the years, there have been strong demands for improved wireless Systems. However, the problem confronting the design of wireless communication Systems come from some limiting factors associated with wireless environments, such as multipath fading, Doppler effect and co-channel interference. The negative effect of multipath fading of wireless channels results in inter-symbol interference (ISI). This in turn imposes a limit on the transmission rate of single-carrier Systems. In conventional single-carrier communication Systems of chapter 3, the problem of ISI is mostly addressed by employment of a time domain channel equalizer. Nevertheless, when the signal rate increases, the symbol duration decreases and as a result the equalizer structure becomes very complex. Recently, Orthogonal Frequency Division Multiplexing (OFDM) scheme was introduced as a robust solution to the problem ISI as well as to produce a high-bit-rate transmission over mobile wireless channel [21, 224]. However, as emphasized in [225], the availability of accurate channel state information remains a crucial factor in maximizing both the channel capacity and the integrity of communication Systems. It is therefore obvious that the efficient system performance in the single antenna OFDM Systems depends largely on the availability of robust and accurate channel estimation technique. In this chapter, decision directed channel estimation scheme is therefore proposed for OFDM Systems. The proposed scheme is based on one of the algorithms proposed in the previous chapter and a subspace algorithm.

The rest of this chapter is organized as follows. Section 4.2 briefly describes SISO OFDM system model, while channel model is presented in Section 4.3. Detail of the proposed decision directed channel estimator for SISO OFDM system is presented in Section 4.4. Section 5 and

Section 6 respectively described both soft demapper and soft mapper that are used in this chapter. Simulation results are presented and discussed in Section 4.7. Section 4.8 presents comparative computational complexity of the proposed DDCE scheme for SISO OFDM Systems, while the chapter is finally summarized in Section 4.9.

4.2 SISO OFDM System Model

The block diagram of the SISO OFDM transceiver considered in this chapter is shown in Figure 4.1. The transmitter part comprises a turbo encoder with two Recursive Systematic Encoder (RSE) used as the Forward Error Correcting (FEC) code for the information data sequence b_p. The interleaver that follows the encoder interleaves the output of the turbo encoder c to c'. A Quadrature Phase Shift keying (QPSK) modulator is used to modulate the two consecutive interleaved bits c' to message QPSK symbol, y[n]. The modulated message symbols are multiplexed with QPSK pilot symbols, t[n] with the aid of multiplexer. The multiplexed symbols are passed through the serial-parallel (S/P) converter. A K-point Inverse Fast Fourier Transform (IFFT) is then applied to the multiplexed symbols, resulting in the OFDM symbols, x[n, k]. In order to combat intersymbol interference due to multipath channel, a guard time in form of cyclic prefix (CP) is inserted between consecutive OFDM symbols before transmission in the frequency selective fading channel. At the receiver, the reverse operation takes place. As shown in Figure 4.1, the receiver incorporates the DDCE for the purpose of estimating the channel state information needed for coherent detection of the transmitted OFDM symbols. The channel estimate is fed into the Soft Demapper that calculates the soft information about each transmitted bit. The interleaved soft information is used by the turbo decoder to make the final decision about the possible transmitted bits.

4.3 Channel Model

The considered channel model is the complex baseband representation of a multipath Rayleigh fading channel of a mobile wireless system given as [42, 154]:

$$h(t,\tau) = \sum_{m=1}^{M} \gamma_m(t) c(\tau - \tau_m) , \tag{4.1}$$

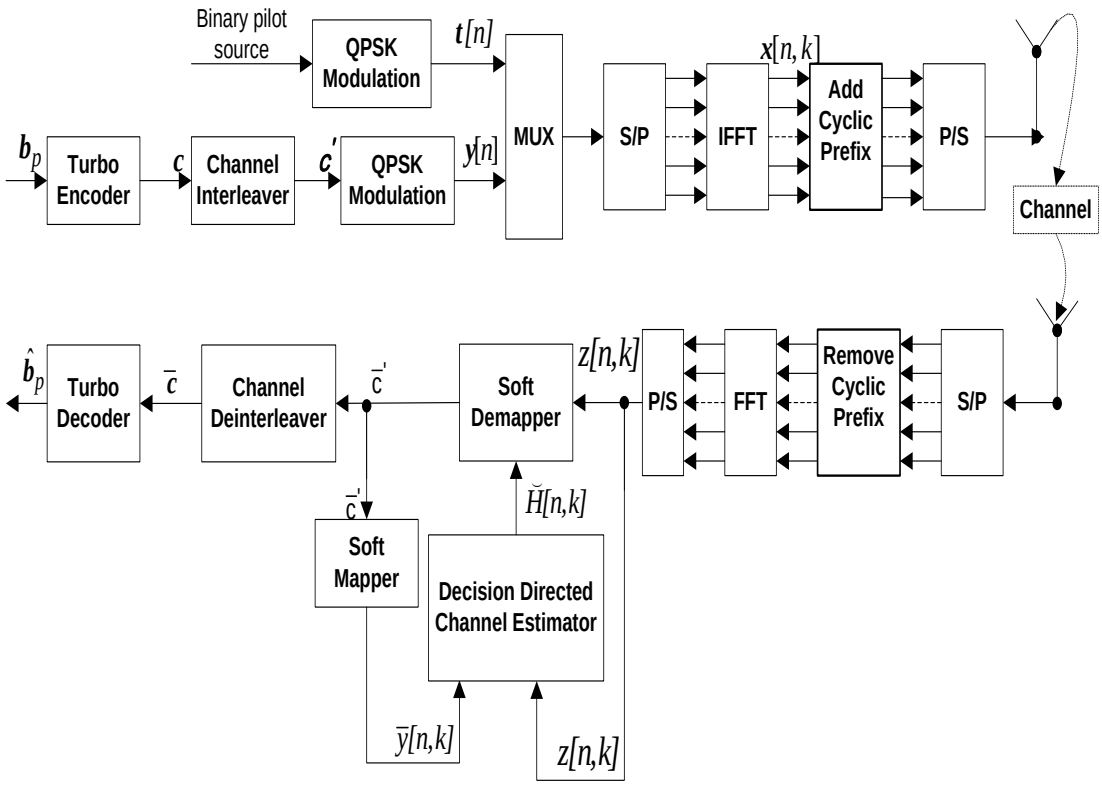

Figure 4.1 SISO OFDM System Transceiver with Decision Directed Channel Estimator

where $\gamma_m(t)$ is the different path time-varying complex gains, τ_m is the different path time delays, $c(\tau)$ is the aggregate impulse response of the transmitter-receiver pair that corresponds to the square-root raised-cosine Nyquist filter, and M is the number of paths. The symbols $\gamma_m(t)$ are always modeled to be wide sense stationary (WSS) narrowband complex Gaussian processes. These are independent for different paths in the fading channel as a result of the motion of one of the communicating terminals. The frequency response of (4.1) at time t is described as [31]

$$H(t,f) \triangleq \int_{-\infty}^{\infty} h(t,\tau) e^{-j2\pi f\tau} d\tau \ ,$$

$$= C(f) \sum_{m} \gamma_m(t) e^{-j2\pi f \tau_m} \qquad (4.2)$$

where $C(f) \triangleq \int_{-\infty}^{\infty} c(\tau) e^{-j2\pi f\tau} d\tau$ is the Fourier transform pair of the transceiver's impulse response $c(\tau)$. It is further stated in [31] that for OFDM Systems with proper cyclic extension and adequate synchronization, the discrete subcarrier-related Channel Transfer Function (CTF) can be expressed as:

$$H[n,k] \triangleq H(nT, k\Delta f) = \sum_{l=0}^{K_0-1} h[n,l] W_K^{kl}$$

$$= C(k\Delta f) \sum_{m=1}^{M} \gamma_m[n] W_K^{k\tau_m / T_s}, \tag{4.3}$$

where

$$h[n,l] \triangleq h(nT, lT_s) = \sum_{m=1}^{M} \gamma_m[n] c(lT_s - \tau_m), \tag{4.4}$$

is the Sampled Spaced-Channel Impulse Response (SS-CIR) and $W_K = \exp(-j2\pi / K)$. The quantities *M*, *K*, K_0 and T_s denote the number of Fractionally Spaced (FS) channel paths, the number of OFDM subcarriers, the number of equivalent Sample Spaced (SS)-CIR taps, and the base-band signal's sample duration respectively. However, in realistic channel conditions associated with non-sample spaced time-variant path-delays $\tau_m(n)$, the receiver, as noted in [154], will encounter received signal components dispersed over several neighboring samples owing to the convolution of the transmitted signal with the system's CIR, which is referred to as leakage. But this phenomenon is unavoidable and therefore the resultant SS-CIR $h[n,l]$ will comprise numerous correlated non-zero taps as indicated in (4.1). In contrast to this, the fractionally-spaced CIR (FS-CIR), also known as non-Sample Spaced-CIR, $\gamma_m(n) = \gamma_m(nT)$ will be constituted by a low number of $M \le K_0 \le K$ statistically independent non-zero taps associated with distinctive propagation paths [154]. Because it is more computationally efficient to estimate this low number of fractionally-spaced CIR-related taps experienced in a realistic channel condition than estimating all the correlated non-zero SS-CIR taps, the fractionally-spaced CIR channel model is best fit into the implementation of OFDM system.

The time-domain and frequency-domain correlation properties of the discrete CTF coefficients $H[n,k]$ associated with different OFDM blocks and subcarrier is characterized by the cross-correlation function $r_H[l,m]$, for $l = \Delta t$ and $m = \Delta f$, given as [225, 226]

$$r_H[l,m] \triangleq E\ \ H[n+l,k+m]H^*[n,k]$$

$$= \sigma_H^2 r_t[l] r_f[m], \tag{4.5}$$

where σ_H^2 is the total average power of the CIR defined as

$$\sigma_H^2 = \sum_{m=1}^{M} \sigma_m^2, \tag{4.6}$$

where $\sigma_m^2 \cong E\ |\gamma_m[n]|^2$.

The time-domain correlation function of the cross correlation function that characterizes CIR component γ_m associated with an individual channel path is denoted as $r_t[l]$ in (4.5). This is generally modeled by a wide sense stationary (WSS) narrow-band complex Gaussian process, and it is described as follows

$$r[l,j] = E\ \ \gamma_i[n]\gamma_j^*[n-l]$$

$$= r_{t;i}[l]\delta[i-j]. \tag{4.7}$$

In (4.5), the frequency-domain correlation functions is denoted as $r_f[m]$ and is given as [149]

$$r_f[m] = |C(m\Delta f)|^2 \sum_{m=1}^{M} \frac{\sigma_m^2}{\sigma_H^2} e^{j2\pi m\Delta f \tau_m}. \tag{4.8}$$

As a result of the insertion of cyclic prefix (CP) after OFDM modulation, the channel matrix will become circulant matrix whose columns are composed of circularly shifted versions of a zero-added channel vector. Hence, the linear convolution performed by the channel is converted to a circular convolution. The received signal in the discrete frequency domain, after the CP has been removed, is given as

$$z[n,k] = H[n,k]x[n,k] + w[n,k], \tag{4.9}$$

for $k = 0,1,...,K-1$ and all *n*'s. In (4.9), $x[n,k]$, $w[n,k]$ and $H[n,k]$ are the transmitted symbol, additive white Gaussian noise sample and the complex CTF coefficient respectively, associated with the *kth* subcarrier of the *nth* OFDM symbol.

4.4 Proposed Decision Directed Channel Estimator for SISO OFDM Systems

In order to come out with robust channel estimation techniques for single antenna OFDM Systems, efforts have been directed towards obtaining efficient channel estimation techniques for OFDM Systems by researchers as indicated in Chapter 2. Decision Directed Channel Estimation (DDCE) method [39, 48, 149, 154] happened to be the most recent channel estimation technique which has emerged from these efforts. In the absence of symbol errors, the DDCE method has been proved to provide better and accurate CSI than the well known purely pilot-assisted channel estimation techniques. The reason for this is because in the absence of transmission errors, the DDCE scheme could be viewed as a pilot assisted channel estimation scheme employing approximately hundred percent pilot information for the channel estimation as against the purely pilot assisted scheme with sparsely available pilot symbols for the same estimation [48, 149, 154]. The DDCE scheme comprises three modules as depicted in Figure 4.2. The first one is the temporary CTF estimator referred to in [5, 6] as *a posteriori* CTF estimator, followed by parametric CIR estimator, while the last stage is the CIR predictor referred to as *a prior* CIR predictor module in [48, 154].

In this chapter, we propose the use of Fast Data Projection Method (FDPM) algorithm, recently developed in [227], to implement the CIR estimator module of the DDCE scheme. We also derive a Variable Step Size Normalized Least Mean Square (VSSNLMS)-based predictor following the method in [42]. This is employed to implement the adaptive predictor module of the DDCE scheme. The DDCE scheme is implemented in the context of a more realistic Fractionally Spaced-Channel Impulse Response (FS-CIR) channel model, as described above, as against the channel that is characterized by a Sample Spaced (SS)-CIR which is assumed in [149].

The inputs to the CTF estimator are the received symbols $z[n,k]$ and the output of the soft mapper $\bar{y}[n,k]$. During the initialization stage of the estimation scheme, pilot symbols, $t[n]$ multiplexed to all the carriers, are used instead of the soft mapper's output $\bar{y}[n,k]$, to initiate the estimation process, while $\bar{y}[n,k]$ are used in the subsequent estimation stages. The inputs to the CTF estimator are used to make a temporary estimate of the CTF coefficients $\hat{\boldsymbol{H}}[n]$ that correspond to the current channel state. The output of the CTF estimator is fed into the parametric

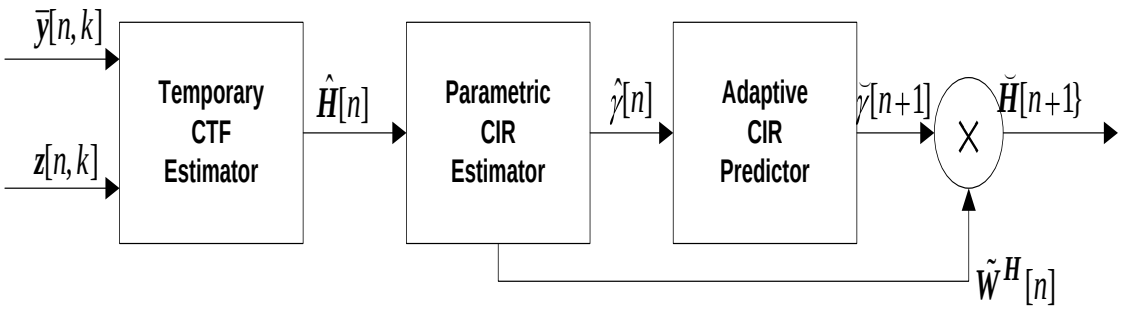

Figure 4.2 Decision Directed Channel Estimator Modules for SISO OFDM Systems [154]

CIR estimator to generate the FS-CIR $\hat{\gamma}[n]$. This is employed by the adaptive CIR predictor to predict an *a priori* estimate $\breve{\gamma}_{n+1}$ of the next CIR on a tap-by-tap-basis [1, 2]. The predicted CIR is convolved with the transformation matrix $\tilde{W}[n]$ to obtain the Frequency Domain FD-CTF $\breve{H}[n+1]$. During the $_{n+1\ th}$ OFDM-symbol period, the FD-CTF $\breve{H}[n+1]$ is employed by the soft demapper to produce the soft input for the decoder. This process continues until all the symbols are detected.

4.4.1 Temporary CTF Estimator

The Temporary CTF estimator module of the DDCE scheme is based on the Minimum Mean Square Error (MMSE) estimator [228]. This is similar to what is employed in [154]. By assuming the parameters *H[n,k]* to be complex-Gaussian distributed with a zero mean and variance of σ_H^2, the noisy MMSE estimate of the FD-CTF coefficients *H[n,k]* of the scalar linear model described by (4.9), using the two inputs signals to the CTF Estimator, is given as [226, 228]

$$\tilde{H}[\mathrm{n,k}] = \left(\frac{\bar{y}[\mathrm{n,k}]\bar{y}[\mathrm{n,k}]}{\sigma_w^2} + \frac{1}{\sigma_H^2} \right)^{-1} . \frac{\bar{y}[\mathrm{n,k}]z[\mathrm{n,k}]}{\sigma_w^2}$$

$$= \frac{\bar{y}[\mathrm{n,k}]z[\mathrm{n,k}]}{|\bar{y}[\mathrm{n,k}]|^2 + \frac{\sigma_w^2}{\sigma_H^2}}, \qquad (4.10)$$

where the noisy estimate $\tilde{H}[\mathrm{n},\mathrm{k}]$ could be written as

$$\tilde{H}[\mathrm{n},\mathrm{k}] = H[\mathrm{n},\mathrm{k}] + v[\mathrm{n},\mathrm{k}], \tag{4.11}$$

and $v[\mathrm{n},\mathrm{k}]$ denotes the *i.i.d.* complex-Gaussian noise samples with a zero mean and a variance of $\sigma_v^2 = MSE_H$. Additive white Gaussian noise's variance, $\sigma_\omega^2 = N_0/2$, where N_0 is the noise power. The symbol MSE_H denotes the average Mean Square Error (MSE) associated with the MMSE CTF estimator of (4.10).

4.4.2 Parametric CIR Estimator based on FDPM Algorithm

The idea of employing the signal subspace technique for estimation of parametric channel model for OFDM Systems is first deployed in [229] and is followed up in [154]. Nevertheless, the approach of parametric channel model has earlier been applied to Global System for Mobile Communications system [230] and the high-speed digital video broadcast system [91] to enhance the performance of channel equalizer and estimator. As stated in [229], the main reason behind the deployment of subspace technique here is because there is always a low number of M (the number of FS-CIR taps) in comparison with K (the total number of FD-CIR taps), that is $M \ll K$. Consequently, it is more computationally efficient to estimate a low number of CIR-related taps in the low dimensional signal subspace than having to estimate all the FD-CTF coefficients.

By following the approach in [226], the substitution of $H[\mathrm{n},\mathrm{k}]$ in (4.11) with (4.3) results in

$$\tilde{H}[n,k] = C(k\Delta f)\sum_{m=1}^{M}\gamma_m[n]W_K^{k\tau_m/T_s} + v[n,k], \tag{4.12}$$

where $C(f)$ denotes the frequency response of the transceiver's pulse-shaping filter and $W_k = e^{-j2\pi\frac{1}{K}}$, while γ_m and τ_m are the amplitudes and the relative delays of the FS-CIR taps respectively. In matrix form (4.12) becomes

$$\tilde{\boldsymbol{H}}[n] = \tilde{\boldsymbol{W}}\gamma[n] + v[n], \tag{4.13}$$

where $\tilde{\boldsymbol{W}} = diag(C[k])\boldsymbol{W}$ is defined as ($K \times M$)-dimensional matrix in which $diag(C[k])$ is a ($K \times K$)-dimensional diagonal matrix with the corresponding elements of the vector $C(f)$ on the main diagonal [226]. Symbol $\boldsymbol{W}$ is the Fourier Transform matrix defined by

$W_{km} = W_K^{k\tau_m / T_s}$ for all *K's* and *M's*. Since the channel's Power Delay Profile (PDP) and the associated transformation matrix $(\tilde{\boldsymbol{W}})$ will be time-varying if one of the communication terminals is in motion, and might not be known *a priori*, there is need for accurate tracking of this channel's parameter.

In [154] results of recursive tracking of OFDM channel's PDP and the associated transformation matrix employing PASTd algorithm are presented. However, some shortcomings of the PASTd algorithm are highlighted in [227]. One of these is the fact that the deflation technique applied on PAST algorithm to arrive at PASTd version causes a stronger loss of orthonormality between eigenvector $\boldsymbol{w}_m[n]$ of the transformation matrix $\tilde{\boldsymbol{W}}_n$ for $m=1,...,M$. Therefore, if there are some post-processing methods that use the signal subspace estimate, from which an orthonormal basis of the signal subspace is required in order to extract the desired signal information, the transformation matrix has to be re-orthonormalized. This will result in increase in the computational complexity of the process. Another shortcoming mentioned in [227] is the fact that PASTd algorithm exhibits an increase in computational complexity if $K \gg M$. In a bid to avoid these shortcomings, the FDPM algorithm [227] that possesses a simple structure with a single parameter (the step-size of the algorithm) to be specified is hereby proposed for the first time and employed in this chapter for accurate tracking of the FS-CIR's PDP instead of the PASTd algorithm used in [154]. The FDPM algorithm has an extremely high convergence rate towards orthonormality. It is also the fastest among all competing subspace algorithms of the same computational complexity, including the PAST and the PASTd algorithms, as observed in [227].

The description of FDPM algorithm, as adapted to parametric CIR estimation, is given as follows. If $\boldsymbol{C}_H$ is a symmetric, nonnegative, definite, covariance matrix of the observation vectors $\hat{\boldsymbol{H}}[n]$ of size *K*, its singular vectors corresponding to the *M* dominant singular values can be computed with the aid of an iterative procedure referred to as orthogonal iteration [231] that has the following variants [227]

$$\tilde{\boldsymbol{W}}[n] = orthnorm \quad \boldsymbol{I}_K \pm \mu \boldsymbol{C}_H \quad \tilde{\boldsymbol{W}}[n-1] \ , \quad n=1,2,... \tag{4.14}$$

while $\mu > 0$ is a small scalar parameter known as *step size* and *"orthnorm"* stands for orthonormalization process. In the case where matrix $\boldsymbol{C}_H$ is unknown and the data vector

sequence $\hat{\boldsymbol{H}}[n]$ is acquired sequentially, $\boldsymbol{C}_H$ in (4.14) can be replaced with an adaptive estimate $\boldsymbol{C}_H[n]$ that satisfies $E\ \boldsymbol{C}_H[n] = \boldsymbol{C}_H$. This results in the Adaptive Orthogonal Iterative algorithm given as [227]:

$$\tilde{\boldsymbol{W}}[n] = orthnorm\ \ \boldsymbol{I}_K \pm \mu \boldsymbol{C}_H[n]\ \tilde{\boldsymbol{W}}[n-1]\ ,\ n = 1,2,\ldots\ . \tag{4.15}$$

The choice of $\boldsymbol{C}_H[n]$ will lead to different subspace tracking algorithms. However, the simplest selection for $\boldsymbol{C}_H[n]$ is the instantaneous estimate of the covariance matrix, $\boldsymbol{C}_H[n] = \hat{\boldsymbol{H}}[n]\hat{\boldsymbol{H}}^H[n]$ which results in the Data Projection Method (DPM) introduced in [42] and given as follows:

$$\hat{\gamma}[n] = \tilde{\boldsymbol{W}}^{\boldsymbol{H}}[n-1]\hat{\boldsymbol{H}}[n]\,, \tag{4.16}$$

$$\boldsymbol{T}[n] = \tilde{\boldsymbol{W}}[n-1] \pm \mu \hat{\boldsymbol{H}}[n]\hat{\gamma}^H[n]\ , \tag{4.17}$$

$$\hat{\boldsymbol{W}}[n] = orthnorm\ \ \boldsymbol{T}[n]\ \ , \tag{4.18}$$

while the orthonormalization is performed using Gram-Schmidt. In [227], Gram-Schmidt part is removed and a faster orthonormalization procedure based on Housholder transformation is applied to the DPM algorithm that reduces the overall complexity to order $O(KM)$ which eventually results in the FDPM algorithm. The summary of the FDPM algorithm as applied to the tracking of the FS-CIR's PDP is given in Table I.

Table 4.1 Fast Data Projection Method Algorithm [227]

- For faster convergence, $\tilde{\boldsymbol{W}}[0]$is initialized to orthonormal matrix (typically the first *M* columns of the identity matrix) with *K* rows.
- With the new observation $\hat{\boldsymbol{H}}[n]$, the FDPM algorithm is applied as follow:

For $n = 1, 2, \ldots$

$$\hat{\gamma}[n] = \tilde{\boldsymbol{W}}^{\boldsymbol{H}}[n-1]\hat{\boldsymbol{H}}[n]$$

$$\bar{\mu} = \mu \Big/ \left\| \hat{\boldsymbol{H}}[n] \right\|^2$$

$$\boldsymbol{T}[n] = \tilde{\boldsymbol{W}}[n-1] \pm \bar{\mu}\hat{\boldsymbol{H}}[n]\hat{\gamma}^H[n]$$

$$\boldsymbol{a}[n] = \hat{\gamma}[n] - \left\|\hat{\gamma}[n]\right\| \boldsymbol{e}_1\ , \qquad \text{where } \boldsymbol{e}_1 = 10\ldots0^{\,T}$$

$$\boldsymbol{Z}[n] = \boldsymbol{T}[n] - \frac{2}{\left\|\boldsymbol{a}[n]\right\|^2}\ \boldsymbol{T}[n]\boldsymbol{a}[n]\ \boldsymbol{a}^H[n]$$

$$\tilde{\boldsymbol{W}}[n] = normalize\ \ \boldsymbol{Z}[n]\ \ , \quad \text{this is the normalization of each column of } \boldsymbol{Z}[n]\,.$$

end

The performance index for FDPM subspace tracking algorithm, in order to compare it with PASTd algorithm, is defined in terms of the MSE criterion as follows

$$MSE = E\ |\boldsymbol{e}(n)|^2\ , \tag{4.19}$$

where $\boldsymbol{e}(n)$ is given as

$$\boldsymbol{e}(n) = \hat{\boldsymbol{H}}[n] - \tilde{\boldsymbol{W}}[n-1]\hat{\boldsymbol{\gamma}}[n]\ . \tag{4.20}$$

4.4.3 Channel Impulse Response (CIR) Predictor

In [152] three variants of MMSE predictors and two types of adaptive predictors for implementation of the proposed DDCE scheme for OFDM Systems are presented. The variants of the MMSE prediction techniques presented includes the full-blown MMSE predictor, reduced complexity MMSE predictor, and the DFT implementation-based MMSE predictor. In the class of adaptive predictors, also presented in [152], are the Recursive Least Square (RLS) and the Normalized Least Means Square (NLMS) predictors. In [234], comparative results are presented for both robust MMSE predictor and the adaptive RLS predictor. In both [152] and [234] it is concluded that the adaptive predictor outperforms its MMSE counterpart especially in a fast time varying channels because of its ability to track time-varying channel and noise statistics. This is due to the fact that the adaptive predictors do not require *a priori* knowledge of channel and noise statistics, the channel correlation functions and the noise variance, which change slowly with time. On the other hand, the performance of the MMSE predictor depends largely on the *a priori* knowledge of the channel and noise statistics (which are time-varying and are not known *a priori*), in the absence of which its performance is grossly affected. Hence, the adaptive predictors are considered as a better alternative for employment in wireless communications Systems.

Between the two adaptive predictors proposed in [152], the RLS predictor is said to perform better than the NLMS predictor. This is due to the fact that the RLS algorithm converges faster with smaller excess Mean Square Error (MSE) in comparison with the NLMS algorithm as mentioned and demonstrated in Chapter 3. However, the computational complexity in terms of the coefficient update is said to be significantly more costly for RLS than NLMS, in particular for large filter length [152]. This, in a way, imposes a limitation to the deployment of the RLS predictor in a real time implementation. It is against this background that we seek to derive an improved version of NLMS-based predictor with faster convergence rate close to, but with less

complexity when compared with the RLS-based predictor. This predictor is hereby tagged Variable Step Size NLMS (VSSNLMS)-based CIR predictor. The CIR predictor predicts the *a priori* estimate of the CIR taps, $\breve{\gamma}_m\ n+1$, associated with the next OFDM symbol, for m = 0, 1,..., M -1 on a tap-by-tap basis by employing the previous CIR taps tagged *a posteriori* CIR taps [152]. However, in the time domain, the *mth* CIR component $\gamma_m(n)$ will experience a narrowband fading process that is characterized by an associated cross-correlation function. This cross-correlation function can be described as[152]

$$E\ \gamma_m[n]\gamma_m^*[n-l]\ = r_t[l]\delta[i-j], \tag{4.21}$$

where $r_t[l]$ denotes the time-domain correlation function and $\delta[.]$ is the Kronecker delta function. The narrowband process of (4.21) can be approximately modeled as an autoregressive process of the order L_{prd} [152]. The *a priori* estimate of the *mth* CIR component predicted by the predictor is given as

$$\breve{\gamma}_m[n+1]=\boldsymbol{p}_m^H[n]\hat{\boldsymbol{\gamma}}_m[n], \tag{4.22}$$

where the *mth* CIR tap's finite impulse response prediction filter coefficient vector is denoted as $\boldsymbol{p}_m=\{p_m[0], p_m[1],..., p_m[L_{prd}-1]\}$,

and

$\hat{\gamma}_m[n]=\{\hat{\gamma}_m[n], \hat{\gamma}_m[n-1],..., \hat{\gamma}_m[n-L_{prd}+1]\}^T$.

The two adaptive predictors, the RLS and the NLMS predictors proposed in [152] with the VSSNLMS predictor derived in this chapter are presented in the next sub-sections.

4.4.3.1 Adaptive RLS Predictor

The RLS based CIR tap predictor [152, 215] calculates the *mth* predictor filter $\boldsymbol{p}_m[n]$ such that it minimizes the scalar cost function

$$\Omega_{RLS,m}[n]=\sum_{j=1}^{n}\lambda^{n-j}\left|\gamma_m\ \ j\ -\boldsymbol{p}_m^H\ \ n\ \gamma_m\ \ j-1\right|^2, \tag{4.23}$$

where λ is a forgetting factor that accounts for possible time varying attribute of the fading process of the mobile channel, and it can assume a value within the range $\mathbf{0}<\lambda\leq\mathbf{1}$. The RLS based predictor filter $\boldsymbol{p}_m[n]$ is updated by the following equation [152, 215]

$$\boldsymbol{p}_m[n]=\boldsymbol{p}_m[n-1]+\boldsymbol{k}_m\ \ n-1\ e_m^*[n], \tag{4.24}$$

where $e_m[n]$ is the prediction error and it is given as

$$e_m[n] = \hat{\gamma}_m[n] - \bar{\gamma}_m[n]$$
$$= \hat{\gamma}_m[n] - \boldsymbol{p}_m^H[n-1]\hat{\boldsymbol{\gamma}}_m[n-1], \quad (4.25)$$

and $\boldsymbol{k}_m\ n$ is the RLS gain vector given as [152, 215]:

$$\boldsymbol{k}_m\ n = \frac{\boldsymbol{G}_m\ n-1\ \hat{\gamma}_m^H\ n}{\lambda + \hat{\gamma}_m^H\ n\ \boldsymbol{G}_m\ n-1\ \hat{\gamma}_m\ n}. \quad (4.26)$$

In (4.26), the matrix $\boldsymbol{G}_m\ n$ is the inverse of the $L_{prd} \times L_{prd}$ sample covariance matrix of the *mth* CIR tap. The matrix $\boldsymbol{G}_m\ n$ can be obtained recursively as

$$\boldsymbol{G}_m\ n = \frac{1}{\lambda}\ I - \boldsymbol{k}_m\ n\ \hat{\gamma}_m^H\ \boldsymbol{G}_m\ n-1\ . \quad (4.27)$$

4.4.3.2 Adaptive NLMS Predictor

With NLMS algorithm, the CIR tap's predictor filter coefficients $\boldsymbol{p}_m[n]$ of length L_{prd} are updated as [152]

$$\boldsymbol{p}_m[n] = \boldsymbol{p}_m[n-1] + \frac{\mu}{\left\|\hat{\boldsymbol{\gamma}}_m[n-1]\right\|^2} e_m^*[n]\hat{\boldsymbol{\gamma}}_m[n-1], \quad (4.28)$$

where μ is the constant step size and $e_m[n]$ is as expressed in (4.25). For stable operation, the NLMS algorithm requires μ to be within the range $0 < \mu < 2$ [215]. The selection of μ goes a long way to determine the convergence speed of excess Mean Square Error (MSE), as well as the ability to track the time-varying channel parameters. The values of $\mu \approx 0.5$ is said to give a good result in [152]. For n = 0, the predictor filters are initialized [152] as $\boldsymbol{p}_m[n] = 1\ \ 0\ \ 0\ \ \ldots\ \ 0^T$.

4.4.3.3 Adaptive VSSNLMS Predictor

Since it is the selection of the step size that determines the convergence rate of the adaptive NLMS predictor as well as its ability to track the fast time-varying channel, we hereby derive a variable step size version of the NLMS predictor tagged the Variable Step Size Normalized Least Mean Square (VSSNLMS) Predictor. By following the approach used to derive the VSSNLMS-based channel estimator for Turbo Equalizer-based communications receiver in Chapter 3 [232, 233], the VSSNLMS-based predictor is hereby derived as follow. The CIR tap's predictor filter coefficients $\boldsymbol{p}_m[n]$ are updated as

$$\boldsymbol{p}_m[n] = \boldsymbol{p}_m[n-1] + \frac{\mu[n]}{\|\hat{\gamma}_m[n-1]\|^2} e_m^*[n]\hat{\gamma}_m[n-1]. \quad (4.29)$$

The VSSNLMS-based predictor then predict the *a priori* estimate of the *mth* CIR component as

$$\bar{\gamma}_m[n+1] = \boldsymbol{p}_m^H[n]\hat{\gamma}_m[n], \quad (4.30)$$

where $e_m[n]$, the prediction error, is as expressed in (4.25) and $\mu[n]$ is the variable step-size which is updated following [232, 233] as

$$\hat{\mu}[n] = \mu[n-1] - \frac{\rho}{2}\frac{\partial e^2[n]}{\partial \mu[n-1]} \quad (4.31a)$$

$$\hat{\mu}[n] = \mu[n-1] - \frac{\rho}{2}\frac{\partial e^2[n]}{\partial \boldsymbol{p}_m[n]}.\frac{\partial \boldsymbol{p}_m[n]}{\partial \mu[n-1]} \quad (4.31b)$$

$$\hat{\mu}[n] = \mu[n-1] + \frac{\rho e[n,k]e^*[(n-1),k]\hat{\gamma}_m^T[n]\hat{\gamma}_m[n-1]}{\|\hat{\gamma}_m[n-1]\|^2}. \quad (4.32)$$

For the complex input signal and complex channel tap, (4.32) becomes

$$\hat{\mu}[n] = \mu[n-1] + \frac{\rho \,\mathrm{Re}\; e[n,k]e^*[(n-1),k]\hat{\gamma}_m^H[n]\hat{\gamma}_m[n-1]}{\|\hat{\gamma}_m[n-1]\|^2}. \quad (4.33)$$

In order to restrict the variable step size $\mu[n]$ to the range $0 < \mu[n] < 2$ which makes for stable operation of NLMS algorithm as stated above, the variable step size $\mu[n]$ in (4.29) is then confined to within the range given as

$$\mu[n] = \begin{cases} \mu_{\max} & if \quad \hat{\mu} > \mu_{\max} \\ \mu_{\min} & if \quad \hat{\mu} < \mu_{\min} \\ \hat{\mu}[n] & otherwise \end{cases}, \quad (4.32)$$

where $0 < \mu_{\min} < \mu_{\max} < 2$.

As with the NLMS predictor, for $n = 0$, the predictor filter's coefficient, using VSSNLMS-based predictor, are initialized as $\boldsymbol{p}_m[n] = \begin{bmatrix} 1 & 0 & 0 & \ldots & 0 \end{bmatrix}^T$.

4.5 Soft Demapper

For the QPSK constellation used for modulation of the coded bits in this chapter, $y^{i,j}[n]$ denotes one of the four QPSK symbols obtained, at the transmitter end of the system, by mapping two

successive interleaved bits c'_{μ} and $c'_{\mu+1}$ to QPSK constellation with *μMod2=0* as given in Table 4.2. Using the approach in [235], the soft demapper calculates log-likelihood ratios $L\ c'_{\mu} \mid z[n,k]$ and $L\ c'_{\mu+1} \mid z[n,k]$ of the two successive interleaved bits c'_{μ} and $c'_{\mu+1}$ respectively as

$$L\ c'_{\mu} \mid z[n,k] = \ln\left(\frac{\Pr\ z \mid c'_{\mu}=1, c'_{\mu+1}=0 + \Pr\ z \mid c'_{\mu}=1, c'_{\mu+1}=1\ \exp L_a\ c'_{\mu+1}}{\Pr\ z \mid c'_{\mu}=0, c'_{\mu+1}=0 + \Pr\ z \mid c'_{\mu}=0, c'_{\mu+1}=1\ \exp L_a\ c'_{\mu+1}}\right)$$

$$= \ln\left(\frac{B_n^{10} + B_n^{11} e^{L_a\ c'_{\mu+1}}}{B_n^{00} + B_n^{01} e^{L_a\ c'_{\mu+1}}}\right), \tag{4.33}$$

$$L\ c'_{\mu+1} \mid z[n,k] = \ln\left(\frac{\Pr\ z \mid c'_{\mu}=0, c'_{\mu+1}=1 + \Pr\ z \mid c'_{\mu}=1, c'_{\mu+1}=1\ \exp L_a\ c'_{\mu}}{\Pr\ z \mid c'_{\mu}=0, c'_{\mu+1}=0 + \Pr\ z \mid c'_{\mu}=0, c'_{\mu+1}=1\ \exp L_a\ c'_{\mu}}\right)$$

$$= \ln\left(\frac{B_n^{01} + B_n^{11} e^{L_a\ c'_{\mu}}}{B_n^{00} + B_n^{10} e^{L_a\ c'_{\mu}}}\right). \tag{4.34}$$

Table 4.2 QPSK constellation

Modulation Input bits: c'_{μ}, $c'_{\mu+1}$	Modulation Output Symbol $y^{i,j}[n,k]$
00	$y^{0,0}$ = exp(jπ/4)
01	$y^{0,1}$ = exp(3jπ/4)
10	$y^{1,0}$ = exp(-jπ/4)
11	$y^{1,1}$ = exp(-3jπ/4)

The probabilities $B_n^{i,j}$, with $i, j \in 0,1$ in (4.33) and (4.34) are obtained by employing probability function [235] given as

$$B_n^{i,j} = \Pr\ z[n,k] \mid y^{i,j}[n,k]$$

$$= \frac{1}{2\pi\sigma_w^2} \exp\left[-\frac{1}{2\sigma_w^2} \left| z[n,k] - \breve{H}[n,k] y^{i,j}[n,k] \right|^2 \right], \tag{4.35}$$

where σ_w^2 is the noise variance. The *a priori* values of bits $c_\mu^{'}$ and $c_{\mu+1}^{'}$: $L_a\ c_\mu^{'}$ and $L_a\ c_{\mu+1}^{'}$ respectively, are set to zero since there is no feedback from the decoder.

4.6 Soft Mapper

The soft mapper is used to estimate the symbols $\bar{y}[n,k]$ by using the outputs of the soft demapper. Hence, symbols $\bar{y}[n,k]$, at each *kth* subcarrier, can be computed using $L\ c_\mu^{'} \mid z[n,k]$ and $L\ c_{\mu+1}^{'} \mid z[n,k]$ as follow [179]

$$\bar{y}[n,k] = D_n^{00} + D_n^{01} + D_n^{10} + D_n^{11}, \tag{4.36}$$

where,

$$D_n^{i,j} = \Pr\left[c_\mu^{'} = i \right] \times \Pr\left[c_{\mu+1}^{'} = j \right] \times y^{i,j}[n,k]. \tag{4.37}$$

The probabilities $\Pr\left[c_\mu^{'} = 1 \right]$ and $\Pr\left[c_\mu^{'} = 0 \right]$ can be expressed respectively as

$$\Pr\left[c_\mu^{'} = 1 \right] = \frac{1}{2}\left(1 + \tanh\left(\frac{L\ c_\mu^{'} \mid z[n,k]}{2} \right) \right), \tag{4.38}$$

and

$$\Pr\left[c_\mu^{'} = 0 \right] = \frac{1}{2}\left(1 - \tanh\left(\frac{L\ c_\mu^{'} \mid z[n,k]}{2} \right) \right). \tag{4.39}$$

Similarly, the probabilities $\Pr\left[c_{\mu+1}^{'} = 1 \right]$ and $\Pr\left[c_{\mu+1}^{'} = 0 \right]$ can be expressed respectively for as

$$\Pr\left[c_{\mu+1}^{'} = 1 \right] = \frac{1}{2}\left(1 + \tanh\left(\frac{L\ c_{\mu+1}^{'} \mid z[n,k]}{2} \right) \right), \tag{4.40}$$

and

$$\Pr\left[c'_{\mu+1}=0\right]=\frac{1}{2}\left(1-\tanh\left(\frac{L\ c'_{\mu+1}\mid z[n,k]}{2}\right)\right). \tag{4.41}$$

4.7 Simulation Results and Discussion

This section presents the results of the simulation work conducted for the proposed DDCE for SISO OFDM system. For all the results presented, the QPSK-modulated OFDM system with K = 64 subcarriers and a total bandwidth of 800kHz are assumed. A rate 1/3 turbo encoder of octal generator polynomial 7/5, consisting of a random interleaver with size N = 2304 bits is employed. The symbol duration, *Ts* is 80μs, the CP length is 16 samples (1/4 of the symbol period) and the guard interval, *Tg* = 20μs. As a result the total block period, T is 100μs. The six-path time-varying Rayleigh fading COST 207 Typical Urban (TU) channel model of [43] with Doppler frequencies of 50Hz and 100Hz is employed. These parameters are tabulated in Table 4.3. The first OFDM symbol with 64 subcarriers comprises the pilot symbols which are used for the initialization of the channel estimation scheme. In our simulation, we assume M = 6 FS-CIR taps, η is set to 0.95 for PASTd algorithm. The length of the CIR predictor (L_{prd}) is set to 10, ρ is set to 0.002, and μ_0 = 0.5 is used for the NLMS-based predictor and to initialize the VSSNLMS-based predictor. The forgetting factor value λ for RLS-based predictor is set to 0.99. The optimal SISO turbo decoder, the Maximum A-Posteriori (MAP) decoder implemented as log-MAP in [221] is employed in this simulation.

The optimum value for the step size μ in Table 4.1, for convergence of the proposed FDPM algorithm, is between zero and unity ($0<\mu<1.0$) [227]. A value of μ close to unity is confirmed in [227] to give good result. Hence, this simulation commences by varying the value μ in Table 4.1 between 0.90 and 1.0 for FDPM algorithm, while using the NLMS-based predictor to implement the DDCE scheme of Figure 4.2. Figure 4.3 and Figure 4.4 correspond to the MSE results of FDPM for various values of μ, both in slow and fast fading channels respectively, while Figure 4.5 depicts the MSE as a function of the normalized fading frequency (fD) exhibited by FDPM based CIR estimator of the DDCE scheme for fixed SNR of 3dB, while using NLMS-based predictor for various values of μ. Figure 4.6 show the plot of the MSE versus μ exhibited by FDPM based CIR estimator of the DDCE scheme at fixed SNR of 3dB for fD =0.005 and 0.02 respectively, while Figure 4.7 shows corresponding plot for fD =0.01 and 0.015 respectively. The

results in Figure 4.3, Figure 4.4 and Figure 4.5 suggest that the optimum value of μ largely depends more on the fading rate than the SNR. The value of $\mu = 0.98$ appears to be a compromise between the slow and fast fading channels, and this value is used for the remaining simulations. This optimum value becomes more visible in the plots of Figure 4.6 and Figure 4.7 respectively. From Figure 4.3, Figure 4.4 and Figure 4.5, the value of $\mu = 1.0$ results in poor performance of the proposed FDPM algorithm. This is apparently due to instability in the algorithm as a result of using $\mu = 1.0$. The optimum value is expected to be a value in the region of $0 < \mu < 1.0$.

Table 4.3 System Parameters

Parameters	**Value**
FFT Size, Number of carriers (K)	64
Channel bandwidth, B	800kHz
Sample Period,1/B	12.5μs
Subcarrier spacing (Δf =B/K)	12.5kHz
Symbol duration,T (1/ Δf)	80μs
Guard interval (Tg)	20μs
Guard type	Cyclic extension
Total symbol duration (Ts = T+Tg)	100μs
Modulation	QPSK
Channel model	6-paths Rayleigh fading COST 207 Typical Urban (TU) channel model of Ref [12]
Maximum delay spread	20μs
Channel coding	1/3 rate, (7, 5) Turbo code

Simulations were also carried out in order to demonstrate the achievable performance of the proposed VSSNLMS predictor employed in the context of the decision-directed channel estimation for SISO OFDM system in comparison with the RLS-based predictor and NLMS-based

predictor. Figure 4.8 depicts the comparative prediction MSE versus the normalized Doppler frequency (fD) for the proposed VSSNLMS predictor and the adaptive RLS and NLMS predictors, while holding the SNR constant at 5dB. The normalized Doppler frequency (fD) is varied between the slow fading channel of normalized Doppler frequency fD= 0.001 and the fast fading channel of normalized Doppler frequency fD= 0.1. The achievable MSE performance gain of the proposed adaptive VSSNLMS predictor is observed to be far better than that of the NLMS predictor and close to that of the RLS predictor over the whole range of the normalized Doppler frequencies. The better performance could be attributed to the variable step size employed by the VSSNLMS-based predictor. In Figure 4.9, the MSE performance of the adaptive predictors is illustrated for the fast fading channel scenario with the normalized Doppler frequency fD=0.02, while SNR is increased from 0dB to 10dB. Once again, the proposed VSSNLMS predictor exhibits a better performance in comparison with the NLMS predictor, and its performance is close to that of the RLS predictor.

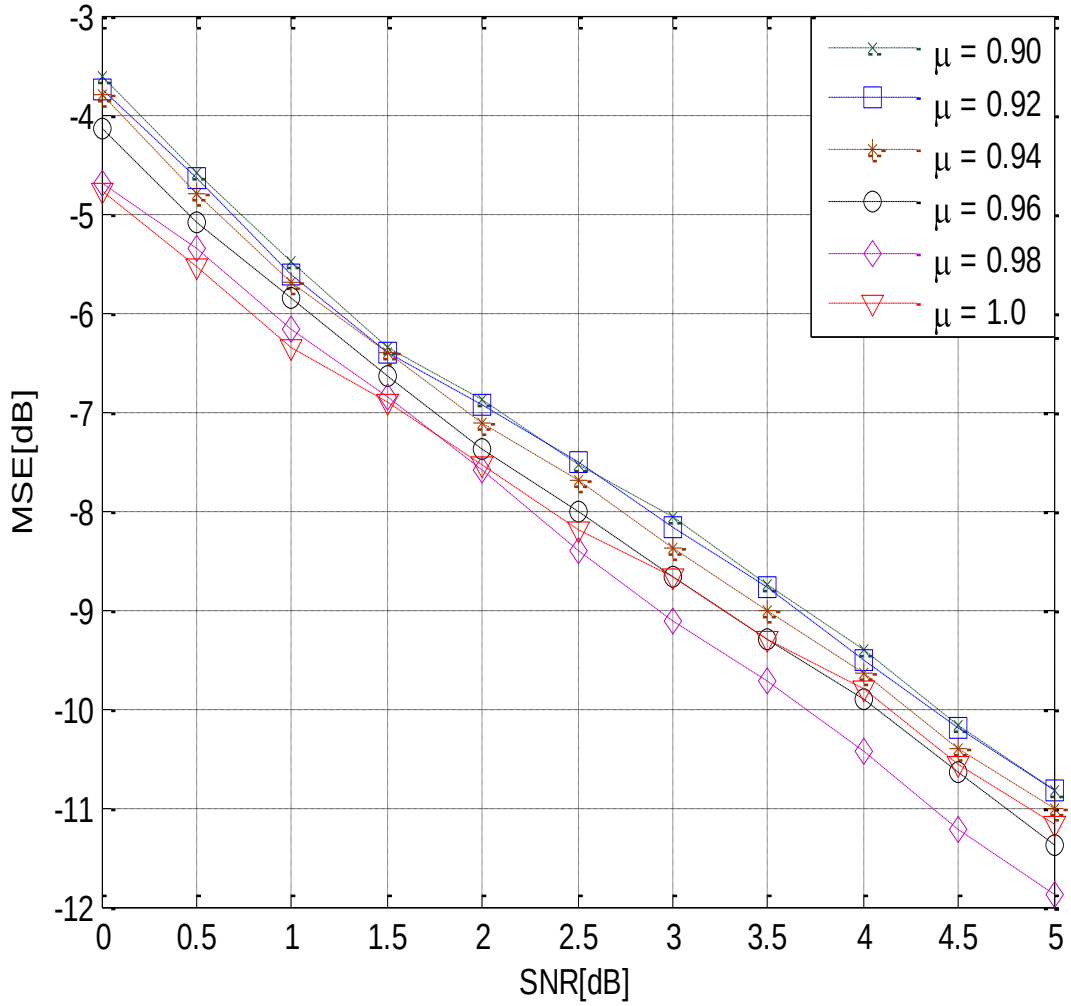

Figure 4.3 MSE exhibited by FDPM based CIR estimator of the DDCE scheme operating in slow fading Channel fD = 0.005 while using NLMS-based predictor for values of μ ranges between 0.90 and 1.0.

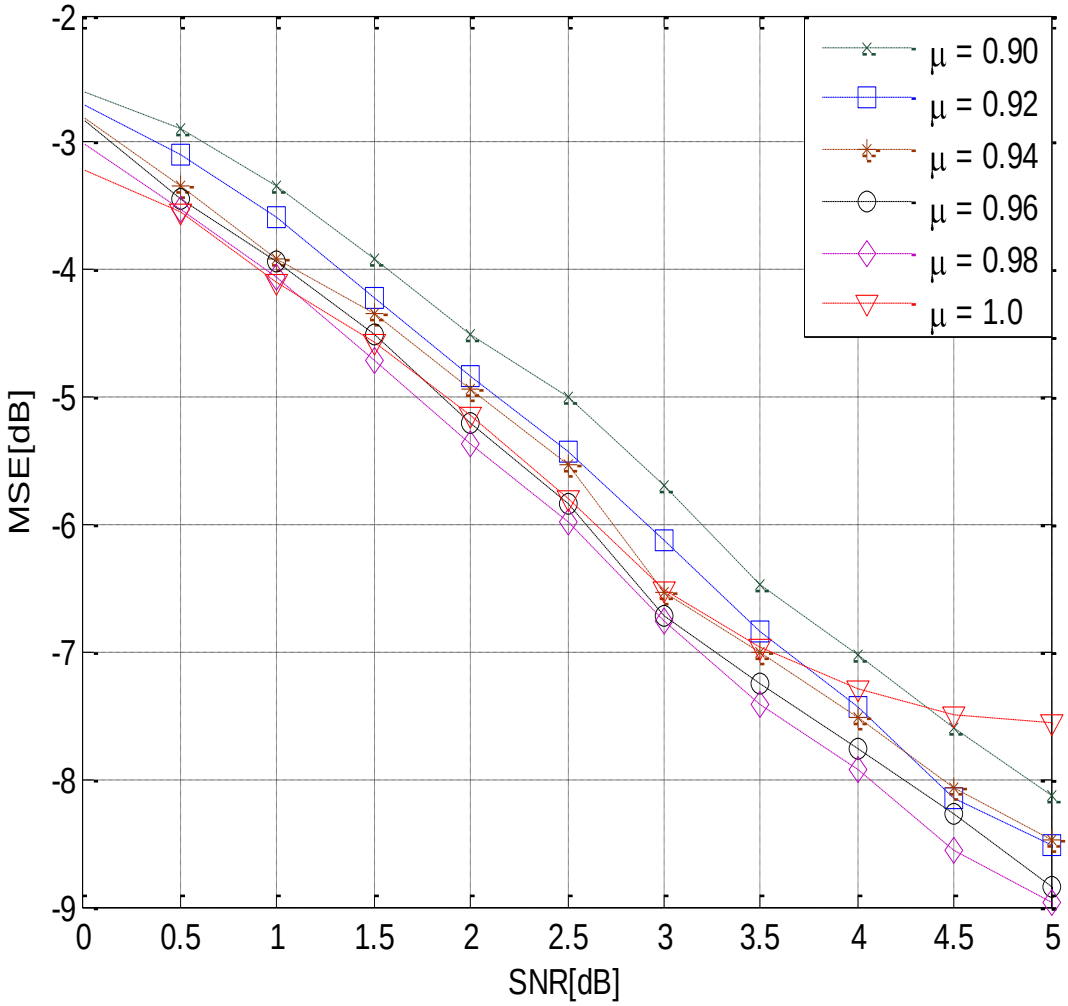

Figure 4.4 MSE versus SNR exhibited by FDPM based CIR estimator of the DDCE scheme operating in fast fading Channel fD = 0.02 while using NLMS-based predictor for values of μ ranges between 0.90 and 1.0

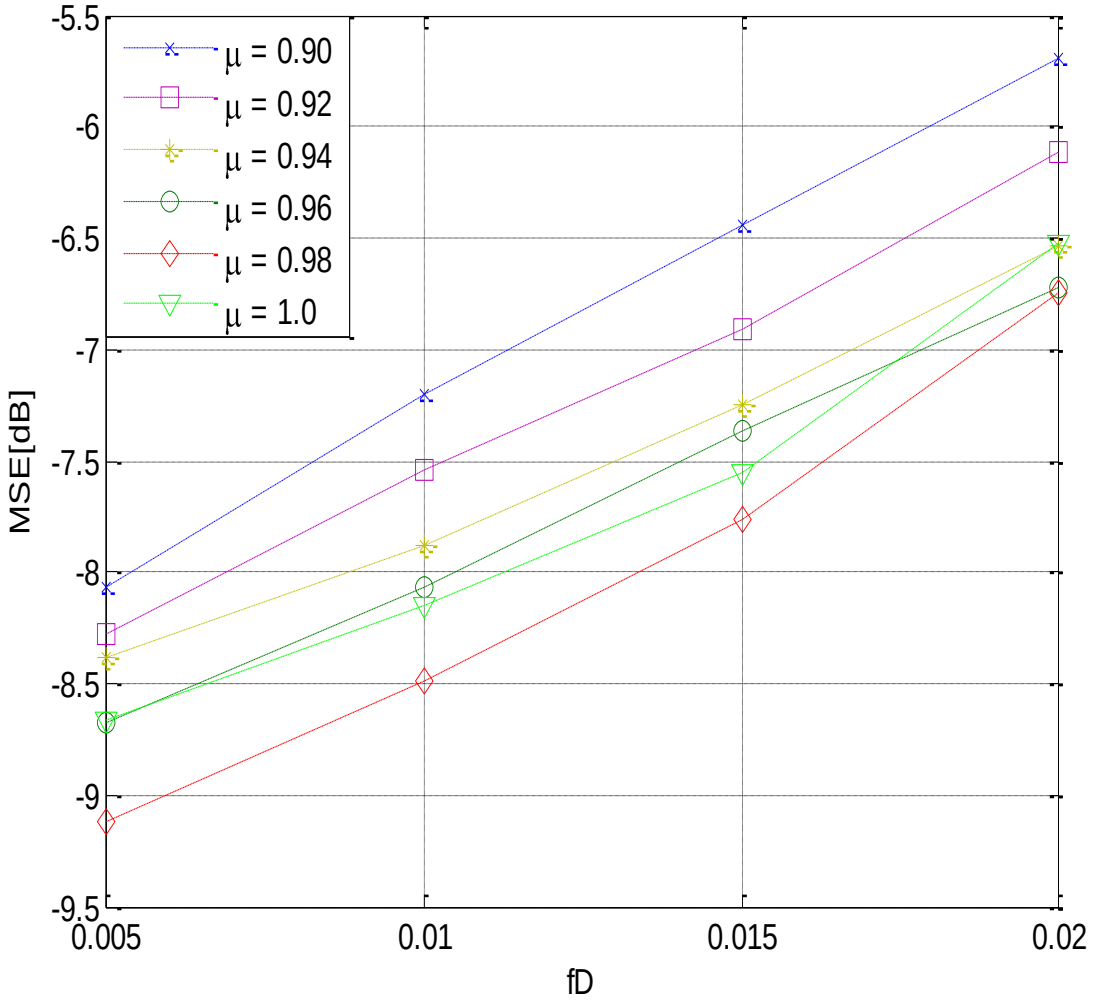

Figure 4.5 MSE versus fD exhibited by FDPM based CIR estimator of the DDCE scheme for fixed SNR = 3dB while using NLMS-based predictor for values of μ ranges between 0.90 and 1.0.

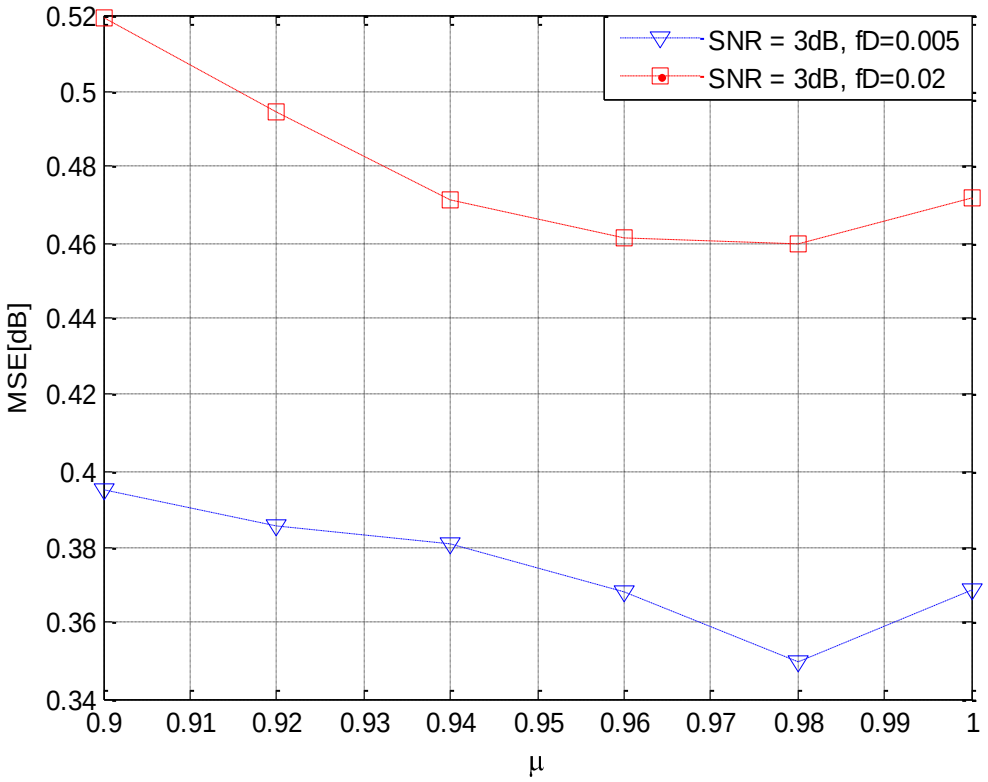

Figure 4.6 Plot of MSE versus μ exhibited by FDPM based CIR estimator of the DDCE scheme at fixed SNR=3dB and fD=0.005 and 0.02 respectively

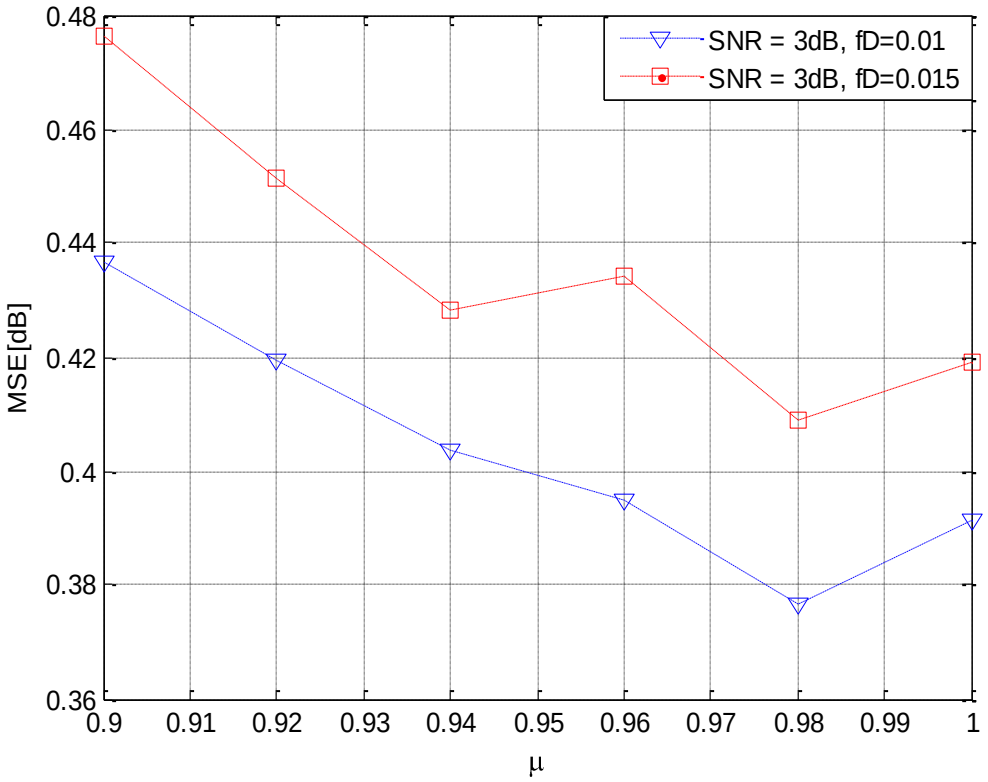

Figure 4.7 Plot of MSE versus μ exhibited by FDPM based CIR estimator of the DDCE scheme at fixed SNR=3dB for fD=0.01 and 0.015 respectively

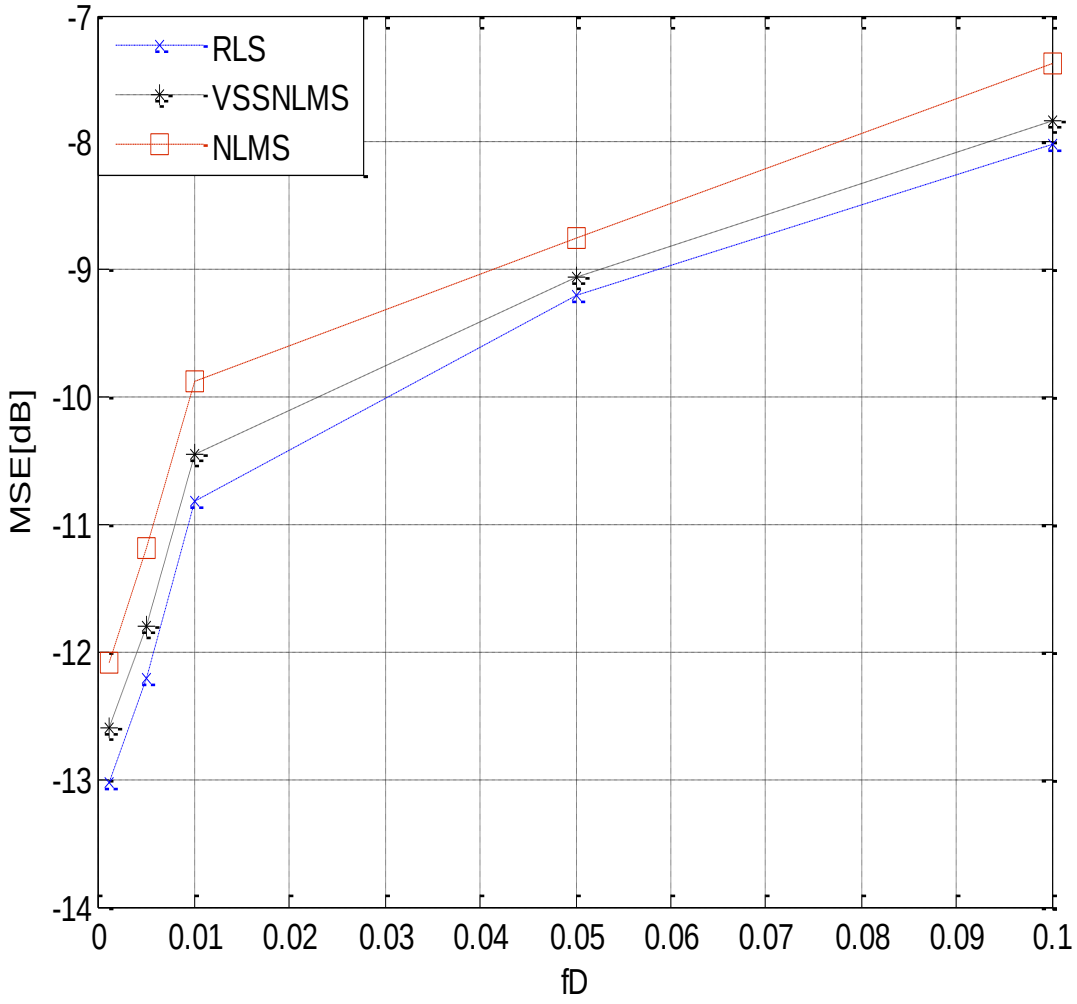

Figure 4.8 MSE exhibited y the RLS, VSSNLMS and NLMS -based CIR Adaptive Predictors for SNR = 5dB

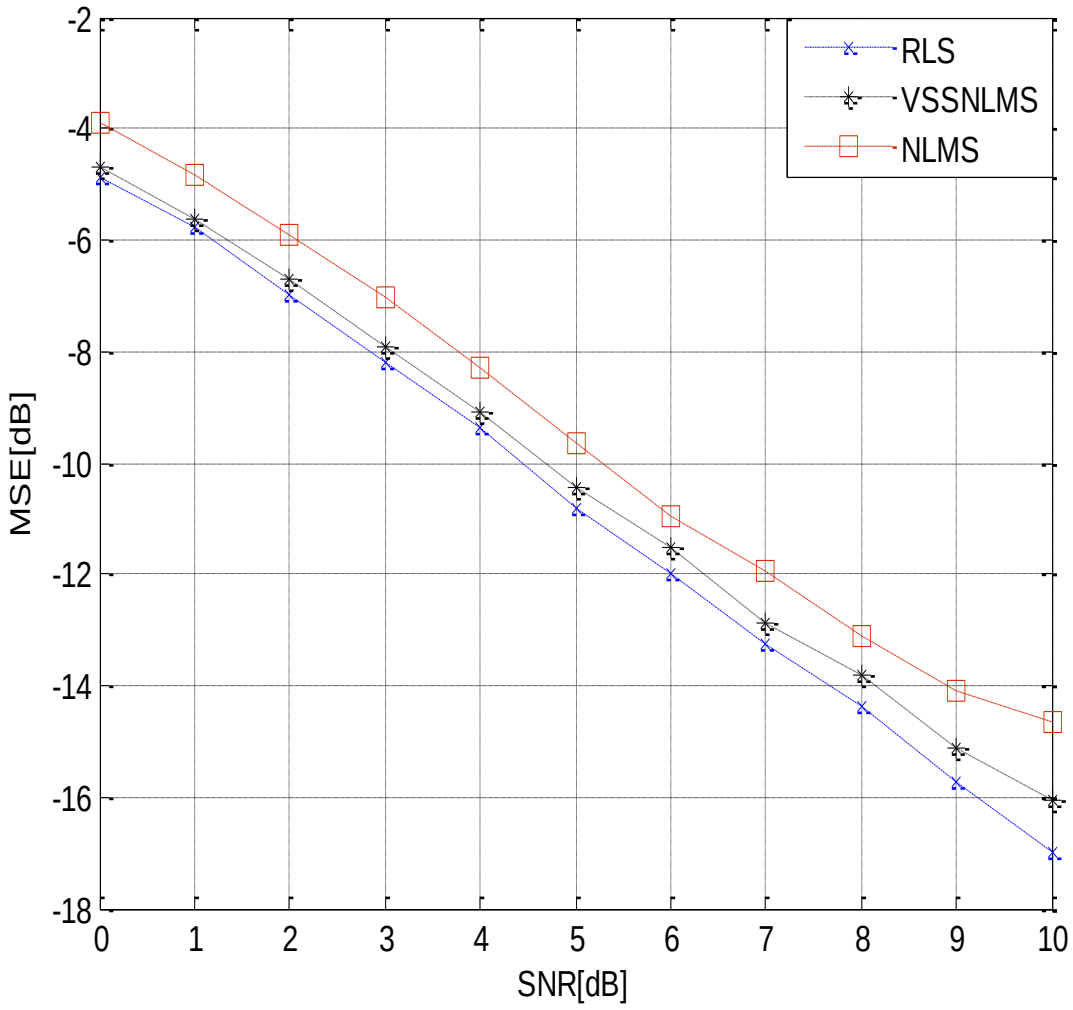

Figure 4.9 MSE exhibited by the RLS, VSSNLMS and NLMS -based CIR Adaptive Predictors during fast fading channel of normalized Doppler frequency fD=0.02

Figure 4.10 and Figure 4.11 show convergence behaviour of the proposed adaptive VSSNLMS predictor in comparison with RLS-based predictor and NLMS-based predictor, for both slow and fast fading channel scenarios, respectively. It is observed that the performance for slow fading scenario, in all cases, is better than that of the fast fading scenario. This shows that the scheme finds it easy to track the slow fading channel than its fast fading counterpart. The results also show how DDCE employing VSSNLMS-based predictor outperforms its NLMS counterpart and its performance is very close to that of RLS-based predictor, especially at the lower part of Signal to Noise Ratio (SNR) considered. The improved performance of the DDCE employing

VSSNLMS-based predictor could be associated with the rate of convergence of the VSSNLMS-based predictor that is improved as a result of the variable step size in the predictor in contrast to the fixed step size employed in the NLMS-based predictor.

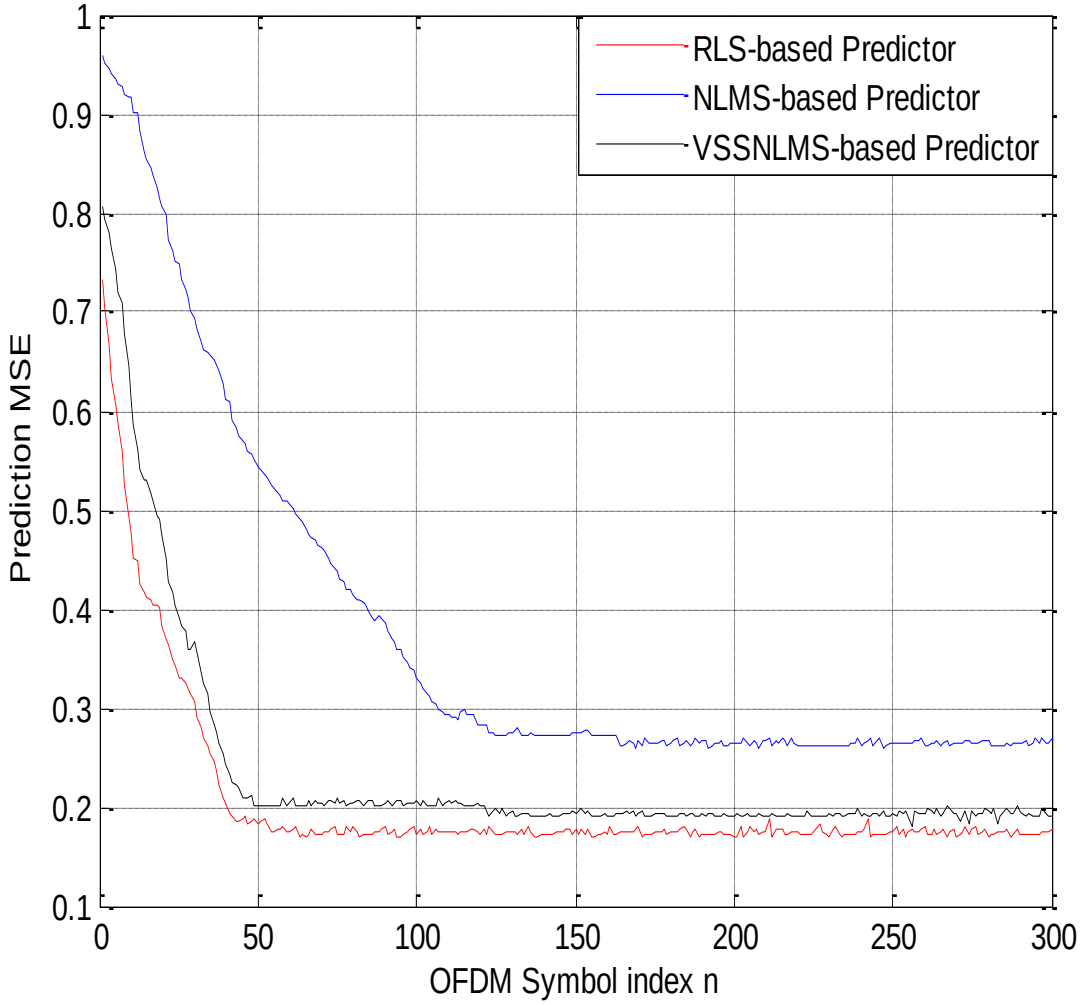

Figure 4.10 Convergence behaviour of the VSSNLMS-based predictor, RLS-based predictor and NLMS-based predictor for slow fading channel with normalized fading frequency, fD = 0.005.

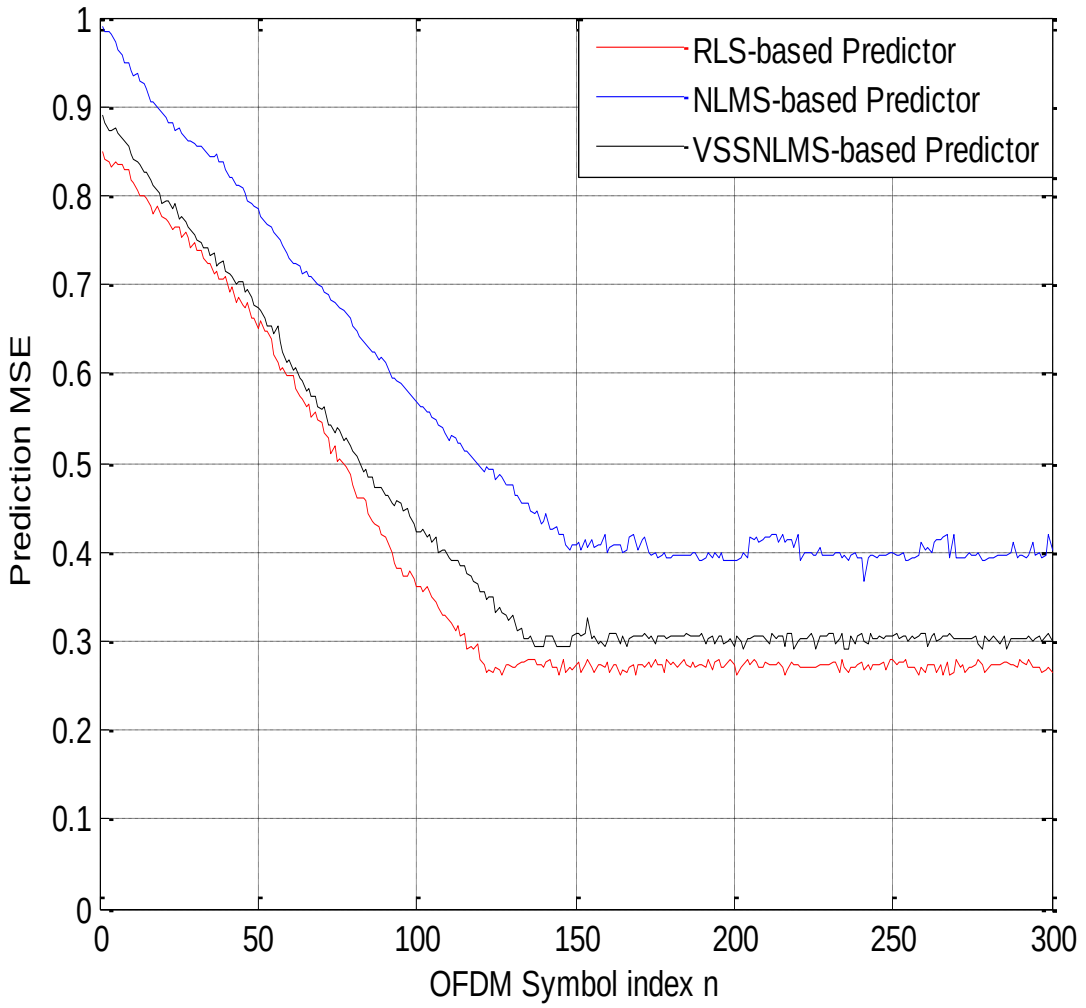

Figure 4.11 Convergence behaviour of the VSSNLMS-based predictor, RLS-based predictor and NLMS-based predictor for fast fading channel with normalized fading frequency, fD = 0.02.

Finally comparative performances between the FDPM and PASTd subspace algorithm for CIR estimator in combination with NLMS-based predictor and the proposed VSSNLMS-based predictor are presented. Figure 4.12 and Figure 4.13 show the comparative performance gain of FDPM-based DDCE over PASTd-based DDCE in form of Bit Error Rate (BER) for both slow and fast fading scenarios respectively. The curves labeled 'perfect channel state' information (CSI) correspond to detection using the perfect knowledge of channel at the receiver, and serve as benchmark for the two cases of fading channels. The achievable MSE exhibited by the FDPM-based DDCE in comparison with PASTd-based DDCE while employing VSSNLMS and NLMS predictors are shown in Figure 4.14 and Figure 4.15 for slow and fast fading channels respectively.

Furthermore, Figure 4.16 and Figure 4.17 illustrate the achievable BER versus SNR and the MSE versus SNR as a function of normalised Doppler frequency (fD) respectively, for both FDPM- and PASTd-based DDCE employing VSSNLMS adaptive predictor. In general, the good performance exhibited by the whole system at lower part of Signal to Noise Ratio (SNR) is obviously aided by the type of the channel encoder (the Turbo encoder) and the SISO Turbo decoder employed, which are known to exhibit good performance at lower SNR. This is the more reason why Turbo encoder rather than the convolution encoder is employed in the Systems.

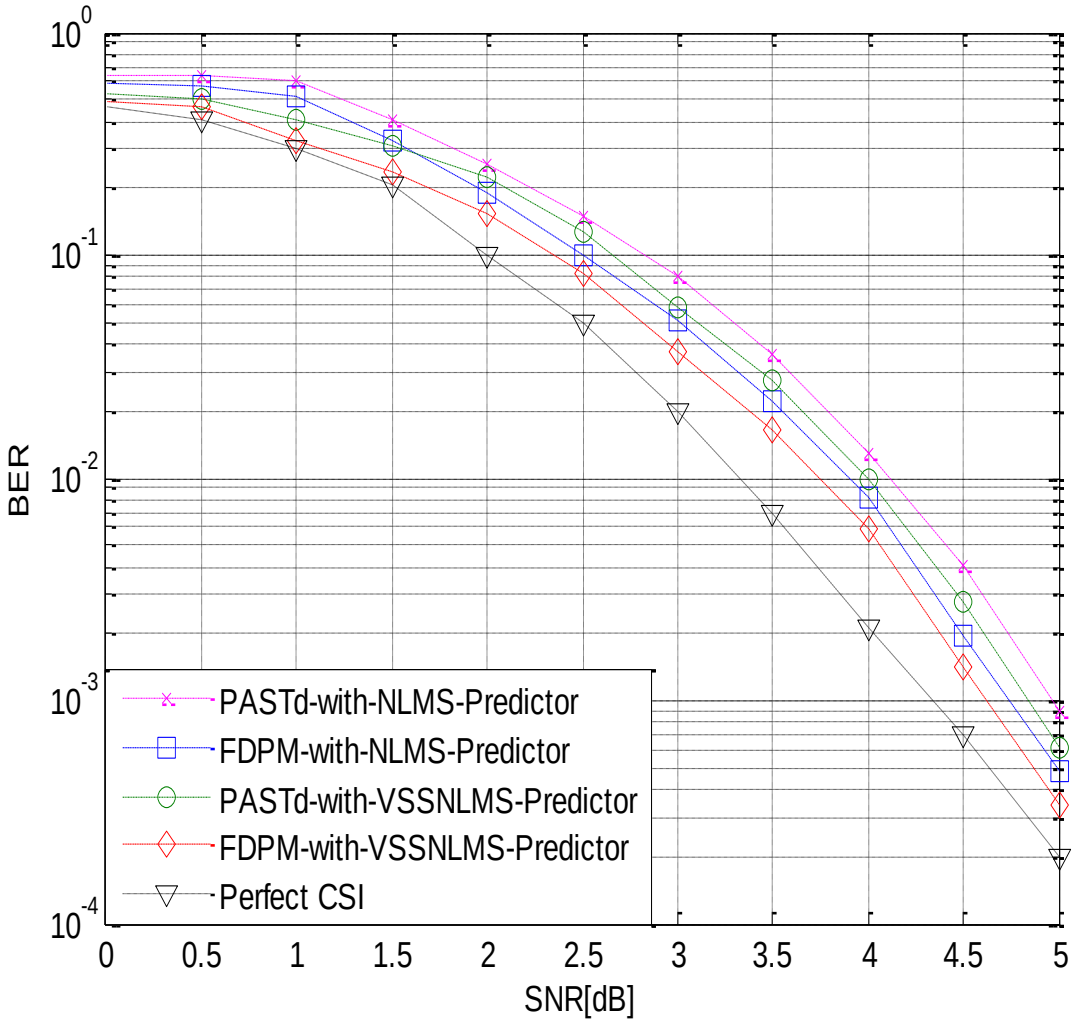

Figure 4.12 BER exhibited by FDPM- and PASTd-based DDCE employing NLMS and VSSNLMS adaptive predictors for normalized Doppler frequency fD=0.005

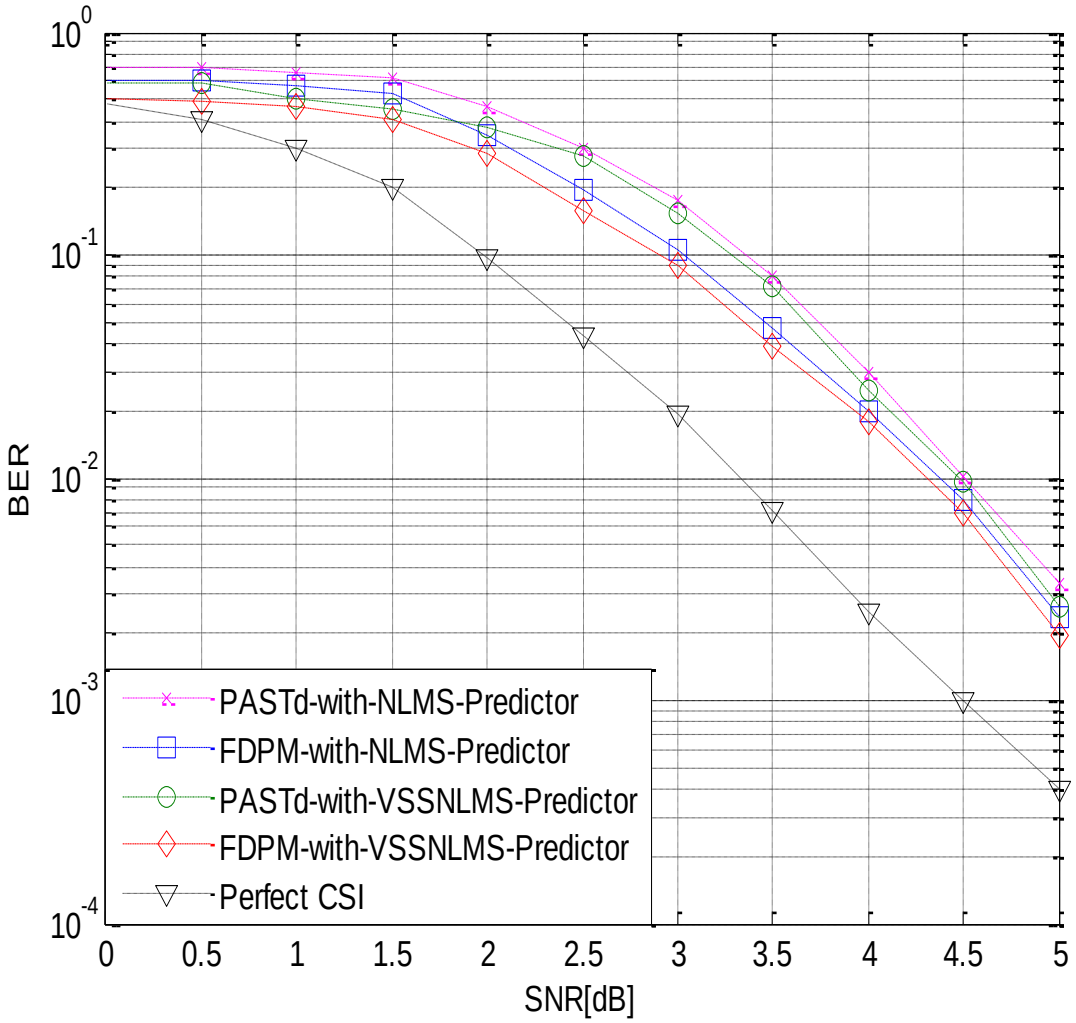

Figure 4.13 BER exhibited by FDPM- and PASTd-based DDCE employing NLMS and VSSNLMS adaptive predictors for normalized Doppler frequency fD=0.02

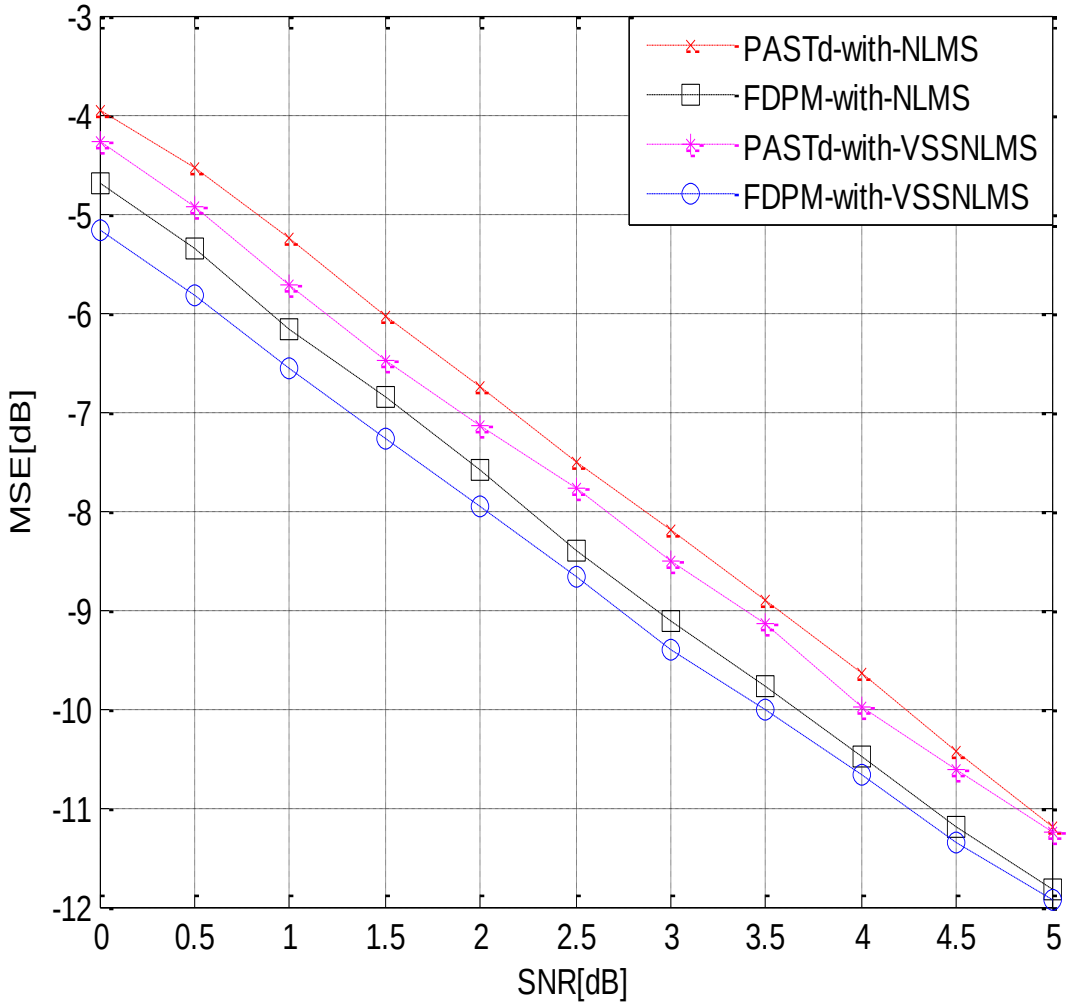

Figure 4.14 MSE exhibited by FDPM- and PASTd-based DDCE employing NLMS and VSSNLMS adaptive predictors for normalized Doppler frequency fD=0.005

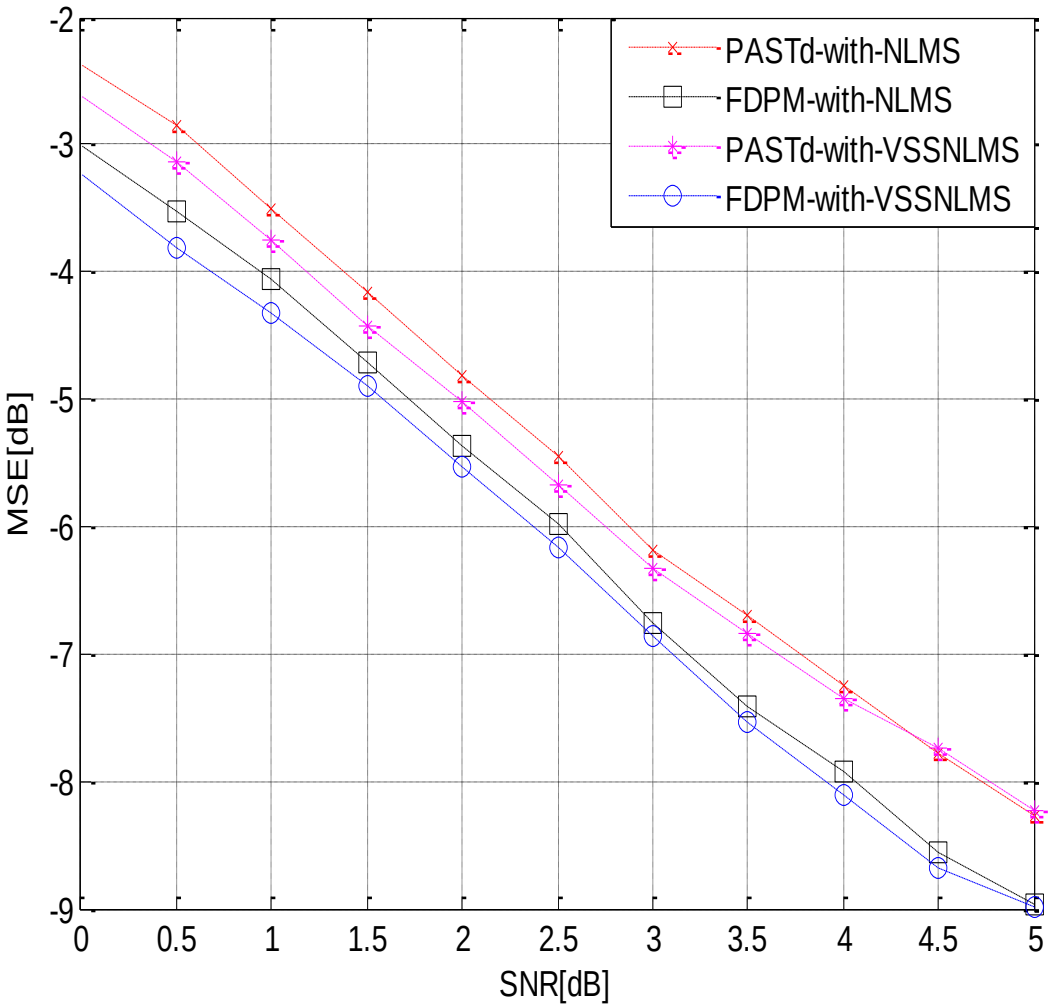

Figure 4.15 MSE exhibited by FDPM- and PASTd-based DDCE employing NLMS and VSSNLMS adaptive predictors for normalized Doppler frequency fD=0.02

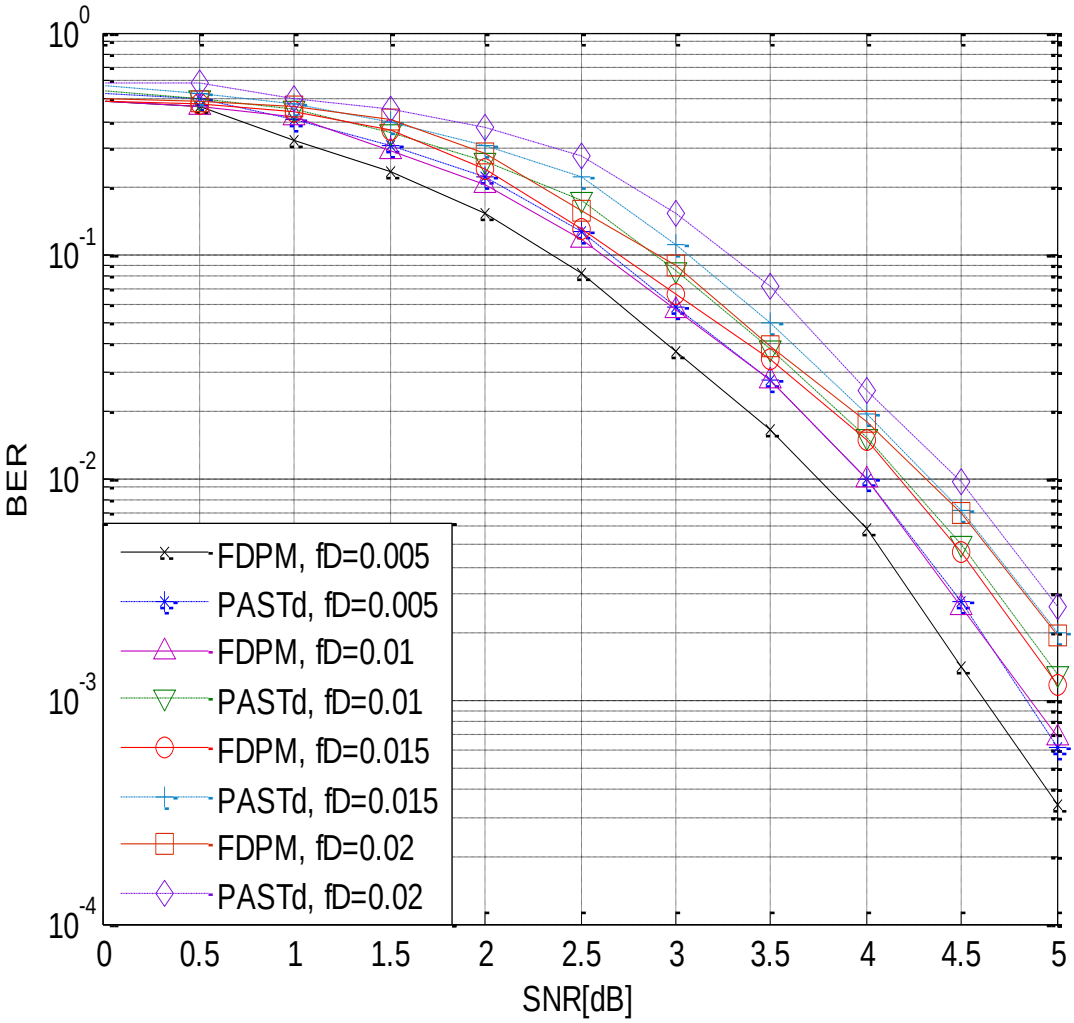

Figure 4.16 BER versus SNR as a function of normalized Doppler frequency (fD) exhibited by FDPM- and PASTd-based DDCE employing VSSNLMS adaptive predictors

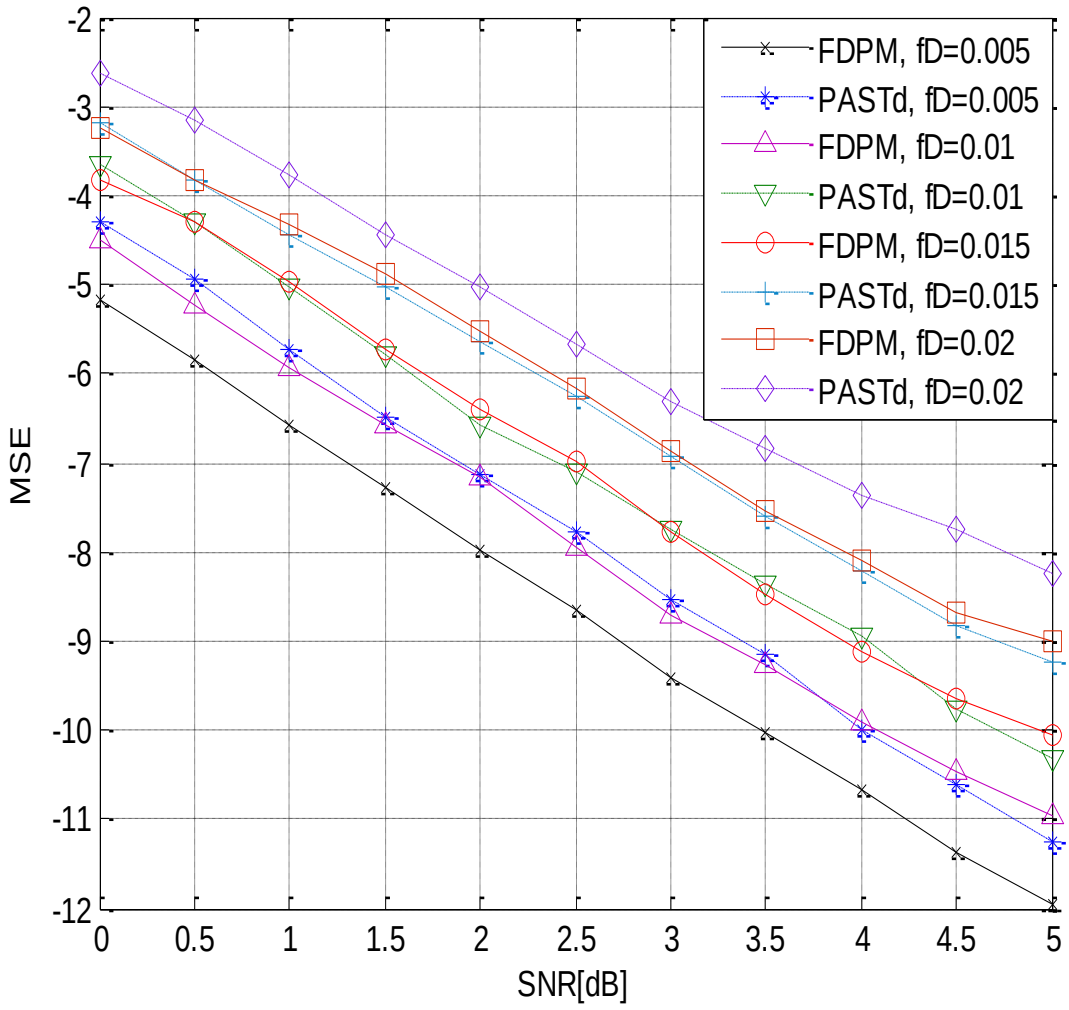

Figure 4.17 MSE versus SNR as a function of normalized Doppler frequency (fD) exhibited by FDPM- and PASTd-based DDCE employing VSSNLMS adaptive predictors

4.8 Comparative Computational Complexity of the proposed DDCE Scheme

Computational complexity of the proposed scheme employing FDPM-based CIR estimator and VSSNLMS-based CIR predictor in comparison with the one proposed in [154] are shown in Table 4.4. The FDPM-based CIR estimator, which is confirmed in [227] to be the fastest among

Table 4.4 Comparative Computational Complexity o the proposed DDCE scheme for SISO OFDM System

Subspace algorithm for DDCE CIR Estimator	**Computational Complexity**	**Adaptive CIR-based Predictor**	**Computational Complexity (Coefficient Update)**
PASTd algorithm(without re-orthonormalization	$4KM + O(M) \approx O(5KM)$	RLS-based Predictor	$O\ ML_{prd}^2$
PASTd algorithm(with re-orthonormalization	$6KM + O(M) \approx O(7KM)$	RLS-based Predictor	$O\ ML_{prd}^2$
Proposed FDPM algorithm	$6KM + O(M) \approx O(7KM)$	**Proposed VSSNLMS-**based Predictor	$O\ \ 3L_{prd} + 4\ M$
		NLMS-based Predictor	$O\ ML_{prd}$

all competing subspace algorithms of the same computational complexity (including the PAST and the PASTd algorithms) exhibits similar computational complexity: $6KM + O(M) \approx O(7KM)$, as the PASTd algorithms with re-orthornomalzation. In [42] the computational complexity in terms of the coefficient update of the adaptive NLMS and RLS predictors are compared and are given as order $O\ ML_{prd}$ and $O\ ML_{prd}^2$ respectively where L_{prd} is the length of the CIR predictor filter. Similarly to the case of VSSNLMS-based estimator proposed in Chapter 3, the proposed adaptive VSSNLMS predictor only requires L_{prd} extra additions and $L_{prd} + 4$ extra multiplications (divisions) compared with the adaptive NLMS predictor. It then turns out that the coefficient update of the proposed adaptive VSSNLMS predictor will be of order $O\ \ 3L_{prd} + 4\ M$, which is still far lower than that of RLS-based adaptive predictor for large filter length.

4.9 Chapter Summary

In this chapter, channel estimation for SISO OFDM system is presented. Specifically, Decision Directed Channel Estimation scheme is investigated for single antenna OFDM Systems in the context of a more realistic Fractionally Spaced-Channel Impulse Response (FS-CIR) channel model, as against the channel characterized by a Sample Spaced (SS)-CIR. Simulation results to validate the proposed scheme is presented and also discussed. The main contributions in this chapter include the application of the FDPM subspace tracking algorithm for the implementation of the CIR estimator module of the DDCE scheme, derivation of the VSSNLMS predictor for the implementation of the CIR predictor module of the DDCE scheme. Comparative complexity issues with the proposed scheme are also discussed. The presented simulation results show how the FDPM-based CIR estimator outperforms the PASTd-based CIR estimator. The results also indicate that the VSSNLMS-based CIR predictor improves the performance of the DDCE scheme in comparison with when NLMS-based predictor is employed. The simulation results with the DDCE scheme based on the proposed VSSNLMS-based CIR predictor is also observed to be very close to a more complex RLS-based predictor earlier employed by other authors in literature.

CHAPTER 5

ITERATIVE DECISION DIRECTED CHANNEL ESTIMATION FOR SISO OFDM SYSTEMS

5.1 Introduction

Iterative technique, based on turbo principle, has received special attention in the signal processing as well as error correcting coding research fields. This is because the technique has been confirmed to exhibit some gains over its non-iterative counterpart. In this chapter, we re-consider a turbo-coded single input single output (SISO)-OFDM system presented in Chapter 4. However, here the design of its receiver is made to be iterative implying that its module comprises Turbo decoder and the Iterative Decision Directed Channel Estimation (DDCE) scheme that are working together in an iterative mode in conjunction with the soft Demapper.

The rest of the chapter is organized as follows. Section 5.2 describes turbo principle, while the system model is presented in Section 5.3. Section 5.4 describes the iterative DDCE scheme. The soft demapper and soft mappers employ in this chapter are presented in Section 5.5. Simulation results for the proposed iterative DDCE schemes are discussed in Section 5.6. Section 5.7 gives the summary of the whole chapter.

5.2 Turbo Principle

In [236] concatenated coding scheme as a means of achieving improved coding gain was initially proposed by Forney. This was achieved by combining two or more constituent codes as channel encoder. Turbo Code proposed in [209] emerged as a refinement of the concatenated encoding structure, in addition with an iterative algorithm for decoding the constituent code sequence. Excellent gain in terms of bit error rate (BER) performance, as low as 10^{-5}, at a signal to noise

ration (SNR) of about 0.7 dB is achieved through this scheme in order to achieve the Shannon's capacity. The idea in this chapter is based on the iterative decoding structure of the turbo code. Before presenting the proposed structure, it is important to have insight into the encoding structure for better understanding of the decoding structure of the turbo code on which the proposal in this chapter is based.

5.2.1 Generic Turbo Encoder

As shown in Figure 5.1, turbo encoder is made up of two constituent encoders. Each of the encoder are usually 1/2 rate Recursive Systematic Convolutional (RSC) encoder. Consequently, the sequence of input bits is encoded twice with these constituent encoders. The input bits of the second encoder are the interleaved version of the input of the first encoder. The output of the Turbo encoder comprises the Systematic bits c (the input bits), parity bits c_1 (output of the first constituent encoder), and parity bits c_2 (output of the second constituent encoder). These are multiplexed together before transmission. In order to obtain better coding rates, the two parity sequences could be punctured before being multiplexed with the systematic bits.

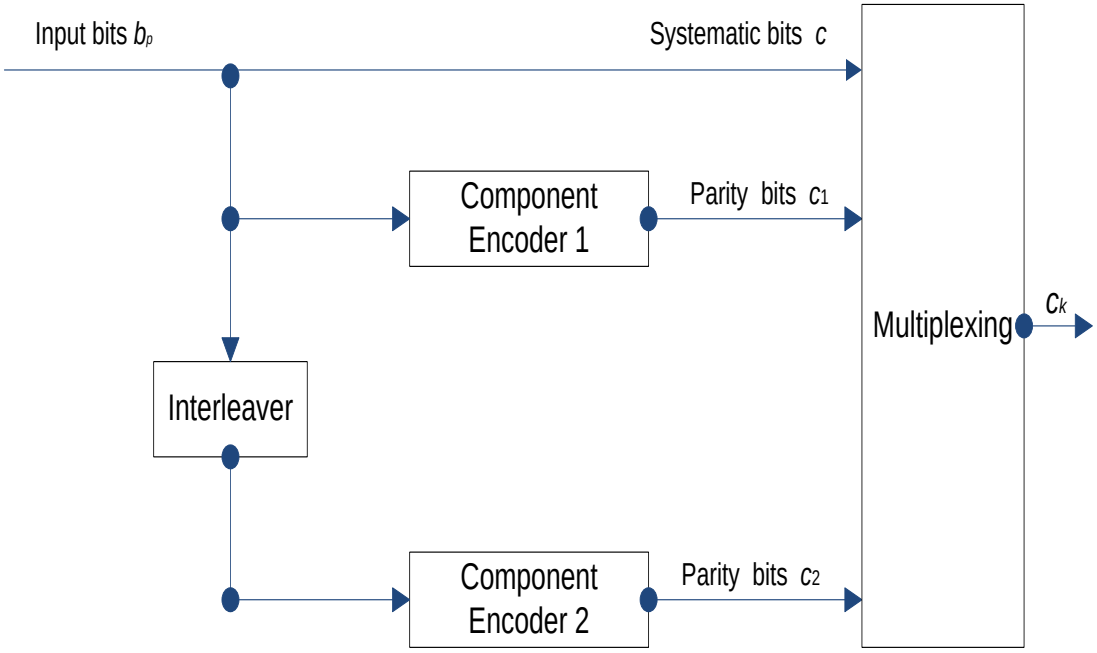

Figure 5.1 Schematic diagram of the generic turbo encoder

5.2.2 Iterative Turbo Decoder

The schematic diagram of iterative Turbo decoder is shown in Figure 5.2. It comprises of two RSC component serially concatenated via an interleaver that is similar to that of the encoder. Decoder 1 takes as its inputs the received soft information sequence corresponding to the systematic bits, the received parity 1 sequence (corresponding to the first encoder), and the information from decoder 2 about the likely values of the bits being decoded (known as *a priori* information). The interleaved version of the soft information sequence, corresponding to the systematic bits, along side the received parity 2 sequence (corresponding to the second encoder), and the information from decoder 1 about the likely values of the bits being decoded are fed into decoder 2. In addition to computing the decoded output bit sequence, each decoder must also produce the associated probabilities for each bit being decoded as well as soft output for the decoded bits. The soft outputs are generally represented in terms of Log Likelihood Ratios (LLRs). The decoder can either be based on Maximum A-Posteriori (MAP) algorithm proposed in [237] or the Soft Output Viterbi Algorithm (SOVA) presented in [238].

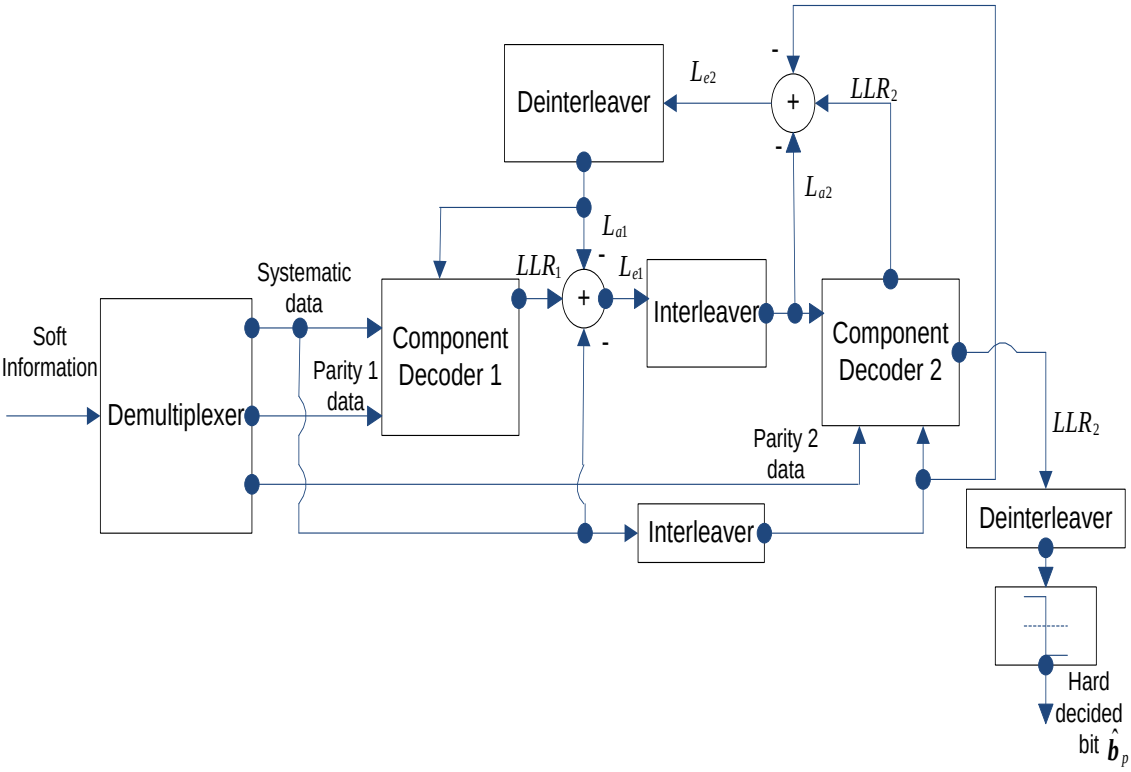

Figure 5.2 Schematic diagram of iterative turbo decoder

5.2.2.1 Log-Likelihood Ratios

In [239] the concept of Log likelihood Rations (LLRs) is introduced to simplify the iterative feedback from one component decoder to other in the iterative turbo decoding. For a data bit b_p, the soft information in terms of LLRs, is defined as the ratio of the probability that b_p is equal to +1 to the probability that b_p is equal to -1, and given by

$$L\ b_p\ = \ln\left(\frac{\Pr\ \ b_p = +1}{\Pr\ b_p = -1}\right). \tag{5.1}$$

The sign of the decoded bit corresponds to the most probable hard decision on the bit, and it is determined from the magnitude of LLRs. The amplitude of LLRs corresponds to the reliability of this decision. Most often, the interest is to determine the probability of b_p equal to +1 or -1 conditioned on some received soft information $\bar{z}$. Consequently, (5.1) will be conditioned LLRs and is given as:

$$L\ b_p \mid \bar{Z}\ = \ln\left(\frac{\Pr\ \ b_p = +1 \mid \bar{Z}}{\Pr\ b_p = -1 \mid \bar{Z}}\right), \tag{5.2}$$

while

$$\Pr\ \ b_p = \pm 1 \mid \bar{Z}\ = \frac{\exp\ \pm L\ b_p \mid \bar{Z}}{1 + \exp\ \pm L\ b_p \mid \bar{Z}}. \tag{5.3}$$

By using Bayes' theorem, the conditioned LLRs of (5.2) is equivalent to

$$\begin{aligned} L\ b_p \mid \bar{Z}\ &= \ln\left(\frac{\Pr\ \ \bar{Z} \mid b_p = +1\ \Pr\ \ b_p = +1}{\Pr\ \ \bar{Z} \mid b_p = -1\ \Pr\ \ b_p = -1}\right) \\ &= \ln\left(\frac{\Pr\ \ \bar{Z} \mid b_p = +1}{\Pr\ \ \bar{Z} \mid b_p = -1}\right) + \ln\left(\frac{\Pr\ \ b_p = +1}{\Pr\ \ b_p = -1}\right). \end{aligned} \tag{5.4}$$

This LLRs so obtained are used to compute the extrinsic L_e . information that is used as *a priori* information input, L_a . , for the next component decoder. Thus, extrinsic information from component decoder 1 in Figure 5.2 is

$$L_{e1}\ b_p\ = L_1\ b_p \mid \bar{Z}\ - L_{a1}\ b_p\ . \tag{5.5}$$

More detail about iterative turbo decoding principle and the associated algorithms can be found in the following references therein [240, 241]. The iterative DDCE structure for SISO OFDM that follows in the subsequent sections is built based on the iterative turbo decoding principle described.

5.3 System Model

The block diagram of the system model incorporating the iterative DDCE scheme is as shown in Figure 5.3. At the transmitter, in the same way as the one in Chapter 4, there is a turbo encoder with a two Recursive Systematic Encoder (RSC) and random bit interleaver. Following this is the Quadrature phase shift keying (QPSK) modulation that used for modulating both the message and pilot bits. The multiplexed QPSK symbols are fed into the IFFT modulation after which the cyclic prefix (CP) is added before transmission over the frequency selective fading channel. The receiver performs the reverse operations. After the parallel-to-serial conversion of the received message

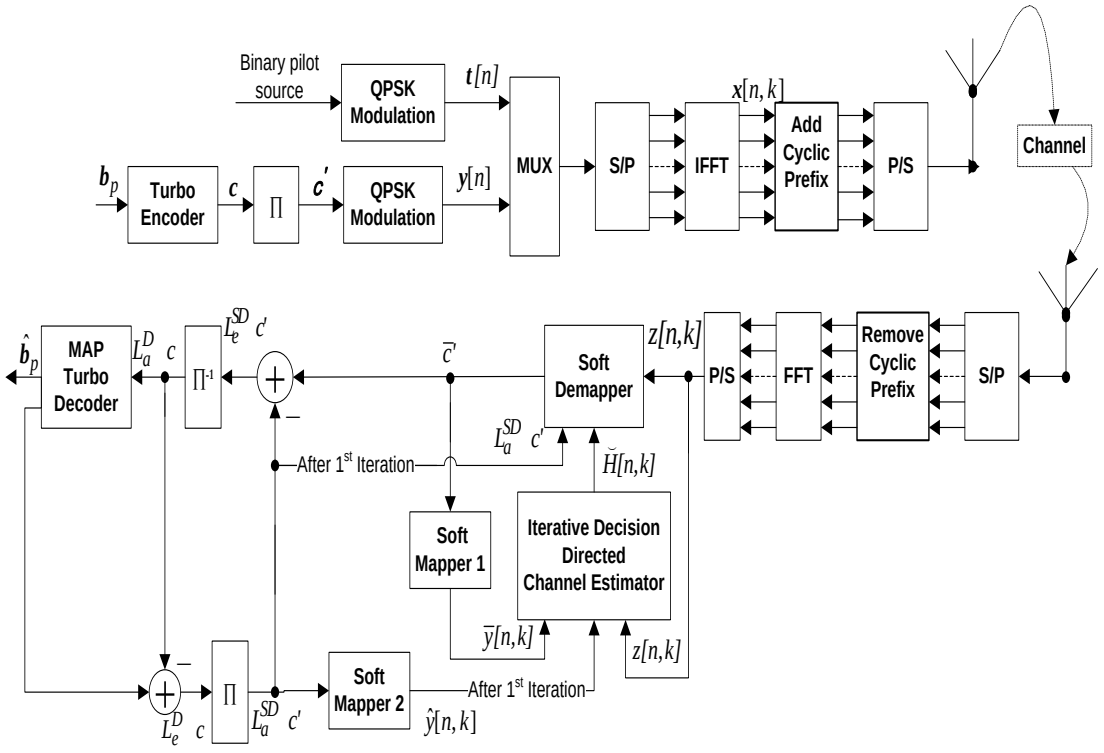

Figure 5.3 OFDM Transceiver with Iterative Decision Directed Channel Estimator

symbols, the iterative DDCE is employed to estimate the channel behaviour. This is fed into the soft demapper that employs the channel estimate in combination with the received message symbol to compute the soft information about each of the transmitted bits. The outputs of the soft demapper are thereafter deinterleaved to *a posteriori L-values* and sent to the turbo decoder. The turbo decoder, in turn, computes extrinsic information from where *a priori* values that are fed back to the soft demapper and the Iterative DDCE are obtained. This process continues over a pre-determined numbers of iteration. The turbo decoder makes the estimate of the transmitted bits during the last iteration and returns $\hat{b}_p$.

The channel characteristic employed follows after the one described in Chapter 4. Hence, the continuous-time CIR adopted is the complex baseband representation of the mobile wireless system given as

$$h(t,\tau)=\sum_{m}^{M}\gamma_m(t)c(\tau-\tau_m), \tag{5.6}$$

where $\gamma_m(t)$ and τ_m are the time-variant complex amplitude and the delay of the *m*th path respectively, and $c(\tau)$ is the aggregate impulse response of the transmitter-receiver pair that corresponds to the square-root raised-cosine Nyquist filter. By virtue of the motion of one of the communicating terminals, $\gamma_m(t)$'s are always modeled to be WSS narrowband complex Gaussian processes which are independent for different paths. Consequently, at the receiver, after the cyclic prefix (CP) has been removed from the OFDM symbols, the received signal in the discrete frequency domain is given as [1]

$$z[n,k]=H[n,k]x[n,k]+w[n,k], \tag{5.7}$$

For $k=0,1,...,K-1$ and all *n*'s. In (4.9), $x[n,k]$, $w[n,k]$ and $H[n,k]$ are the transmitted symbol, additive white Gaussian noise sample and the frequency domain complex CTF coefficient respectively, associated with the *kth* subcarrier of the *nth* OFDM block.

5.4 Iterative Decision Directed Channel Estimation Scheme

The Iterative DDCE scheme is shown in Figure 5.4. Similar to the DDCE scheme of Chapter 4, it comprises of three majour parts namely the temporary CTF estimator, which is referred to as a *posteriori* CTF estimator, the parametric CIR estimator, and the CIR predictor (also known as *a*

prior CIR predictor). In each of the iteration cycles, the known pilot symbols $t[n]$ are used to initialize the decision directed channel estimation process between the estimator and the Soft Demapper, while the detected symbol $\bar{y}[n]$ is used in the subsequent estimation process during each of the iterations. At any iteration stage, the CTF estimator uses its input to make a temporary estimate of the CTF coefficients $\hat{\boldsymbol{H}}[n]$ that corresponds to the current channel state. The output of the CTF estimator is fed into the parametric CIR estimator to generate the FS-CIR $\hat{\gamma}[n]$. This is employed by the adaptive CIR predictor to predict an *a priori* estimate $\breve{\gamma}_{n+1}$ of the next CIR on a tap-by-tap-basis. The Frequency Domain (FD)-CTF $\breve{\boldsymbol{H}}[n+1]$ is obtained from the predicted CIR convolved with the transformation matrix $\tilde{\boldsymbol{W}}[n]$. The FD-CTF $\breve{\boldsymbol{H}}[n+1]$ is employed by the Soft Demapper to compute the next soft input $\bar{c}'_{n+1}$ to the Soft Mapper-1. Soft Mapper-1 in turn uses this to calculate the next detected symbol $\bar{y}[n+1]$ that is fed into the Iterative DDCE during the $n+1\ th$ OFDM-symbol period. Each of the iterative DDCE modules are based on the various algorithms proposed in Chapter 4.

At the end of the estimation /detection process during each of the iteration stages, the *a priori L-values* $L_a^{SD}\ c'$ from the decoder is subtracted from the soft detected symbols $\bar{c}'$ (the a-posteriori *L- values* from the Soft Demapper) to form the extrinsic *L-values* $L_e^{SD}\ c'$. After deinterleaving, the *extrinsic L-values* become the *a-priori L values* $L_a^D\ c$ fed to the Turbo decoder. However, in

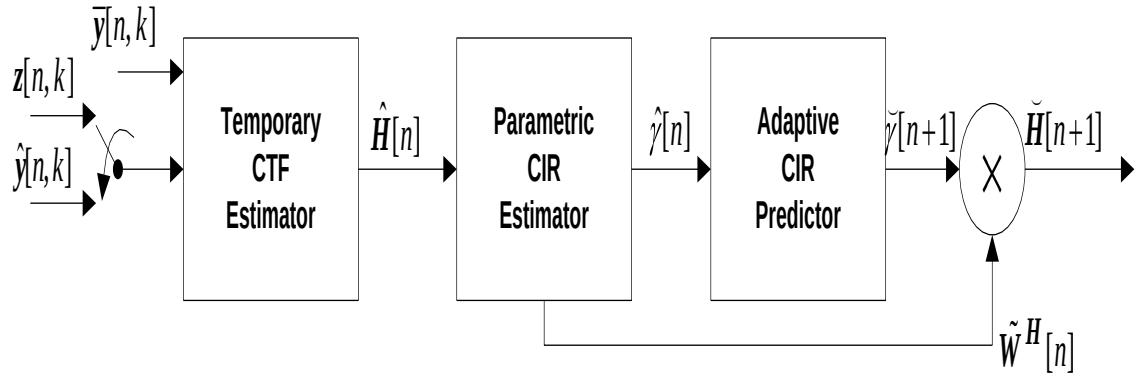

Figure 5.4 Iterative Decision Directed Channel Estimator

the first iteration, the *a priori L-values* $L_a^{SD}\ c'$ from decoder are assumed to be zeros since there is no soft information available at the output of the decoder at this stage. The Turbo decoder in turns calculate the *a-posteriori L- values* for all the code bits by employing the Maximum A-Posteriori (MAP) decoder implemented as log-MAP [12]. The *extrinsic L-values* $L_e^D\ c$ is obtained by substracting the *a-priori L values* $L_a^D\ c$ from the *a-posteriori* L-values. The *extrinsic L-values* $L_e^D\ c$ is then interleaved to form the *a-priori L values* $L_a^{SD}\ c$ that are fed to the Soft Demapper and Soft Mapper-2. These are used in combination with the known pilot symbols $t[n]$, during the second iteration and upward, for estimation and detection processes. Soft Mapper-2 is employed to calculate the probability of the possible transmitted symbols (the soft symbols $\hat{y}[n,k]$) from the *a priori* L- values $L_a^{SD}\ c$. These soft symbols are then used as the input to the iterative DDCE in the subsequent iteration after the first iteration instead of the received symbols. The iterative estimation, detection, and decoding processes continue for a number of predetermined iterations. At the final iteration stage, the decoder makes a final decision and returns hard decision estimate $\hat{b}_p$ of the possible transmitted bits.

5.5 Soft Demapper and Soft Mappers

In this section the soft demapper and the two soft mappers, 1 and 2 of Figure 5.3 are presented in context of the proposed iterative DDCE.

5.2.1 Soft Demapper

The soft demapper follows after the one presented in Chapter 4 except that instead of setting the *a priori* values to zero, the *a priori* values are obtained from the feedback from the Turbo decoder after the first iteration. Consequently, the soft demapper calculates log-likelihood ratios $L\ c'_{\mu} \mid z[n,k]$ and $L\ c'_{\mu+1} \mid z[n,k]$, of the two successive interleaved bits c'_{μ} and $c'_{\mu+1}$ respectively, as

$$L\ c'_{\mu} \mid z[n,k] = \ln\left(\frac{\Pr\ z \mid c'_{\mu}=1, c'_{\mu+1}=0\ + \Pr\ z \mid c'_{\mu}=1, c'_{\mu+1}=1\ \exp L_a\ c'_{\mu+1}}{\Pr\ z \mid c'_{\mu}=0, c'_{\mu+1}=0\ + \Pr\ z \mid c'_{\mu}=0, c'_{\mu+1}=1\ \exp L_a\ c'_{\mu+1}}\right)$$

$$= \ln\left(\frac{B_n^{10} + B_n^{11} e^{L_a\ c'_{\mu+1}}}{B_n^{00} + B_n^{01} e^{L_a\ c'_{\mu+1}}} \right), \tag{5.8}$$

$$L\ c'_{\mu+1} \mid z[n,k] = \ln\left(\frac{\Pr\ z \mid c'_{\mu} = 0, c'_{\mu+1} = 1 + \Pr\ z \mid c'_{\mu} = 1, c'_{\mu+1} = 1\ \exp L_a\ c'_{\mu}}{\Pr\ z \mid c'_{\mu} = 0, c'_{\mu+1} = 0 + \Pr\ z \mid c'_{\mu} = 0, c'_{\mu+1} = 1\ \exp L_a\ c'_{\mu}} \right)$$

$$= \ln\left(\frac{B_n^{01} + B_n^{11} e^{L_a\ c'_{\mu}}}{B_n^{00} + B_n^{10} e^{L_a\ c'_{\mu}}} \right). \tag{5.9}$$

The probabilities $B_n^{i,j}$, with $i, j \in 0,1$ in (5.8) and (5.9) are obtained by employing probability density function [215] given as

$$B_n^{i,j} = \Pr\ z[n,k] \mid y^{i,j}[n,k]$$

$$= \frac{1}{2\pi\sigma_w^2} \exp\left[-\frac{1}{2\sigma_w^2} \left| z[n,k] - \breve{H}[n,k] y^{i,j}[n,k] \right| \right], \tag{5.10}$$

where σ_w^2 is the noise variance. As stated above, the *a priori* values of bits c'_{μ} and $c'_{\mu+1}$, $L_a\ c'_{\mu}$ and $L_a\ c'_{\mu+1}$ respectively, are set to zero during the first iteration since there is no feedback from the decoder at this stage, but assume their respective values at the subsequent iterations.

5.2.2 Soft Mapper 1

The soft mapper 1 estimates the soft symbol $\bar{y}[n,k]$, input to the iterative DDCE, by using the outputs of the soft demapper. Therefore, the soft symbol $\bar{y}[n,k]$, at each *kth* subcarrier, is computed using $L\ c'_{\mu} \mid z[n,k]$ and $L\ c'_{\mu+1} \mid z[n,k]$ from the soft demapper as follow [179]

$$\bar{y}[n,k] = D_n^{00} + D_n^{01} + D_n^{10} + D_n^{11}, \tag{5.11}$$

where,

$$D_n^{i,j} = \Pr\left[c'_\mu = i\right] \times \Pr\left[c'_{\mu+1} = j\right] \times y^{i,j}[n,k]. \tag{5.12}$$

The probabilities $\Pr\left[c'_\mu = 1\right]$ and $\Pr\left[c'_\mu = 0\right]$ can be expressed respectively as

$$\Pr\left[c'_\mu = 1\right] = \frac{1}{2}\left(1 + \tanh\left(\frac{L\ c'_\mu \mid z[n,k]}{2}\right)\right), \tag{5.13}$$

and

$$\Pr\left[c'_\mu = 0\right] = \frac{1}{2}\left(1 - \tanh\left(\frac{L\ c'_\mu \mid z[n,k]}{2}\right)\right). \tag{5.14}$$

Similarly, the probabilities $\Pr\left[c'_{\mu+1} = 1\right]$ and $\Pr\left[c'_{\mu+1} = 0\right]$ can be expressed respectively as

$$\Pr\left[c'_{\mu+1} = 1\right] = \frac{1}{2}\left(1 + \tanh\left(\frac{L\ c'_{\mu+1} \mid z[n,k]}{2}\right)\right), \tag{5.15}$$

and

$$\Pr\left[c'_{\mu+1} = 0\right] = \frac{1}{2}\left(1 - \tanh\left(\frac{L\ c'_{\mu+1} \mid z[n,k]}{2}\right)\right). \tag{5.16}$$

5.5.3 Soft Mapper 2

Soft Mapper-2 calculates the probability of the possible transmitted symbols (the soft symbols $\hat{y}[n,k]$) from the *a priori* L- values $L_a^{SD}\ c$. The output of the soft mapper 2 is then used as the input to the iterative DDCE in the subsequent iteration, after the first iteration, instead of the received symbols $z[n,k]$.

The soft symbol is calculated as follow [179]

$$\hat{y}[n,k] = M_n^{00} + M_n^{01} + M_n^{10} + M_n^{11}. \tag{5.17}$$

Similarly to the case of Soft Mapper 1, we have

$$M_n^{i,j} = \Pr\left[c'_\mu = i\right].\Pr\left[c'_{\mu+1} = j\right].y^{i,j}[n,k], \tag{5.18}$$

where the probabilities $\Pr\left[c'_\mu = 1\right]$ and $\Pr\left[c'_\mu = 0\right]$ can be expressed respectively as

$$\Pr\left[c'_\mu = 1\right] = \frac{1}{2}\left(1 + \tanh\left(\frac{L_a^{SD}\ c'_\mu}{2}\right)\right), \text{ and} \tag{5.19}$$

$$\Pr\left[c'_\mu = 0\right] = \frac{1}{2}\left(1 - \tanh\left(\frac{L_a^{SD}\ c'_\mu}{2}\right)\right). \tag{5.20}$$

Correspondingly, the probabilities $\Pr\left[c'_{\mu+1} = 1\right]$ and $\Pr\left[c'_{\mu+1} = 0\right]$ can be expressed respectively as

$$\Pr\left[c'_{\mu+1} = 1\right] = \frac{1}{2}\left(1 + \tanh\left(\frac{L_a^{SD}\ c'_{\mu+1}}{2}\right)\right), \text{ and} \tag{5.21}$$

$$\Pr\left[c'_{\mu+1} = 0\right] = \frac{1}{2}\left(1 - \tanh\left(\frac{L_a^{SD}\ c'_{\mu+1}}{2}\right)\right). \tag{5.22}$$

The values $L_a\ c'_\mu$ and $L_a^{SD}\ c'_{\mu+1}$, are the *a priori* values of the bits c'_μ and $c'_{\mu+1}$ to the Soft Demapper respectively, obtained from the extrinsic information($L_e^D\ c$) that is available at the output of the decoder.

5.6 Simulation Results and Discussion

In this section simulation results are presented and discussed in a bid to characterize the achievable performance of the iterative DDCE scheme in comparison with its non-iterative counterpart presented in Chapter 4. Simulations are also run to confirm the performance of the proposed iterative DDCE scheme employing FDPM subspace tracking algorithm and VSSNLMS predictor in comparison with using PASTd subspace tracking algorithm and the NLMS predictor.

A rate 1/3, octal generator polynomial of (7, 5), turbo-coded QPSK-modulated OFDM system with K = 64 subcarriers and a total bandwidth of 800kHz is assumed. The symbol duration, Ts is 80μs, while the CP length is 16 samples (1/4 of the symbol period) with the CP period, Tg = 20μs. Consequently, the total block period, T is 100μs. Random interleavers are employed in

the system. The six-path time-varying Rayleigh fading COST 207 Typical Urban (TU) channel model of [43] with Doppler frequencies of 50Hz and 100Hz is employed. The first OFDM symbol of 64 subcarriers comprises the pilot symbols. These are used to initialize the channel estimation process. In all the simulation, we assumed having M = 6 FS-CIR taps, and we set $\bar{\mu}$ = 0.98 for FDPM algorithm, while η is set to 0.95 for PASTd algorithm. The length of the CIR predictor (L_{prd}) is set to 10, while μ_0 = 0.5 is used for NLMS-based predictor and to initialize VSSNLMS-based predictor, ρ is set to 0.002.

Figure 5.5 and Figure 5.6 show the performance improvement in terms of BER as iteration increase, for the system employing the proposed Iterative DDCE scheme of Figure 5.3 with FDPM-based CIR estimator and NLMS based predictor under slow and fast fading scenario respectively. Also shown in the figures are the results after the 8th iteration of Turbo decoder for the system employing non-iterative DDCE scheme presented in Chapter 4, with FDPM-based CIR estimator and NLMS based predictor. The 8th iteration results of Turbo decoder for the system employing non-iterative DDCE scheme presented in Chapter 4 is chosen because this is the point where the results start to decline for the system. The curves labeled perfect channel state information (CSI) correspond to detection with perfect knowledge of channel at the receiver, and serve as benchmarks in the two cases of channel fading. It is observed that the results for Iterative DDCE scheme begin to show no further improvement after the 7th iteration for both fading scenarios. It is also observed that the results of the non-iterative DDCE scheme are just a little bit better than the 6th iteration results of the iterative DDCE scheme. However, the 7th and 8th iterations results of the iterative DDCE scheme are better than that of the non-iterative DDCE scheme (with turbo decoder).

Figure 5.7 shows the comparative performance gain, in terms of BER, of FDPM-based iterative DDCE over PASTd-based iterative DDCE while using NLMS based predictor for both slow and fast fading channel scenarios respectively. The corresponding Means Square Error (MSE) exhibits by both subspace tracking algorithms during both slow and fast fading channel scenarios after the 7th iteration are as shown in Figure 5.8. It is obvious from the figures that FDPM-based iterative DDCE outperforms its PASTd-based iterative DDCE counterpart and its results are closer to the ideal channel estimator (the perfect CSI).

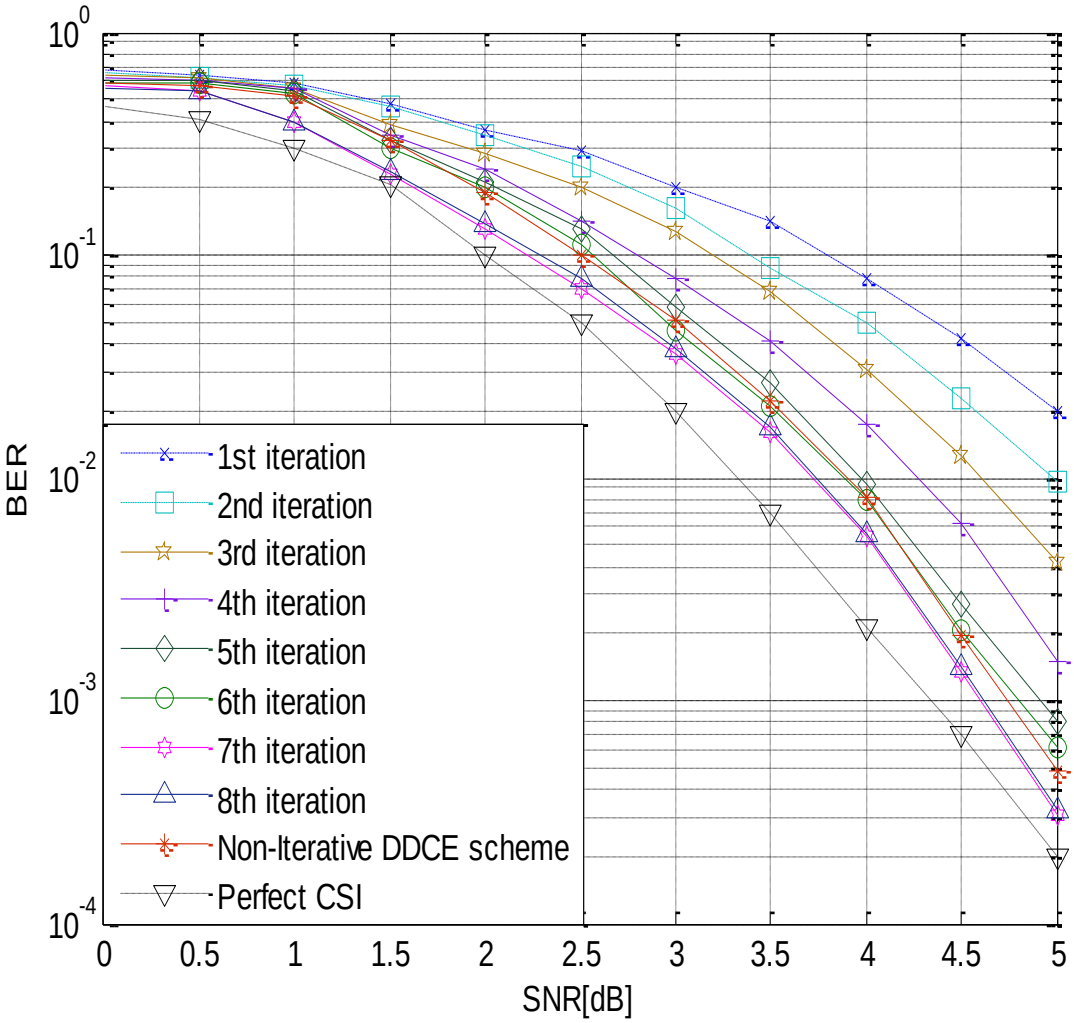

Figure 5.5 BER performance of the proposed Iterative DDCE scheme employing FDPM-based CIR estimator and NLMS based predictor, fD=0.005

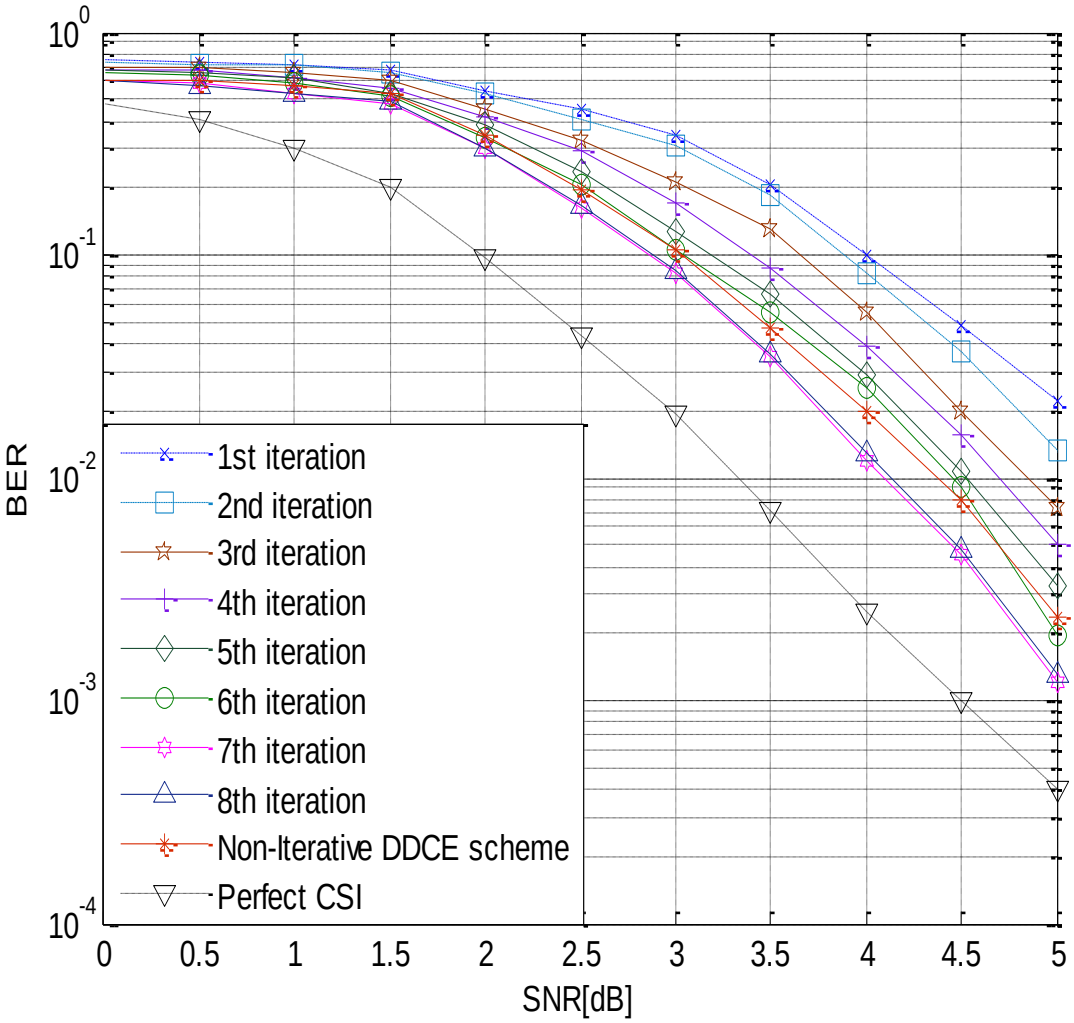

Figure 5.6 BER performance of the proposed Iterative DDCE scheme employing FDPM-based CIR estimator and NLMS based predictor, fD=0.02

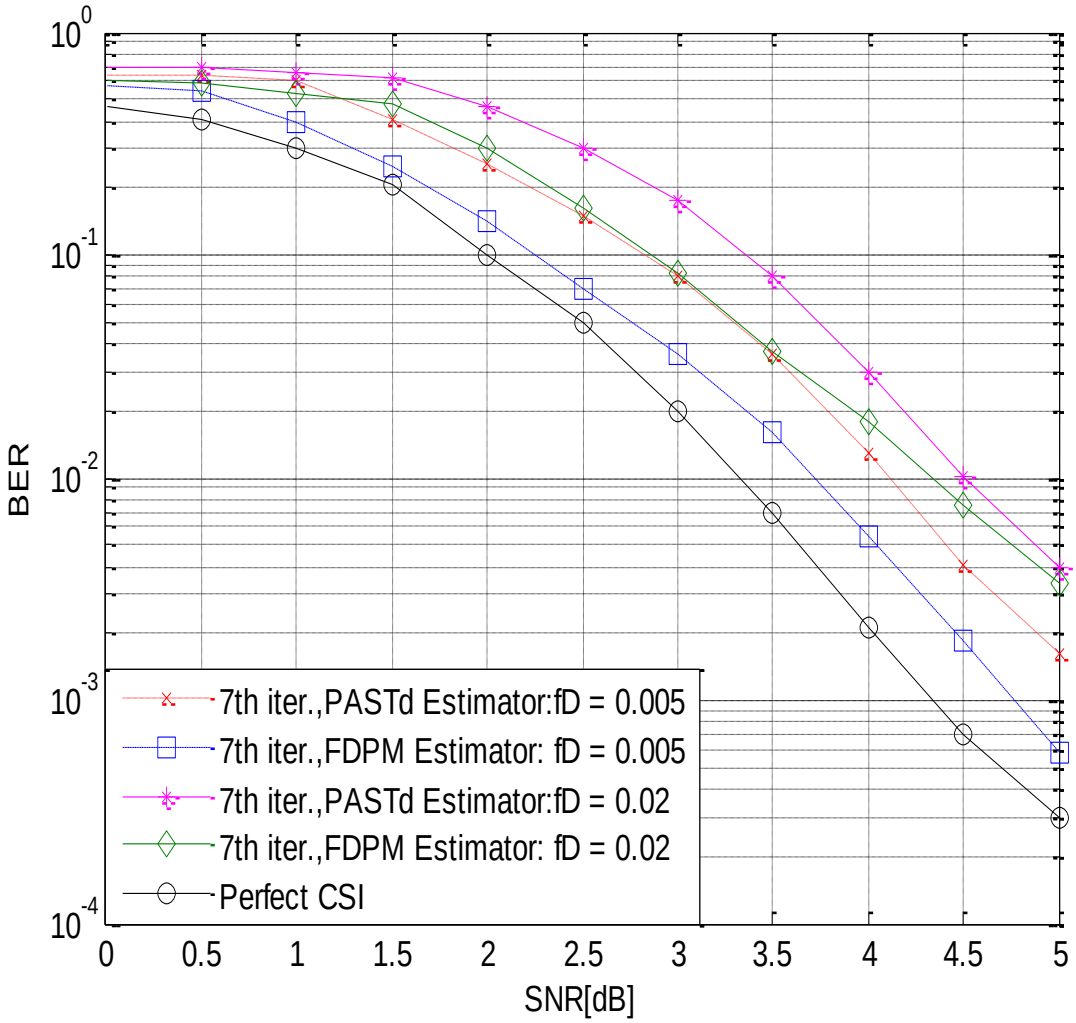

Figure 5.7 BER performance of the Iterative DDCE scheme with both FDPM-based CIR estimator and PASTd-based CIR estimator while employing and NLMS based predictor for both normalized Doppler frequencies fD = 0.005 and fD = 0.02.

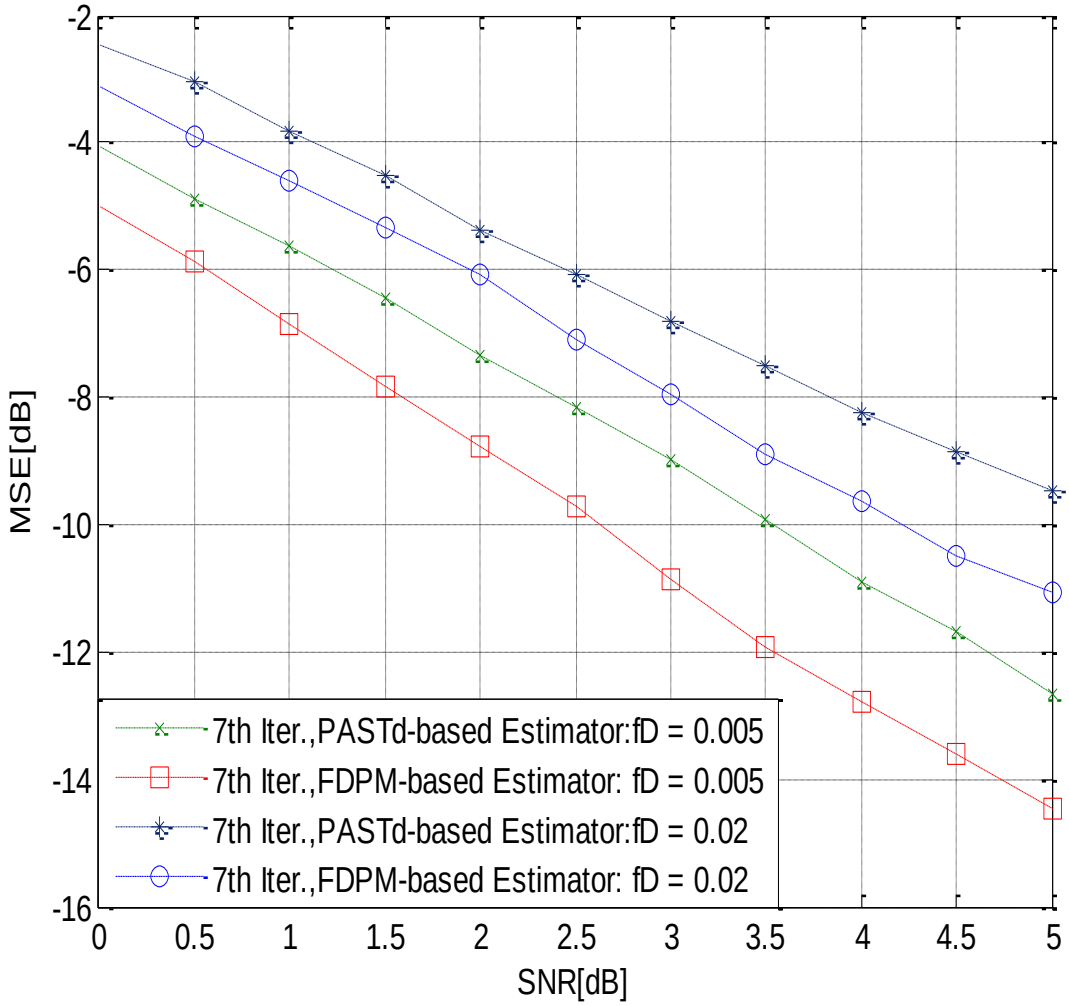

Figure 5.8 MSE at 7th Iteration exhibited by FDPM- and PASTd-based Iterative DDCE while employing and NLMS based predictor for both normalized Doppler frequencies fD = 0.005 and fD = 0.02.

In Figure 5.9, comparative performance gain of FDPM-based iterative DDCE in comparison with PASTd-based iterative DDCE, as well as performance gain achievable while employing VSSNLMS-based predictor and NLMS-based predictor are shown in terms of BER for both slow and fast fading channel scenarios. In the figure, the results indicate that FDPM-based iterative DDCE employing NLMS and VSSNLMS predictors show better performance than PASTd-based iterative DDCE employing the two predictors respectively. The figure also indicates performance improvement introduced by the employment of the proposed VSSNLMS predictor over its NLMS counterpart for each case of FDPM-based iterative DDCE and PASTd-based iterative DDCE

schemes. The corresponding Means Square Error (MSE) results are shown in Figure 5.10 and Figure 5.11 for slow and fast fading channel respectively. During the slow fading channel scenario shown in Figure 5.10, the MSE performances of the FDPM-based iterative DDCE employing NLMS and VSSNLMS predictors are better than that of PASTd-based iterative DDCE employing the two predictors respectively. There is also MSE performance improvement for both FDPM-based iterative DDCE and PASTd-based iterative DDCE schemes as NLMS predictor is replaced with VSSNLMS predictor. However, for the fast fading channel scenario shown in Figure 5.11, the performance gain of the FDPM- and PASTd- based DDCE schemes employing VSSNLMS predictor in comparison with the one with NLMS predictor is very small. This narrow marginal gain might be due to the fact that the improvement brought upon the scheme by the iterative techniques overrides the improvement the VSSNLMS predictor offers during this fast fading channel scenario.

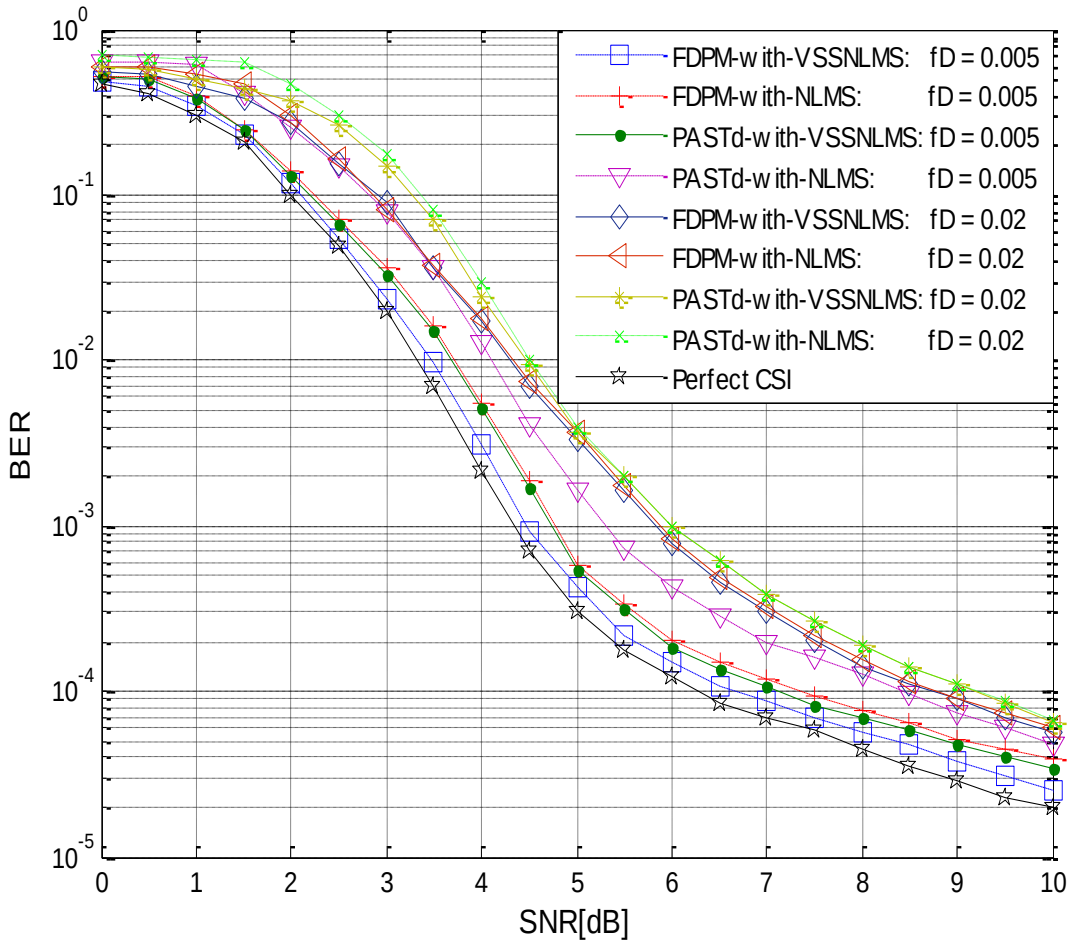

Figure 5.9 BER at the 7th iteration for the proposed DDCE-based FDPM and PASTd algorithms, employing NLMS and VSSNLMS predictors, fD = 0.005 and fD =0.02

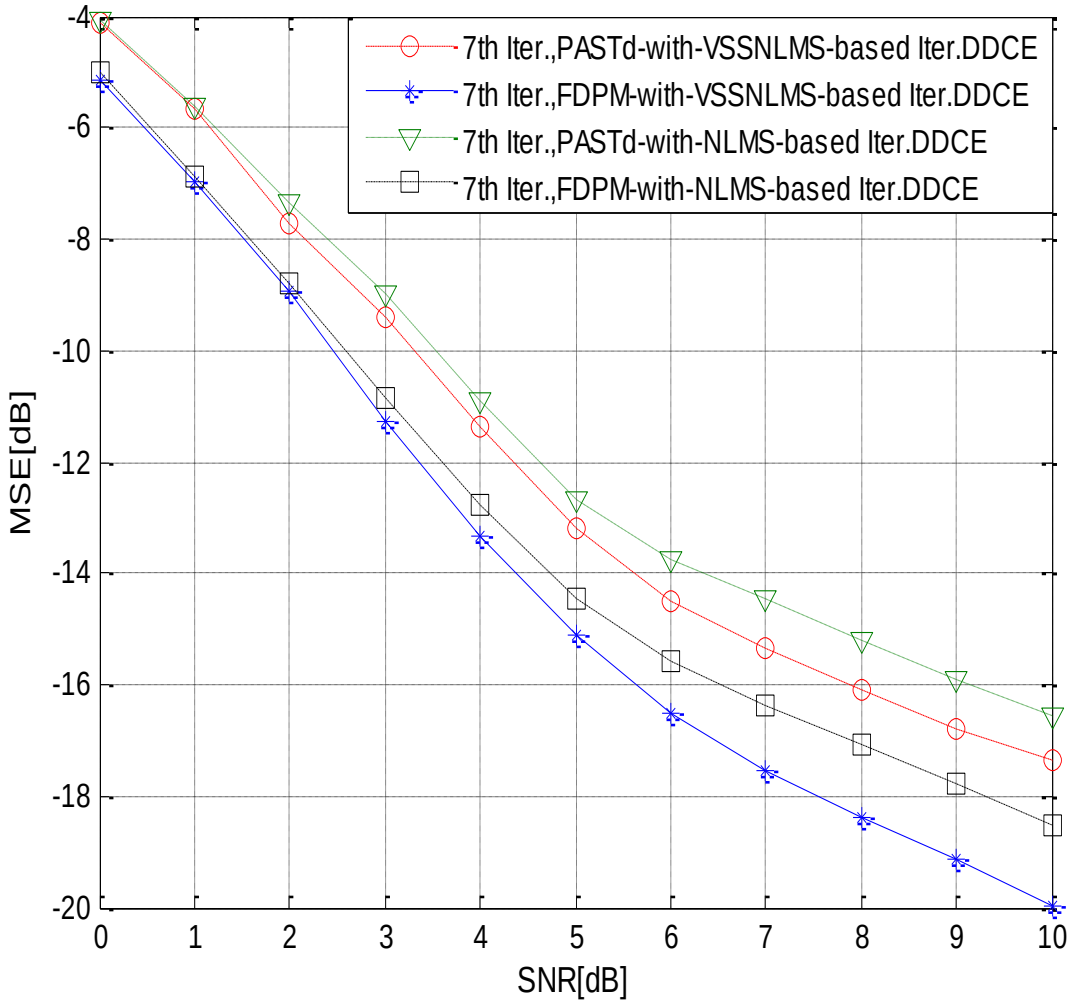

Figure 5.10 MSE at the 7th iteration for the proposed DDCE-based FDPM and PASTd algorithms, employing NLMS and VSSNLMS predictors, fD = 0.005

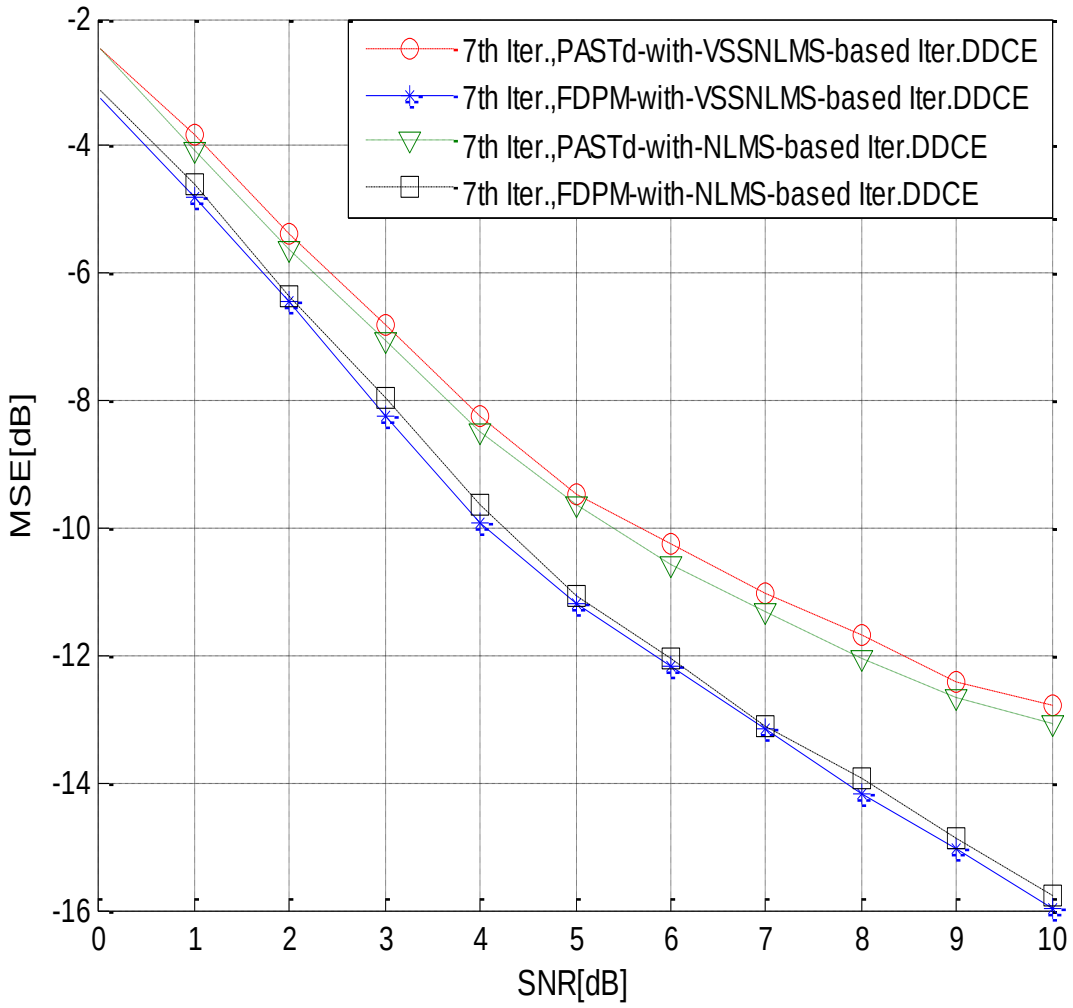

Figure 5.11 MSE at the 7th iteration for the proposed DDCE-based FDPM and PASTd algorithms, employing NLMS and VSSNLMS predictors, fD = 0.02.

5.7 Computational Complexity of the Iterative DDCE Scheme

The computational complexity of the proposed iterative DDCE scheme employing FDPM-based CIR estimator and VSSNLMS-based CIR predictor is the same with that of its non-iterative counterpart presented in Chapter 4 detailed in Section 4.8. However, as a result of the iterative paths introduced in the system receiver, the complexity of the OFDM receiver in comparison with its non-iterative counterpart of Chapter 4 will increase by an additional extra one soft mapper and an interleaver as can be seen from Figure 4.1 and 5.3 respectively.

5.8 Chapter Summary

In this Chapter the concept of iterative DDCE technique proposed for SISO OFDM system is presented. The scheme is based on a Fast Data Projection Method subspace tracking algorithm as well as VSSNLMS-based predictor derived in the previous Chapter. Simulation results suggest that improved performance can be achieved with a reasonable number of iterations. The results also indicate that the iterative DDCE scheme, at an optimal iteration number, outperforms its non-iterative DDCE counterpart proposed in Chapter 4. The simulation results further show improvement in the performance of the proposed iterative scheme employing the FDPM algorithm over its counterpart that employs the PASTd algorithm. The results also indicate that the VSSNLMS-based CIR predictor brings about an improvement to the performance of the DDCE scheme in comparison with the DDCE scheme employing NLMS-based predictor, especially during slow channel fading scenario. In the whole, the Iterative DDCE scheme confirms the added advantage offered by the iterative technique in comparison with the non-iterative technique. However, the proposed scheme will exhibit some disadvantages in terms of hardware complexity and also the implementation issues such as additional time required for iteration in comparison with its non-iterative counterpart presented in Chapter 4. This will definitely bring about some delay in the processing time at the system receiver.

CHAPTER 6

CHANNEL ESTIMATION FOR MIMO-OFDM SYSTEMS

6.1 Introduction

Employment of multiple antennas at both transmitter and receiver ends of wireless communication Systems, termed as MIMO system, has received attention both from industries as well as from academic communities. The reason for this is due to the various gains attached to the deployment of the multiple antennas in the communication Systems. Prominent among these gains are the diversity gain and the multiplexing gain.

Diversity gain can be achieved with the aid of space time coding technique. The deployment of the space-time coding enables the transmission of the same data symbol from multiple transmit antennas. The received data symbols, at each of the receive antennas, are the superposition of all the transmitted data symbols. As such, the receiver will detect the same transmitted data symbol several times and at different antenna position in space. As long as the fading for each transmission links between a pair of transmit and receive antennas in the MIMO Systems can be assumed to be independent of each other, such that at least one link is not in a fading dip at the same time with the other links, the transmitted data symbols can be detected with higher accuracy at the receiver of MIMO Systems. In this way, the bit error rate (BER) performance of the system can be significantly enhanced. This performance improvement is referred to as diversity gain. The space time coding techniques for MIMO Systems can be found, for example, in [242]. There are different types and improved versions of space time coding techniques that have been proposed in literatures. Some of these are the Space-Time Trellis Codes (STTC) in [243], the Orthogonal Space-Time Block Code (OSTBC) in [244, 245], and the Super-Orthogonal Space-Time Trellis Codes (SOSTTC) in [246, 247]. Since the focus of this thesis is on channel estimation techniques for wireless communication system including MIMO-OFDM system, space time coding

technique is not considered. Consequently, MIMO encoding (space-time coding) is not pursued further.

Multiplexing gain is achieved with the aid of Spatial Multiplexing technique. In this technique, stream of data symbols are independently transmitted on different transmit antennas simultaneously. Consequently, multiplexing gain, which is the increase of data rate, is obtained at no additional power consumption or bandwidth expenditure. The main difference in the system architecture for achieving diversity gain and multiplexing gain is that the former can be achieved when multiple antennas are employed at either ends of the communication system. However, for the multiplexing gain to be achieved, multiple antennas are required at both end of the transmission link [248]. As mentioned in Chapter 1, the MIMO system that employs spatial multiplexing technique will have its data rate/ capacity growing proportionally with the minimum of the numbers of transmit, M_T and receive, M_R antennas (that is $min\{M_T, M_R\}$). There are different algorithms that have been employed to implement spatial multiplexing. The first of these is the diagonally-layered space-time known as diagonal Vertical Bell laboratories Layered Space Time (D-BLAST) proposed in [244]. In [249, 250], a simplified version of D-BLAST known as V-BLAST is proposed. Coding gain can be achieved by encoding the data in advance with convolutional code [251]. In [252] spatial multiplexing approach based on the serial concatenation of a convolutional encoder, a bit interleaver, and a space-time signal constellation mapper is proposed, where it is shown that the presented structure approaches the optimal performance. In this approach, information bits are encoded with a convolutional encoder after which the encoded bits are appropriately interleaved and demultiplexed into several parallel streams. Each of these streams is then mapped unto signal constellation points such as M-PSK/M-QAM constellation, and independently transmitted on a transmit antenna. Linear superposition of the transmitted signals corrupted by channel noise is captured by each receive antenna at the receiver end of the MIMO Systems. This approach is said to be a space-time extension of the bit-interleaved coded modulation idea of [253]. Hence, the scheme is referred to as space-time bit-interleaved coded modulation (ST-BICM) [252].

In a broadband communication occasioned by higher data rate, MIMO channel exhibits strong frequency selectivity. However, Orthogonal Frequency Division Multiplexing (OFDM) has become a convenient technique for wideband transmission where the frequency selective channels are converted to an equivalent set of frequency flat sub-channels. The joint deployment of both MIMO and OFDM techniques, referred to as MIMO-OFDM Systems, is considered as a

promising technology for the future generation of broadband wireless Systems, as it decouples the frequency selective MIMO channel into an equivalent numbers of parallel MIMO channels while still maintaining the higher data rate achievable in the MIMO system.

In this chapter, soft input iterative DDCE scheme employing adaptive VSSNLMS and subspace tracking FDPM algorithms is proposed for estimation of MIMO CSI at the receiver of the bit interleaved turbo coded MIMO-OFDM Systems. The proposed iterative DDCE operates in an iterative mode in conjunction with the MIMO demappers and the Turbo decoder at the receiver of the MIMO-OFDM Systems.

The rest of this chapter is therefore organized as follows. Section 6.2 briefly introduces iterative DDCE scheme for MIMO-OFDM Systems, while the MIMO-OFDM Systems model is described in Section 6.3. Different modules of the proposed iterative DDCE for MIMO-OFDM Systems are described in Section 6.4. Section 6.5 and Section 6.6 present soft MIMO demapper and soft MIMO mapper respectively. Simulation results for the proposed iterative DDCE for MIMO-OFDM system are discussed in Section 6.7. Finally, Section 6.8 summarized the chapter.

6.2 Iterative DDCE Scheme for MIMO-OFDM Systems

The ST-BICM architecture has been presented for MIMO-OFDM Systems in [254-257]. Iterative detection and decoding for the ST-BICM MIMO-OFDM architecture is presented in [258]. In [259] optimal decoding of the bit-interleaved coded modulation (BICM) MIMO-OFDM Systems where an imperfect channel estimate is available at the receiver is investigated. In this thesis however, iterative DDCE scheme [263, 264] similar to the one in Chapter 5 is proposed for the MIMO-OFDM system, which is based on ST-BICM structure described above. The proposed iterative DDCE operates in an iterative mode in conjunction with the MIMO demappers (also called detectors) and the Turbo decoder at the receiver of the MIMO-OFDM Systems.

6.3 MIMO-OFDM Systems Model

Figure 6.1 shows block diagram of MIMO-OFDM based on space-time bit-interleaved coded modulation (ST-BICM) transmission scheme. Figure 6.2 depicts the block diagram of the receiver of the MIMO-OFDM system based on ST-BICM including the proposed iterative DDCE scheme.

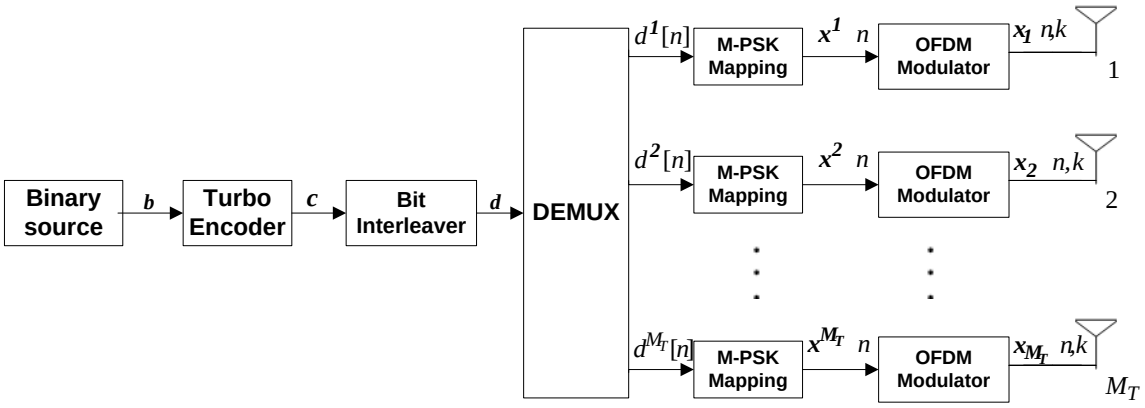

Figure 6.1 Block diagram of MIMO-OFDM based on ST-BICM transmission scheme

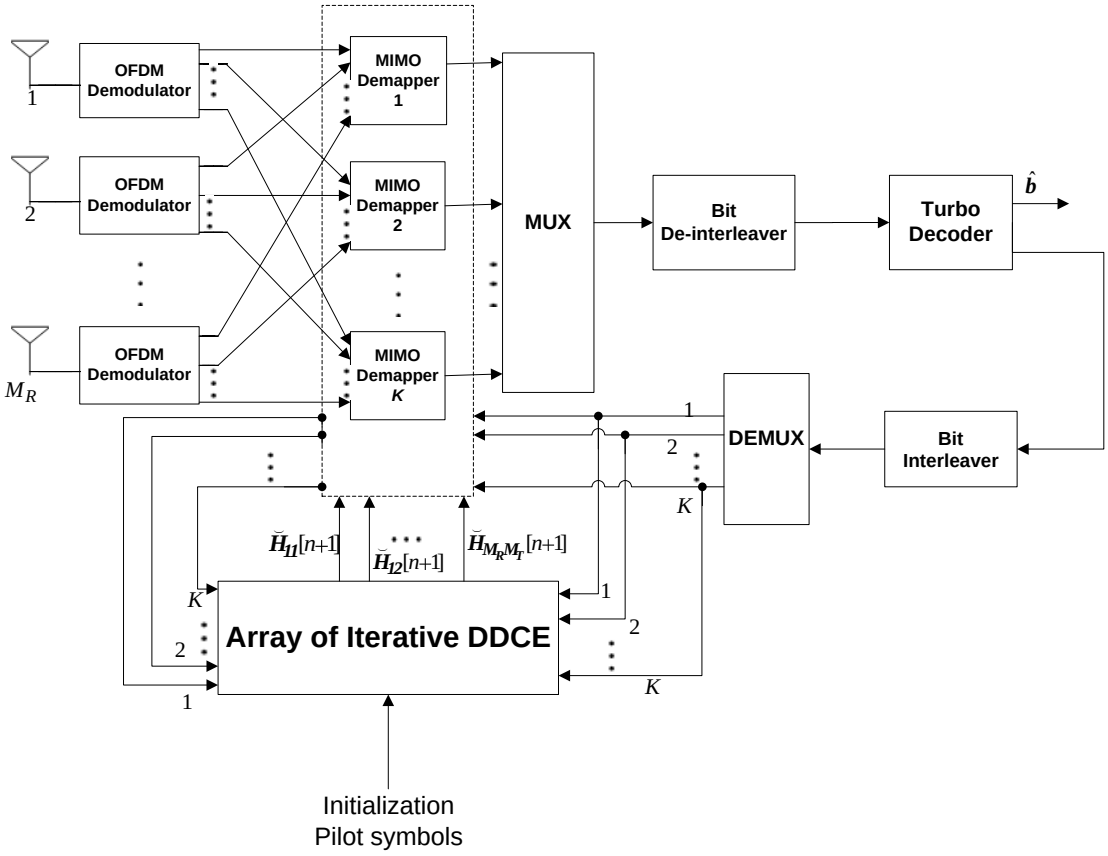

Figure 6.2 Block diagram of MIMO-OFDM receiver with Iterative DDCE scheme

6.3.1 ST-BICM Transmitter Structure

In the Space-Time Bit Interleaved Coded Modulation (ST-BICM) transmitter structure shown in Figure 6.1, binary source bits $\boldsymbol{b} = b_1, b_2, ..., b_{N_b}$, $\in +1, -1$ are encoded by a turbo encoder having code rate R_c . The encoder output sequence $\boldsymbol{c} = c_1, c_2, ..., c_{N_c}$, $\in +1, -1$, where $N_c = N_b / R_c$, are interleaved to $\boldsymbol{d} = d_1, d_2, ..., d_{N_c}$, $\in +1, -1$ by employing a random interleaver of length N_c. The interleaved code bit stream, $\boldsymbol{d}$, are demultiplexed to M_T transmit antenna as $\boldsymbol{d}^i[n]$, $i = 1, ... M_T$, at a time instant *n*. Each of the M_T parallel streams is then mapped to complex symbol, $\boldsymbol{x}\ n = x^1[n], x^2[n], ..., x^{M_T}[n]$, chosen from *M*-ary signal constellation χ, such as QPSK employed in this work. The outputs of the mapper are modulated by the OFDM modulator to each subcarrier as $\boldsymbol{x}\ n,k = x_1[n,k], x_2[n,k], ..., x_{M_T}[n,k]$, and transmitted through M_T antennas.

6.3.2 Channel Statistics

Considering a single user MIMO-OFDM system of Figure 6.1 and Figure 6.2 with M_T transmit and M_R receive antennas, with each OFDM subcarrier of length *K*, the MIMO channel will experience frequency selective fading occasioned by M independent paths in each of the $M_T \times M_R$ Single Input Single Output (SISO) propagation links. Each of these SISO links is similar to SISO channel considered in the previous chapters. Hence, the SISO links of the MIMO channel can be characterized as a multipath SISO channel employed in the previous chapters. As it is with the previous multipath SISO channel, the OFDM transmission scheme converts each of the broadband frequency selective MIMO channels to a set of *K* parallel flat fading channels.

With reference to the previous chapters, the complex baseband representation of the continuous-time CIR of a mobile wireless system is described as [242, 246]

$$h(t,\tau) = \sum_m \gamma_m(t) c(\tau - \tau_m), \tag{6.1}$$

where $\gamma_m(t)$ and τ_m are the time-variant complex amplitude and the delay of the *m*th path respectively, and $c(\tau)$ is the aggregate impulse response of the transmitter-receiver pair that corresponds to the square-root raised-cosine Nyquist filter. Consequent upon the motion of one of the communicating terminals, $\gamma_m(t)$'s are always modeled to be WSS narrowband complex Gaussian processes which are independent for different paths.

The average power of $\gamma_m(t)$'s is a function of the channel delay profiles, which are dependent upon the environment. In the case of MIMO Systems, the channels that are related to different transmit and receive antennas usually experience the same delay profiles as with the SISO Systems [260]. Consequently, the time domain channel impulse response (CIR) from the *ith* transmit antenna to the *jth* receive antenna, following equation (6.1), can be denoted by

$$h_{ji}(\tau) = \sum_{m=0}^{M-1} \gamma_{ji} \; m\, c(\tau - \tau_m) \tag{6.2}$$

However, for OFDM Systems with proper cyclic extension and adequate synchronization, the discrete subcarrier-related Channel Transfer Function (CTF) can be expressed as:

$$H_{ji}[n,k] \triangleq H_{ji}(nT, k\Delta f) = \sum_{l=0}^{K_0-1} h_{ji}[n,l] W_K^{kl}$$

$$= C(k\Delta f) \sum_{m=1}^{M} \gamma_{ji}[n,m] \; W_{ji}^{\;k\tau_m/T_s}{}_{K}, \tag{6.3}$$

where

$$h_{ji}[n,l] \triangleq h_{ji}(nT, lT_s)$$

$$= \sum_{m=1}^{M} \gamma_{ji}[n,m] c(lT_s - \tau_m), \tag{6.4}$$

is the Sample Spaced Channel Impulse Response SS-CIR and $W_K = \exp(-j2\pi/K)$. In (6.4) $\gamma_{ji}(n,m) = \gamma_{ji}(nT,m)$ is the Fractionally Spaced Channel Impulse Response (FS-CIR), and it will be constituted by a low number of $M \le K_0 \le K$ statistically independent non-zero taps associated with distinctive propagation paths. The symbols *K*, *T*, Δf, and T_s in (6.3) are the number of subcarrier, OFDM symbol length, subcarrier spacing, and OFDM symbol duration respectively. In matrix form, equation (6.3) can be written as:

$$\boldsymbol{H}_{ji}\; n = \boldsymbol{W}_{ji}\; n\; \gamma_{ji}\; n\,, \tag{6.5}$$

where $\boldsymbol{W}_{ji} = diag(C[k])\boldsymbol{W}_{ji}$ is defined as ($K \times M$)-dimensional matrix in which $diag(C[k])$ is a ($K \times K$)-dimensional diagonal matrix with the corresponding elements of vector $C(f)$ on the main diagonal [161]. Symbol $\boldsymbol{W}_{ji}$ is the Fourier Transform matrix defined by $W_{ji}\; km = W_{ji}^{\;k\tau_m/T_s}{}_{K}$ for each propagation links between the *ith* transmit and *jth* receive antenna, and for all *k's* and *m's*.

6.3.3 ST-BICM Receiver

At the receiver of the MIMO-OFDM system based on ST-BICM scheme, if perfect time and frequency synchronization are assumed, after the cyclic prefix (CP) has been discarded and OFDM demodulation has be carried out, the signal received at the *jth* receive antenna is the superposition of M_T distorted transmitted signals. Hence, the signal received at the *jth* receive antenna associated with the *kth* subcarrier of the *nth* OFDM block can be written as

$$z_j\ n,k = \sum_{i=1}^{M_T} H_{ji}\ n,k\ x_i\ n,k + w_j[n,k] \quad , \tag{6.6}$$

where $z_j\ n,k$, $x_i\ n,k$ and $w_j[n,k]$ denotes the receive symbol at the *jth* antenna, the transmitted symbol from the *i-th* transmit antenna, and the complex zero-mean white Gaussian noise sample encountered at the *jth* receive antenna respectively.

In vector form, the received signal of (6.6) is given as

$$\boldsymbol{z}\ n,k = \boldsymbol{H}\ n,k\ \boldsymbol{x}\ n,k + \boldsymbol{w}\ n,k \tag{6.7}$$

where,

$$\boldsymbol{H}\ n,k = \begin{bmatrix} H_{11}\ n,k & . & . & . & H_{1M_T}\ n,k \\ . & . & & & . \\ . & & . & & . \\ . & & & . & . \\ H_{M_R1}\ n,k & . & . & . & H_{M_RM_T}\ n,k \end{bmatrix}, \tag{6.8}$$

$$\boldsymbol{z}\ n,k = \left[z_1\ n,k\ , z_2\ n,k\ , \ldots , z_{M_R}\ n,k\ \right]^T, \tag{6.9}$$

and

$$\boldsymbol{w}\ n,k\ = \left[w_1\ n,k\ , w_2\ n,k\ , \ldots , w_{M_R}\ n,k\ \right]^T. \tag{6.10}$$

The received signals are fed into the $1\times K$ array of MIMO demapper. The demappers, with the aid of estimated MIMO CSI provided by the proposed iterative DDCE scheme, compute soft information about the transmitted message bits. These, after being de-interleaved, are fed into the turbo decoder that makes final decision about the possible transmitted bits following a number of iteration. Soft information are fed back to both the MIMO demappers and the array of the iterative DDCE scheme in order to complete the iterative loop of the receiver of the MIMO-OFDM system based on ST-BICM.

6.4 Iterative Decision Directed Channel Estimator Modules for MIMO-OFDM System

Each of the $M_T \times M_R$ array of Iterative Decision Directed Channel Estimator at the receiver of the MIMO-OFDM system of Figure 6.3 comprises three majour component namely, Temporary Channel Transfer Function (CTF) Estimator, Parametric Channel Impulse Response (CIR) Estimator, and the Adaptive Channel Impulse Response Predictor as shown in Figure 3. Details of these are given in the following sections.

6.4.1 Temporary Channel Transfer Function (CTF) Estimator

6.4.1.1 CTF Estimator based on Minimum Mean Square Error (MMSE) Criterion

By extending the MMSE employed in the previous chapters for single antenna OFDM Systems to MIMO channel, the MMSE estimate of the MIMO FD-CTF coefficients *H[n,k]* of the scalar linear model described by (6.7), using the two inputs signals to the CTF Estimator, is given as [226, 228]

$$\tilde{H}_{ij}[\mathrm{n,k}] = \left(\frac{\sum_{i=1}^{M_R} \bar{y}_i[\mathrm{n,k}]\bar{y}_i[\mathrm{n,k}]}{\sigma_{w_i}^2} + \frac{1}{\sigma_{H_{ij}}^2} \right)^{-1} \cdot \frac{\sum_{i=1}^{M_R} \bar{y}_i[\mathrm{n,k}] z_i[\mathrm{n,k}]}{\sigma_{w_i}^2}$$

$$= \frac{\sum_{i=1}^{M_R} \bar{y}_i[\mathrm{n,k}] z_i[\mathrm{n,k}]}{\sum_{i=1}^{M_R} \left|\bar{y}_i[\mathrm{n,k}]\right|^2 + \frac{\sigma_{w_i}^2}{\sigma_{H_{ij}}^2}}, \tag{6.11}$$

where the noisy estimate $\tilde{H}_{ij}[\mathrm{n,k}]$ could be similarly written as

$$\tilde{H}_{ij}[\mathrm{n,k}] = H_{ij}[\mathrm{n,k}] + v_i[\mathrm{n,k}], \tag{6.12}$$

and $v_i[\mathrm{n,k}]$ denotes the *i.i.d*. complex-Gaussian noise samples with a zero mean and a variance of $\sigma_v^2 = MSE_{H_{ij}}$ at the *i-th* receive antenna. The symbol $MSE_{H_{ij}}$ denotes the average Mean Square Error (MSE) associated with the MMSE CTF estimator of (6.11). In the simulation results that will be shown later, it is observed that the performance of MMSE based CTF estimator for

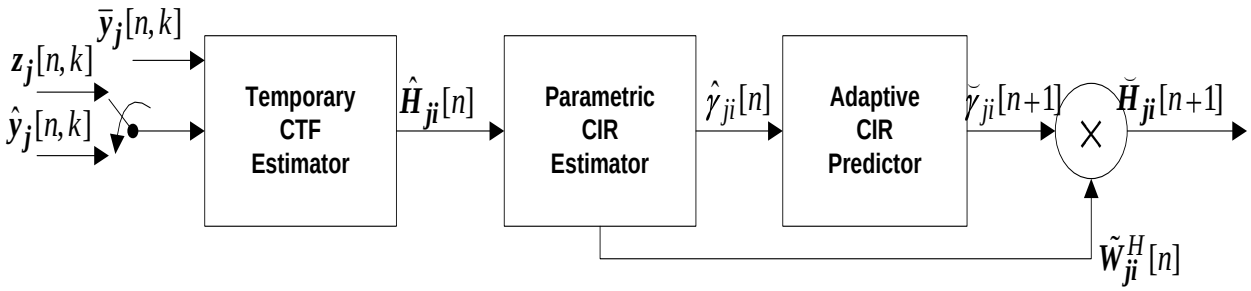

Figure 6.3 Iterative Decision Directed Channel Estimator for MIMO-OFDM Systems

MIMO-OFDM system is worse when compared with how it performed in the case of single antenna OFDM Systems. The simple reason for this is due to the problem of rank deficiency nature associated with the estimation of the MIMO channel. This problem is similarly alluded to in [161]. In order to mitigate this problem, arrays of VSSNLMS based adaptive channel estimator of Chapter 3 are then proposed to implement the CTF estimator, instead of the linear MMSE based CTF estimator, to independently estimate the $M_R \times M_T$ uncorrelated channel coefficient of the MIMO CTF matrix rather that the RLS-based channel estimation applied by the authors in [161]. The use of the VSSNLMS based adaptive channel estimator is inspired by its low complexity and its performance that is close to the performance of the more complex RLS based adaptive channel estimator as indicated in Chapter 3.

6.4.1.2 Variable Step Size Normalized Least Mean Square (VSSNLMS) Adaptive CTF Estimator

The derivation of the Adaptive VSSNLMS-based CTF estimator for the proposed Iterative DDCE scheme for MIMO OFDM system is presented in this section. By omitting the indices *i* and *j* for simplicity, the VSSNLMS-based CTF recursively estimates $\hat{\boldsymbol{H}}[n]$ as follows.

$$\hat{\boldsymbol{H}}[n] = \hat{\boldsymbol{H}}[n-1] + \mu[n]\boldsymbol{e}[n]\frac{\hat{\boldsymbol{x}}^H[n]}{\left\|\hat{\boldsymbol{x}}[n]\right\|^2}, \tag{6.13}$$

where superscript '*H*' is a Hermitian (conjugate transpose),

$$\boldsymbol{e}[n] = \boldsymbol{z}[n] - \boldsymbol{H}^H[n]\hat{\boldsymbol{x}}[n], \tag{6.14}$$

and $\hat{\boldsymbol{x}}[n]$ are the soft value of the detected symbols. The variable step size $\mu[n]$ is updated as [232, 233]

$$\mu[n] = \mu[n-1] - \frac{\rho}{2}\frac{\partial \boldsymbol{e}^2[n]}{\partial \mu[n-1]} \tag{6.15a}$$

$$\mu[n] = \mu[n-1] - \frac{\rho}{2}\frac{\partial \boldsymbol{e}^2[n]}{\partial \hat{\boldsymbol{H}}[n]} \cdot \frac{\partial \hat{\boldsymbol{H}}[n]}{\partial \mu[n-1]} \tag{6.15b}$$

By substituting (6.15a) into (6.15b), and the result substituted into the result obtained from the result of the substitution of (6.13) into (6.15b), we have

$$\mu[n] = \mu[n-1] + \frac{\rho \,\mathrm{Re}\;\boldsymbol{e}[n]\boldsymbol{e}^*[n-1]\hat{\boldsymbol{x}}^H[n]\,\hat{\boldsymbol{x}}[n-1]}{\left\|\hat{\boldsymbol{x}}[n-1]\right\|^2}. \tag{6.16}$$

When the input signal and the channel tap are real (6.16) becomes:

$$\mu[n] = \mu[n-1] + \frac{\rho \boldsymbol{e}[n]\boldsymbol{e}[n-1]\hat{\boldsymbol{x}}^T[n]\,\hat{\boldsymbol{x}}[n-1]}{\left\|\hat{\boldsymbol{x}}[n-1]\right\|^2}\ . \tag{6.17}$$

The values of $\mu[n]$ are restricted within the range $0 < \mu[n] < 2$ in order to make for stable operation of the algorithm [232, 233].

6.4.2 FDPM Subspace Tracking Algorithm-based MIMO CIR Estimator

The time domain MIMO CIR estimator is based on the FDPM algorithm [227] earlier proposed for single antenna CIR estimator in the previous chapters. This is hereby re-derived in the context of MIMO-OFDM Systems. If the symmetric, nonnegative, definite, covariance matrix of the observation vectors $\hat{\boldsymbol{H}}_{ji}[n]$ of size *K* is represented as $\boldsymbol{C}_{H_{ji}}$, its singular vectors corresponding to the *M* dominant singular values can be computed with the aid of an iterative procedure referred to as orthogonal iteration [231] that has the following variants [227]

$$\tilde{\boldsymbol{W}}_{ji}[n] = orthnorm\quad \boldsymbol{I}_K \pm \mu \boldsymbol{C}_{H_{ji}}\ \tilde{\boldsymbol{W}}_{ji}[n-1]\ . \tag{6.18}$$

Replacing $\boldsymbol{C}_{H_{ji}}$ with adaptive estimate $\boldsymbol{C}_{H_{ji}}[n]$, (6.18) results in an adaptive orthogonal iterative algorithm given as

$$\tilde{\boldsymbol{W}}_{ji}[n] = orthnorm\quad \boldsymbol{I}_K \pm \mu \boldsymbol{C}_{H_{ji}}[n]\ \tilde{\boldsymbol{W}}_{ji}[n-1]\ . \tag{6.19}$$

If $\boldsymbol{C}_{H_{ji}}[n]$ is replaced with instantaneous estimate of the covariance matrix represented as $\boldsymbol{C}_{H_{ji}}[n]=\hat{\boldsymbol{H}}_{ji}[n]\hat{\boldsymbol{H}}_{ji}^{H}[n]$, (6.19) results in Data Projection Method (DPM) algorithm given as

$$\hat{\boldsymbol{\gamma}}_{ji}[n]=\tilde{\boldsymbol{W}}_{ji}^{\boldsymbol{H}}[n-1]\hat{\boldsymbol{H}}_{ji}[n], \tag{6.20}$$

$$\boldsymbol{T}_{ji}[n]=\tilde{\boldsymbol{W}}_{ji}[n-1]\pm\mu\hat{\boldsymbol{H}}_{ji}[n]\hat{\boldsymbol{\gamma}}_{ji}^{H}[n]\ , \tag{6.21}$$

$$\hat{\boldsymbol{W}}_{ji}[n]=orthnorm\ \boldsymbol{T}_{ji}[n]\ \ . \tag{6.22}$$

The FDPM algorithm [227], which is herein re-derived in the context of MIMO channel and employed to track the time-domain MIMO CIR, is obtained through the application of a faster orthonomalization procedure (Housholder Transformation) to the DPM algorithm. This application of the faster orthonomalization procedure to obtain the FDPM algorithm is the basis for its better performance in comparison with other subspace tracking algorithms with the same order of computational complexity.

In summary, the time-domain CIR estimates $\hat{\gamma}_{ij}[n]$ of length *M* is tracked based on the temporary FD-CTF observation, $\hat{\boldsymbol{H}}_{ji}[n]$, using the subspace FDPM tracking algorithm as follows.

- At time index n =0, the $\tilde{\boldsymbol{W}}_{\boldsymbol{ij}}[n]$is initialized to orthonormal matrix (typically the first *M* columns of the identity matrix) with *K* rows for faster convergence.

For i = 1, 2, ..., M_R

Do

For j = 1, 2, ..., M_T

Do

For n = 1, 2, .

$$\hat{\gamma}_{\boldsymbol{ij}}[n]=\tilde{\boldsymbol{W}}_{\boldsymbol{ij}}^{H}[n-1]\hat{\boldsymbol{H}}_{\boldsymbol{ij}}[n] \tag{6.23}$$

$$\bar{\mu}=\frac{\mu}{\left\|\hat{\boldsymbol{H}}_{\boldsymbol{ij}}[n]\right\|^{2}} \tag{6.24}$$

$$\boldsymbol{T}_{\boldsymbol{ij}}[n]=\tilde{\boldsymbol{W}}_{\boldsymbol{ij}}[n-1]\pm\bar{\mu}\hat{\boldsymbol{H}}_{\boldsymbol{ij}}[n]\hat{\gamma}_{\boldsymbol{ij}}^{H}[n] \tag{6.25}$$

$$\boldsymbol{a}_{\boldsymbol{ij}}[n]=\hat{\gamma}_{\boldsymbol{ij}}[n]-\left\|\hat{\gamma}_{\boldsymbol{ij}}[n]\right\|\boldsymbol{e}_1\ , \qquad \text{where } \boldsymbol{e}_1=10...0^{\,T} \tag{6.26}$$

$$\boldsymbol{Z}_{\boldsymbol{ij}}[n]=\boldsymbol{T}_{\boldsymbol{ij}}[n]-\frac{2}{\left\|\boldsymbol{a}_{\boldsymbol{ij}}[n]\right\|^{2}}\ \boldsymbol{T}_{\boldsymbol{ij}}[n]\boldsymbol{a}_{\boldsymbol{ij}}[n]\ \boldsymbol{a}_{\boldsymbol{ij}}^{H}[n] \tag{6.27}$$

$$\tilde{\boldsymbol{W}}_{\boldsymbol{ij}}[n] = normalize\ \ \boldsymbol{Z}_{\boldsymbol{ij}}[n] \quad , \tag{6.28}$$

end for n

end for M_T

end for M_R

The performance FDPM subspace tracking algorithm in terms of mean square error (MSE) criterion is as follows.

$$MSE = E\ \left|\boldsymbol{e}(n)\right|^2 \quad , \tag{6.29}$$

where $\boldsymbol{e}(n)$ is given as

$$\boldsymbol{e}(n) = \hat{\boldsymbol{H}}_{\boldsymbol{ij}}[n] - \tilde{\boldsymbol{W}}_{\boldsymbol{ij}}[n-1]\hat{\boldsymbol{\gamma}}_{\boldsymbol{ij}}[n]. \tag{6.30}$$

6.4.3 Adaptive VSSNLMS Algorithm-based MIMO CIR Predictor

The MIMO CIR predictor for the proposed iterative DDCE for MIMO-OFDM Systems is based on VSSNLMS algorithm and it is similar to the one in the previous chapters for single antenna OFDM Systems, except that it is herein adapted to the case of MIMO channels. The choice of VSSNLMS-based predictor over its counterpart, the (RLS)-based adaptive predictor is similarly based on the reasons for employing VSSNLMS-based CTF estimator instead of the RLS-based CTF estimator, the computation complexity issues [261, 262] detailed in Chapter 4.

The VSSNLMS algorithm updates the *mth* CIR tap's predictor coefficients $\boldsymbol{p}_{ij}[n][m]$ of length L_{prd} as [261, 263, 265]

$$\boldsymbol{p}_{ij}[n, m] = \boldsymbol{p}_{ij}[n-1, m] + \frac{\mu_{ij}[n]}{\left\|\hat{\gamma}_{ij}[n-1, m]\right\|^2} e_{ij}^{*}[n, m]\hat{\gamma}_{ij}[n-1, m], \tag{6.31}$$

where,

$$e_{ij}[n, m] = \hat{\gamma}_{ij}[n, m] - \boldsymbol{p}_{ij}^{H}[n-1, m]\hat{\gamma}_{ij}[n-1, m]. \tag{6.32}$$

The MIMO CIR is then predicted for the next time index n+1 as

$$\breve{\gamma}_{ij}[n+1, m] = \boldsymbol{p}_{ij}^{H}[n, m]\hat{\gamma}_{ij}[n, m], \tag{6.33}$$

and the variable step size of (6.31) is obtained as

$$\hat{\mu}_{ij}[n] = \mu_{ij}[n-1] + \frac{\rho\,\mathrm{Re}\ e_{ij}[n, m]e_{ij}^{*}[n-1, m]\hat{\gamma}_{ij}^{H}[n, m]\hat{\gamma}_{ij}[n-1, m]}{\left\|\hat{\gamma}_{ij}[n-1, m]\right\|^2}. \tag{6.34}$$

In order to restrict the variable step size $\mu_{ij}[n]$ to the range $0<\mu_{ij}[n]<2$ which makes for the stable operation of the NLMS algorithm as stated above, the variable step size $\mu_{ij}[n]$ in (6.31) is restricted within the range given as

$$\mu_{ij}[n]=\begin{cases}\mu_{\max} & if \quad \hat{\mu}_{ij}[n]>\mu_{\max}\\ \mu_{\min} & if \quad \hat{\mu}_{ij}[n]<\mu_{\min}\\ \hat{\mu}_{ij}[n] & otherwise\end{cases}, \tag{6.35}$$

where $0<\mu_{\min}<\mu_{\max}<2$.

At time index n = 0, the predictor filters are initialized as [152] $\boldsymbol{p}_{ij}[n,m]=1\ \ 0\ \ 0\ \ldots\ 0^{T}$. The operation of the VSSNLMS based MIMO CIR predictor is summarized as follow:

For i = 1, 2, …, M_R
Do
For j = 1, 2, …, M_T
Do
For n = 1, 2, . .
Do
For m = 1, 2, …, M
if n = 0,
set $\boldsymbol{p}_{ij}[m][n]=1\ \ 0\ \ 0\ \ldots\ 0^{T}$

$$e_{ij}[n,m]=\hat{\gamma}_{ij}[n,m]-\boldsymbol{p}_{ij}^{H}[n-1,m]\hat{\gamma}_{ij}[n-1,m] \tag{6.36a}$$

$$\boldsymbol{p}_{ij}[n,m]=\boldsymbol{p}_{ij}[n-1,m]+\frac{\mu_{ij}[n]}{\left\|\hat{\gamma}_{ij}[n-1,m]\right\|^{2}}e_{ij}^{*}[n,m]\hat{\gamma}_{ij}[n-1,m] \tag{6.36b}$$

$$\breve{\gamma}_{ij}[n+1,m]=\boldsymbol{p}_{ij}^{H}[n,m]\hat{\gamma}_{ij}[n,m] \tag{6.36c}$$

$$\hat{\mu}_{ij}[n]=\mu_{ij}[n-1]+\frac{\rho\,\mathrm{Re}\ e_{ij}[n,m]e_{ij}^{*}[n-1,m]\hat{\gamma}_{ij}^{H}[n,m]\hat{\gamma}_{ij}[n-1,m]}{\left\|\hat{\gamma}_{ij}[n-1,m]\right\|^{2}} \tag{6.36d}$$

end for M
end for n
end for M_T
end for M_R

The predicted CIR is finally converted to the frequency domain CTF using the transformation matrix $\tilde{\boldsymbol{W}}_{\boldsymbol{ij}}[n]$ as

$$\breve{\boldsymbol{H}}\ n,k\ =\tilde{\boldsymbol{W}}_{\boldsymbol{ij}}[n]^{*}\breve{\gamma}_{ij}[n+1,m]\,. \tag{6.37}$$

The CTF obtained is then fed to the soft MIMO demapper for the purpose of obtaining soft information for the next OFDM symbol.

6.5 Soft MIMO Demapper

The soft MIMO Demapper is fed with the outputs of the OFDM demodulators, the estimated MIMO CTF, as well as the extrinsic (soft) information returns by the Turbo decoder. The demapper computes the *a posterior* log likelihood ratios of the coded and interleaved transmitted bits for *i-th* antenna branch mapped at *k-th* subcarrier into the *q-th* bit position ($i = 1, \ldots, M_T$; and $q = 1, \ldots Q$ from the 2^Q-ary signal constellation) as

$$L\ d[n]^{i,q} = \ln\left(\frac{\Pr\ d[n]^{i,q} = +1}{\Pr\ d[n]^{i,q} = -1}\right) \tag{6.38}$$

6.5.1 Soft MIMO Demapper Formulation

If the *q-th* bit corresponding to the symbol $x_i\ n,k$, transmitted from the *i-th* transmit antenna and on the *k-th* subcarrier, at time instant *n*, is represented as $d^{i,q}[n,k]$, then its log-likelihood ratios can be denoted as $L\ d^{i,q}[n,k]$, where $i = 1, \ldots, M_T$; and $q = 1, \ldots, Q$ (from the 2^Q-ary signal constellation). In the case where QPSK constellation is used for modulation at the transmitter end of the system, $Q = 2$. Hence, the log-likelihood ratios $L\ d^{i,q}[n,k]$ of (6.38) conditioned on the estimated channel state information, $\breve{\boldsymbol{H}}\ n,k$ (made available by the proposed iterative DDCE scheme) as shown in Figure 6.2, is given as [252]

$$\begin{aligned} L\ d^{i,q}[n] &= \ln\left(\frac{\Pr\ d^{i,q}[n]=+1 \mid \boldsymbol{z}[n], \breve{\boldsymbol{H}}[n]}{\Pr\ d^{i,q}[n]=-1 \mid \boldsymbol{z}[n], \breve{\boldsymbol{H}}[n]}\right) \\ &= \ln\left(\frac{\sum_{\boldsymbol{x}[n]\in\chi\ d^{i,q}[n]=+1} \Pr\ \boldsymbol{x}[n],\boldsymbol{z}[n],\boldsymbol{H}[n]}{\sum_{\boldsymbol{x}[n]\in\chi\ d^{i,q}[n]=-1} \Pr\ \boldsymbol{x}[n],\boldsymbol{z}[n],\boldsymbol{H}[n]}\right), \end{aligned} \tag{6.39}$$

where $\chi\ d^{i,q}[n]=b; b\in+1,-1$ is the set of all possible vectors having bit $d^{i,q}[n]=+1 or -1$. The number of elements in such a set is $2^{M_T Q-1}$ [252] .The subcarrier index *k*, is dropped for convenience purpose. The joint probability density of (6.39), obtained from the product of the conditioned channel probability density function, and the *a priori* probability of the symbol vector, under AWGN assumption, is given as [252]

$$\Pr\ \boldsymbol{x}[n],\boldsymbol{z}[n],\boldsymbol{H}[n]\ = K\exp\left(\frac{1}{N_0}\sum_{j=1}^{M_R}\left\|z_j[n]-\sqrt{E_s}\sum_{i=1}^{M_T}H_{ji}[n]x^i[n]\right\|^2+\frac{1}{2}\sum_{i=1}^{M_T}\sum_{q=1}^{Q}d^{i,q}[n]L_a\ \ d^{i,q}[n]\right), \quad (6.13)$$

where K is a constant. The elements of the symbol vector $\boldsymbol{x}[n]$ and the bits that are mapped to such a vector are denoted as $x^i[n]$ and $d^{i,q}[n]$ respectively. The *a priori* log-likelihood ratios $L_a\ \ d^{i,q}[n]$ are set to zero at the initial stage of the iterative process, since there is no *a priori* information on the coded bit at this stage. During the subsequent iterations, the *a priori* ratios of the bits of each transmit antenna branch are derived from the output of the Map turbo decoder. The *a priori* log-likelihood ratios from the decoder are also employed by another *soft mapper* to compute soft symbols that are fed into the proposed iterative DDCE scheme for the estimation of the channel state information in the second iteration and beyond.

6.6 Soft MIMO Mapper

The soft MIMO Mapper follows after the soft Mapper of the previous chapters for single antenna OFDM Systems scenario. In order to make for effective performance of the soft mappers, different *M-PSK* constellation arrangement are used on each of the *ith* antenna branch at the transmitter end of the system, ranging from gray to anti-gray mapping arrangements.

6.7 Simulation Results and Discussions

In order to evaluate the performance of the proposed soft input iterative DDCE scheme for the MIMO-OFDM Systems, computer simulations were conducted for the $M_T \times M_R$ MIMO-OFDM Systems based on the ST-BICM transmission scheme shown in Figure 6.1 and Figure 6.2. The time-variant six-path COST 207 Typical Urban (TU) channel model of [43] with normalized Doppler frequencies of 0.005, 0.02, and 0.01 is employed, while the channel gains associated with transmit and receive antenna pairs are independent but with the same statistical properties. A total channel bandwidth of 800 kHz divided into K = 64 subcarriers is assumed. In order to make the subcarriers orthogonal to each other, the symbol duration, *Ts* is set to 80μs, while the CP length is 16 samples (1/4 of the symbol period) and additional guard interval *Tg* = 20μs is employed to give protection from intersymbol interference occasioned by channel multipath delay spread. Consequently, the total block period, *T* sum up to 100μs. The turbo encoder of rate

1/3 and octal generator polynomial of (7, 5) is serially concatenated with random interleaver in order to achieve the bit interleaved coded modulation technique. A realistic non sample-spaced CIR of length M = 6 is assumed in all the simulations. The step size μ for FDPM-based CIR estimator is set to 0.98, while η is set to 0.95for PASTd algorithm. The length of the CIR predictor (L_{prd}) is set to 10, while initialization values of $\mu[n]$ and $\mu_{ij}[n]$ are set to 0.5, and ρ set to 0.002 for both the VSSNLMS-based CTF estimator and the VSSNLMS-based predictor respectively.

The simulation work begins with extension of the linear MMSE CTF estimator employed in the previous chapters for single antenna OFDM Systems to the case of MIMO-OFDM Systems. Subsequently, the proposed VSSNLMS-based CTF estimator is employed. In order to ensure error free estimate from the proposed iterative DDCE for MIMO-OFDM Systems, the first N_{pil}-th OFDM symbols comprises the known pilot symbol out of the total ($N = N_{pil} + N_{mes}$) OFDM symbols per frame as shown in Figure 6.4. Figure 6.5 depicts the corresponding pilot-messages OFDM symbols pattern. Both Iterative DDCE and the soft MIMO demapper operate in an iterative mode with the Turbo decoder during which they exchange soft information with Turbo decoder in a bid to refine their outputs over a number of iterations. During the last iteration, the hard decision about the transmitted bits $\hat{b}_p$ is made by the Turbo decoder. At this initial stage, the OFDM frame length N is set to 25, while N_{pil} =1 and N_{mes} = 24 resulting in 4% = $\left(\frac{\mathrm{N_{pil}}}{\mathrm{N}}\times 100\%\right)$ pilot message overhead. The number of transmit and receive antennas are set to $M_T = M_R = 2$. The comparative results exhibit by the two estimators for both slow and fast fading channels are as shown in Figure 6.6. It is observed that the performance of the linear MMSE CTF estimator in comparison with the adaptive VSSNLMS-based CTF estimator is very poor for both fading channel scenarios, and the margin between the MSE performance of VSSNLMS-based CTF estimator in comparison with linear MMSE CTF estimator become wider as the SNR increases. The reason for this poor performance of the linear estimator is apparently due to the problem of highly rank-deficient nature associated with the estimation of MIMO CTF, which a linear estimator like MMSE will find difficult to accurately estimate. This problem is similarly alluded to in [161], where RLS-based CTF estimator is employed to mitigate the problem. However, it is confirmed in [184] that the complexity cost associated with RLS algorithm would not lend it to real time implementation. This is the reason while the VSSNLMS-based CTF estimator is proposed in this Chapter.

The effect of iteration between the three modules, soft MIMO demapper, Turbo decoder and the proposed iterative DDCE over a number of iterations is also investigated. At this stage, the iterative DDCE is constituted by VSSNLMS-based CTF estimator, FDPM-based parametric CIR estimator, and adaptive VSSNLMS-based predictor. The achievable bit error rate (BER) over six iterations are displayed in Figure 6.7 and Figure 6.8 for slow and fast fading channels respectively. The results show an improvement for both fading channels up to the fifth iteration. The result is more noticeable for the fast fading channel scenario. Simulation is further run for the proposed iterative DDCE for MIMO-OFDM Systems employing PASTd-based CIR estimator proposed in [161]. Figure 6.9 and Figure 6.10 show comparative BER and MSE performance respectively between the FDPM-based iterative DDCE and the PASTd-based DDCE schemes after the fifth iteration. The proposed FDPM-based iterative DDCE exhibits better performance in comparison with its PASTd counterpart, especially at higher SNR.

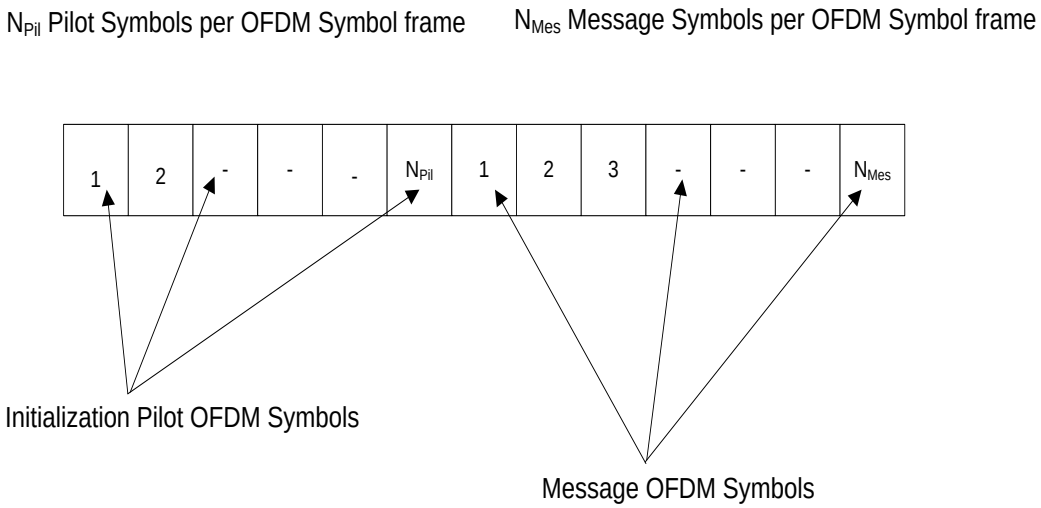

Figure 6.4 Initialization Pilot OFDM symbols and Message OFDM symbols arrangement per OFDM symbol frame for the Iterative DDCE Scheme.

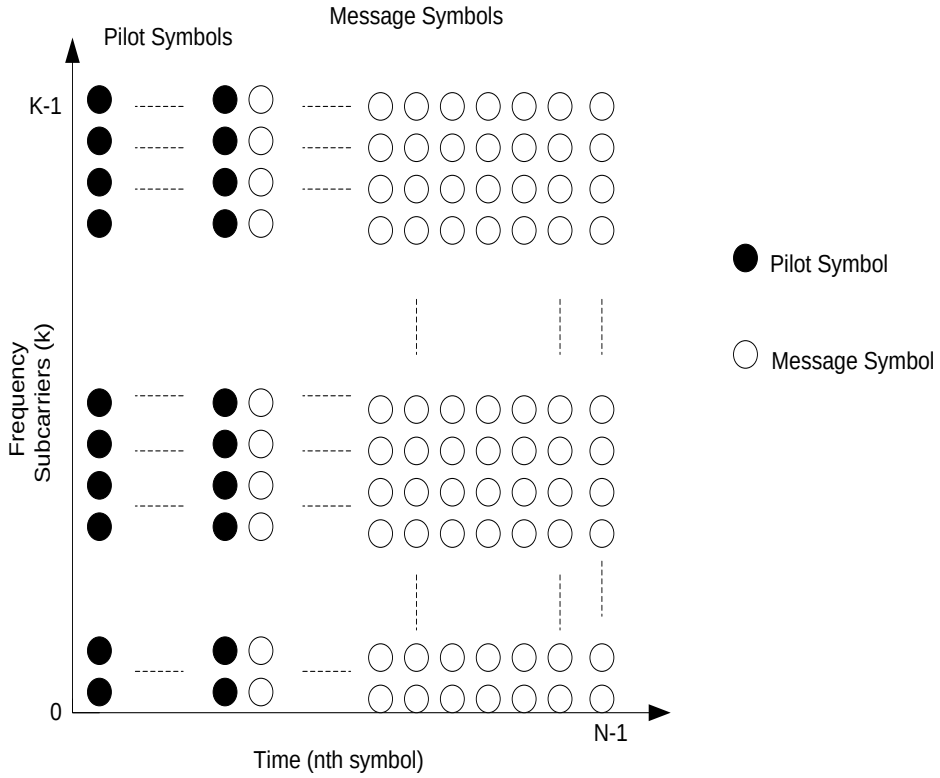

Figure 6.5 Corresponding Pilot OFDM symbols / Message OFDM symbols pattern for the Iterative DDCE Scheme ($N = N_{Pil} + N_{Mes}$).

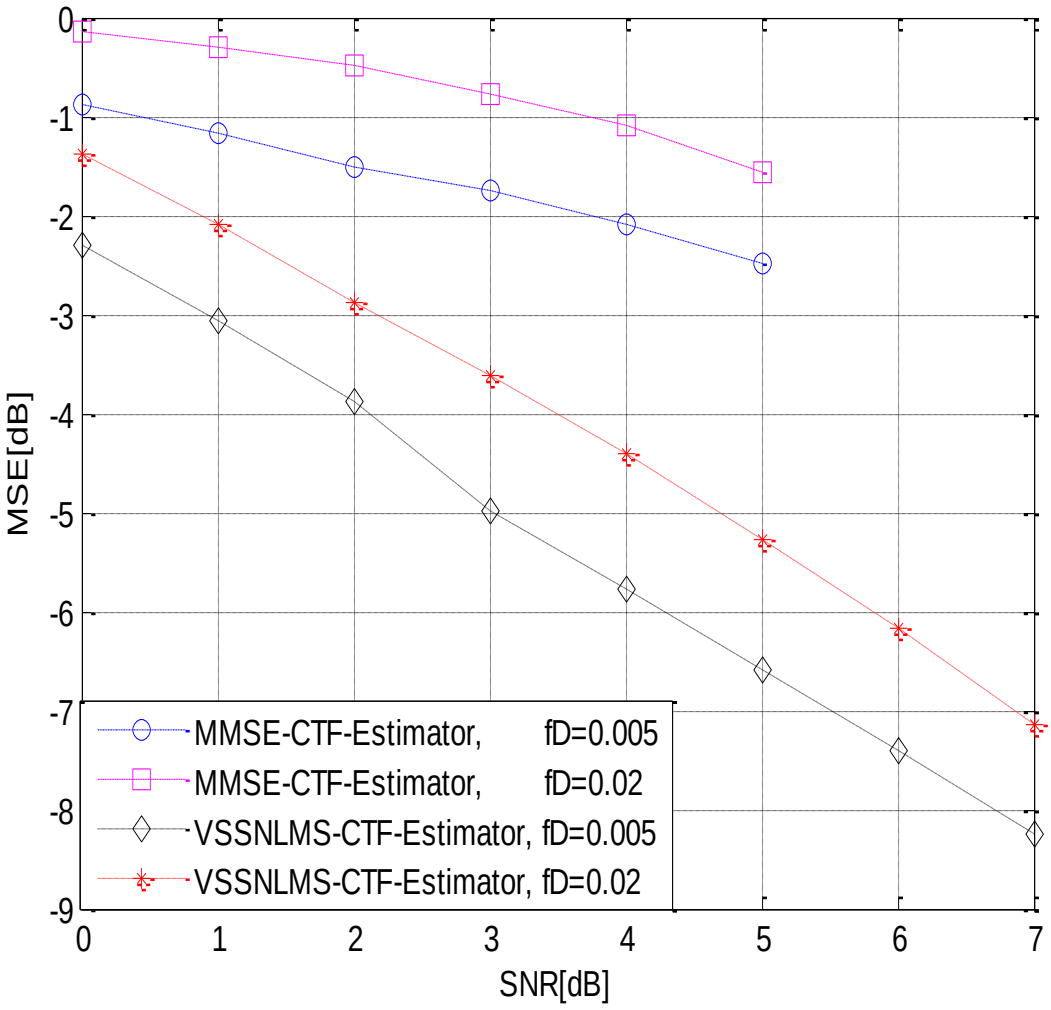

Figure 6.6 Comparative MSE exhibited by the MMSE-based and VSSNLMS-based Temporary CTF Estimators operating in both slow fading Channel fD = 0.005 and fast fading channel fD = 0.02.

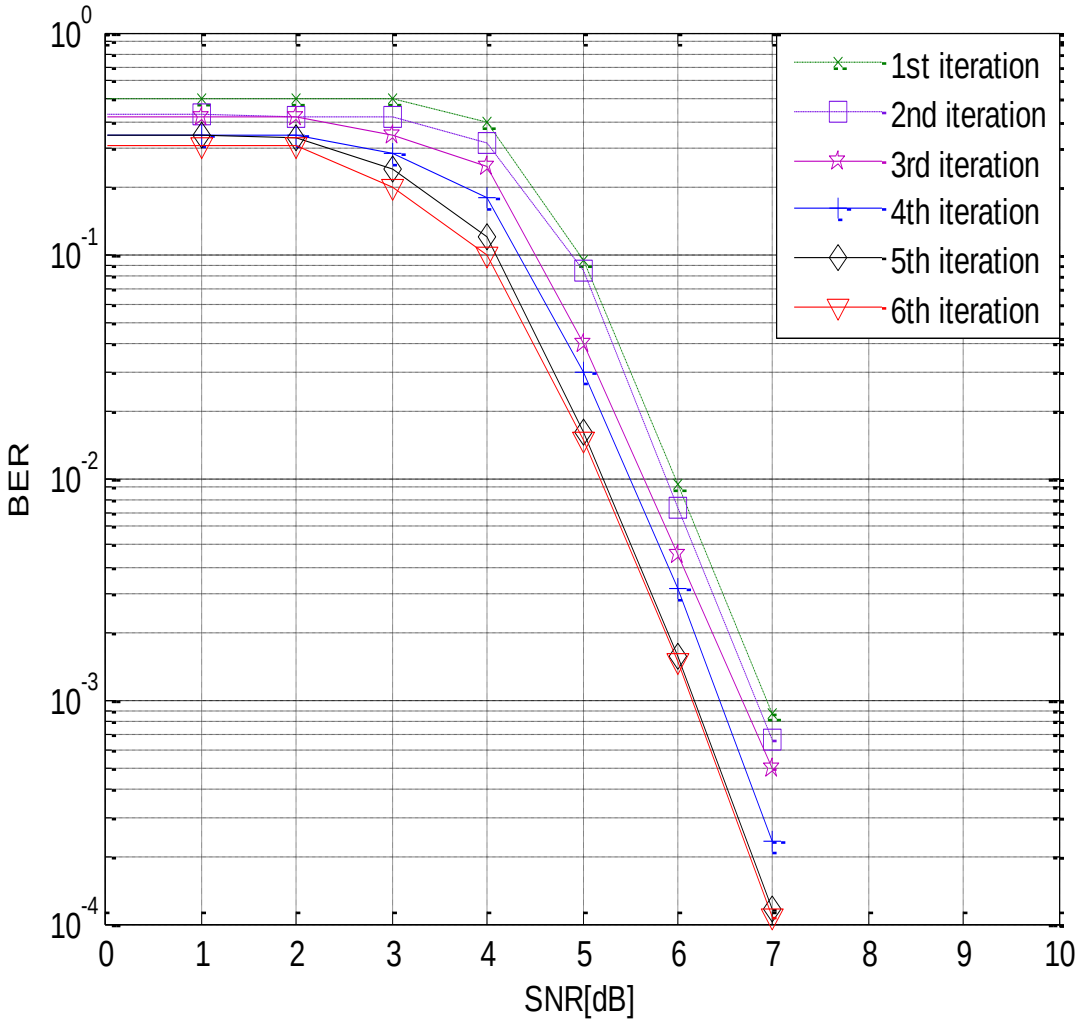

Figure 6.7 BER versus SNR exhibited by the 2 × 2 iterative FDPM-based DDCE scheme for BICM Bit interleaved turbo coded MIMO-OFDM System, fD=0.005.

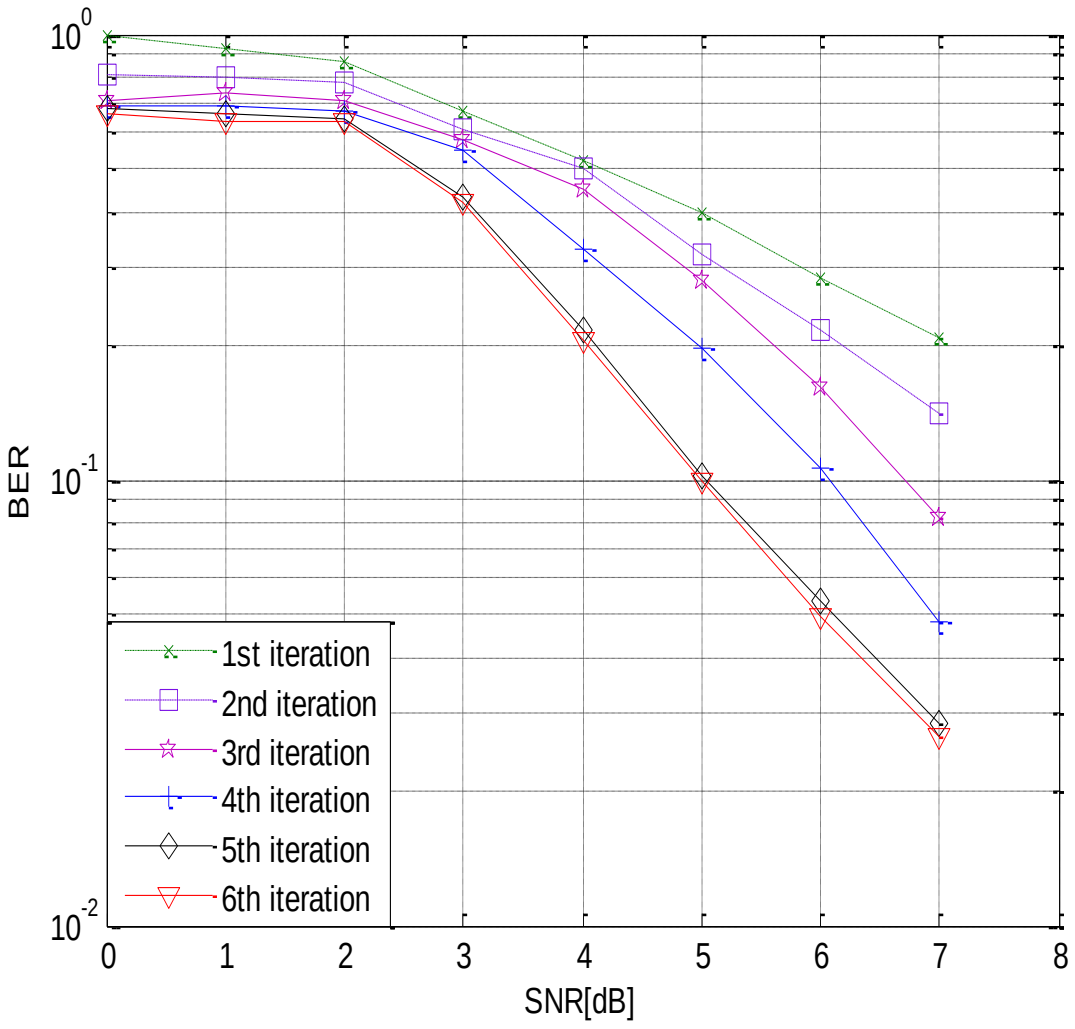

Figure 6.8 BER versus SNR exhibited by the 2 × 2 iterative FDPM-based DDCE scheme for Bit interleaved turbo coded MIMO-OFDM System, fD=0.02.

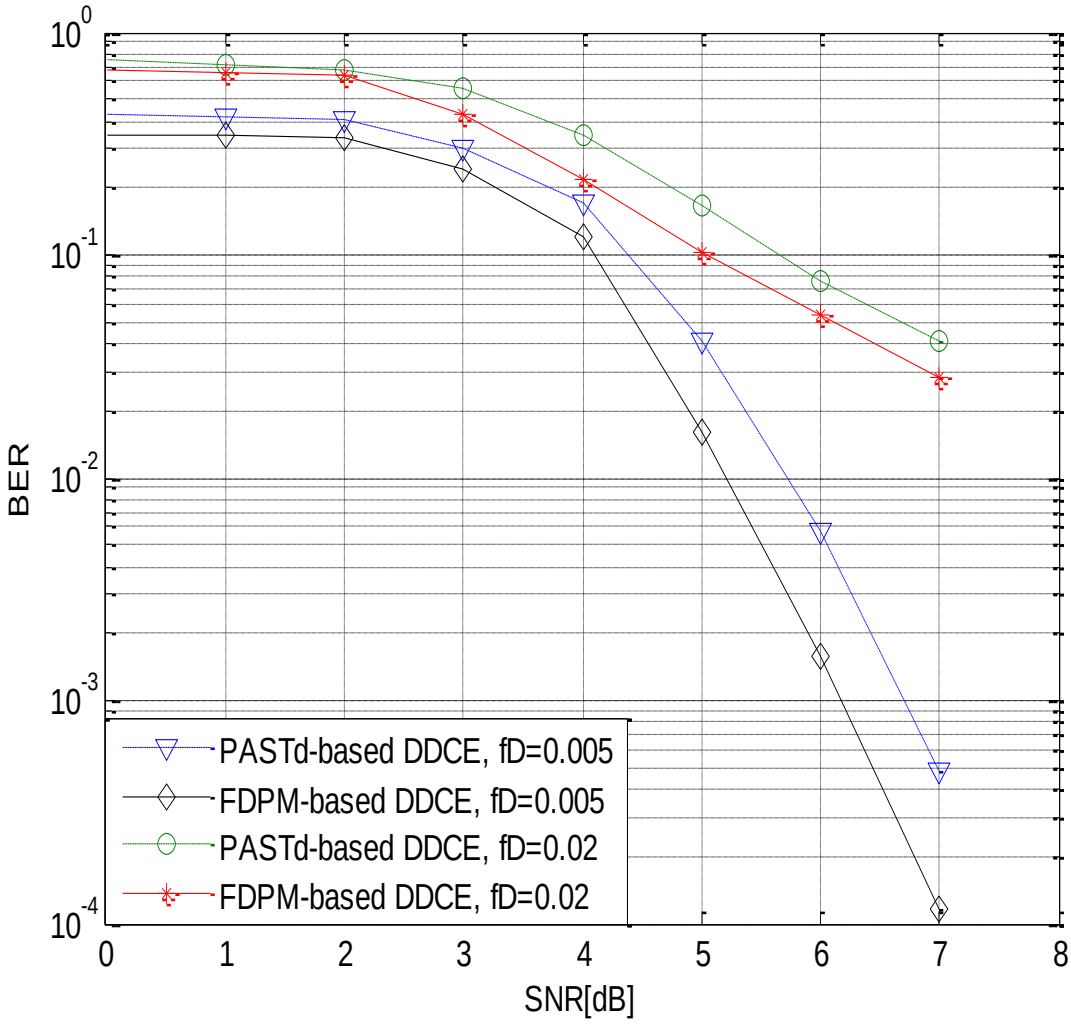

Figure 6.9 BER versus SNR at 5th iteration as a function of normalized Doppler frequencies exhibited by the 2 × 2 iterative FDPM-based and iterative PASTd-based DDCE schemes for Bit interleaved turbo coded MIMO-OFDM System.

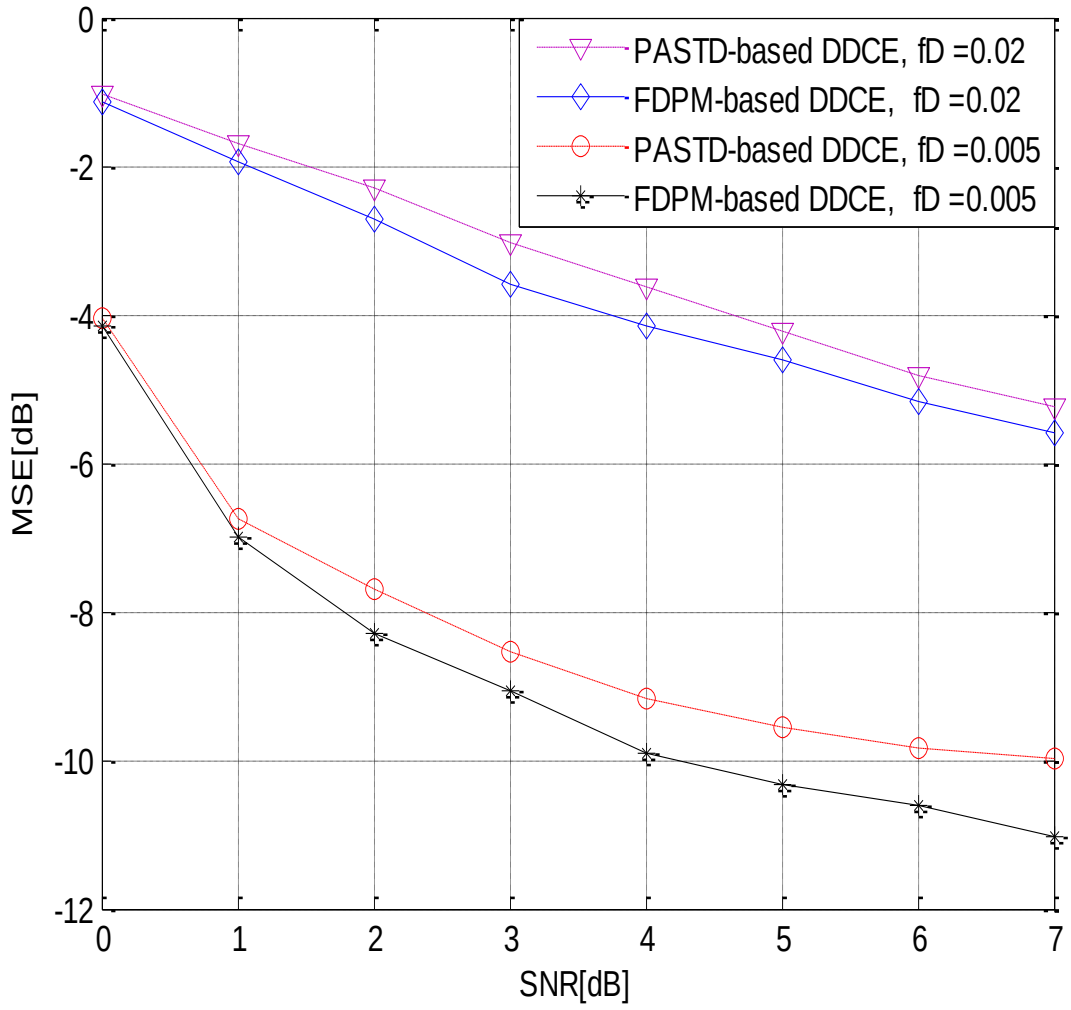

Figure 6.10 MSE versus SNR at 5th iteration as a function of normalized Doppler frequencies exhibited by the 2 × 2 iterative FDPM-based and iterative PASTd-based DDCE schemes for Bit interleaved turbo coded MIMO-OFDM System.

Figure 6.11 further shows the achievable BER performance of the proposed FDPM-based iterative DDCE as a function of normalized Doppler frequencies 0.005, 0.02, and 0.01. The results indicate a poor performance at higher normalized Doppler frequency of 0.01. This suggests that the proposed estimator finds it difficult to track a very rapid fading MIMO channel.

Furthermore, the effect of the pilot overhead $\left(\frac{N_{pil}}{N}\times 100\%\right)$ in the OFDM frame is investigated. Figure 6.12 and Figure 6.13 illustrate the BER performance after the fifth iteration for the FDPM-based iterative DDCE under slow and fast fading MIMO channels respectively while varying the percentage overhead of the initialization pilot symbols between 4%, 16% and 28% per OFDM symbol frame. The results indicates improvement in the obtainable channel estimate when the pilot overhead increases from 4% to 16%, but with less improvement when it is increased from 16% to 28 % in both cases of fading MIMO channel conditions. Lastly, the effect of the antenna diversity on the proposed iterative DDCE for the bit interleaved turbo coded MIMO-OFDM Systems is investigated. Figure 6.14 and Figure 6.15 portray the achievable result with 1×1, 2×2, and 4×4 MIMO-OFDM Systems for slow and fast fading MIMO channels. It is observed that the increment of M_T and M_R from $M_T = M_R = 1$ to $M_T = M_R = 4$ brings about improvement to the BER performance of the estimator for both slow and fast fading channel cases. This is largely due to the increased spatial diversity advantage associated with higher number of antenna at both ends of the MIMO communication Systems. However, it is noted that there is degradation in the performance of the proposed iterative DDCE scheme for MIMO-OFDM Systems when compared with performance obtainable with the single antenna OFDM Systems at lower SNR during the fast fading channel. The simple explanation for this is that the high complexity-based iterative DDCE scheme for MIMO-OFDM Systems (in the order of $M_T \times M_R$ compared with that of single antenna system) finds it difficult to track the channel estimate accurately during the fast fading MIMO channel scenario in comparison with the low complexity-based iterative DDCE scheme for single antenna system at low SNR.

In order to validate the various results presented hitherto, effort was made to reproduce results for PASTD-based channel estimation proposed for similar scheme in [205] employing Turbo coding with code rate 1/2. Figure 6.16 illustrates the achievable results of the PASTD-based estimator for 1×1, 2×2, and 4×4 QPSK MIMO-OFDM systems corresponding to results of Figure 6.0 of [205]. With close comparison with the previous results, it is obvious that the FDPM-based estimator proposed in this thesis, whose results are earlier presented, exhibits better performance that the PASTD-based channel estimation of [205].

In a bid to investigate the effect of code rate on the overall performance of the system, plot of PASTD-based estimator for 1×1 systems employing Turbo coding with code rate 1/3 is included in Figure 6.16. It is observed that the there is a significant improvement in the result by reducing

the code rate from 1/2 to 1/3 especially at higher SNR. The performance exhibits by PASTD-based estimator for 1 × 1 systems employing Turbo coding with code rate 1/3 is closed to its equivalent in Figure 4.16 of Chapter 4. The little observable difference could be associated to the differences in the number of data per frame, number of iteration, and fading rate. It is noted herein that 1/3 code rate for Turbo coding employed in this thesis rather than 1/2 code rate used in the various cited literature has brought significant improvements upon various results presented in the thesis.

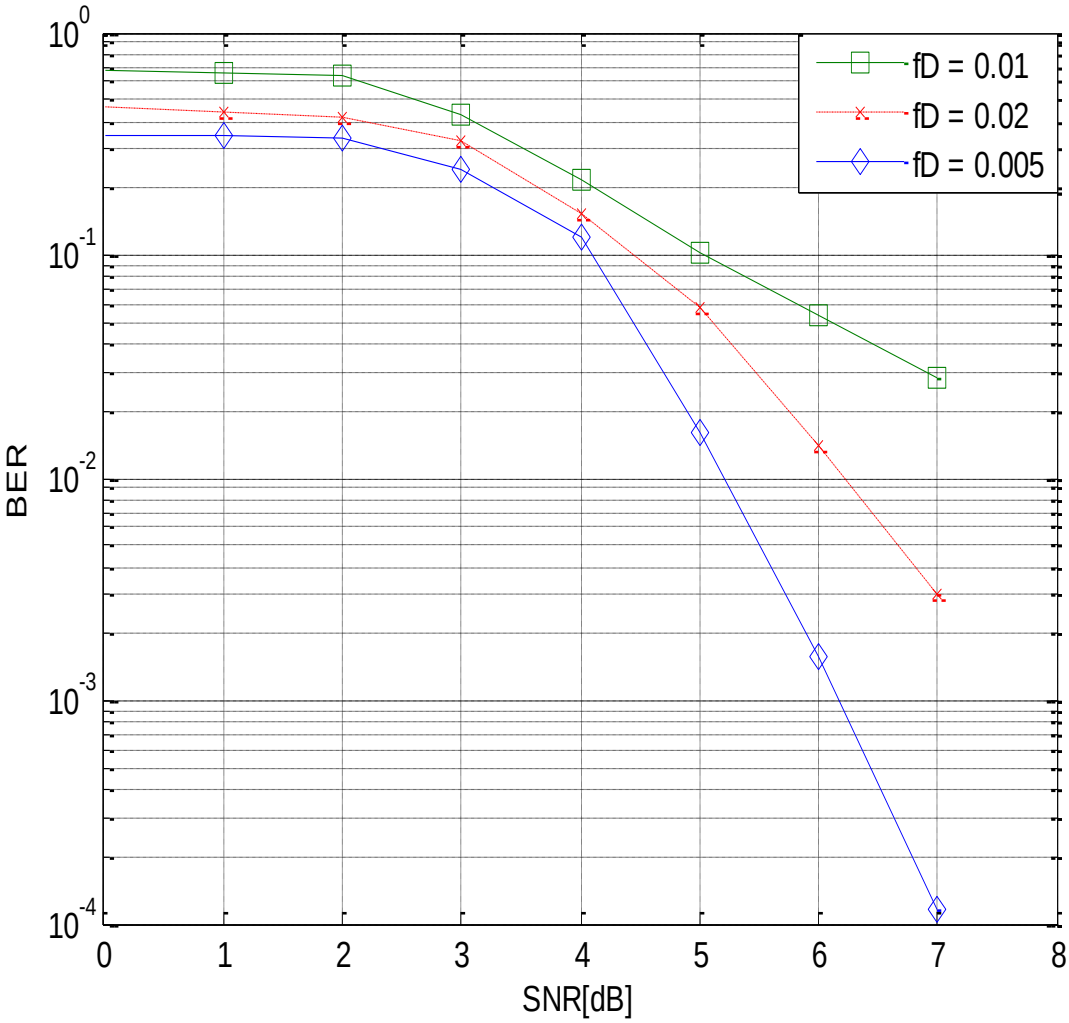

Figure 6.11 BER versus SNR at 5th iteration as a function of normalized Doppler frequencies exhibited by the 2 × 2 iterative FDPM-based for Bit interleaved turbo coded MIMO-OFDM System.

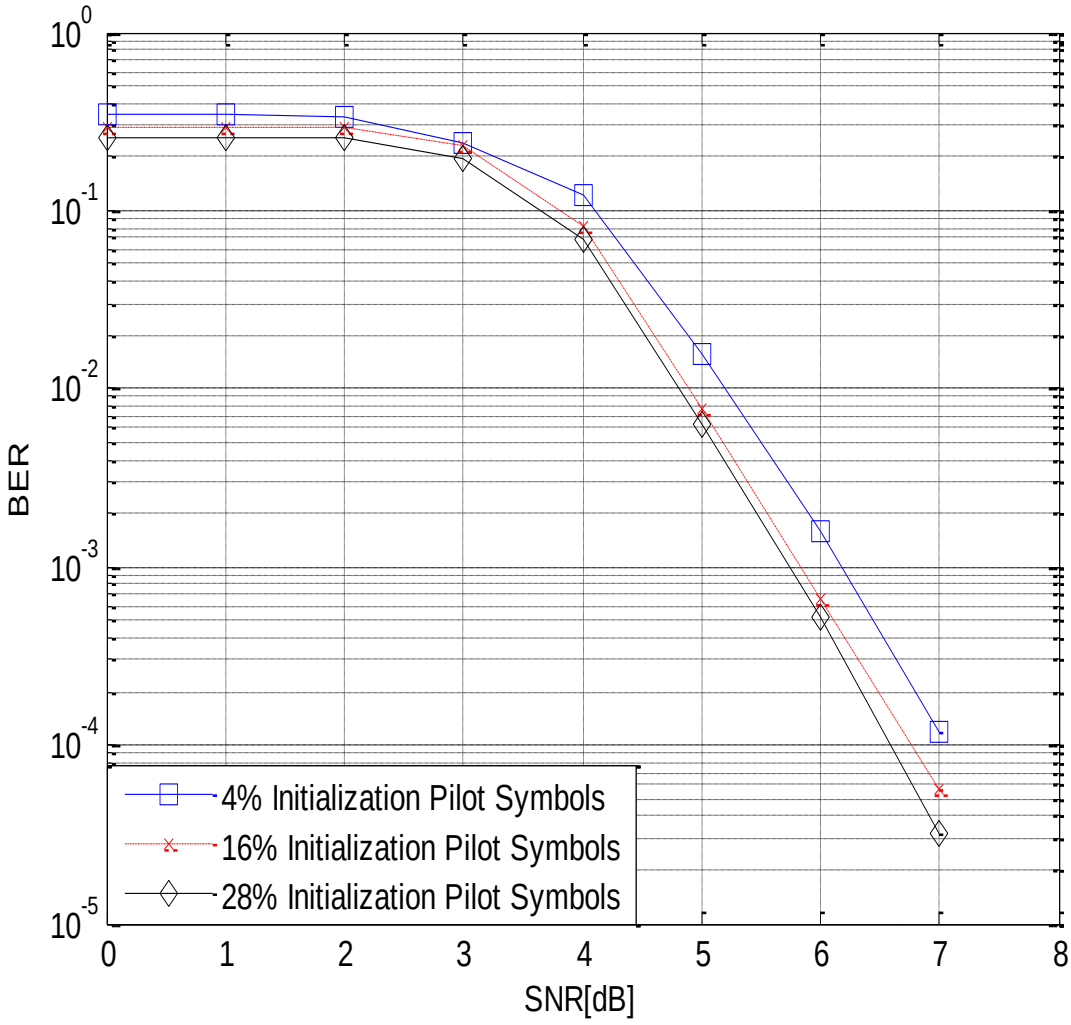

Figure 6.12 BER versus SNR after the 5th iteration as a function of percentage pilot overhead during slow fading scenario of normalized Doppler frequency, fD = 0.005 for FDPM- based -based iterative DDCE for MIMO-OFDM Systems.

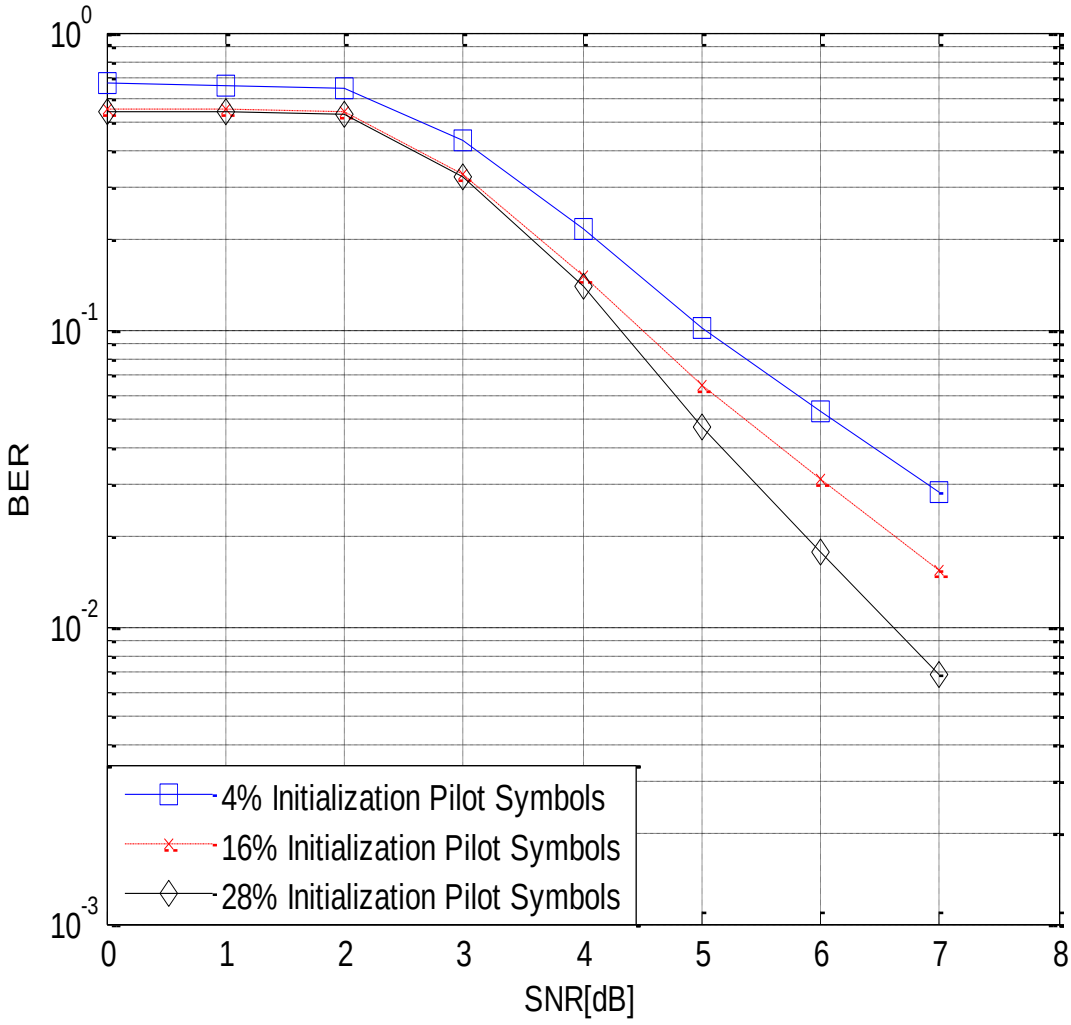

Figure 6.13 BER versus SNR after the 5th iteration as a function of percentage pilot overhead during fast fading scenario of normalized Doppler frequency, fD = 0.02 for FDPM- based iterative DDCE for MIMO-OFDM Systems.

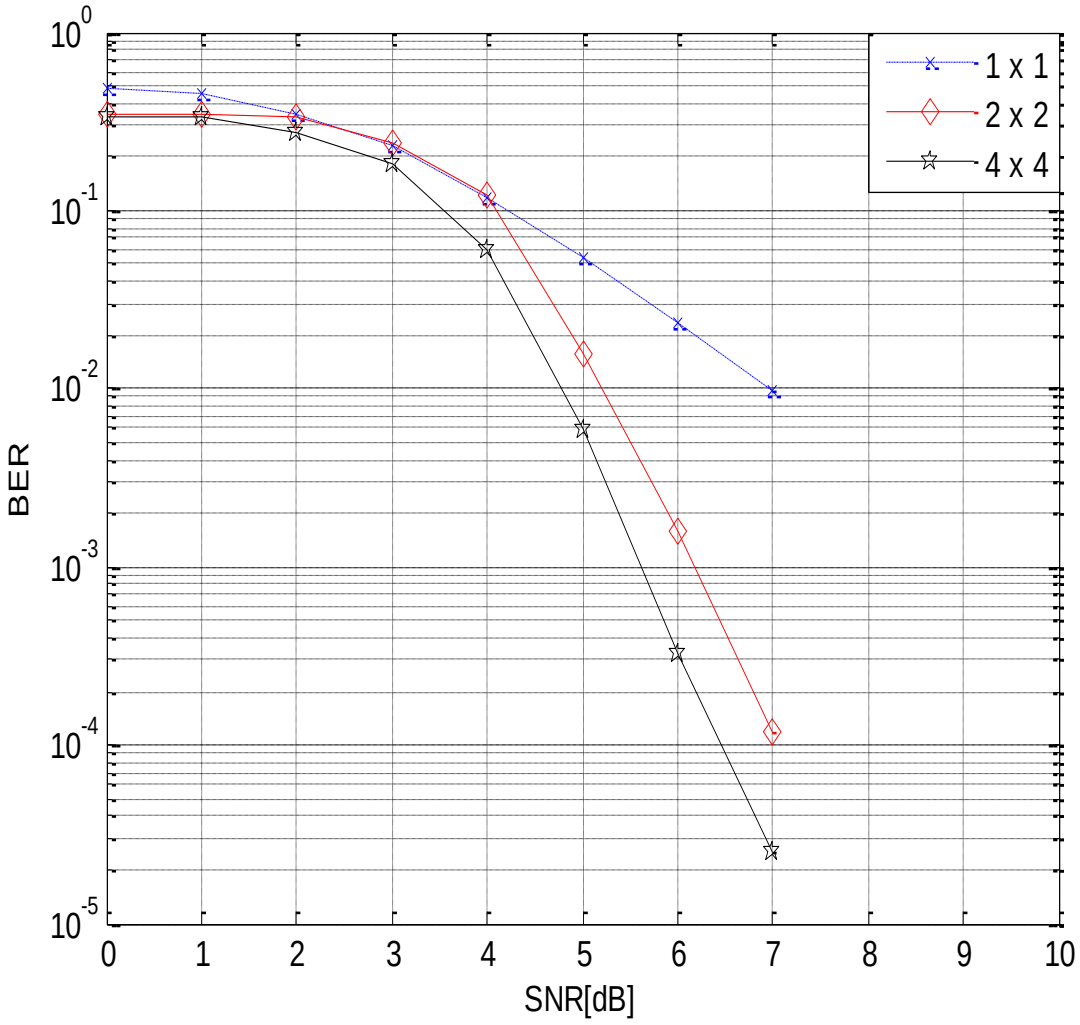

Figure 6.14 BER versus SNR after the 5th iteration for FDPM-based iterative for 1 × 1, 2 × 2, and 4 × 4 MIMO-OFDM Systems during slow fading scenario of normalized Doppler frequency, fD = 0.005.

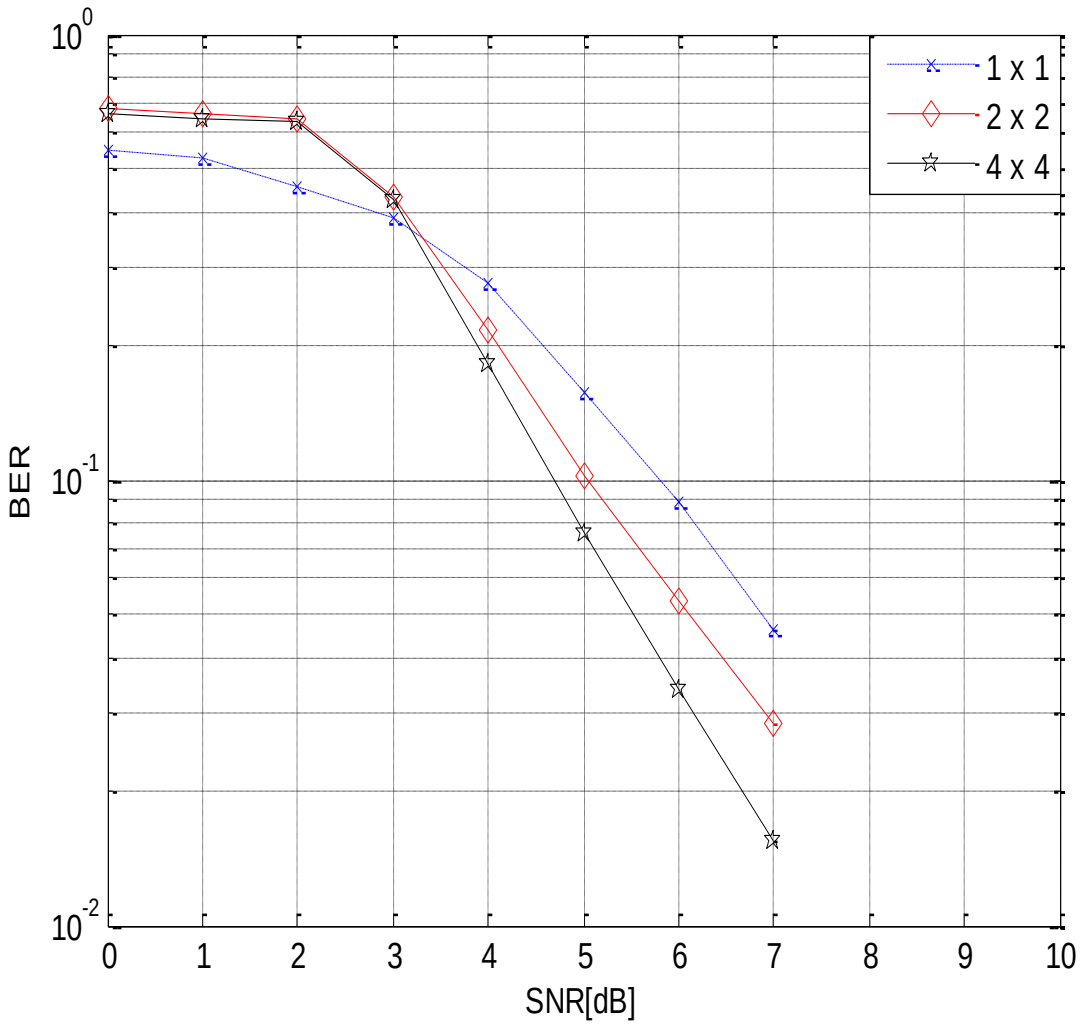

Figure 6.15 BER versus SNR after the 5th iteration for FDPM-based iterative for 1 × 1, 2 × 2, and 4 × 4 MIMO-OFDM Systems during slow fading scenario of normalized Doppler frequency, fD = 0.02.

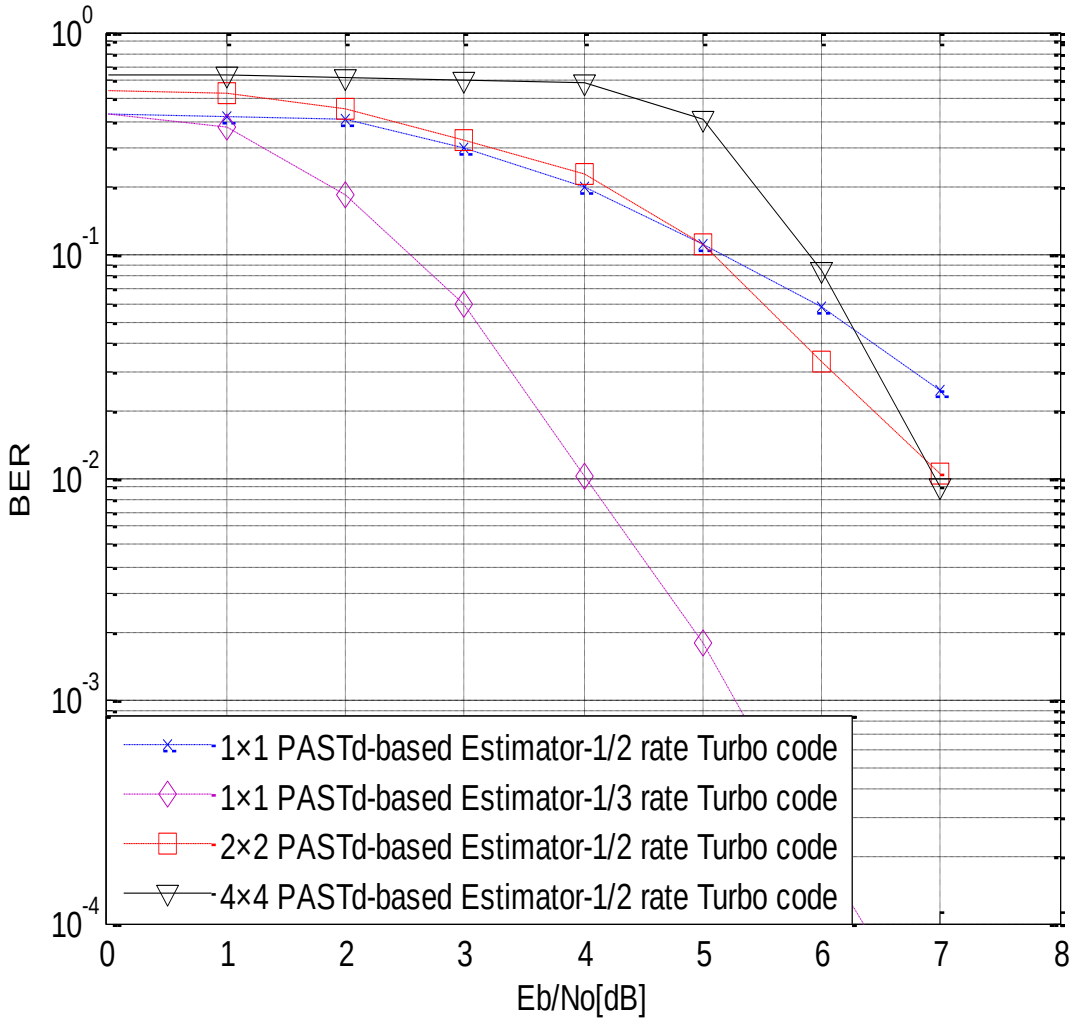

Figure 6. 16 BER results for PASTD-based iterative channel estimator [205] for 1 × 1, 2 × 2, and 4 × 4 MIMO-OFDM Systems during normalized Doppler frequency, fD = 0.003

6.8 Computational Complexity of the proposed Iterative DDCE scheme for MIMO-OFDM Systems

In order to have idea of the computational complexity of the proposed iterative DDCE scheme for MIMO-OFDM system, computational complexity of each module is examined. The computational complexity of adaptive VSSNLMS algorithm is of order $O\ \ 3L_{prd}+4\ M$ [8], while the computational complexity of the FDPM subspace tracking algorithm is of order $6KM+O(M)\approx O(7KM)$. It implies that each of the arrays of the iterative DDCE will constitute a computational complexity of twice $O\ \ 3L_{prd}+4\ M$ to take care of the CTF estimator and the predictor, plus $O(7KM)$ to take care of the CIR parametric estimator module, in the context of SISO-OFDM system. Consequently, for the bit interleaved turbo coded MIMO-OFDM, the order of computational complexity of the proposed iterative DDCE will grow linearly in order of $M_T \times M_R$ in comparison with the SISO-OFDM system of Chapter 5. However, if RLS algorithm of complexity order $O\ \ ML_{prd}^2$ is employed as used in [161] for implementation of CTF estimator and CIR predictor, each of the arrays of the iterative DDCE for MIMO-OFDM system will constitute a computational complexity of twice $O\ \ ML_{prd}^2$. This will definitely be more costly if larger predictor filter length L_{prd} is used.

6.9 Chapter Summary

In this chapter, MIMO-OFDM based on space time-BICM is presented. In order to make for coherent detection of the transmitted signal in the system, soft input iterative DDCE scheme based on adaptive VSSNLMS and subspace tracking FDPM algorithms is proposed for estimation of MIMO CSI at the receiver of the bit interleaved turbo coded MIMO-OFDM Systems. The VSSNLMS-based temporary CTF estimator, the FDPM-based parametric CIR estimator, and the adaptive VSSNLMS-based CIR predictor are derived in the context of MIMO channel for the proposed iterative Decision Directed Channel Estimation scheme. Simulation results portraying the performance trends of the proposed iterative DDCE for both slow and fast fading channel scenarios have been presented and discussed. In the overall, the proposed

estimator for MIMO-OFDM system employing the VSSNLMS-based CTF estimator and VSSNLMS-based predictor derived in this chapter, as well as the FDPM-based CIR estimator is shown to outperform its counterpart based on MMSE criterion and PASTd subspace algorithm. However, the order of computational complexity of the proposed iterative DDCE scheme grows linearly as $M_T \times M_R$ (the number of transmit and receive antennas) in comparison with the computational complexity of the similar scheme proposed in the previous chapters for SISO-OFDM system.

CHAPTER 7

CONCLUSIONS AND RECOMMENDATIONS

7.1 THESIS SUMMARY

In this thesis, the issue of channel estimation for single input single output (SISO), multiple input multiple output (MIMO) Systems in combination with orthogonal frequency division multiplexing transmission scheme is addressed. This is necessitated with the understanding that without availability of perfect channel state information (CSI) at the receiver end of either the SISO or MIMO OFDM Systems, the achievable advantages associated with the Systems and the OFDM transmission scheme would not be maximally exploited. Having reviewed previous contributions in this area of research, we proposed computationally efficient and robust channel estimation schemes for single antenna communication Systems, SISO-OFDM communication Systems and MIMO-OFDM communication Systems.

Specifically in Chapter 3, soft input based iterative channel estimation scheme is proposed for turbo equalization-based receiver for single antenna communication system over frequency selective fading channel. Single-VSSNLMS and multiple-VSSNLMS algorithms are derived for the implementation of the proposed channel estimator in a bid to address the problem of slow convergence rate and poor channel tracking capabilities associated with the LMS and NLMS-based channel estimation algorithms. From the presented results the proposed VSSNLMS-based iterative channel estimation algorithm shows faster convergence rate than both APRmodRLS algorithm and the LMS algorithm earlier recommended for the same purpose in literatures. The presented simulation results also show that both single and multiple-VSSNLMS-based iterative channel estimation algorithms outperform both the LMS and the NLMS algorithms and their performances are very close to that of the well know computationally complex RLS algorithm. We concluded that the single-VSSNLMS algorithm which is less complex than both multiple-

VSSNLMS and RLS algorithms is suitable for the tracking and the estimation of a fast-varying frequency selective fading channel in single antenna communication Systems.

In the subsequent Chapter, Decision Directed Channel Estimation scheme for SISO OFDM system in the context of a more realistic Fractionally Spaced-Channel Impulse Response (FS-CIR) channel model is investigated. We proposed the use of the Fast Data Projection Method (FDPM) subspace tracking algorithm for the implementation of the CIR estimator module of the DDCE scheme. The presented results show how the FDPM-based CIR estimator outperforms the PASTd-based CIR estimator proposed by another authors in literature. VSSNLMS-based predictor is further derived for the implementation of the CIR predictor module of the DDCE scheme. The presented results also indicate that the VSSNLMS-based CIR predictor improved the performance of the DDCE scheme in comparison with when NLMS-based predictor is employed. The obtainable results of the DDCE scheme employing the proposed VSSNLMS-based CIR predictor is also observed to be very close to the scheme that employs a more complex RLS-based predictor. In terms of computational complexities, we have been able to show that the proposed DDCE scheme employing FDPM-based CIR estimator and VSSNLMS-based CIR predictor is less complex in comparison with the one proposed in the literature; hence the proposed estimator scheme for SISO OFDM communication system is more appropriate for real time implementation.

The concept of iterative technique based on turbo principle is applied, in Chapter 5, to the DDCE scheme proposed in Chapter 4 for SISO OFDM communication system. Based on this principle an iterative structure is designed to implement the proposed iterative DDCE scheme for SISO OFDM communication system. The presented results suggest that improved performance can be achieved with a reasonable number of iterations. The results also indicate that the iterative DDCE scheme, at an optimal iteration number, outperforms its non-iterative DDCE counterpart proposed in the previous Chapter. In summary we have been able to confirm the added advantage offered by the proposed iterative DDCE scheme in comparison with the non-iterative scheme.

Lastly, soft input iterative DDCE scheme is proposed for space-time bit-interleaved coded modulation (ST-BICM) MIMO-OFDM communication system. For the MIMO-OFDM system, VSSNLMS-based temporary CTF estimator, FDPM-based parametric CIR estimator and adaptive VSSNLMS-based CIR predictor are derived in the context of MIMO channel for the proposed iterative Decision Directed Channel Estimation scheme. The derivation and the proposal of the VSSNLMS-based temporary CTF estimator for MIMO-OFDM system is informed by the poor

performance exhibited by the CTF estimator based on minimum mean square error (MMSE) criterion that has been employed in the case of SISO OFDM system in the previous Chapters. In the overall, the proposed iterative DDCE estimator for MIMO-OFDM system employing the VSSNLMS-based CTF estimator and the VSSNLMS-based predictor, as well as the FDPM-based CIR estimator is shown to outperform its counterpart based on MMSE criterion and PASTd subspace algorithm. From the foregoing, it could be concluded that the proposed iterative DDCE scheme, employing the algorithms, is robust enough for estimation of CSI for MIMO-OFDM communications system.

7.2 SUGGESTIONS FOR FUTURE RESEARCH WORK

In this thesis the issue of channel estimation for both single antenna and multiple antenna-based OFDM Systems is investigated. However, we believe that there are quite a lot of research works that need to be carried out especially for MIMO-OFDM communication Systems. This is because it is of common knowledge that MIMO-OFDM technique will have a crucial role to play in the implementation of the future generation of the mobile wireless Systems, especially the fourth generation (4G) and fifth generation (5G) Systems and even higher generation that could be conceived. Hence, the work presented in this thesis could be used as a platform for some future research works, some of which are highlighted in the following:

- In the various communication Systems presented in this thesis, single user rather than multiple users is assumed in all the simulation works as stated in Section 1.5. The proposed estimation schemes can be extended to the case of multi-user single antenna and MIMO Systems.

- The proposed iterative estimator is implemented for the multi level phase shift keying (M-PSK) Systems. The scheme could be implemented for the case of multi level quadrature amplitude modulation (M-QAM) Systems in order to investigate its performance trend.

- Perfect time and frequency synchronization is assumed in all our simulations, but we know that this is not the case in the practical world. Hence, it will be necessary to investigate the possibility of time and frequency synchronization in conjunction with the

proposed channel estimation scheme. In addition, a way of incorporating interference cancellation with the proposed channel estimation process should be considered.

- Extension of the proposed iterative DDCE scheme for space-time bit-interleaved coded modulation MIMO-OFDM communication system to the space time coded MIMO-OFDM in a bid to exploit both the coding and diversity gains should also be considered.

- It is obvious that the computational complexity of the proposed iterative DDCE scheme for MIMO-OFDM communications system increases linearly with the number of transmits and receives antennas. A method by which reduction in the computational complexity could be achieved should be looked into.

- Besides, the iterative DDCE scheme should also be extended to the case of virtual antenna arrays technique employing cooperative and relay station-aided communication antenna Systems.

REFERENCES

[1] C. Oestges and B Clerckx, *Wireless Communications_from Real-World Propagation to Space-Time Code Design*. Elsevier Academic Press, 480 pages, Mar. 2007.

[2] A. J. Paulraj and T. Kailath, "Increasing capacity in wireless broadcast Systems using distributed transmission/directional reception," *U. S. Patent*, no. 5,345,599, 1994.

[3] G. J. Foschini, "Layered space-time architecture for wireless communication in a fading environment when using multielement antennas," *Bell Labs Tech. J.*, pp. 41-59, 1996.

[4] I. E. Telatar, "Capacity of multi-antenna Gaussian channels," *European Trans. Tel.*, vol. 10, no. 6, pp. 585-595, Nov./Dec.1999.

[5] H. Bolcskei, D. Gesbert, and A. J. Paulraj, "On the capacity of OFDM-based spatial multiplexing Systems," *IEEE Transaction on Communication*, vol. 50, no. 2, pp. 225-234, Feb. 2002.

[6] R. W. Chang, "Synthesis of band-limited orthogonal signals for multichannel data," *BSTJ*., pp. 1775-1797, Dec. 1966.

[7] B. R. Saltzburg, "Performance of an efficient parallel data transmission Systems," *IEEE Transaction on Communication*, pp. 805-811, Dec. 1967

[8] Sklar, B, "Rayleigh fading channels in mobile digital communication Systems, Part I: Characterization," *IEEE Communication Magazine*, vol. 35, no. 7, pp. 90-100, July 1997.

[9] T. S. Rappaport, "Wireless Communication Principles and Practice," Upper Saddle River, NJ, USA: Prentice Hall, First Ed., 1996.

[10] O. Oyman, R. U. Nabar, H. B¨olcskei, and A. J. Paulraj, "Characterizing the statistical properties of mutual information in MIMO channels," *IEEE Transaction on. Signal Processing*, vol. 51, no. 11, Nov. 2003.

[11] G. G. Raleigh and J. M. Cioffi, "Spatio-temporal coding for wireless communication," *IEEE Transaction on Communication*, vol. 46,pp 357-366, Mar. 1998.

[12] A.J. Paulraj, D. A. Gore, R.U. Nabar, H. Bolcskei, "An overview of MIMO communications - a key to gigabit wireless," *Proceedings of the IEEE* , vol.92, no.2, pp. 198-218, Feb. 2004.

[13] G. J. Foschini, "Layered space-time architecture for wireless communication in a fading environment when using multielement antennas," *Bell Labs Tech. J.*, pp. 41-59, 1996.

[14] H. Atarashi., S. Abeta, and M. Sawahashi, ''Broadband Packet Wireless Access Appropriatefor High-speed and High-Capacity Throughput,'' *Proceedings of IEEE VTC2001-Spring*, Rhodes, Greece, pp. 566–570, May 2001.

[15] IEEE Standard 802.11a-1999, Part 11: Wireless LAN Medium Access Control (MAC) and Physical Layer (PHY) specifications: High-speed Physical Layer in the 5 GHz Band.

[16] K. Miyoshi, A. Matsumoto, and M. Uesugi, ''A Study on Time Domain Spreading for OFCDM (in Japanese),'' *IEICE Technical Report*, RCS2001-179, pp. 13-18, November 2001.

[17] J. Benesty, H. Rev, L.R. Vega, and S. Tressens, "A Nonparametric VSS NLMS Algorithm" IEEE Signal Processing Letters, vol. 13, no 10, pp. 581-584, October 2006.

[18] Y. Hara, T. Kawabata, J. Duan, T. Sekiguchi ''MC-CDM System for Packet Communications Using Frequency Scheduling (in Japanese),'' *IEICE Technical Report*, RCS2002-129, pp. 61-66, July 2002.

[19] IEEE Standard IEEE 802.16a, for Local and Metropolitan Area Networks -Part 16, Air Interface for Fixed Broadband Wireless Access Systems- http://grouper.ieee.org/groups/802/16/

[20] S. Hara and R. Prasad, *Multicarrier Techniques for 4G Mobile Communications*. Artech House, Inc. Norwood, MA, USA, 268 pages, 2003.

[21] S. B. Weinstein and P. M. Ebert, "Data transmission by frequency-division multiplexing using the discrete Fourier transform," *IEEE Transaction on Communication,* vol. COM- 19, pp. 628-634, Oct. 1971.

[22] W. Y. Zou, and Y. Wu, "COFDM: an overview," *IEEE Transaction on Broadcasting,* vol. 41, no. 1, pp. 1 - 8, March 1995.

[23] Hongwei Yang, "A road to future broadband wireless access: MIMO-OFDM-Based air interface," *IEEE Communications Magazine*, Vol. 43, No. 1, pp. 53 - 60, Jan. 2005.

[24] R. Van Nee and R. Prasad, *OFDM for Wireless Multimedia Communications*, Artech House, Inc. Norwood, MA, USA, 280 pages, 2000.

[25] E.G. Larsson and J. Li, "Preamble Design for Multiple-Antennas OFDM-Based WLANs with Null Subcarriers," *IEEE Signal Processing Letter*, vol. 8, no. 11, pp. 258-288, Nov. 2001.

[26] Y. (G.) Li, "Simplified Channel Estimation for (OFDM) Systems with Multiple Transmit Antennas," *IEEE Transaction on Wireless Communication,* vol. 1, no. 1, pp. 67-75, Jan. 2002,

[27] W.G. Jeon, K.H. Paik, and Y.S. Cho, "Two-Dimensional Pilot-Symbol-Aided Channel Estimation for OFDM System with Transmitter Diversity," *IEICE Transaction on Communication,* vol. E85-B, no. 4, pp. 840-844, Apr. 2002.

[28] R.J. Piechocki, P.N. Fletcher, A.R. Nix, C.N. Canagarajah, and J.P.McGeehan, "Performance Evaluation of BLAST-OFDM Enhanced Hiperlan/2 Using Simulated and Measured Channel Data," *Electronics Letter*, vol. 37, no. 18, pp. 1137-1139, Aug. 2001.

[29] G. L. Stuber, J. R. Barry, S. W. McLaughlin, Y. (G.) Li, M. A. Ingram, and T. G. Pratt, "Broadband MIMO-OFDM Wireless Communications," *IEEE Proceedings*, vol. 92, no. 2, pp. 271-294, Feb. 2004.

[30] H. Bolcskei, "MIMO-OFDM wireless Systems: basic, perspectives, and challenges," *IEEE Wireless Communications*, Vol.1, No. 4, pp. 31-37, Aug. 2006.

[31] Y. Li, L. Cimini, and N. Sollenberger, "Robust channel estimation for OFDM Systems with rapid dispersive fading channels," *IEEE Transactions on Communications*, vol. 46, no. 7, pp. 902-915, July 1998.

[32] R. Prasad, *OFDM for Wireless Communications Systems*, Artech House, Inc. Norwood, MA, USA, 291 pages, 2000.

[33] D. J. young and N.C. Beaulieu, "A quantitative evaluation of generation methods for correlated rayleigh random variate," *in Proceedings IEEE GLOBECOM*, Sydney, Austrialia, pp. 3332-3337, Nov. 8-12, 1998.

[34] D. J. young and N.C. Beaulieu, "The generation of correlated rayleigh random variates by inverse discrete Fourier transform," *IEEE Transaction on Communication.*, vol. 48, pp. 1114-1127, July 2000.

[35] D. Verdin and T. C. tozer, "Generating a fading process for the simulation of land-mobile radio communications," *Electronic Letters*, vol. 29, no.23, pp. 2011-2012, Nov. 1993

[36] S. A. fechtel, "A novel approach to modeling and efficient simulation of frequency-s elective fading radio channels," *IEEE Journal of Selected Areas in communications*, vol. 11, pp. 422-431, April. 1993.

[37] W. C. Jakes, Ed., Microwave mobile communications. New York: Wiley, 1974. reprinted by IEEE Press in 1994.

[38] M. F. Pop and N. C. Beaulieu, "Limitation of sum-of-sinusoids fading channel simulators," *IEEE Transaction on Communication*, vol. 49, no.4, pp. 699-708, April 2001.

[39] P. Dent, G. E. Bottomley, and T. Croft, "Jakes fading model revisited," *Electronic Letters*, vol. 29, no. 13, pp. 1162-1163, June 1993.

[40] M. Patzold, U. killat, and F. Laue, "A deterministic digital simulation model for zuzuki processes with application to a shadowed Rayleigh land mobile radio channel," *IEEE Transaction in Vehicular. Technology*, vol. 45, no. 2, pp. 318-331, May 1996.

[41] P. M. Crespo and J. Jimenez, "Computer simulation of radio channels using a harmonic decomposition technique," *IEEE Transaction in Vehicular. Technology*., vol. 44, no. 3, pp. 414-419, Aug 1995.

[42] R. Steele and L. Hanzo, Eds., *Mobile Radio Communications*, 2nd ed. New York, USA: John Wiley and IEEE Press, 1090 pages, 1999.

[43] M. Failli, "*Digital land mobile radio communications COST 207*," European Commission, Tech. Rep., 1989.

[44] V. Kuhn, "*Wireless Communication over MIMO Channels, applications to CDMA and Multiple Antenna Systems*" John Wiley & Sons, Ltd. the Atrium, Southern Gate, Chichester, West Sussex, England. 2006.

[45] Roald Otnes, "Fractionally Spaced Linear MMSE Turbo Equalization," *in Proceedings 12th European Signal Processing Conference (EUSIPCO 2004)*, Vienna, Austria, pp. 465-468, Sep. 6-10, 2004.

[46] W. A. Gardner, *Introduction to Random Processes: with Application to Signals and Systems*, 2nd Ed.; New York, McGraw-Hill, 1989.

[47] M. Ibnkahla, *Signal Processing for Mobile Communications Handbook*, CRC Press New York, Washington, D.C. USA. 2005.

[48] L. Hanzo, M. Munster, B. J. Choi, and T. Keller. *OFDM and MC-CDMA for Broadband Multi-User Communications, WLANs and Broadcasting*. John Wiley and IEEE Press, 992 pages, 2003.

[49] J. H. Lodge and M. L. Moher, "Time diversity for mobile satellite channels using trellis coded modulations,"*in Proceedings IEEE Global Telecommunication Conference,* Tokyo, vol. 1, pp. 303-307, 15th-18th Nov. 1987.

[50] M. L. Moher and J. H. Lodge, "TCMP-a modulation and coding strategy for Rician fading channels," *IEEE Journal in Selected Areas in Communications*, vol. 7, no. 9, pp. 1347-1355, Dec. 1989.

[51] S. Sampei and T. Sunaga, "Rayleigh fading compensation method for 16QAM in digital land mobile radio channels," in *Proceedings IEEE Vehicular Technology Conference,* San Francisco, CA, pp. 640-646, May 1989.

[52] J. K. Cavers, "An analysis of pilot symbol assisted modulation for Rayleigh fading channels," *IEEE Transaction in Vehicular Technology*, vol. 40, no.4, pp. 686-693, Nov. 1991.

[53] J. K. Cavers, and M. Liao, "A comparison of pilot tone and pilot symbol techniques for digital mobile communication," *in Proceedings IEEE Global Telecommunications Conference*, pp. 915–921, Dec. 1992.

[54] P. Hoeher, and F. Tufvesson, "Channel estimation with superimposed pilot sequence," *in Proceedings IEEE Global Telecommunications Conference*, pp. 2162-2166, Dec. 1999.

[55] X. Tang, M. S. Alouini, and A. J. Goldsmith, "Effect of channel estimation error on M-QAM BER performance in rayleigh fading," *IEEE Transaction on Communications*, vol. 47, no. 12, pp. 1856-1864, Dec. 1999.

[56] M. Dong, L. Tong, and B. M. Sadler, "Optimal insertion of pilot symbols for transmissions over time-varying flat fading channels," *IEEE Transactions on Signal Processing*, vol. 52, pp. 1403–1418, May 2004.

[57] X. Cai, and G. B. Giannakis, "Adaptive PSAM accounting for channel estimation and prediction errors," *IEEE Transaction On Wireless Communications*, vol. 4, no.1, pp. 246-256, Jan.2005.

[58] P. Hoher, "TCM on frequency-selective land-mobile fading channels," *in International Workshop on Digital Communications*, (Tirrenia, Italy), pp. 317-328, September 1991.

[59] P. Hoher, S. Kaiser, and P. Robertson, "Two-dimensional pilot-symbol-aided channel estimation by Wiener filtering," *in Proceedings IEEE International Conference on Acoustics, Speech and Signal Processing*, Munich, Germany, pp.1845–1848, April 1997.

[60] P. H¨oher, S. Kaiser, and P. Robertson, "Pilot-symbol-aided channel estimation in time and frequency," *in Proceedings IEEE Global Telecommunications Conference: The Mini-Conference*, Phoenix, AZ, pp. 90-96 November 1997.

[61] J. Rinne and M. Renfors, "Pilot spacing in orthogonal frequency division multiplexing Systems on practical channels," *IEEE Transaction on Consumer Electronic*, vol. 42, no. 4, pp. 959-962, Nov. 1996.

[62] R. Negi and J. Cioffi, "Pilot tone selection for channel estimation in a mobile OFDM system," *IEEE Transaction on Consumer Electronic*, vol. 44, no.3, pp.1122–1128, Aug. 1998.

[63] Y. Li, "Pilot-symbol-aided channel estimation for OFDM in wireless Systems," *IEEE Transactions on Vehicular Technology*, vol. 49, no.4, pp. 1207-1215, July 2000.

[64] H. Minn and V. K. Bhargava "An Investigation into Time-Domain Approach for OFDM Channel Estimation," *IEEE Transactions on Broadcasting*, vol. 46, no. 4, pp. 240–248, December 2000.

[65] M. Morelli and U. Mengali, "A Comparison of Pilot-Aided Channel Estimation Methods for OFDM Systems," *IEEE Transactions on Signal Processing*, vol. 49, no. 12, pp. 3065–3073, December 2001.

[66] B. Yang, Z. Cao, and K. Letaief, "Analysis of low-complexity windowed DFT- based MMSE channel estimation for OFDM Systems," *IEEE Transactions on Communications*, vol. 49, no. 11, pp. 1977-1987, November 2001.

[67] M.X. Chang and Y. Su, "Model-based channel estimation for OFDM signals in Rayleigh fading, "*IEEE Transactions on Communications*, vol. 50, no. 4, pp. 540-544, April 2002.

[68] W. G. Jeon, K. H. Paik, and Y. S. Cho, "An efficient channel estimation technique for OFDM Systems with transmitter diversity," *in IEEE Proceedings International Symposium Personal Indoor Mobile*, vol. 2, pp. 1246-1250, 18th-21st Sept. 2000.

[69] V. Jungnickel, T. Haustein, E. Jorswieck, V. Pohl, and C. von Helmolt, "Performance of a MIMO system with overlay pilots," *in Proceedings Global Telecommunications Conference, 2001. GLOBECOM '01.IEEE*, vol. 1, pp. 594–598, 25th-29th Nov. 2001.

[70] S. Ohno and G. B. Giannakis, "Optimal training and redundant precoding for block transmissions with applications to wireless OFDM," *in Proceedings IEEE ICASSP*, Salt Lake City, UT, pp. 2389–2392, May 2001.

[71] S. Ohno and G. B. Giannakis, "Capacity maximizing pilots for wireless OFDM over rapidly fading channels," *in Proceedings. International. Symposium in Signals, System, Electronic*, Tokyo, Japan, pp. 246–249, 24th-27th July 2001.

[72] S. Coleri, M. Ergen, A. Puri, and A. Bahai, "Channel Estimation Techniques based on Pilot Arramngement in OFDM Systems," *IEEE Transactions on Broadcasting*, vol. 48, no. 3, pp. 223–229, September 2002.

[73] W. Zhang, X-G, Xia and P. C. Ching, "Optimal Training and Pilot Pattern Design for OFDM Systems in Rayleigh Fading," *IEEE Transactions on Broadcasting*, vol. 52, no. 4, pp. 50-57, December 2006.

[74] I. Barhumi, G. Leus and M. Moonen ,"Optimal Training Design for MIMO OFDM Systems in Mobile Wireless Channels," *IEEE Transactions on Signal Processing*, vol. 51, no. 6, pp. 1615-1624, June 2003.

[75] B. Song, L. Gui, and W. Zhang, "Comb Type Pilot Aided Channel Estimation in OFDM Systems with Transmit Diversity," *IEEE Transactions on Broadcasting*, vol. 52, no. 1, pp. 50-57, March 2006.

[76] H. Minn and N. Al-Dhahir ,"Optimal Training Signals for MIMO OFDM Channel Estimation," *IEEE Transactions on Wireless Communications*, vol. 5, no. 5, pp. 1158-1168, May 2006.

[77] H. Minn, N. Al-Dhahir and Y. Li,"Optimal Training Signals for MIMO OFDM Channel Estimation in the Presence of Frequency offset and Phase Noise," *IEEE Transactions on Communications*, vol. 54, no. 10, pp. 1754-1759, October 2006.

[78] A. Petropulu, R. Zhang and R. Lin,"Blind OFDM Channel Estimation through Simple Linear Precoding," *IEEE Transactions on Wireless Communications*, vol. 3, no. 2, pp. 647-655, March 2004.

[79] A. Benveniste, M Goursat, and G. Ruget, "Robust identification of a non-minimum phase system: blind adjustment of a linear equalizer in data communications", *IEEE Transaction on Automatic Control*, vo. 25, no. 3, pp. 385-399, June 1980.

[80] J. K. Tugnait, “Identification of linear stochastic system via second and fourth-order cumulant matching", *IEEE Transaction on Information Theory*, vol. 33, no. 3, pp. 393-407, May 1987.

[81] D. Hatzinakos and C. Nikias, “Estimation of multipath channel response in frequency selective channels”, *IEEE Journal in Selected Areas in Communications*, vol. 7, no.1, pp.12-19, January 1989.

[82] O. Shalvi and E. Weinstein, “New Criteria for Blind Deconvolution of Non-minimum Phase Systems (Channels)", *IEEE Transaction on Information Theory*, vol. 36, no. 2 pp. 312-320, March 1990.

[83] Z. Ding, R. A. Kennedy, B. D. O. Anderson, and C. R. Johnson, “Ill-convergence of Godard blind equalizers in data communication Systems”, *IEEE Transaction on Communications*, vol. 39, no. 9, pp. 1313-1327, September 1991.

[84] A. P. Petropulu and C. L. Nikias, “Blind Deconvolution Using Signal Reconstruction from Partial Higher Order Cepstral Information,” *IEEE Transaction on Signal Processing*, vol. 41, no. 6, pp.2088-2095, June 1993.

[85] W. A. Gardner, “Exploitation of spectral redundancy in cyclostationary signals,” *IEEE Signal Processing Magazine*, vol. 8, no. 2, pp. 14-36, Apr. 1991.

[86] L. Tong, G. Xu, and T. Kailath, “A new approach to blind identification and equalization of multipath channel,” *in Proceedings of the 25th Asilomar Conference on Signals, Systems, and Computers*, Pacific Grove, CA, Nov. 1991.

[87] L. Tong, G. Xu, and T. Kailath, “Blind identification and equalization using spectral measures, Part II: A Time Domain Approach,” *in W.A. Gardner Ed., editor, Cyclostationarity in Communications and Signal Processing*. IEEE Press, 1993.

[88] L. Tong, G. Xu, and T. Kailath, “Blind identification and equalization based on second order statistics: A time domain approach,” *IEEE Transaction on Information Theory*, vol. 40, no. 2, pp. 340-349, Mar. 1994.

[89] H. H. Zeng, L. Tong: 'Blind Channel Estimation Using the Second-Order Statistics: Asymptotic Performance and Limitations', *IEEE Transactions on Signal Processing*, vol. 45, no. 8, pp. 2060–2071, August 1997.

[90] D. Boss, K. Kammeyer, and T. Petermann, "Is blind channel estimation feasible in Mobile communication Systems?; a study based on GSM," *IEEE Journal on Selected Areas in Communications*, vol. 16, no. 8, pp. 1479–1492, October 1998.

[91] I. Kang, M. P. Fitz, and S. B. Gelfand, "Blind Estimation of Multipath Channel Parameters: Amodal Analysis Approach," *IEEE Transactions on Communications*, vol. 47, no. 8, pp. 1140-1150, Aug. 1999.

[92] S. Yatawatta, A. P. Petropulu, and R. Dattani, "Blind Channel Estimation Using Fractional Sampling," *IEEE Transactions on Vehicular Technology*, vol. 53, no. 2, pp. 363-371, March. 2004.

[93] J. P. Delmas, Y. Meurisse and P. Comon, "Performance Limits of Alphabet Diversities for FIR SISO Channel Identification," *IEEE Transaction on Signal Processing*, vol. 57, no. 1, pp.73-82, Jan. 2009.

[94] Y. Bresler and A. Macovski, "Exact maximum likelihood parameter estimation of superimposed exponential signals in noise," *IEEE Transaction on Audio, Speech, Signal Processing*, vol. 34, no. 5, pp. 1081-1089, Oct. 1986.

[95] H. Liu, G. Xu, and L. Tong, "A deterministic approach to blind equalization," *in Proceedings of 27th Asilomar Conference on Signals, Systems, and Computers*, Pacific Grove, CA, vol.1, pp. 751-755, 1-3 Nov. 1993.

[96] G. Xu, L. Tong, and T. Kailath, "A Least-squares approach to blind channel identification," *IEEE Transaction on Signal Processing*, vol. 43, no. 8, pp.2982- 2993, Dec. 1995.

[97] B. Muquet, M. de Courville: 'Blind and Semi-Blind Channel Identification Methods using Second Order Statistics for OFDM Systems', *in IEEE Proceedings ICASSP '99*, vol. 5, pp. 2745–2748, March 1999

[98] F.-C. Zheng, S. McLaughlin, B. Mulgrew: 'Blind equalization of nonminimum phase channels: higher order cumulant based algorithm', *IEEE Transactions on Signal Processing*, vol. 41, no. 2, pp. 681 – 691, Feb. 1993.

[99] S. Chen, S. McLaughlin: 'Blind channel identification based on higher order cumulant fitting using genetic algorithms', in *IEEE Proceedings Signal Processing Workshop on Higher-Order Statistics* (SPW-HOS '97), Banff Canada, pp. 184-188, 21st-23rd July 1997.

[100] M. de Courville, P. Duhamel, P. Madec and J. Palicot, "Blind equalization of OFDM Systems based on the minimization of a quadratic criterion," *in IEEE Proceedings of International Conference on Communications.*, vol. 3, pp. 1318 -1322, 23rd-27th Mar. 1996.

[101] U. Tureli, H. Liu: 'Blind Carrier Synchronization and Channel Identification for OFDM Communications', *in Proceedings of IEEE ICASSP '98*, vol. 6, pp. 3509-3512, May 1998.

[102] B. Muquet and M. de Courville, "Blind and semi-blind channel identification methods using second order statistics for OFDM Systems" *in Proceedings of IEEE ICASSP '99*, vol. 5, pp. 2745 -2748, 1999.

[103] R. W. Heath, Jr. and G. B. Giannakis, "Exploiting input cyclo-stationarity for blind channel identification in OFDM system," *IEEE Transaction on Signal Processing*, vol. 47, no. 3, pp. 848-856, Mar. 1999.

[104] X. Cai and A. N. Akansu, "A subspace method for blind channel identification in OFDM Systems," in *Proceedings of International Conference on Communications (ICC2000)*, vol. 2, pp. 929–933, 18th-22nd June 2000.

[105] H. B¨olcskei, R. W. Heath, and A. J. Paulraj, "Blind equalization in OFDM-based multi-antenna Systems," in *IEEE Proceedings of Adaptive Systems for Signal Processing, Communications, and Control Symposium*, pp. 58-63, 1-4 Oct. 2000.

[106] B. Muquet, M. de Courville, P. Duhamel: 'Subspace-Based Blind and Semi-Blind Channel Estimation for OFDM Systems', *IEEE Transactions on Signal Processing*, Vol. 50, pp. 1699-1712, July 2002.

[107] S. Roy and C. Li, "A subspace blind channel estimation method for OFDM Systems without cyclic prefix," *IEEE Transaction on Wireless Communications.* vol. 1, no.4, pp. 572-579, Oct. 2002.

[108] C. Li and S. Roy, "Subspace-based blind channel estimation for OFDM by exploiting virtual carriers," *IEEE Transaction on Wireless Communications*, vol.2, no. 1, pp. 141-150, Jan. 2003.

[109] X. G. Doukopoulos and G. V. Moustakides, "Blind adaptive channel estimation in OFDM Systems," *IEEE Transaction on. Wireless Communications*, vol. 5, no. 7, pp. 1716-1725, Jul. 2006.

[110] S. Zhou and G. Giannakis, "Finite-alphabet based channel estimation for OFDM and related multicarrier Systems," *IEEE Transactions on Communications*, vol. 49, no. 8, pp. 1402-1414, August 2001.

[111] T. Petermann, S. Vogeler, K-D. Kammeyer, D. Boss: "Blind Turbo Channel Estimation in OFDM Receivers", in *Proceedings of 35th Asilomar Conference on Signals, Systems and Computers*, vol. 2, pp. 1489 -1493, 4th-7th November 2001.

[112] L. Lin, J. C.-I. Chuang, and Y. Li, "Near optimal joint channel estimation and data detection for COFDM Systems," in *Proceedings of IEEE Global Telecommunication Conference (GLOBECOM)*, vol. 2, pp. 726-730, San Francisco, CA, Nov. 2000.

[113] B. Lu, X. Wang and K. R. Narayanan, "LDPC-based space time coded OFDM Systems over correlated fading channels: Analysis and receiver design," *IEEE Transaction on Communications*, vol. 50, no. 1, pp. 74-88, Jan. 2002.

[114] R. Chen, S. Liu and X. Wang, "Convergence Analyses and Comparisons of Markov Chain Monte Carlo algorithms in Digital Communications," *IEEE Transactions on Signal Processing*, vol. 50, no. 2, pp. 255-270, Feb. 2002.

[115] N. Chotikakamthorn, H. Suzuki, "On Identifiability of OFDM Blind Channel Estimation," in *Proceedings Vehicular Technology Conference (VTC 1999-Fall), Amsterdam, Netherlands*, vol. 4, pp. 2358-2361, 19th-22nd Sept. 1999.

[116] M. Necker and G. Stuber, "Totally Blind Channel Estimation for OFDM over Fast Varying Mobile Channels," *IEEE Transaction on Wireless Communications*, vol. 3, no. 5, pp. 1514-1525, Sept. 2004.

[117] H. Bolcskei, R. Heath, and A. Paulraj, "Blind channel identification and equalization in OFDM based multiantenna Systems," *IEEE Transactions on Signal Processing*, vol. 50, no. 1, pp. 96–109, Jan 2002.

[118] S. Zhou, B. Muquet, and G. B. Giannakis, "Subspace based blind channel estimation for block precoded space time OFDM," *IEEE Transactions on Signal Processing*, vol. 50, no. 5, pp. 1215-1228, May 2002.

[119] C. Gao, m. Zhao, S. Zhou, and Y. Yao, "Blind channel estimation algorithm for MIMO-OFDM Systems," *IEEE Electronic Letters*, vol. 39, no. 19, pp.1420-1422, Sep. 2003.

[120] S. Yatawatta, A. P. Petropulu, "Blind Channel Estimation in MIMO OFDM Systems," *in Proceedings of IEEE Statistical Signal Processing Workshop*, St, Louis, MO, USA, pp. 349-352, 28th September- 1st October 2003.

[121] S. Yatawatta, A. P. Petropulu, "Blind Channel Estimation in MIMO OFDM Systems with Multiuser Interference," *IEEE Transactions on Signal Processing*, vol. 54, no. 3, pp. 1054-1068, March 2006.

[122] J. K. Tugnait, "Identification and deconvolution of multichannel linear non-Gaussian processes using higher order statistics and inverse filter criteria," *IEEE Transactions on Signal Processing*, vol. 45, no. 3, pp. 658-672, March 1997.

[123] Y. Inouye, K. Hirano, "Cumulant-based blind identification of linear multi-input-multi-output Systems driven by colored inputs," *IEEE Transactions on Signal Processing*, vol. 45, no.5 pp. 1543-1552, June 1997.

[124] G. B. Giannakis and J. M. Mendel, "Identification of nonminimum phase system using higher order statistics," *IEEE Transactions on Acoustic, Speech, Signal Processing*, vol. 37, no. 3, pp. 360-377, March 1989.

[125] B. Chen, A. P. Petropulu, "Frequency Domain Blind MIMO System Identification Based on Second and Higher Order Statistics," *IEEE Transactions on Signal Processing*, vol. 49, no. 8, pp. 1677-1688, Aug. 2001.

[126] M. Castella, J. C. Pesquet and A. P. Petropulu, "Family of frequency and Time-Domain Contrasts for Blind Separation of convolutive Mixtures of Temporally dependent Signals," *IEEE Transaction on Signal Processing*, vol. 53, no. 1, pp. 107-120 Jan. 2005.

[127] T. Acar, Y. Yu and A. P. Petropulu, "Blind MIMO System estimation based on PARAFAC decomposition of higher-order output tensors," *IEEE Transaction on Signal Processing*, vol. 54, no. 11, pp. 4156-4168, Nov. 2006.

[128] H. Liu and G. Xu, "A deterministic approach to blind symbol estimation," *IEEE Signal Processing Letters*, vol. 1, no. 12, pp. 205-207, Dec. 1994.

[129] W. Liu, L. L. Yang, and L. Hanzo, "Subspace Tracking based blind MIMO Transmit Preprocessing," in *Proceedings of IEEE Vehicular Technology Conference (VTC)*, pp. 2228-2232, Dublin Ireland, 22nd-27th April 2007.

[130] C. –C. Tu and B. Champagne, "Subspace Blind MIMO-OFDM Channel Estimation with Short Averaging Periods: Performance Analysis," in *Proceedings of IEEE Wireless*

Communication and Networking Conference (WCNC), pp. 24-29, Las Vegas, USA, 31st March -3rd April 2008.

[131] B. Farhang-Boroujeny, "Pilot-based channel identification: proposal for semi-blind identification of communication channels," *Electronic Letters*, vol. 31, no. 13, pp. 1044-1046, June 1995.

[132] C. K. Ho, B. Farhang-Boroujeny and F. Chin, "Added pilot semi-blind channel estimation scheme for OFDM in fading channels," in *Proceedings of IEEE Global Telecommunications Conference,* pp. 3075-3079, Nov. 2001.

[133] G. T. Zhou, M. Viberg, and T. McKelvey, "A first-order statistical method for channel estimation," *IEEE Signal Processing Letters,* vol. 10, no. 3 pp. 57-60, March 2003.

[134] V. Buchoux, O. Cappe, E. Moulines, and A. Gorokhov, "On the performance of semi-blind subspace-based channel estimation," *IEEE Transactions on Signal Processing*, vol. 48, no. 6, pp. 1750-1759, June 2000.

[135] E. Aktas and U. Mitra. "Semiblind channel estimation for CDMA Systems with parallel data and pilot signals," *IEEE Transactions on Communications*, vol. 52, no. 7, pp. 1102-1112, July 2004.

[136] E. de Carvalho and D. Slock. "Blind and semi-blind FIR multichannel estimation: (global) identifiability conditions". *IEEE Transactions on Signal Processing*, vol. 52, no. 4, pp. 1053-1064, Apr.2004.

[137] S. Zhou, B. Muquet, and G. B. Giannakis, "Semi-blind channel estimation for block precoded space-time OFDM transmissions," in *Proceedings of IEEE 11th Signal Processing Workshop on Statistical Signal Processing*, pp. 381-384, Aug. 2001.

[138] J. Choi. "Equalization and semi-blind channel estimation for space-time block coded signals over a frequency-selective fading channel". *IEEE Transactions on Signal Processing*, vol. 52, no. 3, pp. 774–785, March 2004.

[139] T. Wo and P. A. Hoeher "Semi-blind channel estimation for frequency-selective MIMO Systems," in *Proceedings of 14th Ist mobile & wireless Communication Summit*, Dresden, Germany, paper no 548, 19th-23rd June 2005.

[140] A.Medles, D. T. M. Slock and E. de Carvalho, "Linear prediction based semi-blind estimation of MIMO FIR channels," in *Proceedings of 3rd IEEE Workshop Signal Processing Advances in Wireless Communications (SPAWC)*, Taiwan, R.O.C., pp. 58-61, March 2001.

[141] A. K. Jagannetham and B. D. Rao, "A semi-blind technique for MIMO channel matrix estimation," in *Proceedings of IEEE Workshop Signal Processing Advances in Wireless Communications (SPAWC)*, Rome, Italy., pp. 304-308, Jun. 2003.

[142] A. Jagannatham and B. Rao, "Whitening-rotation-based semi-blind MIMO channel estimation," *IEEE Transactions on Signal Processing*, vol. 54, no. 3, pp. 861-869, March 2006.

[143] C. Murthy, A. Jagannatham, and B. Rao, "Training-based and semiblind channel estimation for MIMO Systems with maximum ratio transmission," *IEEE Transactions on Signal Processing*, vol. 54, no. 7, pp. 2546-2558, July 2006.

[144] J.-J. van de Beek, O. Edfors, M. Sandell, S. Wilson, and P. B¨orjesson, "On channel estimation in OFDM Systems," in *Proceedings of* IEEE *Vehicular Technology Conference*, vol. 2. pp. 815-819, Chicago, IL USA, July 1995.

[145] O. Edfords, M. Sandell, J.-J. van de Beek, S. Wilson, and P. B¨orjesson, "OFDM channel estimation by singular value decomposition," in *Proceedings of IEEE Vehicular Technology Conference*, vol. 2. pp. 923-927, Atlanta GA. USA, 28th April – 1st May 1996.

[146] O. Edfords, M. Sandell, J.-J. van de Beek, S. Wilson, and P. B¨orjesson, "OFDM channel estimation by singular value decomposition," *IEEE Transactions on Communications*, vol. 46, no. 7, pp. 931–939, July1998.

[147] Y. Li and N. Sollenberg, "Clustered OFDM with channel estimation for high rate wireless data," *IEEE Transactions on Communications*, vol. 49, no. 12, pp. 2071–2076, Dec. 2001.

[148] M. Munster and L. Hanzo ,"MMSE channel prediction assisted symbol-by-symbol adaptive OFDM," in *Proceedings of IEEE International Conference on Communications*, vol. 1, pp. 416–420, New York, USA, 28 April-2 May 2002.

[149] J. Akhtman and L. Hanzo, "Generic reduced-complexity MMSE channel estimation for OFDM and MC-CDMA," in *Proceedings of Spring'05 IEEE Vehicular Technology Conference (VTC)*, vol.1, pp. 528-532, Stockholm, Sweden, May 30 - June 1 2005.

[150] J. Akhtman and L. Hanzo, "Sample-Spaced and Fractionally-Spaced CIR Estimation Aided Decision Directed Channel Estimation for OFDM and MC-CDMA," in *Proceedings of Fall'05 IEEE Vehicular Technology Conference (VTC)*, vol.3, pp. 1916-1920, Stockholm, Sweden, 25-28 Sept. 2005.

[151] B. Yang, "Projection approximation subspace tracking," *IEEE Transaction on Signal Processing*, vol. 43, no. 1, pp. 95–107, January 1995.

[152] D. Schafhuber and G. Matz, "MMSE and adaptive prediction of time-varying channels for OFDM Systems," *IEEE Transaction on Wireless Communications*, vol. 4, no. 2, pp. 593–602, Mar. 2005.

[153] J. Akhtman and L. Hanzo, "Decision Directed Channel Estimation Employing Approximation Subspace Tracking," in *Proceedings of Spring'05 IEEE Vehicular Technology Conference (VTC)*, pp. 3056-3060, Dublin Ireland, Sweden, 22-25 April 2007.

[154] J. Akhtman and L. Hanzo, "Decision Directed Channel Estimation Aided OFDM Employing Sample-Spaced and Fractionally-Spaced CIR Estimators," *IEEE Transaction on Wireless Communications*, vol. 6, no 4, pp. 1171-1175, April 2007.

[155] Y. (G.) Li, N. Seshadri, and S. Ariyavisitakul, "Channel estimation for OFDM Systems with transmitter diversity in mobile wireless channels," *IEEE Journal on Selected. Areas in Communication,* vol. 17, no. 3, pp. 461-471, Mar. 1999.

[156] Y. Li, J.Winters, and N. Sollenberger, "MIMO-OFDM for wireless communications: signal detection with enhanced channel estimation," *IEEE Transactions on Communications*, vol. 50, no. 9, pp. 1471–1477, Sept. 2002

[157] M. Munster and L. Hanzo, "RLS-adaptive parallel interference cancellation assisted decision-directed channel estimation for OFDM," in *Proceedings of IEEE Wireless Communications and Networking Conference*, vol. 1, pp. 50–54, New Orleans, Lousiana, USA, 16-20 March 2003.

[158] P. Strobach, "Low-rank adaptive filters," *IEEE Transaction on Signal Processing*, vol. 44, no. 12, pp. 2932-2947, Dec. 1996.

[159] J. Du, and Y. Li, "MIMO-OFDM Channel estimation based on subspace tracking," in *IEEE Proceedings of Vehicular Technology Conference (VTC)*, vol. 2, pp.1084-1088, April 2003.

[160] M. Munster and L. Hanzo, "Parallel-interference-cancellation decision-directed channel estimation for OFDM Systems using multiple transmit antennas," *IEEE Transactions on Wireless Communications*, vol. 4, no. 5, pp. 2148-2162, Sept. 2005.

[161] J. Akhtman and L. Hanzo, "Advance Channel Estimation for MIMO-OFDM in realistic channel conditions," in *Proceedings of IEEE International Conference on Communications* , vol.3, pp. 2528-2533, , *Glasgow, UK* Stockholm, Sweden, 24-28, June 2007.

[162] G. Kaleh and R. Vallet, "Joint parameter estimation and symbol detection for linear or nonlinear unknown channels," *IEEE Transactions on Communications*, vol. 42, no. 7, pp. 2406–2413, July 1994.

[163] V. Mignone and A. Morello, "CD3-OFDM : a novel demodulation scheme for fixed and mobile receivers," *IEEE Transactions on Communications*, vol. 44, no. 9, pp. 1144-1151, Sep. 1996.

[164] M. Sandell, C. Luschi, P. Strauch, and R. Yan, "Iterative channel estimation using soft decision feedback," in *Proceedings of IEEE Global Telecommunications Conference*, vol. 6, Sydney, NSW, pp. 3728–3733, 8-12 Nov.1998.

[165] E. Baccarelli, R. Cusani, and S. Galli, "A novel adaptive receiver with enhanced channel tracking capability for TDMA-based mobile radio communications," *IEEE Journal on Selected Areas in Communications*, vol. 16, no. 9, pp. 1630–1638, Dec. 1998.

[166] H. Zamiri-Jafarian and S. Pasupathy, "EM-based recursive estimation of channel parameters," *IEEE Transactions on Communications*, vol. 47, no. 9, pp. 1297–1302, Sep. 1999.

[167] E. Al-Susa and R. F. Ormondroyd, "A Predictor-Based Decision Feedback Channel Estimation Method for COFDM with High Resilience to Rapid Time-Variations," in *Proceedings of IEEE Vehicular Technology Conference*, vol. 1, Amsterdam, Netherlands , pp. 273–278, 19-22 September 1999.

[168] M. Valenti, "Iterative channel estimation for turbo codes over fading channels," in *Proceedings of IEEE Wireless Communications and Networking Conference*, vol. 3, 23-28, pp.1019–1024, Sep. 2000.

[169] M. C. Valenti and B. D. Woerner, "Iterative channel estimation and decoding of pilot symbol assisted Turbo codes over flat-fading channels," *IEEE Journal on Selected Areas in Communications*, vol. 19, no. 9, pp. 1697–1705, Sept. 2001.

[170] Q. Li, C. N. Georghiades, and X. Wang, "An iterative receiver for Turbo-coded pilot-assisted modulation in fading channels," *IEEE Communication Letters*, vol. 5, no. 4, pp.145-147, April 2001.

[171] K.-D. Kammeyer, V. K¨uhn, and T. Petermann, "Blind and non-blind turbo estimation for fast fading GSM channels," *IEEE Journal on Selected Areas in Communications*, vol. 19, no. 9, pp. 1718-1728, Sep. 2001.

[172] C. Komninakis and R. Wesel. "Joint iterative channel estimation and decoding in flat correlated Rayleigh fading". *IEEE Journal on Selected Areas in Communications*, vol. 19, no. 9, pp. 1706–1717, Sep. 2001.

[173] A. Berthet, B. Unal, and R. Visoz, "Iterative decoding of convolutionally encoded signals over multipath Rayleigh fading channels," *IEEE Journal on Selected Areas in Communications*, vol. 19, no. 9, pp. 1729–1743, Sep. 2001.

[174] M. Kobayashi, J. Boutros, and G. Caire, "Successive interference cancellation with SISO decoding and EM channel estimation," *IEEE Journal on Selected Areas in Communications*, vol. 19, no. 8, pp. 1450–1460, Aug. 2001.

[175] H.-J. Su and E. Geraniotis, "Low-complexity joint channel estimation and decoding for pilot symbol-assisted modulation and multiple differential detection Systems with correlated Rayleigh fading," *IEEE Transactions on Communications*, vol. 50, no. 2, pp. 249-261, Feb. 2002.

[176] B. Mielczarek, A. Svensson, "Improved iterative channel estimation and turbo decoding over flat-fading channels," in *IEEE Proceedings of Vehicular Technology Conference (VTC)*, pp. 975-980, 24-28 Sep.2002.

[177] B.-L. Yeap, C.Wong, and L. Hanzo, "Reduced complexity in-phase/quadrature- phase M-QAMturbo equalization using iterative channel estimation," *IEEE Transactions on Wireless Communications*, vol. 2, no. 1, pp. 2-10, Jan. 2003.

[178] N. Nefedov, M. Pukkila, R. Visoz, and A. Berthet, "Iterative data detection and channel estimation for advanced TDMA Systems," *IEEE Transactions on Communications*, vol. 51, no. 2, pp. 141–144, Feb. 2003.

[179] F. Sanzi, S. Jelting and J. Speidel, "A comparative study of iterative Channel Estimators for mobile OFDM Systems," *IEEE Transactions on Wireless Communications*, vol. 2, no. 5, pp. 849–859, Sep. 2003.

[180] J. -H. Lee, Y. -H. Kim, S. -C. Kim, J. C. Han "Pilot symbol initiated iterative channel estimation and decoding for QAM modulated OFDM signals," in *Proceedings IEEE 57th Semiannual Vehicular Technology Conference (VTC)*, vol.2, pp. 1322 -1326, 22-25 April 2003.

[181] L. T. Son, and K. M. Ahmed, "Performance of coherent direct sequence ultra wideband receiver with iterative channel estimation and detection," in *Proceedings of IEEE International Symposium on Communication and information technology*, pp.1218-1223, 26-29 Oct. 2004.

[182] H. Mai, A. Burr, and S. Hirst, "Iterative channel estimation for turbo equalization," in *Proceedings. IEEE International Symposium on Personal Indoor and Mobile Radio Communications, PIMRC*', pp. 1327–1331, Barcelona, Spain, Sep. 2004.

[183] R. Otnes and M. Tuchler, "Soft iterative channel estimation for Turbo equalization: comparison of channel estimation algorithms," in *Proceedings. IEEE International Conference on Communications (ICC)*, vol. 1, pp.72-76, 25-28 Nov. 2002.

[184] R. Otnes and M. Tuchler, "Iterative Channel Estimation for Turbo equalization of Time Varying Frequency selective Channel," *IEEE Transactions on Communications*, vol. 3, no. 6, pp.1918- 1923, Nov. 2004.

[185] A. Dowler, A. Nix, and J. McGeehan, "Data-derived iterative channel estimation with channel tracking for a mobile fourth generation wide area OFDM system," in *Proceedings IEEE Global Telecommunications Conference (Glocom'03)*, vol. 2, pp.804-808, 1-5 Dec. 2003.

[186] S. Song, A. C. Singer, and K. Sung, "Soft input channel estimation for turbo equalization," *IEEE Transactions on Signal Processing*, vol. 52, no. 10, pp. 2885–2894, Oct. 2004.

[187] Y. Li, X. –G. Xia, R. Yao, and W. Zhu, "Coding assisted iterative channel estimation for impulse radio ultra-side band communication Systems," in *Proceedings IEEE International Conference on Acoustics, Speech, and Signal Processing* (ICASSP apos 05), vol. 3, pp.329-332, 18-23 Mar. 2005.

[188] H. Mai, Y. Zakharov, and A. Burr, "Iterative B-spline channel estimation for fast flat fading channels," in *Proceedings of IEEE International Conference on Communications,* vol. 4, pp. 2145-2149, 16-20 May 2005.

[189] M. Morelli, and L. Sanguinetti, "Estimation of channel statistics for iterative detection of OFDM signals," *IEEE Transactions on Wireless Communications*, vol. 4, no. 4, pp. 1360-1365, July 2005.

[190] B. Ozbek, D. L. Ruyet, and C. Panazio, "Pilot-aided iterative channel estimation for OFDM-based Systems, in *Proceedings. of European Signal Processing Conference (EUSIPCO),* Antalya, Turkey, 5page, 4-8 Sep. 2005.

[191] S. Sand, A. Dammann, and A. R. Usmani, "Iterative OFDM receiver with channel estimation," in *Proceedings 9th International Symposium on Wireless Personal Multimedia Communication (WPMC),* San Diego, USA, pp.5pages, Sep. 2006.

[192] M. L. Ammari, and F. Gagnon, "Iterative channel estimation and decoding of Turbo-coded OFDM symbols in selective Rayleigh channel, "*Canadian Journal of Electrical and Computer Engineering*, vol. 32, no. 1, pp. 9-18, Winter 2007.

[193] J. -G. Kim, T. –J. Kim, J. –S. Lee, and J. –T. Lim, "Channel estimation for OFDM over fast fading channels, in *Proceedings of World Academy of Science, Engineering and Technology*, vol. 21, pp. 455-458, Jan. 2007.

[194] S. Ferrara, T. Matsumoto, M. Nicoli, and U. Spagnolini, "Soft iterative channel estimation with subspace and rank tracking," *IEEE Signal Processing Letters*, vol.14, no. 1, pp. 5-8, Jan. 2007.

[195] M. F. Flanagan, and A. D. Fagan, "Iterative channel estimation, equalization, and decoding for pilot-symbol assisted modulation over frequency selective fast fading channels," *IEEE Transactions on Vehicular Technology*, vol.56, no. 4, pp. 1661-1670, Jul. 2007.

[196] H. Zhu, B. Farhang-Boroujeny, and C. Schlegel, "Pilot embedding for joint channel estimation and data detection in MIMO communication Systems," *IEEE Communications Letters*, vol. 7, no. 1, pp. 30-32, Jan. 2003.

[197] X. Deng, A. M. Haimovich, and J. G-Frias, "Decision directed iterative channel estimation for MIMO system, in *Proceedings of International Conference on Communications (ICC)*, Seattle Washington, vol. 4, pp. 11-15, May 2003.

[198] T. Abe, S. Tomisato, and T. Mastumoto, "A MIMO turbo equalizer for frequency-selective channels with unknown interference," *IEEE Transactions on Vehicular Technology*, vol. 52, no. 3, pp. 476-482, May 2003.

[199] C. Cozzo and B. Hughes, "Joint channel estimation and data detection in space- time communications," *IEEE Transactions on Communications*, vol. 51, no. 8, pp. 1266–1270, Aug. 2003.

[200] L. Lu, and Y. Xiao, "Joint iterative channel estimation for space-time multiuser detection," in *Proceedings. of IEEE Region 10 TENCON 2004 Conference*, vol. 1, pp.491-494, Nov. 2004.

[201] J. Choi, M. Bouchard, and T. H. Yeap, "Adaptive filtering-based iterative channel estimation for MIMO wireless communications," in *Proceedings of IEEE International Symposium on Circuit and System (ISCAS)*, vol. 5, pp. 4951-4954, May 2005.

[202] H.-C. Won and G.-H. Im, "Iterative cyclic prefix reconstruction and channel estimation for STBC OFDM system," *IEEE Communications Letters*, vol. 9, no.4, pp. 307-309, Apr. 2005.

[203] B. Song, W. Zhang, and L. Gui, "Iterative joint channel estimation and signal detection in MIMO OFDM System," in *Proceedings of IEEE International Conference on Wireless Communications, Networking and Mobile Computing (WCNC)*, vol.1, pp.39-43, 23-26 Sep. 2005.

[204] J. Chen, S. Li: 'Iterative channel estimation for MIMO OFDM Systems', in *Proceedings IEEE International Conference on Communications, Circuits and Systems*, vol.1, pp. 180-184, 27-30 May 2005.

[205] J. Akhtman and L. Hanzo, "Iterative receiver architectures for MIMO-OFDM," in *Proceedings of IEEE International Conference on Wireless Communications, Networking and Mobile Computing (WCNC),* pp.825-829, 11-12 March 2007.

[206] P. Beinschob, M. Lieberei and U. Zolzer, "Improving MIMO-OFDM decision-directed channel estimation by utilizing error-correcting codes," *Advances in Radio Science*, vol. 7, pp. 83-88, May. 2009.

[207] M. Jiang, J. Akhtman and L. Hanzo, "Iterative joint channel estimation and multi-user detection for multiple-antenna aided OFDM system," *IEEE Transactions on Wireless Communications*, vol. 6, no. 8, pp. 2904-2914, Aug. 2007.

[208] R. Li, Y. Li, and B. Vucetic, "Iterative receiver for MIMO-OFDM Systems with joint ICI cancellation and channel estimation," in *Proceedings. of IEEE Wireless Communication and Networking Conference (WCNC)*, pp. 7-12, Las Vegas, USA, 31 March -3 April 2008.

[209] C. Berrou, A. Glavieus, and P. Thitimajshima, "Near Shannon limit error correcting coding and decoding: Turbo-codes," in *Proceedings IEEE International Conference on Communications*, pp. 1064-1070, May 1993.

[210] C. Berrou, A. Glavieus, "Near optimum error correcting coding and decoding: Turbo codes," *IEEE Transactions on Communications*, vol. 44, no. 10, pp. 1261-1271, Oct. 1996.

[211] M. Tuchler, R. Koetter, and A. C. Singer, "Turbo equalization: principles and new results unknown," *IEEE Transactions on Communications*, vol. 50, no. 5, pp. 754–767, May 2002.

[212] M. Tuchler, A. C. Singer, and R. Koetter, "Minimum mean squared error equalization using a priori information," *IEEE Transactions on Signal Processing*, vol. 50, no. 3, pp. 673-683, Mar. 2002.

[213] C. Heegard and S. B. Wicker, Turbo Coding. Norwell, MA, USA: Kluwer Academic Publisher, First Ed., 1999.

[214] W. N. Furman and J. W. Nieto, "Understanding HF channel simulator requirements in order to reduce HF modem performance measurement variability," in *Proceedings of 6th Nordic Shortwave Conf. HF*, Fårö, Sweden, pp. 6.4.1-6.4.13, Aug. 2001

[215] S. Haykin, *Adaptive Filter Theory, 3rd Edition*, Prentice Hall, Upper Saddle River, NJ, USA, 1996.

[216] V.J. Mathews, Z. Xie, "A stochastic gradient adaptive filter with gradient adaptive step-size," *IEEE Transaction on Signal Processing*, vol.41, no.6, pp. 2075-2087, June 1993.

[217] Y. K. Shin, J. G. Lee, "A study on the fast convergence algorithm for the LMS adaptive filter design," in *KIEE Proceedings.*, vol.19 , no. 5, pp. 12-19, October 1985,

[218] M. Tarrab, A. Feuer, "Convergence and performance analysis of the normalized LMS algorithm with uncorrelated Gaussian data *IEEE Transaction on Information Theory*, vol.34, no.4, pp.680- 691, July 1988.

[219] C. Komninakis, "A Fast and Accurate Rayleigh Fading Simulator," in *Proceedings of IEEE Global Communications Conference, GLOBECOM 2003*, GC01-8, San Francisco, Vol. 6, pp. 3306-3310, Dec. 1-5, 2003.

[220] R. Otnes and M. Tüchler, " Low-complexity turbo equalization for time-varying channels," in *Proceedings 55th IEEE Vehicular Technology Conference(VTC 2002) Spring*, Birmingham, AL, USA, vol. 1, pp. 140 -144, 6-9 May 2002.

[221] D. Raphaeli, and Y. Zarai, "Combined turbo equalization and turbo decoding," *IEEE Communication Letters*, vol.2, no.4, pp. 107-109, April 1998.

[222] O. O. Oyerinde and S. H. Mneney, "Single and Multiple - Variable Step Size Normalized Least Mean Square Algorithms for Network Echo Cancellation," *in Proceedings of the 5th International Conference on Cybernetics and Information Technologies, Systems and Applications: CISTA 2008, in the context of International Multi-Conference on Engineering and Technological Innovation: IMETI 2008*, Orlando, Florida, USA, pp 1-5, 29th June - 2nd July, 2008.

[223] O. O. Oyerinde and S. H. Mneney, "Variable Step Size Algorithms for Network Echo Cancellation," *Ubiquitous Computing and Communication (UBICC) Journal*, vol. 4, no. 3, pp. 746-757, August 2009.

[224] L. J. Cimini, Jr., "Analysis and simulation of a digital mobile channel using orthogonal frequency division multiplexing," *IEEE Transaction on Communications*, vol. 33, no. 7, pp. 665-765, July 1985.

[225] A. Goldsmith, S.A. Jafar, N. Jindal, and S. Vishwanath, "Capacity limits of MIMO channels," *IEEE Journal on Selected Areas in Communications*, vol. 21, no. 5, pp. 684-702, June 2003.

[226] J. G. Proakis, Digital communications, 4th ed., New York, McGraw-Hill, 2000.

[227] X. G. Doukopoulos and G. V. Moustakides, "Fast and Stable Subspace Tracking," *IEEE Transactions on Signal Processing*, vol. 56, no. 4, pp. 1452–1465, April 2008.

[228] S. M. kay, *Fundamentals of Statistical Signal Processing*. Englewood Cliffs, NJ, USA: Prentice-Hall, 1998.

[229] B. Yang, K. Letaief, R. Cheng, and Z. Cao, "Channel estimation for OFDM transmission in multipath fading channels based on parametric channel modeling," *IEEE Transactions on Communications*, vol. 49, no. 3, pp. 467-479, March 2001.

[230] J. T.Chen, A. Paulraj, and U. Reddy, "Multichannel Maximum-Likelihood Sequence estimation (MLSE) Equalizer for GSM using a parametric channel model" *IEEE Transactions on Communications*, vol. 47, no. 1, pp. 53-63, Jan. 1999.

[231] G. H. Golub and C. F. van Loan, *Matrix Computation*, 2nd ed. Baltimore, MD: The John Hopkins Univ. Press, 1993.

[232] O. O. Oyerinde, and S. H. Mneney, "Soft Input Iterative Channel Estimation for Turbo Equalization over Time Frequency Selective Fading Channel," *in Proceedings of South Africa Telecommunication Networks and Applications Conference (SATNAC) 2008*, Wild Coast Sun, Eastern Cape Coast, South Africa**,** pp. 77-82, September 7 - 10, 2008.

[233] O. O. Oyerinde and S. H. Mneney, "Improved Soft Iterative Channel Estimation for Turbo Equalization of Time Varying Frequency Selective Channels," *Wireless Personal Communication Journal*, vol. 52, no.2, pp. 325-340, January 2010.

[234] J. Akhtman and L. Hanzo, "Channel Impulse Response Tap Prediction for Time-Varying Wireless Channels," *IEEE Transactions on Vehicular. Technology*, vol. 56, no 5, pp. 2767-2769, Sep. 2007.

[235] S. ten Brink, J. Speidel, and R.-H. Yan, "Iterative demapping for QPSK modulation," *Electronic Letter*, vol. 34, no. 15, pp. 1459–1460, 1998.

[236] G.D. Forney, Concatenated Codes, Cambridge, MA: MIT Press, 1966.

[237] L. R. Bahl, J. Cocke, F. Jelinek, and J. Raviv, "Optimal decoding of linear codes for minimizing symbol error rate," *IEEE Transactions on Information Theory*, vol. 20, no.2, pp. 284-287, March 1974.

[238] J. Hagenauer and P. Hoeher, "A Viterbi algorithm with soft-decision output and its applications," in *Proceedings of IEEE Global Communications Conference, GLOBECOM 1989,* vol. 3, pp. 1680-1686, 1989.

[239] P. Robertson, "Illuminating the structure of code and decoder of parallel concatenated recursive systematic (turbo) codes," in *Proceedings of IEEE Global Communications Conference, GLOBECOM 1994,* vol. 3, pp. 1298-1303-1686, 1994.

[240] J. P. Woodard and L. Hanzo, "Comparative study of Turbo Decoding Techniques: an Overview," *IEEE Transactions on Vehicular Technology*, vol. 49, no 6, pp. 2208-2233, Nov. 2000.

[241] J. Hagenauer, E. Offer, and L. Papke, "Iterative Decoding of binary block and Convolutional Codes," *IEEE Transactions on Information Theory*, vol. 42, no.2, pp. 429-445, March 1996.

[242] J. Guey, M. P. Fitz, M. R. Bell, and W. Kuo, "Signal design for transmitter diversity wireless communication Systems over Rayleigh fading channels," *IEEE Transactions on Communications*, vol.47, no. 4, pp. 527-537, April 1999.

[243] V. Tarokh, N. Seshadri, and A. R. Calderbank, "Space-time codes for high data rate wireless communication: Performance criterion and code construction," *IEEE Transaction on Information Theory*, vol. 44, no. 2, pp. 744-765, March 1998.

[244] S. M. Alamouti, "A simple transmit diversity technique for wireless communications," *IEEE Journal in Selected Areas Communications*, vol. 16, no. 8, pp. 1451-1458, Oct. 1998.

[245] V. Tarokh, H. Jafarkhani, and A. Calderbank, "Space-time block codes from orthogonal designs," *IEEE Transaction on Information Theory*, vol. 45, no. 5, pp. 1456-1467, July 1999.

[246] H. Jafarkhani and N. Seshadri, " Super-Orthogonal Space-Time Trellis Codes," *IEEE Transaction on Information Theory*, vol. 49, no. 4, pp. 937-950, April 2003.

[247] J. N. Pillai and S. H. Mneney, " Turbo Decoding of Super-Orthogonal Space-Time Trellis Codes in Rayleigh Fading Channels," *Journal Wireless Personal Communications,* vol. 37, no. 3-4 , pp.371-385 , May 2006.

[248] H. Bolcskei and A. J. Paulraj, "Multiple Input Multiple Output (MIMO) wireless Systems," *IEEE The Communication Handbook, J. Gibson,* Ed., CR Press, 2nd edition, 2002.

[249] P. W. Wolniansky, G. J. Foschini, G. D. Golden, and R. A. Valenzuela, "V-BLAST: an architecture for realizing very high data rates over the rich-scattering wireless channel," in *Proceedings URSI International Symposium on Signals, Systems and Electronics,* Pisa, Italy, pp. 295-300, 29 Sept.-2 Oct. 1998.

[250] G. D. Golden, G. J. Foschini, and R. A. Valenzuela, P. W. Wolniansky, "Detection algorithm and initial laboratory results using V- BLAST space-time communication architecture," *Electronic Letter*, vol. 35, no. 1, pp. 14-15, 1999.

[251] A. Van Zelst, R. Van Nee, and G. A. Awater, "Space division multiplexing (SDM) for OFDM Systems ," in *Proceedings of IEEE Vehicular Technology Conference (VTC)*, vol. 2, Tokyo, Japan, pp. 1070-1074, 15-18 May 2000.

[252] A. M. Tonello, "Space-time bit-interleaved coded modulation with an iterative decoding strategy in *Proceedings of IEEE Vehicular Technology Conf. (VTC)*, Boston, US, pp. 473-478, 24-28 Sept. 2000.

[253] G. Caire, G. Taricco, E. Biglieri, "Bit-interleaved coded modulation*," IEEE Transaction on Information Theory*, vol. 44, no. 3, pp. 927-946, May 1998.

[254] D. Zuyderhoff, X. Wautelet, A. Dejonge, and L. Vanderdorpe, "MMSE turbo receiver for space–frequency bit–interleaved coded OFDM," in *Proceedings of IEEE Vehicular Technology Conference(VTC'03) Fall*, Orlando, USA, Oct. 2003.

[255] I. Lee, A. C. Chan, and C. W. Sundberg, "Space–time bit–interleaved coded Modulation for OFDM Systems," *IEEE Transaction on Signal Processing*, vol. 52, no.3, pp. 820-825, March 2004.

[256] A. Assalini, F. Osnato, and S. Pupolin, "Space-frequency bit-interleaved convolutional and turbo coded OFDM Systems with simplified iterative approaches," in *Proceedings of Wireless Personal Multimedia Communications (WPMC'04)*, Abano Terme, Italy, Sept. 2004.

[257] A. Assalini, and S. Pupolin, "On the impact of radio channel on the performance of space-time bit-interleaved coded OFDM system," in *Proceedings of International Conference on Global mobile Congress (GMC'05)*, Chongging, China, Oct. 2005.

[258] H. Lee, B. Lee, and I. Lee, "Iterative detection and decoding with an improved V-blast for MIMO-OFDM Systems," *IEEE Journal in Selected Areas Communications*, vol. 24, no. 3, pp. 504-513, Mar. 2006.

[259] S. Sadough, P. Piantanida, and P. Duhamel, "MIMO-OFDM optimal decoding and achievable information rates under imperfect channel estimation," in *Proceedings IEEE 8th Workshop on Signal Processing Advance in Wireless Communications (SPAW'07)*, pp. 1-5, 17-20 June 2007.

[260] Y. Li, L. Cimini, J. H. Winter and N. R. Sollenberger, "MIMO-OFDM for Wireless Communications: Signal Detection with Enhanced Channel Estimation," *IEEE Transactions on Communications*, vol. 50, no. 9, pp. 1471-1477, Sep. 2002.

[261] O. O. Oyerinde and S. H. Mneney, "Decision Directed Channel Estimation for OFDM Systems employing Fast Data Projection Method Algorithm," *in Proceedings of IEEE International Conference on Communication (ICC),* Dresden, Germany, 5 pages. 14th - 18th June 2009.

[262] O. O. Oyerinde and S. H. Mneney, "FDPM Aided Decision Directed Channel Estimation with VSSNLMS-based Predictor for OFDM Systems," in *Proceedings*

IEEE International Symposium on Broadband Multimedia System and Broadcasting, Shanghai, China, 6 pages, 24th -26th March 2010.

[263] O. O. Oyerinde and S. H. Mneney, "Soft Iterative Decision Directed Channel Estimation for OFDM Systems employing Adaptive Predictor," *in Proceedings of IEEE 1st International Conference on Wireless Communication Society, vehicular Technology, Information theory and Aerospace & Electronics Systems Technology (Wireless VITAE'09),* Aalborg, Denmark, pp. 857- 861, 17th -20th May 2009.

[264] O. O. Oyerinde and S. H. Mneney, "Iterative OFDM Receiver with Decision Directed Channel Estimation," *in Proceedings of IEEE AFRICON 2009,* Nairobi, Kenya, 6 pages, 23rd -25th September 2009.

[265] O. O. Oyerinde and S. H. Mneney, "Adaptive CIR Prediction of Time-Varying Channels for OFDM System," *in Proceedings of IEEE AFRICON 2009,* Nairobi, Kenya, 5 pages, 23rd -25th September 2009.